



جامعة التنمية البشرية
UNIVERSITY OF HUMAN DEVELOPMENT

p-ISSN 2521-4209
e-ISSN 2521-4217

UHD Journal of Science and Technology

A Scientific periodical issued by University of Human Development

Vol.8 No.(1) June 2024

2024

2724

www.jst.uhd.edu.iq



UHD Journal of Science and Technology

A periodic scientific journal issued by University of Human Development

Editorial Board

Professor Dr. Mariwan Ahmed Rasheed.....	Executive publisher
Assistant Professor Dr. Aso Mohammad Darwesh.....	Editor-in-Chief
Professor Dr. Muzhir Shaban Al-ni.....	Member
Professor Dr. Salih Ahmed Hama.....	Member
Professor Dr. Khalid Al-Quradaghi	Member
Assistant Professor Dr. Tara Mahmood Hassan.....	Member
Assistant Professor Dr. Raed Ibraheem Hamed.....	Member
Dr. Nurouldeen Nasih Qader.....	Member

Technical

Mr. Hawkar Omar Majeed.....	Head of Technical
-----------------------------	-------------------

Advisory Board

Professor Dr. Sufyan Taih Faraj Aljanabi.....	Iraq
Professor Dr. Salah Ismaeel Yahya.....	Kurdistan
Professor Dr. Sattar B. Sadkhan.....	Iraq
Professor Dr. Amir Masoud Rahmani	Kurdistan
Professor Dr. Muhammad Abulaish.....	India
Professor Dr. Parham Moradi	Iran

Introduction

UHD Journal of Science and Technology (UHDJST) is a semi-annual journal published by the University of Human Development, Sulaymaniyah, Kurdistan Region, Iraq. UHDJST member of ROAD, e-ISSN: 2521-4217, p-ISSN: 2521-4209 and a member of Crossref, DOI: 10.21928/issn.2521-4217. UHDJST publishes original research in all areas of Science, Engineering, and Technology. UHDJST is a Peer-Reviewed Open Access journal with Creative Commons Attribution Non-Commercial No Derivatives License 4.0 (CC BY-NC-ND 4.0). UHDJST provides immediate, worldwide, barrier-free access to the full text of research articles without requiring a subscription to the journal, and has article processing charge (APC). UHDJST applies the highest standards to everything it does and adopts APA citation/referencing style. UHDJST Section Policy includes three types of publications: Articles, Review Articles, and Letters.

By publishing with us, your research will get the coverage and attention it deserves. Open access and continuous online publication mean your work will be published swiftly, ready to be accessed by anyone, anywhere, at any time. Article Level Metrics allow you to follow the conversations your work has started.

UHDJST publishes works from extensive fields including, but not limited to:

- Pure Science
- Applied Science
- Medicine
- Engineering
- Technology

Scope and Focus

UHD Journal of Science and Technology (UHDJST) publishes original research in all areas of Science and Engineering. UHDJST is a semi-annual journal published by the University of Human Development, Sulaymaniyah, Kurdistan Region, Iraq. We believe that if your research is scientifically valid and technically sound then it deserves to be published and made accessible to the research community. UHDJST aims to provide a service to the international scientific community enhancing swap space to share, promote and disseminate the academic scientific production from research applied to Science, Engineering, and Technology.

SEARCHING FOR PLAGIARISM

Plagiarism Policy: The UHD Journal of Science and Technology is committed to upholding the highest standards of academic integrity and originality. As such, we do not tolerate plagiarism in any form. Authors submitting manuscripts to the journal must ensure that their work is entirely original and properly cited. Plagiarism, including self-plagiarism and the use of verbatim text from other sources without appropriate attribution, will result in immediate rejection of the submission. To maintain the integrity of scholarly research, all submissions undergo rigorous plagiarism checks using industry-standard software. Authors found to have engaged in plagiarism, at any stage before publication of the manuscript - before or after acceptance, during editing or at page proof

stage, will be barred from submitting to the journal in the future. By submitting their work to the UHD Journal of Science and Technology, authors affirm that their manuscript is their own original work and that any borrowed content is properly cited.

Section Policies

No.	Title	Peer Reviewed	Indexed	Open Submission
1	Articles: This is the main type of publication that UHJST will produce	✓	✓	✓
2	Review Articles: Critical, constructive analysis of the literature in a specific field through summary, classification, analysis, comparison.	✓	✓	✓
3	Letters: Short reports of original research focused on an outstanding finding whose importance means that it will be of interest to scientists in other fields.	✓	✓	✓

PEER REVIEW POLICIES

At UHJST we are committed to prompt quality scientific work with local and global impacts. To maintain a high-quality publication, all submissions undergo a rigorous review process. Characteristics of the peer review process are as follows:

- The journal peer review process is a "double-blind peer review".
- Simultaneous submissions of the same manuscript to different journals will not be tolerated.
- Manuscripts with contents outside the scope will not be considered for review.
- Papers will be refereed by at least 2 experts as suggested by the editorial board.
- In addition, Editors will have the option of seeking additional reviews when needed. Authors will be informed when Editors decide further review is required.
- All publication decisions are made by the journal's Editors-in-Chief on the basis of the referees' reports. Authors of papers that are not accepted are notified promptly.
- All submitted manuscripts are treated as confidential documents. We expect our Board of Reviewing Editors, Associate Editors and reviewers to treat manuscripts as confidential material as well.
- Editors, Associate Editors, and reviewers involved in the review process should disclose conflicts of interest resulting from direct competitive, collaborative, or other relationships with any of the authors, and remove oneself from cases in which such conflicts preclude an objective evaluation. Privileged information or ideas that are obtained through peer review must not be used for competitive gain.
- Our peer review process is confidential and the identities of reviewers cannot be revealed.

Note: UHJST is a member of CrossRef and CrossRef services, e.g., CrossCheck. All manuscripts submitted will be checked for plagiarism (copying text or results from other sources) and self-plagiarism (duplicating substantial parts of authors' own published work without giving the appropriate references) using the CrossCheck database. Plagiarism is not tolerated.

For more information about CrossCheck/iThenticate, please visit <http://www.crossref.org/crosscheck.html>.

OPEN ACCESS POLICY

This journal provides immediate open access to its content on the principle that making research freely available to the public supports a greater global exchange of knowledge. Open Access (OA) stands for unrestricted access and unrestricted reuse which means making research publications freely available online. It access ensures that your work reaches the widest possible audience and that your fellow researchers can use and share it easily. The mission of the UHDJST is to improve the culture of scientific publications by supporting bright minds in science and public engagement.

UHDJST's open access articles are published under a Creative Commons Attribution CC-BY-NC-ND 4.0 license. This license lets you retain copyright and others may not use the material for commercial purposes. Commercial use is one primarily intended for commercial advantage or monetary compensation. If others remix, transform or build upon the material, they may not distribute the modified material. The main output of research, in general, is new ideas and knowledge, which the UHDJST peer-review policy allows publishing as high-quality, peer-reviewed research articles. The UHDJST believes that maximizing the distribution of these publications - by providing free, online access - is the most effective way of ensuring that the research we fund can be accessed, read and built upon. In turn, this will foster a richer research culture and cultivate good research ethics as well. The UHDJST, therefore, supports unrestricted access to the published materials on its main website as a fundamental part of its mission and a global academic community benefit to be encouraged wherever possible.

Specifically:

- The University of Human Development supports the principles and objectives of Open Access and Open Science
- UHDJST expects authors of research papers, and manuscripts to maximize the opportunities to make their results available for free access on its final peer-reviewed paper
- All manuscript will be made open access online soon after final stage peer-review finalized.
- This policy will be effective from 17th May 2017 and will be reviewed during the first year of operation.
- Open Access route is available at <http://journals.uhd.edu.iq/index.php/uhdjst> for publishing and archiving all accepted papers,
- Specific details of how authors of research articles are required to comply with this policy can be found in the Guide to Authors.

ARCHIVING

This journal utilizes the LOCKSS and CLOCKSS systems to create a distributed archiving system among participating libraries and permits those libraries to create permanent archives of the journal for purposes of preservation and restoration.

LOCKSS: Open Journal Systems supports the LOCKSS (Lots of Copies Keep Stuff Safe) system to ensure a secure and permanent archive for the journal. LOCKSS is open source software developed at Stanford University Library that enables libraries to preserve selected web journals by regularly polling registered journal websites for newly published content and archiving it. Each archive is continually validated against other library caches, and if the content is found to be corrupted or lost, the other caches or the journal is used to restore it.

CLOCKSS: Open Journal Systems also supports the CLOCKSS (Controlled Lots of Copies Keep Stuff Safe) system to ensure a secure and permanent archive for the journal. CLOCKSS is based upon the open-source LOCKSS software developed at Stanford University Library that enables libraries to preserve selected web journals by regularly polling registered journal websites for newly published content and archiving it. Each archive is continually validated against other library caches, and if the content is found to be corrupted or lost, the other caches or the journal is used to restore it.

PUBLICATION ETHICS

Publication Ethics and Publication Malpractice Statement

The publication of an article in the peer-reviewed journal UHJST is to support the standard and respected knowledge transfer network. Our publication ethics and publication malpractice statement is mainly based on the Code of Conduct and Best-Practice Guidelines for Journal Editors (Committee on Publication Ethics, 2011) that includes;

- General duties and responsibilities of editors.
- Relations with readers.
- Relations with the authors.
- Relations with editors.
- Relations with editorial board members.
- Relations with journal owners and publishers.
- Editorial and peer review processes.
- Protecting individual data.
- Encouraging ethical research (e.g. research involving humans or animals).
- Dealing with possible misconduct.
- Ensuring the integrity of the academic record.
- Intellectual property.
- Encouraging debate.
- Complaints.
- Conflicts of interest.

ANIMAL RESEARCHES

- For research conducted on regulated animals (which includes all live vertebrates and/or higher invertebrates), appropriate approval must have been obtained according to either international or local laws and regulations. Before conducting the research, approval must have been obtained from the relevant body (in most cases an Institutional Review Board, or Ethics Committee). The authors must provide an ethics statement as part of their Methods section detailing full information as to their approval (including the name of the granting organization, and the approval reference numbers). If an approval reference number is not provided, written approval must be provided as a confidential supplemental information file. Research on non-human primates is subject to specific guidelines from the Weather all (2006) report ([The Use of Non-Human Primates in Research](#)).
- For research conducted on non-regulated animals, a statement should be made as to why ethical approval was not required.
- Experimental animals should have been handled according to the highest standards dictated by the author's institution.
- We strongly encourage all authors to comply with the '*Animal Research: Reporting In Vivo Experiments*' ([ARRIVE](#)) [guidelines](#), developed by [NC3Rs](#).
- Articles should be specific in descriptions of the organism(s) used in the study. The description should indicate strain names when known.

ARTICLE PROCESSING CHARGES

UHDJST is an Open Access Journal (OAJ) and has article processing charges (APCs). The published articles can be downloaded freely without a barrier of admission.

Address

University of Human Development, Sulaymaniyah-Kurdistan Region/Iraq
PO Box: Sulaymaniyah 6/0778

Contact

Principal Contact

Dr. Aso Darwesh

Editor-in-Chief

University of Human Development –
Sulaymaniyah, Iraq

Email: jst@uhd.edu.iq

Support Contact

UHD Technical Support

Phone: +964 773 393 5959

Email: jst@uhd.edu.iq

Contents

No.	Author Name	Title	Pages
1	Jafar A. Ali Loghman Khodakarami Zulfa J. Khudadad Jehan M. Rustam Aya B.Shawkat Srwa S. Ali Bala A. Faqe	Investigating the Influence of Environmental Factors on Corrosion in Pipelines Using Geospatial Modeling	1-12
2	Kardo O. Aziz Ramyar A. Teimoor Tofiq A. Tofiq Dilman S. Abdulla	Kurdish Sorani Dialect Morphology Generation Using a Concatenative Strategy	13-19
3	Rawyer Asaad Rashid Dana Faiq Abd Danyar Awat Othman Hero Abdulqader	Performance Evaluation using Spanning Tree Protocol, Rapid Spanning Tree Protocol, Per-VLAN Spanning Tree, and Multiple Spanning Tree	20-30
4	Bayan Omar Sharif Syamnd Mirza Abdullah Sarwar Arif Star Hadeel Abdulelah Ibrahim Hawar Mardan Muhammad Zhino Raouf Ali Hussein Mustafa Hamasalih	Assessment of Health-care Professional's Knowledge Regarding the Comorbidities of Vitamin D Deficiency and its Relationship with Uterine Fibroids	31-41
5	Hoshmen Murad Mohamedyusf Hawar Othman Sharif Mazen Ismaeel Ghareb	A New Approach for Software Cost Estimation with a Hybrid Tabu Search and Invasive Weed Optimization Algorithms	42-54
6	Azhi Faraj Semih Utku	Comparative Analysis of Word Embeddings for Multiclass Cyberbullying Detection	55-63
7	Bnar Abdulsalam Abdulrahman Nama Ezzaalddin Mustafa	Iraqi Kurd or Arab Male Authenticity Detection Based on Facial Feature	64-77
8	Mudhafar Mohamed M. Saeed	Blood storage impacts on the hematological indices of healthy subjects and patients with iron-deficiency anemia and beta-thalassemia – A comparative study	78-83
9	Dara A. Tahir Sehand Kamaludeen Arif	Enhancing COVID-19 Detection Accuracy: Optimal Gene Combinations, Kit Performance, and Reliable Detection Intervals	84-92

10	Ahmed Sajid Hameed	The Reality of Extension Works in the Directorate of Agricultural Extension and Agricultural Research In Kurdistan Region of Iraq	93-98
11	Fariaa Abdalmajeed Hameed Kanar R. Tariq Harith Raad Hasan Riyam Alaa Johni	Using the Cuckoo Optimization to Initialize the Harmony Memory in Harmony Search Algorithm to Find New Hybrid (CSHS) Algorithm	99-107
12	Ahmed Sajid Hameed	Training Needs of Farmers in the Field of Fig Fruit Breeding in Rania District: Sulaymaniyah Governorate and Relationship with Some Variables	108-114
13	Araz Mohammed Abdulkarim Mahabat Hassan Saeed Akam Mustafa Hassan	Assessment of Symptoms of Depression and Anxiety among Menopause Women in Sulaimani City, Kurdistan: Cross-sectional Study	115-121
14	Thikra Ali Kareem Muzhir Shaban Al-Ani Salwa Mohammed Nejres	Efficient Breast Cancer Dataset Analysis Based on Adaptive Classifiers	122-128
15	Hawar Othman Sharif Mazen Ismaeel Ghareb Hoshmen Murad Mohamedyusf	A Hybrid Artificial Bee Colony and Artificial Fish Swarm Algorithms for Software Cost Estimation	129-141
16	DiSoz Abdalkarim Rashid Marwan B. Mohammed	Black Hole Attack Detection in Wireless Sensor Networks Using Hybrid Optimization Algorithm	142-150
17	Sirwan Aziz Akbar Shkar M J Hassan Zana Muhamad Raof Mudhafar Mohamed M. Saeed	Personalized Skincare: Correlating Genetics with Skin Phenotypes through DNA Analysis	151-163

Investigating the Influence of Environmental Factors on Corrosion in Pipelines Using Geospatial Modeling



Jafar A. Ali*, Loghman Khodakarami, Zulfa J. Khudadad, Jehan M. Rustam, Aya B. Shawkat, Srwa S. Ali, Bala A. Faqe

Department of Petroleum Engineering, Faculty of Engineering, Koya University, Danielle Mitterrand Boulevard, Koya KOY45, Kurdistan Region – F.R. Iraq

ABSTRACT

This study integrated geographic information system (GIS) and remote sensing technology to identify areas around pipelines that are more susceptible to corrosion having the Kurdistan pipeline as a case study. Geospatial data are used to target factors such as rainfall, temperature, rivers, and minerals which increase the corrosion rate. Spatial data such as, the direction of slope, rainfall, proximity to rivers, and minerals, were collected and analyzed; maps were created for every individual factor to visualize their distribution. By overlaying these maps, regions that are at higher risk of corrosion were identified, which can be prioritized for further investigation or preventive measures. This paper's findings are significant for oil and gas industries, including pipeline operators and designers as corrosion can lead to devastating consequences. The novelty of this study is to identify areas along the pipeline at higher risk of corrosion through the application of geospatial information systems and remote sensing. This methodology holds immense potential for industries looking to proactively prevent corrosion through the implementation of preventative maintenance, monitoring programs, and the application of protective coatings and inhibitors. The results of this research demonstrate that environmental data, GIS, and remote sensing can predict corrosion in oil pipelines, offering valuable insights for better managing corrosion risk.

Index Terms: Corrosion, Pipeline, Minerals, Aspect, Geographic information system, Remote sensing

1. INTRODUCTION

The effects of pipeline corrosion have been extensively studied [1]. Pipelines serve as the primary mode for transporting substances between regions and countries. However, corrosion in pipelines poses one of the most significant challenges for the global oil and gas industry [2]. Pipeline corrosion refers to the deterioration of piping material due to exposure to the operating environment which incurs significant costs for the global economy amounting to billions

of dollars annually [3]. Considering that pipelines transport flammable, substances ensuring pipeline safety is of utmost importance. Consequently, the design and selection of the most suitable systems and materials hold great significance for the oil and gas industry [4]. In the current study, it is intended to investigate the corrosion around pipelines using remote sensing and geographic information system (GIS). GIS is commonly used to model pipeline systems, and it plays an important role in the management and operation of pipelines [5].

To detect various types of corrosion, comprehensive monitoring techniques are required. Implementing a combination of these techniques enables effective identification and assessment of different corrosion types [6]. A large number of studies indicate that stress has a significant effect on corrosion processes, leading to the development

Access this article online

DOI: 10.21928/uhdjst.v8n1y2024.pp1-12

E-ISSN: 2521-4217

P-ISSN: 2521-4209

Copyright © 2024 Ali, *et al.* This is an open access article distributed under the Creative Commons Attribution Non-Commercial No Derivatives License 4.0 (CC BY-NC-ND 4.0)

Corresponding author's e-mail: jafar.dalo@koyauniversity.org

Received: 07-10-2023

Accepted: 19-12-2023

Published: 04-01-2024

of pressure corrosion [7]. Wang *et al.* [8] found that stress concentration at the base of corrosion pits can facilitate the transition of pitting corrosion from a metastable state to a stable one. In addition, atmospheric corrosion, which occurs as a result of electrochemical and other reactions between a material's surface and the constituents of the surrounding atmosphere, encompasses various forms of corrosion [9]. The utilization of GIS tools, which encompass computer software, hardware, and data, enables a wide range of functionalities such as data entry, satellite image processing, manipulation, analysis, spatial analytics, transportation management, and data presentation related to specific locations on the earth's surface [10]. By employing GIS technology, significant geological hazards can be mapped and efficiently managed within a GIS database [11]. This approach greatly enhances the efficiency of oil and gas pipeline planning, as potential dangers and risks can be identified in advance [3]. The operations within the oil and gas industry, spanning from locating and extracting resources to managing field labor and transporting materials, are significantly influenced by geography. GIS assists organizations in a variety of pipeline operations such as pipeline planning, taking into account site factors such as terrain, soil type, and population, as well as pipe type and material, pipeline usage, and environmental impact [12].

The majority of previous studies in the field of pipeline corrosion have focused on investigating localized corrosion, primarily attributed to the flow characteristics within the pipe. These studies typically employ various instruments and devices to detect corrosion at specific locations along the pipeline.

The research problem is the characterization monitoring and management of corrosion, primarily within onshore pipelines. The paper aims to provide concise information on the current state of pipeline corrosion control and management. The objective of this study is to use GIS and remote sensing in technology and the advancements made in this field based on the existing knowledge. The results of the current study indicate that multiple elements contribute to the overall deterioration and structural weaknesses observed in the pipes.

2. METHODOLOGY

This research uses GIS to predict and monitor corrosion in pipelines and other infrastructure and create a corrosion risk map by combining data on soil minerals, moisture content,

and other factors that contribute to corrosion. This map can be used to identify areas that are at high risk of corrosion and prioritize maintenance efforts. The information utilized for this investigation comprises a map delineating oil reservoirs and oil and gas transmission lines within the Kurdistan Region of Iraq. This particular map was formulated by the Ministry of Petroleum of the Kurdistan Region. In addition, a digital elevation model (DEM) map, sourced from the archives of the US Geological Survey, was employed. Landsat 8 satellite images, obtained from the US Geological Survey archive, were also incorporated. Furthermore, annual rainfall data for the study area were acquired from the Kurdistan Regional Meteorological Organization.

It uses data that are attached to a unique location [13]. First, we obtained a hard copy of the Ministry of Petroleum's map and georeferenced it. Then, we digitized the oil transmission lines using digital tools [14]. To extract slope information, we utilized the digital elevation model from the map [15]. For the hydrology section, to extract river routes from a DEM, the following steps were undertaken. First, the DEM data were obtained from the US Geological Survey archives, specifically DEM of the study area with a resolution of 28² m. This data can be acquired from various sources such as government agencies, research institutes, or commercial providers. Next, the DEM was pre-processed in hydrology tools in Arc GIS software to eliminate anomalies or errors, such as spikes or dips, which could impact the accuracy of the river extraction process. Subsequently, the flow direction was determined using the D8 algorithm, assigning a flow direction value (e.g., North, Northeast, East) to each cell based on the steepest slope, enabling the identification of potential water paths. A flow accumulation raster was created, representing the total number of cells with the flow in each cell, indicating areas with higher accumulation values that suggest potential river courses with increased flow [16]. In addition, a threshold value was determined based on the flow accumulation raster, which set the minimum accumulation required for a cell to be considered part of the river, thereby influencing the level of detail in the extracted river network. Finally, the river routes were extracted using the threshold flow accumulation raster through raster-to-vector conversion techniques, transforming the raster representation into polyline vectors. The extracted river courses were then validated by comparing them with Google Earth imagery [17,18].

To examine the impact of rainfall on pipeline corrosion rate, the initial step involved gathering data on the total rainfall from the previous year. Subsequently, employing the inverse weighted distance method [19], the precipitation

amount for each pixel was computed. To analyze minerals in the soil, Landsat 8 satellite images of study areas were obtained from the USGS website. Image pre-processing and maps displaying the distribution of minerals were generated using the available remote sensing indices that are presented in equations (1-5) [20]-[22]. It is important to highlight that these indicators were executed within the ArcGIS software.

$$Gossan\ Index = \frac{\frac{Band\ 6}{Band\ 4} - 1}{\frac{Band\ 6}{Band\ 4} + \frac{Band\ 7}{Band\ 5}} \quad (1)$$

$$Fe^{2+}\ Index = \frac{(Band\ 3 + Band\ 4) - (Band\ 2 + Band\ 5)}{(Band\ 3 + Band\ 4) + (Band\ 2 + Band\ 5)} \quad (2)$$

$$Ferric\ Minerals\ Index = \frac{\frac{Band\ 6}{Band\ 4} - 1}{\frac{Band\ 6}{Band\ 4} + 1} \quad (3)$$

$$Laterite\ Index = \left(\frac{Band\ 6}{Band\ 4} - 1 \right) * \left(\frac{Band\ 5}{Band\ 7} - 1 \right) \quad (4)$$

$$Clay\ Minerals\ Index = \frac{\frac{Band\ 7}{Band\ 6} - 1}{\frac{Band\ 7}{Band\ 6} + \frac{Band\ 5}{Band\ 6} + 1} \quad (5)$$

Subsequently, employing the fuzzy membership function [23], [24], the criteria maps were initially standardized, ensuring that the output values fell within the range of 0.0–1.0 [23], [24]. Following this, all standardized maps were overlaid. In the end, the standardized maps were consolidated.

3. THEORETICAL WORK (CASE STUDY – PIPELINE)

In this study, various components need to be considered when discussing matters related to corrosion. These components include factors such as aspect, rivers, rain, and the presence of minerals in the soil, such as clay, gossan, laterite, Fe^{2+} , and Ferrite–Martensite interphase (FMI). By taking into account factors like these, we can improve the accuracy of our predictions regarding the areas on the pipelines that are prone to corrosion reactions.

3.1. Aspect (The Direction of the Slope)

The alignment of the earth's surface with regard to the sun is referred to as an aspect [25]. It is typically represented as an angle in degrees from 0 to 360. ArcGIS calculates the aspect of every cell within the buffer in a DEM based on the slope

and direction of the cell. The direction of the slope can affect the corrosion rate of metals. Water has the biggest impact on the corrosion of slope protection net, followed by anion content. While this study did not directly measure humidity, it was indirectly assessed through geographic direction. This relies on established geographic patterns, where Northern and Western Regions typically have cooler and more humid conditions than southern and eastern areas. Incorporating geographic direction data serves as a proxy for humidity, allowing us to infer these environmental factors without direct measurements.

Total soluble salt has a moderate impact on corrosion [26]. The effect of slope direction on steel depends on the application. It was discovered that distinct impact angles and velocities are determined by varied slope directions and that the peak impact velocity increases with increasing slope direction [27]. Hence, with increasing slope direction (aspect), the corrosion rate of steel will increase.

3.2. Rainfall

Chemicals or other airborne particles known as air pollution can hasten the rate of corrosion. Carbon monoxide (CO), nitrogen oxides (NO and NO_2), sulfur dioxide (SO_2), and last but not least lead (Pb) are examples of air pollutants [28]. When some impurities such as sulfur dissolve in rainwater, the corrosion rate will increase. The rain droplets will catch any pollutants from the air while it falls down and when it reaches the pipelines, the pollutants from the droplets cause the rate of corrosion to speed up rapidly. Rainwater can cause uniform corrosion in pipelines. One of the key elements that cause pipelines to corrode is the presence of moisture. Rainwater may increase the acidity of the soil near the pipeline, which could result in corrosion [29]. The amount of moisture in the soil also has an impact on the pace of corrosion [30]. Water, dirt, and other environmental variables can all cause pipelines to corrode. Where water is present as a distinct phase, pitting corrosion typically develops [31].

3.3. River

First, we should mention that there are two types of rivers (drainage networks): Perennial rivers and seasonal rivers. Rivers that have a continuous flow of water all year round are known as perennial rivers. However, seasonal rivers are ones that only flow during the rainy season at a specific time [32]. Rivers can have a variety of effects on pipeline corrosion. For instance, the dissolved oxygen and other compounds that may be present in river water could cause the pipeline to corrode. The erosion of the soil surrounding a pipeline due to river movement is another factor that may

expose the pipeline to corrosive substances [33]. Rivers can influence the rate of corrosion in various ways, including dampness. The amount of water vapor in the air is gauged by the concept of humidity. Rivers and humidity are related in that rivers have an impact on the humidity of the places around them. For instance, the surrounding air becomes more humid when water evaporates from a river. On the other hand, water flowing downstream from a river can lower the relative humidity in the region [34]. Humidity directly influences how quickly metals corrode. Above a given relative humidity, the corrosion attack or rusting rate is noticeably higher. The rate of corrosion is minimal, however, below the crucial humidity level. The essential humidity is often around 45%; however, it can occasionally be even lower [35]. When the amount of moisture in the air approaches critical humidity – the point at which water no longer evaporates or is absorbed from the atmosphere – humidity can result in atmospheric corrosion. In general, metal components corrode more quickly the longer they are exposed to humid air [36]. When a chemical reaction affects a whole exposed surface, uniform corrosion ensues. Typically, it occurs when metals are exposed to open environments such as water, air, and soil [37]. Then, the rate of corrosion increases with how close the river is. If our pipeline is close to the rivers, the humidity, moisture, and flow rate of the river can affect the corrosion rate.

3.4. Minerals

In the present study, only five mineral types have been taken into account. This selection was made based on their availability within the region under investigation and their suitability for indexing using remote sensing techniques.

3.4.1. Clay

The Clay Minerals Index is a remote sensing index that can be used to map the distribution of clay minerals in soils and rocks. Clay has absorption features in the short-wave infrared spectral region, which can be used to distinguish them from other minerals [38]. All the components of soil, including minerals, living things, and animals, go toward its creation. The minerals, flora, and fauna remnants are ground into tiny particles over time by the pressure of the water [39]. These soils expand and soften during rainy seasons as they absorb more water whereas contracting and hardening during dry seasons as they lose water. Structures constructed on such soils as pipelines are predicted to suffer severe damage due to this behavior [40]. Clay soil can cause corrosion in steel pipes due to the presence of sulfate-reducing bacteria [41] and this will then cause some reactions that will lead to microbial-induced corrosion.

3.4.2. Fe₂

Iron is an element that can be found in plants, animals, soil, and rocks [42], and it belongs to the first transition series and Group 8 of the periodic table. In the field of corrosion, it is commonly acknowledged that the corrosion products of metal ions significantly impact subsequent corrosion processes. For instance, the oxides and hydroxides formed by Fe²⁺/Fe³⁺ play a crucial role in determining the density and structure of the rust layer on the steel's surface [43].

3.4.3. Gossan

Gossan is an iron oxide that forms on the top of sulfide deposits [44]. Its formation is attributed to the acidity of the environment. Steel is susceptible to corrosion when exposed to gossan, leading to general corrosion [44]. The presence of gossamer can serve as an indicator of the existence of sulfide minerals, which can contribute to corrosion in metals [44]. When gossan is present, it suggests the presence of sulfide minerals in the nearby rock, thereby increasing the corrosion rates in metals exposed to the environment. Steel can undergo homogeneous corrosion as a result of gossan [44].

3.4.4. FMI

In Dual-Phase (DP) steels, the area between ferrite and martensite is known as the FMI [39]. There are two stages to the early corrosion process of DP steel. Due to the subsequent appearance of cathodic TM and FM, the steel corrodes more quickly in the first stage than it does in the second stage due to the dissociation of martensite [45].

A particular kind of localized corrosion that affects steel is known as FMI corrosion. It results from the steel's microstructure's inclusion of the phases ferrite and martensite. Corrosion between these two phases occurs at their interface and is characterized by material loss there [46].

3.4.5. Laterite

The Laterite Index is a spectral index calculated from Landsat 8 satellite imagery using specific bands to identify and characterize areas with lateritic soils. The formula for the index is given by $((\text{Band } 6)/(\text{Band } 4) - 1) * ((\text{Band } 5)/(\text{Band } 7) - 1)$. In this equation, "Band 4" represents the red band, "Band 5" corresponds to the near-infrared band, "Band 6" is associated with the shortwave infrared band 1, and "Band 7" represents the shortwave infrared band 2 [47]. The index involves two ratios, (Band 6 / Band 4 - 1) and (Band 5 / Band 7 - 1), which are multiplied together. The resulting index values can be used to highlight areas with lateritic soils, as the combination of specific spectral

bands helps accentuate the unique characteristics of these soils. This type of remote sensing analysis aids in the identification and mapping of lateritic regions, providing valuable information for geological, environmental, and land-use studies [48].

A particular kind of localized corrosion that affects steel is known as FMI corrosion. It results from the steel's microstructure's inclusion of the phases ferrite and martensite. Corrosion between these two phases occurs at their interface and is characterized by material loss there [49].

3.5. Case Study

The theory was applied to real data for the purpose of analysis and further investigation. The Kurdistan pipeline (Fig. 1) was used as a case study, which connects the North Iraqi oil fields from the Topkhana oil field to Turkey. This article paper primarily focuses on crude oil pipelines. The Kurdistan oil pipeline, which was completed by the Kurdistan Regional Government of Iraq in 2013 [44], serves as a central subject of discussion. This functioning oil pipeline connects the Taq Taq oil fields to the broader pipeline network linking Kirkuk to Khurmala. From

Khurmala, the pipeline continues through Dohuk and terminates further North at Fishkabur on the Turkish border. At Fishkabur, it links up with the primary Kirkuk-Ceyhan pipeline [50].

In the subsequent sub-section, the theory will be applied to the pipeline to assess the impact of each factor on an individual map. The map data will then be standardized using Fuzzy logic, ensuring it falls within the range of 0–1, thus becoming dimensionless.

3.5.1. Aspect (Direction of the slope)

Aspect identifies the steepest downslope direction from each cell to its neighbors from the EM. It can be considered the slope direction or the compass direction of a hill face [19]. Regions that face more toward the North tend to have drier climates, resulting in lower humidity levels. Examples of such areas include Fish Khabur and the Tawke oil field. The higher values observed in the aspect map, as depicted in Fig. 2, are predominantly concentrated in these two regions.

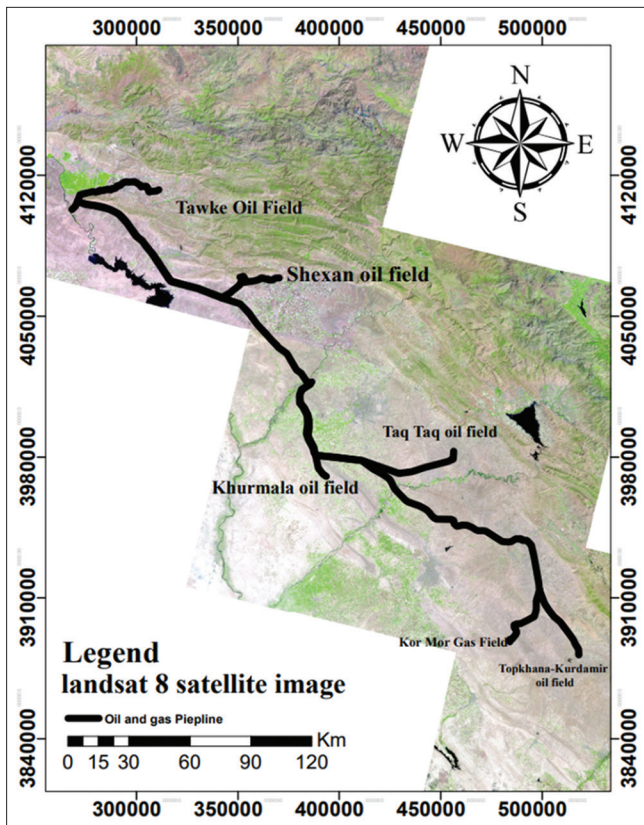


Fig. 1. Kurdistan oil pipeline.

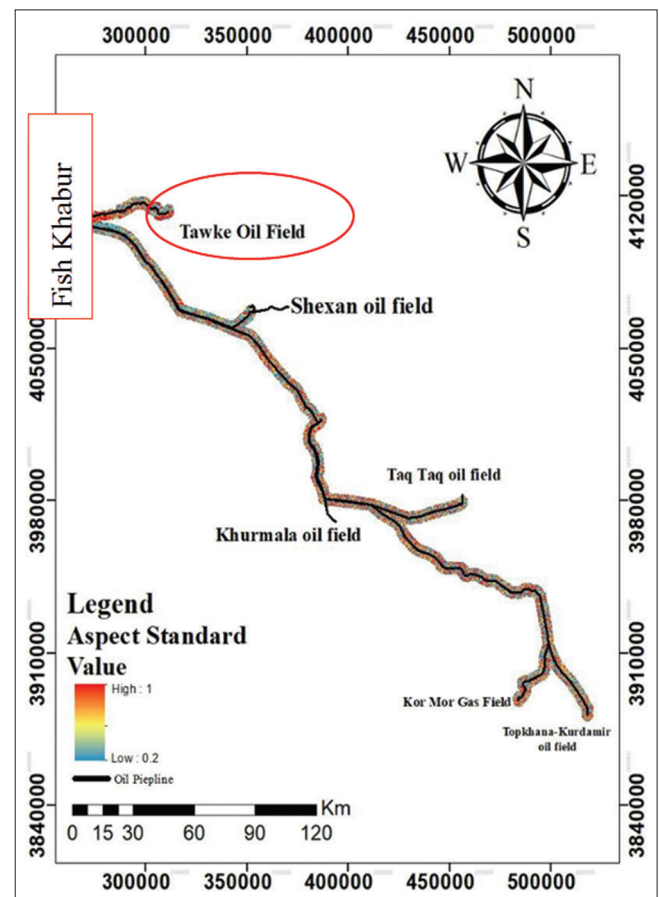


Fig. 2. Standardized aspect map depicting the intersection of oil transmission lines on the ground in different geographical directions

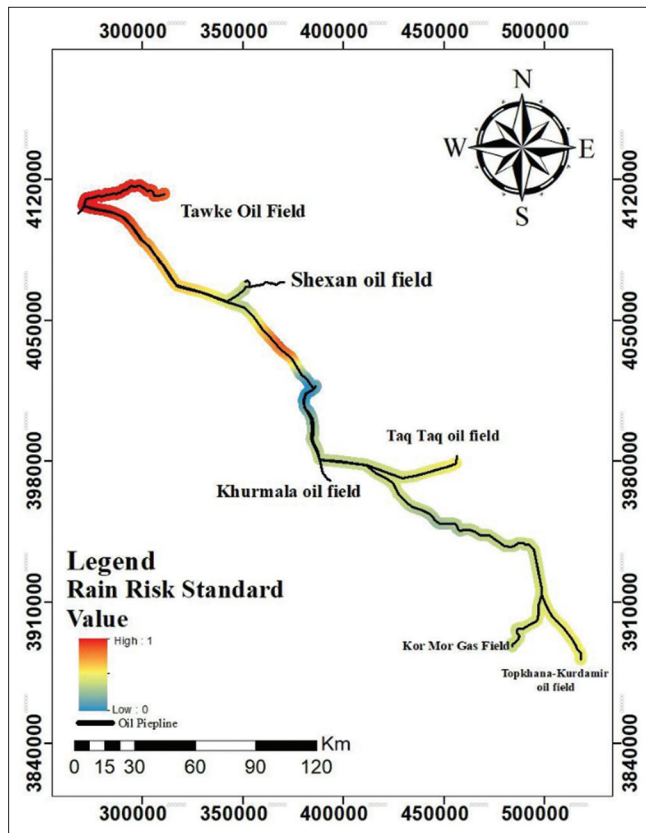


Fig. 3. Standardized spatial distribution map of rainfall.

3.5.2. Rain risk

According to the theory of corrosion, the increase in humidity resulting from rain and snow and the presence of impurities such as sulfur can lead to an increase in the rate of corrosion. When rain droplets collect pollutants from the air during their descent, these pollutants contribute to an accelerated corrosion process upon reaching the pipelines. The standardized spatial distribution map of rainfall depicted in Fig. 3 indicates that the corrosion rate is highest along the route from the Tawke oil field to Fish Khabur, with a ratio range of 0.844–0.990. On the other hand, the lowest corrosion rate is observed in the area between the Shekhan oil field and the Khurmala oil field (Kalak), where the ratio range is between 0.00056 and 0.2579.

3.5.3. River

Rivers can influence the corrosion rate through factors such as dampness. Humidity, which is a measure of water vapor in the air, is related to rivers as they affect the humidity levels of their surrounding areas. River water may contain dissolved oxygen and other compounds that can contribute to pipeline corrosion. Fig. 4 illustrates the river map, indicating

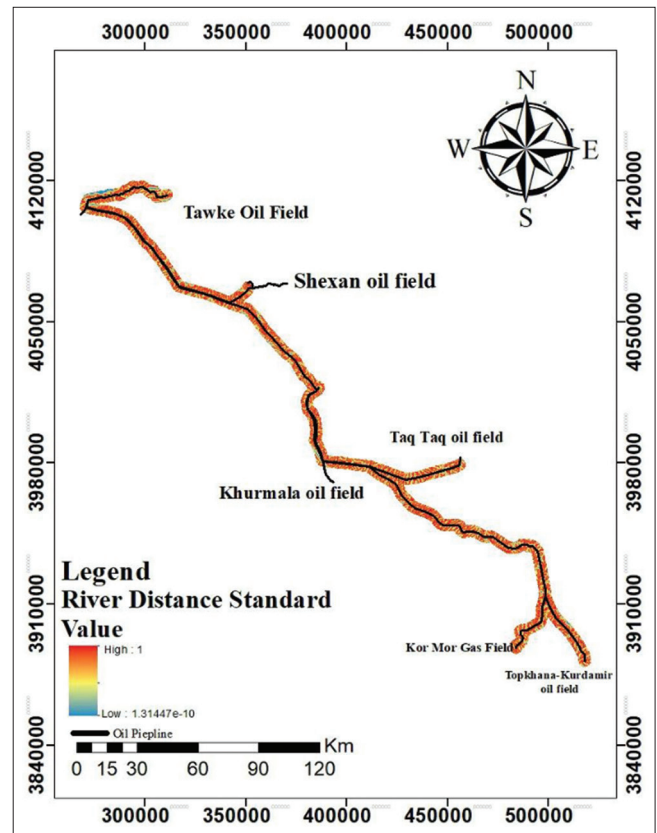


Fig. 4. River map (pipeline proximity to rivers).

the proximity of the pipeline to rivers. With the exception of the region between the Tawke oil field and Fish Khabur, where the ratio range is between 0.071 and 0.908, most regions exhibit similar ratios. This suggests that the corrosion rate remains relatively consistent across these areas, whereas the aforementioned region stands out with a comparatively lower ratio.

3.5.4. Minerals

3.5.4.1. Laterite

Minerals present in the soil have a significant impact on the corrosion rate. In particular, laterite and corrosion rate are closely related, as laterite can accelerate the corrosion of metals that come into contact with it. This is due to the significant presence of iron and aluminum in laterite, which can induce corrosion when in contact with metals [45]. The laterite map in Fig. 5 indicates the distribution of laterite in the region. The highest concentration of laterite is detected from Fish Khabur up until halfway toward the Tawke oil field. There is also a small area with high laterite in the North of the Khurmala oil field, although it is not as extensive as in Fish Khabur. The range of laterite in these

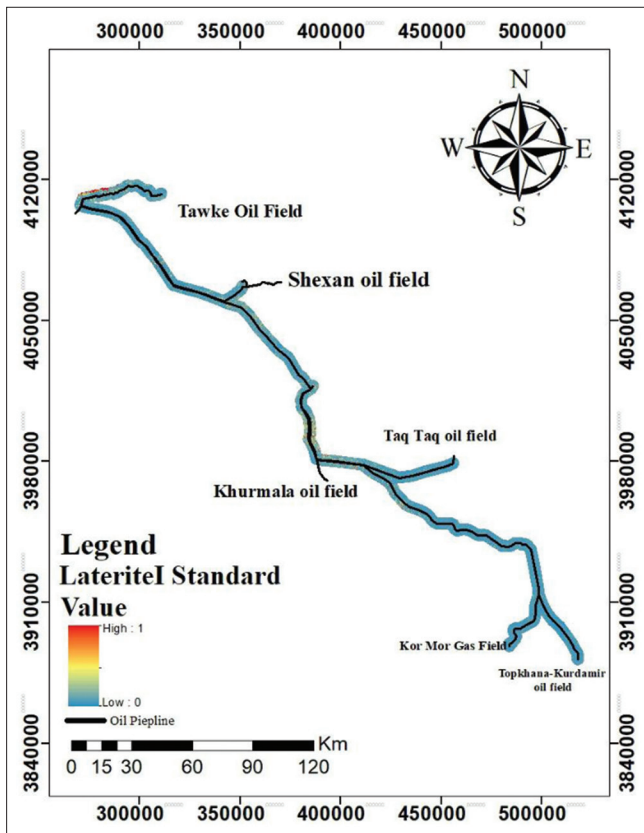


Fig. 5. Standardized laterite map illustrating the intersection of oil transmission lines on the ground.

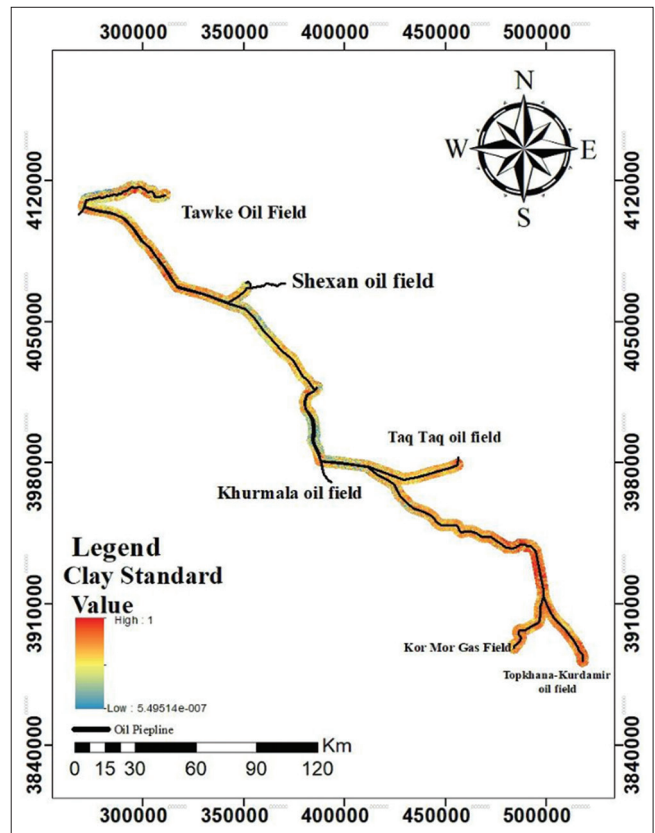


Fig. 6. Standardized clay map illustrating the intersection of oil transmission lines on the ground.

areas varies between 0.658 and 0.9114. The rest of the region exhibits a lower range of laterite, ranging between 0.595 and 0.658.

3.5.4.2. Clay

Clay can trap moisture and corrosive substances against the material of pipelines, because of the presence of clay in soil, these soils expand and soften during rainy seasons as they absorb more water, whereas contracting and hardening during dry seasons as they lose water and cause damages to pipelines. Microbial-induced corrosion also occurs due to the presence of sulfate-reducing bacteria in clay soil. The clay map is illustrated in Fig. 6, lowest value can be seen in the area between the Khurmla oil field and the Shekhar oil field and to be more exact from bina bawe to the Khurmala oil field, where it ranges (0.059–0.061). Most of the oil fields have similar high clay percentages. Except for the area between Shekhan and the Khurmala oil fields, more so starting near Khurmala and stretching southward until it reaches the joint that split into two branches (taq taq and chamchamal) with a range between 0.062 and 0.263.

3.5.4.3. Fe^{2+}

It is well established that the corrosion products of metal ions play a significant role in influencing subsequent corrosion processes. When iron (Fe_2) reacts with water and oxygen, it generates these metal ions. The Fe^{2+} map, as presented in Fig. 7, highlights the areas with the highest concentration of Fe^{2+} from Fish Khabur up to halfway toward the Tawke oil field, with a range between 0.4341 and 0.5482. Conversely, the rest of the region, excluding the mentioned area, exhibits lower levels of Fe^{2+} with a range between 0.3145 and 0.3829.

3.5.4.4. Gossan

The presence of gossan can indicate that there is sulfide which can trap moisture and corrosive substances against metal surfaces in the surrounding rock, which can lead to increased corrosion rates in metals exposed to the environment. Fig. 8 presents a gossan map, it can be seen that the highest gossan amount in the area from the Tawke oil field moves southward until it reaches the pipeline that feeds into the Shekhan oil field and from the Shekhan oil field pipeline moves 37.357828 km South with ranges between

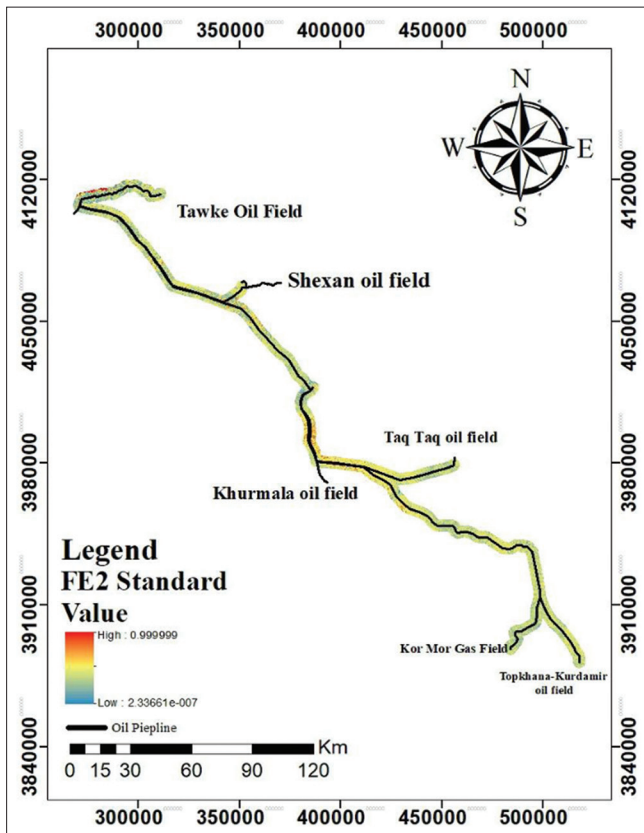


Fig. 7. Standardized Fe²⁺ map illustrating the intersection of oil transmission lines on the ground.

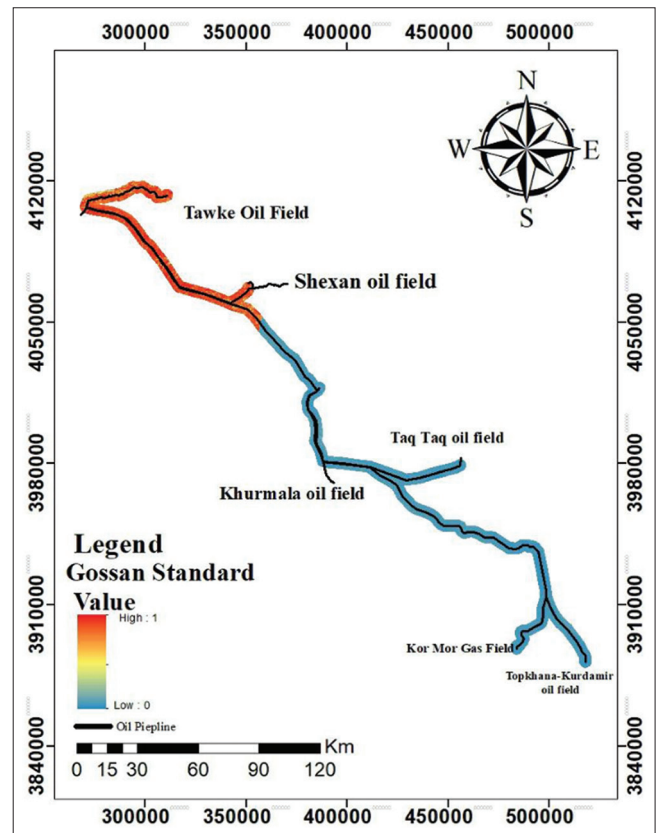


Fig. 8. Standardized Gossan map illustrating the intersection of oil transmission lines on the ground.

0.309 and 0.380. While the lowest gossan rate starts from 37.357828 km down from the Shekhan oil field pipeline and moves southward covering the areas: Khurmala, Taq Taq oil fields, and Kor Mor gas field, until it reaches the Tophkana oil field with a range between 0.168 and 0.226.

3.5.4.5. Ferric minerals index: FMI

A particular kind of localized corrosion that affects steel is known as FMI corrosion. It results from the steel's microstructure's inclusion of the phases ferrite and martensite. Corrosion between these two phases occurs at their interface and is characterized by material loss [11]. The standard FMI map is illustrated in Fig. 9, and the highest FMI area exists from Fish Khabur to the Tawke oil field with ranges between 0.3538 and 0.5180 whereas the lowest FMI values are in the rest of the region (largest area) ranging between 0.3291 and 0.4191.

4. RESULTS AND DISCUSSION

Corrosion is a complex process that can be influenced by a wide range of factors. However, not all factors have the same

impact on corrosion rates, and it is, therefore, necessary to assign appropriate weights to each factor to accurately assess the overall risk of corrosion. Failure to properly weigh each factor can result in inaccurate and erroneous assessments of corrosion risk. To address this issue, we have conducted a study of various criteria that can impact corrosion rates. Our analysis involves assigning weights to each criterion based on its relative contribution and significance in accelerating the corrosion process. By considering the unique characteristics of each criterion, we can develop a more comprehensive and accurate understanding of the overall risk of corrosion. It is important to note that the weighting process is not arbitrary but is based on scientific and engineering principles. By leveraging our collective expertise and experience, we have developed a rigorous and systematic approach to assigning weights which ensures that the assessments are both reliable and consistent in Table 1. With this approach, it can help ensure the safe and effective operation of engineering systems and structures by identifying and mitigating corrosion risk.

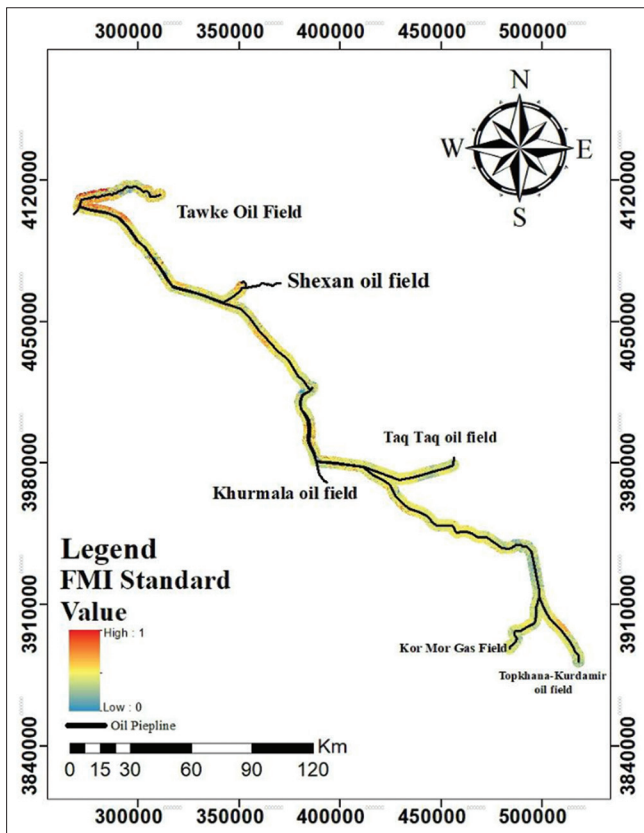


Fig. 9. Standardized Ferrite–Martensite Interphase map illustrating the intersection of oil transmission lines on the ground.

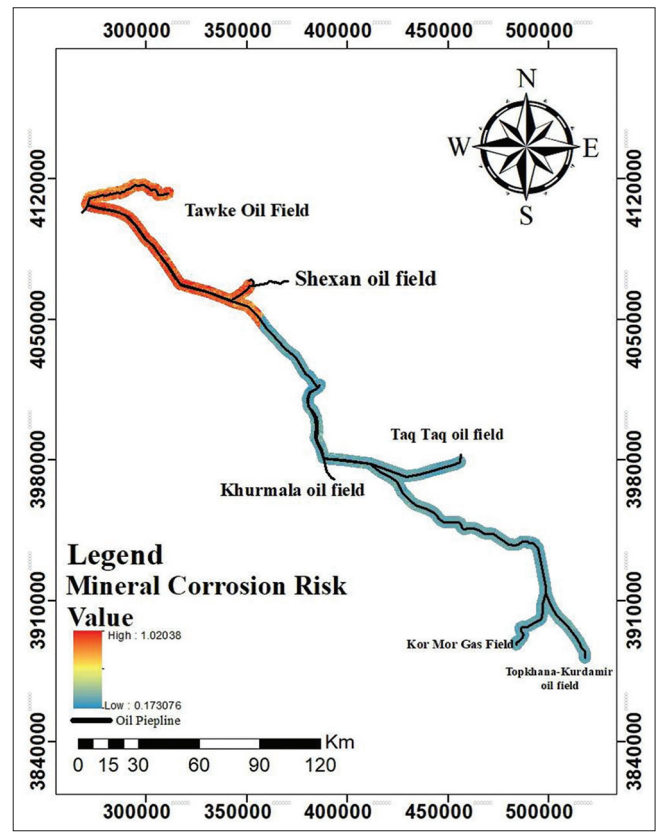


Fig. 10. Minerals corrosion risk map.

In this study, we employed the Delphi method for weighting the criteria. The Delphi method is a structured and iterative communication technique that involves a panel of experts. Through a series of rounds, these experts anonymously share their opinions and insights, and the process continues until a consensus is reached or a pre-defined level of agreement is achieved. The Delphi method helps aggregate the diverse perspectives of experts and is particularly useful in situations where there may be uncertainties or varying opinions regarding the importance of different factors.

The rainfall rate has the highest weight of (22%) since it can contribute most toward corrosion and since there was a high rate of precipitation for the data used during (2019–2020). Fe^{2+} minerals (21%) have a lot of contribution toward corrosion. The river weight is (14%) since it is considered a flow accumulation of greater than 500 ml; the rivers can be seasonal and might not be around all year round. While the weight for the clay is given (13%)

TABLE 1: Factors weights

Factors	Weights (%)
Aspect	8
River	14
Rain	22
Clay	13
Fe^{+2}	21
FMI	8
Gossan	7
Laterite	7

since at times can contribute toward corrosion whereas at other times, it can act as a protective barrier from outside sources. The rest of the minerals are given (8%–7%–7%) for FMI, gossan, and laterite, respectively, since they seem to be less abundant as visible from the mapping of these minerals, and without the presence of moisture or water these minerals cannot contribute much toward corrosion. The process of giving weights is done by multiplying each corrosion factor by its corresponding weights and then overlaying them. Fig. 10 is the overlay map for the minerals only, and Fig. 11 is the overlay map for all the

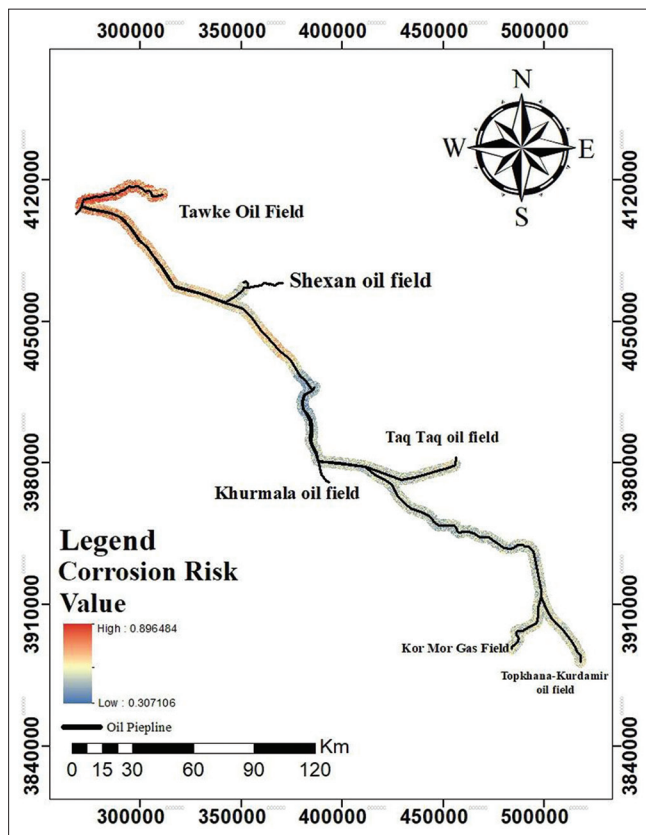


Fig. 11. Corrosion risk map.

factors including minerals with the weights that are given in Table 1. It appears that corrosion is more prevalent in the Northern regions as compared to the Southern regions. This can be attributed to the fact that the areas in the North experience higher levels of precipitation, therefore, are more exposed to moisture and humidity. In addition, the level of minerals is high in that region. Corrosion is strongly influenced by the presence of water and oxygen. As a result, regions with high levels of moisture and humidity, such as those found in the northern areas, are more prone to corrosion than those with lower levels, such as the southern areas.

5. CONCLUSION

This paper demonstrates how GIS technology can be utilized to identify areas at higher risk of corrosion. The data on environmental factors were analyzed to generate maps that could visually display the distribution of these factors. By overlaying these maps, regions that are more susceptible to corrosion were identified.

The use of GIS and remote sensing technologies in identifying areas of higher risk emphasizes the significance of corrosion risk assessment. The findings of the current study are based on the principles of corrosion science and materials engineering. Corrosion occurs due to the interaction between metal structures and their environment. By utilizing GIS technology to identify areas at higher risk of corrosion, industries can take a proactive approach to prevent or mitigate the corrosion process, ultimately ensuring the safe and sustainable operation of critical infrastructure.

REFERENCES

- [1] P. Zhang, D. Xu, Y. Li and K. Yang. "Electron mediators accelerate the microbiologically influenced corrosion of 304 stainless steel by the *Desulfovibrio vulgaris* biofilm". *Bioelectrochemistry*, vol. 101, pp. 14-21, 2015.
- [2] L. Aukett. "The Use of Geographical Information Systems (GIS) in Oil Spill Preparedness and Response. *International Conference of Health, Safety and Environment in Oil and Gas Exploration and Production, Australia*". 2012.
- [3] D. Xu, W. Huang, J. Ruschau, J. Hornemann, J. Wen and T. Gu. "Laboratory investigation of MIC threat due to hydrotest using untreated seawater and subsequent exposure to pipeline fluids with and without SRB spiking". *Engineering Failure Analysis*, vol. 28, pp. 149-159, 2013.
- [4] H. R. Vanaei, A. Eslami and A. Egbewande. "A review on pipeline corrosion, in-line inspection (ILI), and corrosion growth rate models". *Pressure Vessels and Piping*, vol. 149, pp. 43-54, 2017.
- [5] Y. Chang, Y. Wang and W. Fan. "The Applied Research of Embedded GIS in the Corrosion Inspection System of Urban Underground Pipeline. *ICPTT: Advances and Experiences with Pipelines and Trenchless Technology for Water, Sewer, Gas, and Oil Applications*". pp. 1680-1688, 2009.
- [6] N. Saumu. "The Engineers Post". 2022. Available from: <https://www.theengineerspost.com/types-of-corrosion> [Last accessed on 2022 Nov 16].
- [7] X. Liu, G. S. Frankel, B. Zoofan and S. I. Rokhlin. "In-situ observation of intergranular stress corrosion cracking in AA2024-T3 under constant load conditions". *Corrosion Science*, vol. 49, pp. 139-148, 2007.
- [8] M. Laleh, A. E. Hughes, S. Yang, J. Li, W. Xu, I. Gibson and M. Y. Tan. "Two and three-dimensional characterization of localized corrosion affected by lack-of-fusion pores in 316L stainless steel produced by selective laser melting". *Corrosion Science*, vol. 165, p. 108394, 2020.
- [9] J. A. Ali, L. Khodakarami and M. Ahmed. "Pipeline risk assessment using GIS". *UKH Journal of Science and Engineering*, vol. 6, pp. 5-25, 2022.
- [10] E. Ali. "Geographic Information System (GIS): Definition, Development, Applications and Components". Anada Chandra College, Jalpaiguri, India, 2020.
- [11] D. L. Slayter and C. S. Hitchcock. "Development of a GIS Database of Corrosion Hazards for Use in Pipeline Integrity Assessments, *Proceedings of the 2008 7th International Pipeline Conference*". ASME, Alberta, Canada, pp. 347-353, 2008.

- [12] M. Guo and J. Wang. "Environmental Impacts of Shale Gas Development in China: Assessment and Regulation". Springer Nature, Germany, 2021.
- [13] K. Wilson. "Geographic Information Systems (GIS), Earthdata". 2022. Available from: <https://www.earthdata.nasa.gov/learn/backgrounders/gis#:~:text=a%20geographic%20information%20system%20%28gis%29%20is%20a%20computer,sources%20to%20map%20and%20examine%20changes%20on%20earth> [Last accessed on 2022 Nov 18].
- [14] L. Hill. "Geo-referencing: The Geographic Associations of Information". The MIT Press, Cambridge, 2009.
- [15] P. A. Burrough and R. A. McDonnell. "Principle of Geographic Information Systems". Oxford Press, United Kindom, 1998.
- [16] D. G. Tarboton, R. L. Bras and I. Rodriguez-Iturbet. "On the extraction of channel networks from digital elevation data". *Hydrological Processes*, vol. 5, pp. 81-100, 1991.
- [17] S. K. Jenson and J. O. "Domingue, extracting topographic structure from digital elevation data for geographic information-system analysis". *Photogrammetric Engineering and Remote Sensing*, vol. 54, pp. 1593-1600, 1988.
- [18] "ArcGIS Help 10.1". 2012. Available from: <https://resources.arcgis.com/en/help/main/10.1/index.html#/009z000000m000000> [Last accessed on 2022 Nov 10].
- [19] A. R. Soffianian, H. B. Bakir and L. Khodakarami. "Evaluation of heavy metals concentration in soil using GIS, RS and geostatistics". *IJSR*, vol. 9, no. 12, pp. 61-75, 2015.
- [20] L. C. Rowan and J. C. Mars. "Lithologic mapping in the Mountain Pass, California area using advanced spaceborne thermal emission and reflection radiometer (ASTER) data". *Remote Sensing of Environment*, vol. 84, no. 3, pp. 350-366, 2003.
- [21] S. Esmaeili, M. H. Tangestani and M. H. Tayebi. "Sub-pixel mapping of copper-and iron-bearing metamorphic rocks using ASTER data: A case study of Toutak and Surian complexes, NE Shiraz, Iran". *Natural Resources Research*, vol. 29, no. 5, pp. 2933-2948, 2020.
- [22] D. F. Ducart, A. M. Silva, C. L. B. Toledo and L. M. D. Assis. "Mapping iron oxides with Landsat-8/OLI and EO-1/Hyperion imagery from the Serra Norte iron deposits in the Carajás Mineral Province, Brazil". *Brazilian Journal of Geology*, vol. 46, pp. 331-349, 2016.
- [23] K. Xu, C. Kong, J. Li, L. Zhang and C. Wu. "Suitability evaluation of urban construction land based on geo-environmental factors of Hangzhou, China". *Computers and Geosciences*, vol. 37, no. 8, pp. 992-1002, 2011.
- [24] F. Qiu, B. Chastain, Y. Zhou, C. Zhang and H. Sridharan. "Modeling land suitability/capability using fuzzy evaluation". *GeoJournal*, vol. 79, pp. 167-182, 2014.
- [25] R. Krishner. "The earth's elements". *Scientific American*, vol. 271, pp. 58-65, 1994.
- [26] J. Chen, Z. Chen, Y. Ai, J. Xiao, D. Pan, W. Li, Z. Huang and Y. Wang. "Impact of soil composition and electrochemistry on corrosion of rock-cut slope nets along railway lines in China". *Scientific Reports*, vol. 5, p. 14939, 2015.
- [27] S. G. Croll. "Surface roughness profile and its effect on coating adhesion and corrosion protection: A review". *Progress in Organic Coatings*, vol. 148, p. 105847, 2020.
- [28] J. A. Nathanson. "Air pollution: Effects, Causes, Definition, and Facts". Encyclopedia Britannica, United States. Available from: <https://www.britannica.com/science/air-pollution> [Last accessed on 2022 Dec 25].
- [29] M. Wasim and M. B. Djukic. "External corrosion of oil and gas pipelines: A review of failure mechanisms and predictive preventions". *Journal of Natural Gas Science and Engineering*, vol. 100, p. 104467, 2022.
- [30] T. H. Shabangu, A. A. Ponnle, K. B. Adedeji, B. T. Abe, P. A. Olubambi and A. A. Jimoh. "Effects of Soil Properties on Corrosion of Buried Steel Pipeline: A Case Study of Rand Water Pipeline, South Africa, Africon 2015, Addis Ababa, Ethiopia". pp. 1-5, 2015.
- [31] J. M. Race, S. J. Dawson, R. Krishnamurthy and S. Peet. "Pipeline Corrosion Management". 2023. Available from: <https://doi.org/www.rosen-group.com/global/solutions/services/pipeline-corrosion.html#:~:text=the%20main%20threat%20posed%20by%20corrosion%20is%20the> [Last accessed on 2023 Mar 25].
- [32] M. Sturm and C. Benson. "Scales of spatial heterogeneity for perennial and seasonal snow layers". *Annals of Glaciology*. vol. 38, pp. 253-260, 2004.
- [33] T. Olson. "The Science behind the Flint Water Crisis: Corrosion of Pipes, Erosion of Trust". The Conversation, Australia, 2016. Available from: <https://theconversation.com/the-science-behind-the-flint-water-crisis-corrosion-of-pipes-erosion-of-trust-53776> [Last accessed on 2023 Mar 20].
- [34] I. Alkindy. "Hydrologic Cycle: National Geographic Society". 2022. Available from: <https://www.nationalgeographic.org> [Last accessed on 2023 Mar 25].
- [35] Y. C. Ou, L. L. Tsai and H. H. Chen. "Cyclic performance of large-scale corroded reinforced concrete beams". *Earthquake Engineering and Structural Dynamics*, vol. 41, pp. 593-604, 2012.
- [36] M. Zinger. "Getting the Rust Out-Humidity and Corrosion". Latem Industries, Canada, 2017. Available from: <https://latem.com/blog/getting-the-rust-out-humidity-and-corrosion.htm> [Last accessed on 2023 Mar 23].
- [37] Yubi Steel. "23 Different Types of Corrosion: The Definitive Guide". 2021. Available from: <https://www.yubisteel.com/types-of-corrosion> [Last accessed on 2023 Mar 12].
- [38] N. Kumari and C. Mohan. "Basics of Clay Minerals and Their Characteristic Properties". IntechOpen, London, 2021.
- [39] F. I. Shalabi, I. Asi and H. Qasrawi. "Effect of by-product steel slag on the engineering properties of clay soils". *Journal of King Saud University: Engineering Sciences*, vol. 29, pp. 394-399, 2017.
- [40] K. Fortnum. "Where Does Clay Come From, Ceramic". 2022. Available from: <https://www.katherinefortnumceramics.com/post/where-does-clay-come-from#:~:text=It%20is%20made%20from%20minerals> [Last accessed on 2023 Apr 02].
- [41] I. Ahmada, M. Usmana, T. K. Zhaob, S. Qayuma, I. Mahmoodf, A. Mahmood, A. Diallog, C. Obayij, F. I. Ezemah and M. Maazah. "Bandgap engineering of TiO₂ nanoparticles through MeV Cu ions irradiation. *Arabian Journal of Chemistry*, vol. 13, pp.3344-3350, 2022.
- [42] L. D. Michaud. "Is Iron a Mineral or Rock, Mineral Processing and Metallurgy. 2017. Available from: <https://www.911metallurgist.com/blog/iron-mineral-rock> [Last accessed on 2023 Apr 02].
- [43] K. Xiao, Z. Li, J. Song, Z. Bai, W. Xue, J. Wu and C. Dong. "Effect of concentrations of Fe²⁺ and Fe³⁺ on the corrosion behavior of carbon steel in C₁⁻ and SO₄²⁻ aqueous environments". *Metals and Materials International*, vol. 27, pp. 2623-2633, 2020.
- [44] S. Haldar. "Exploration Geochemistry, in Mineral Exploration". Elsevier, Netherlands, pp. 55-71, 2013.
- [45] H. Chen, L. Zhaochong, L. Lu, Y. Huang and X. Li. "Correlation of micro-galvanic corrosion behavior with corrosion rate in the

- initial corrosion process of dual phase steel". *Journal of Materials Research and Technology*, vol. 15, pp. 3310-3320, 2021.
- [46] D. Dwivedi, K. Lepkova and T. Becker. "Carbon steel corrosion: A review of key surface properties and characterization methods". *RSC Advances*, vol. 7, pp. 4580-4610, 2017.
- [47] S. Sinha and G. Lotha. "Laterite: Geology". Encyclopedia Britannica, United States, 1998. Available from: <https://www.britannica.com/science/laterite> [Last accessed on 2023 Apr 05].
- [48] F. Abidin, A. H. G. Widowo, A. A. Ambari and S. Harjanto. "Electrochemical behavior of nickel laterite ores dissolution in sulphuric acid solutions". *IOP Conference Series Materials Science and Engineering*, vol. 833, no. 1, p. 012058, 2020.
- [49] B. Mahajan. "12 Types of Corrosion in Metal with Pictures: A Comprehensive Classification of Corrosion". Civiconcepts, 2023. Available from: <https://civiconcepts.com/blog/types-of-corrosion> [Last accessed on 2023 Apr 12].
- [50] B. Swint. "New Oil Pipeline Boosts Iraqi Kurdistan, the Region Made of three Northern Provinces, *Washington Post*". 2014. Available from: https://www.washingtonpost.com/business/new-oil-pipeline-boosts-iraqi-kurdistan-the-region-made-of-three-northern-provinces/2014/06/12/50635600-ef30-11e3-bf76-447a5df6411f_story.html [Last accessed on 2023 Jan 10].

Kurdish Sorani Dialect Morphology Generation Using a Concatenative Strategy



Kardo O. Aziz¹, Ramyar A. Teimoor², Tofiq A. Tofiq², Dilman S. Abdulla³

¹Department of Computer, College of Science, Chamro University, Iraq, ²Department of Computer, College of Science, University of Sulaimani, Sulaimanyah, Kurdistan Region, Iraq, ³Department of Computer, College of Science, University of Halabja, Halabja, Kurdistan Region, Iraq

ABSTRACT

In natural language processing, morphological generation refers to the creation of the appropriate inflected forms of words based on a predetermined set of morphological rules. However, it might be difficult to generate morphology in languages with intricate morphological systems, like the Kurdish Sorani dialect. The concatenative morphology-based unique technique to morphological generation in Kurdish Sorani is proposed in this research. The suggested strategy tries to get over the drawbacks of current approaches and enhance the precision and effectiveness of morphological generation in Kurdish Sorani. The suggested technique generates all conceivable subjective and objective pronouns in both positive and negative forms, together with the various verb tenses for Kurdish morphology. The study presents a detailed examination of Kurdish Sorani's morphology and points out the difficulties in coming up with the right verbforms. The authors suggest a concatenative morphology-based morphological generating system that comprises of a morphological analyzer and a morphological generator.

Index Terms: Low-resource-language, Kurdish-Sorani, NLP, Word-Generation, Morphology

1. INTRODUCTION

In the digital age, language technology is a growing subject that depends on our understanding of human language and computer techniques to handle it [1]. Even though for some languages, such as English, the field of text processing has been studied very well and many significant efforts can be seen, but for the Kurdish language, despite of having a great number of speakers and computer users, the amount of research in the subject of Kurdish text processing is still rather little [2]–[4].

The Kurdish language is a part of the Indo-Iranian family of Indo-European languages. It is a language spoken by Kurds

and Kurdish people in Kurdistan (also known as “the region of the Kurds”). The most closely related and more widely used language to Kurdish is Persian. There is not a particularly exact statistical survey for the number of native Kurdish speakers in the globe, although it is believed to be more than 45 million [5]. It has diverse dialects. Kurmanji and Sorani are the most frequently spoken dialects in terms of both speakers and degree of standardization [3]. It has limited resources, and the relevant research, information, and tools are still in their infancy [6].

Morphological generation is the process of generating different word forms based on their grammatical properties. In computational linguistics, morphological generation is an important part of natural language processing (NLP), as it enables machines to generate grammatically correct and natural-sounding text. There have been several approaches to morphological generation, including rule-based [4], [7], stochastic, and hybrid methods.

In the Kurdish language, the sheer number of changes that must be developed for Kurdish and Persian verbal

Access this article online

DOI: 10.21928/uhdjst.v8n1y2024.pp13-19

E-ISSN: 2521-4217

P-ISSN: 2521-4209

Copyright © 2024 Aziz, *et al.* This is an open access article distributed under the Creative Commons Attribution Non-Commercial No Derivatives License 4.0 (CC BY-NC-ND 4.0)

Corresponding author's e-mail: Ramyar A. Teimoor, Department of Computer, College of Science, University of Sulaimani, Sulaimanyah, Kurdistan Region, Iraq. ramyar.teimoor@univsul.edu.iq

Received: 14-10-2023

Accepted: 02-01-2024

Published: 10-01-2024

morphology is the main problem. Verbal stems have trilateral or quadrilateral origins (3 or 4 radicals). The conventional combination of root morphemes and vowel melodies forms the derivational foundation for stem construction. Roots, patterns, and stem production are referred to as interdigitation [4], [8].

It is a difficult undertaking to build NLP technology for Arabic and Kurdish. These languages have significant morphology and both derivational and inflectional forms [4], [9]. Furthermore, the complexity of Arabic and Kurdish morphology makes it challenging to analyze or create as a vital component of the whole simulation process. On the one hand, there are now many analysts working in the area of analyzing Kurdish morphemes, which has advanced considerably. These attempts can be seen in [1], [2], [6], [10]. These analyzers provide a variety of outcomes using various techniques. Despite their well-known limitations, they provide a trustworthy source for computational analysis, and in certain situations, even their shortcomings are seen to be beneficial. On the other hand, because of its widespread use in essential everyday applications like spell checking, word generation has also drawn a lot of interest [10]–[13].

In this work, we provide a computational technique that applies a special treatment to the creation of Kurdish morphology that is described in the methodology parts by separating the issue of infixation from other inflectional variations. Since short vowels and diacritical marks are pedagogically advantageous and can always be deleted before presentation, we design Kurdish verbs with them.

The remaining components of this study are listed below. In Section 2, we review the literature on morphological analyzers and stemmers in Kurdish, Arabic, and Persian Language. in Section 3. To assess the effectiveness of the model, categorization results are compared in Section with total accuracy in the fourth section, and the conclusions are in the fifth section.

2. RELATED WORK

There are other works that are connected to this effort, but the most of them are stemmers and word generators for the Arabic language and Persian. We looked at their methodology and developed a new one for our Kurdish Sorani dialect. Most of the related studies work on analyzing morphological tokens and attempt to eliminate the suffixes and prefixes,

while our work is the inverse of their work. We provide the root or the stem and try to append prefixes and suffixes to generate all variations of a single verb.

Ahmadi [4] provides a thorough description of Kurdish-Sorani morphological and morphological constructions in a formal way to tackle complex morphology of Sorani. Ahmadi has presented morphological word generation rules with most of the possibilities and provides a couple examples for each tense. Furthermore, Ahmadi claims that morphemes often have different phonological forms depending on the structure of the word and the surrounding morphemes. Sorani Kurdish clitics and affixes often exhibit allomorphy, that is having more than one single shape for the same morpheme. Ahmadi has done an extensive study on Kurdish Sorani Morphology, but since the study is just in theory and descriptive. Thus, they do not provide a program or system for practical and evaluation or for production. Thus, we exploit this issue and we reuse some of their written rules that is related to Kurdish verbs along with some improvements to create an automatic system to generate words from a list of Kurdish verbs

Naserzade *et al.* [14] offer a thorough morphological analyzer for Central Kurdish (CK) in this study. They initially put together and methodically classified a complete collection of the language's morphological and morphophonological rules, building on the few available literature. A generative lexicon with almost 10,000 verbs, nouns, adjectives, named entity, and other forms of word stem stems was also compiled and carefully categorized. They implemented the CKMorph Analyzer based on finite-state transducers using these rule sets and resources. They gathered test sets for assessing the analyzer's correctness and coverage, personally labeled them, and made them available for public use as a baseline for future study. About 95.9% of the 1000 CK words in the first test set, which CKMorph assessed morphologically and contextually, were properly analyzed. Furthermore, of the 4.22M CK tokens in the second test set, 95.5% were subject to at least one analysis from CKMorph. Their work is almost the inverse of our work. While we work on generating morphological words, specifically verbs, they analyze those morphological words and label each part or section of each word.

Another study which is Saeed *et al.* [15], they study morphological tokens in Kurdish and remove suffixes and prefixes to get the original word or verb that created the word on. Thus, the work uses pre-created tokens which have many prefixes and suffixes. The goal of this study is to develop a method for classifying Kurdish using Reber Stemmer. As a result, a novel method is being researched to get the stem

of Kurdish words by eliminating their longest suffixes and prefixes. This method has a strong capacity and satisfies the criteria when it comes to the process of getting the stem of Kurdish words by removing as many of the necessary affixes as feasible. This stemmer's benefit is that it disregards the list of affixes in the right stem ordering for multiple words with the same format. The eight-class KDC-4007 dataset is used to apply the stemming approach. The categorization is performed using the Support Vector Machine (SVM) and Decision Tree (DT or C 4.5). The Longest-Match stemmer approach has been effectively compared with this stemmer. The F-measure of the Reber stemmer and Longest-Match methods in SVM is greater than DT, the data show. Reber stemmer in SVM achieved higher F-measure for the classes (religion, sport, health, and education), whereas the remainder of the classes are lower in Longest-Match. Reber stemmer had a greater F-measure in DT for the courses (religion, sport, and art), but in the longest match, the rest of the classes had a lower F-measure. The intuition of our study came from this and similar papers. We looked into their dataset and found that most of the datasets that are used for stemming do not cover all the possible morphological words that could be created from a single stem. We believe that to trust a stemmer in real life, it should understand all the possible morphological words. We found that most of the missing cases were those morphological that appear least or not appear at all in the dataset.

Furthermore, Yoosofan *et al.* [16] state that the basic problem with generating non-concatenative languages such as Arabic verbal morphology is the large number of variants that must be generated. They compare Arabic and Persian Stemmers and the features in each language. One of the challenges for stemmers are the enormous variations of a single word.

Each word must be recognized and correctly stemmed by a stemmer. Regarding Arabic, the evolution and variations of these words provide the fundamental challenge to their derivation. When compared to Persian terms, Arabic words exhibit distinct derivational behavior morphologically. In addition, several of these Persian terms have distinctive qualities that allow us to separate them from Arabic counterparts. They have limited their derivation to a few common trilateral roots to get the right results. For Example, Information retrieval, text classification, text summarization, automated phrasal category recognition, translation studies, NLP, etc.

A very similar work which has done the same work as ours but for Arabic is Aqel *et al.* [11]. They have developed a method that will deliver almost all the words that can be

produced out of any submitted word. Their study will address the issue of whether or not derived and inflected words can both be formed using the same process. Furthermore, since morphology analyzes the word structure taking into consideration its fundamental meaningful components, several suggestions for building the method described here are considered. It has consistently been one of the most crucial elements in almost every application of NLP. That idea was applied to Arabic, which resulted in heavily inflected and derived terms. In their work, a method is devised that yields nearly all of the words that may be generated from any given word.

TMT Sembok and Ata [17] show the importance of a good stemmer in information retrieval tools. They showed that a stemmer increases the effectiveness of retrieval systems. The results have demonstrated that retrieval effectiveness has increased when stemming is implemented because document retrieval in information retrieval systems (IRS) often comprises acquiring relevant documents related to information needs. The system's ability to understand document content will boost the efficacy of the retrieval results. However, it takes a lot of work to understand the subject. Both stemmed and unstamped keywords are available. When they stem and conflate keywords during the retrieval process, they improve the usage of semantic technology in IRS. In morphological analysis, which occurs before syntactic and semantic analysis in NLP, word stemming is a step.

In addition, Habash and Rambow [18] provide MAGEAD, a morphological analyzer and generator for Arabic language. Their research is groundbreaking since it specifically addresses the necessity for processing the languages' morphology. MAGEAD combines morphemes from several dialects and conducts an online analysis to or generation from a root+pattern+features representation. It also contains independent phonological and orthographic representations. They give MAGEAD a thorough analysis. MAGEAD has a very similar work to our study. They introduce a number of rules and a list of prefixes and suffixes that will possibly attach to a stem to generate morphological tokens.

3. METHODS

We started by collecting the verbs that we have in Kurdish language from academic and non-academic documents. Generating verbs for all of the tenses and persons including negative and positive tenses are all relays on the verbs' (base, and root). Verbs are chosen for this paper because the

Kurdish language has verbal incorporation features. Incorporation is a morphological process in which a verb is combined with another word, usually a noun or an adjective, to form a complex word that expresses a complete idea or sentence. In Kurdish language, as well as in other languages that use incorporation, the resulting word can act as a standalone sentence without the need for additional words or elements. For example, the word (“ناتاندەمی”/nætəndəmə/) means “I will not give it to you” in English and a whole sentence was required to express the same meaning. It contains the “I” and “you” pronouns, which can be replaced by other personal pronouns to change their meaning. In addition, the negative word is also included which can be removed to get a positive form of the word. Furthermore, prefixes, suffixes, or pronouns cannot be simply replaced or removed to change their meaning. In most cases, the entire sequence of prefixes, suffixes, and stemming is changed.

We have three types of verbs in Kurdish. Simple verbs have a single word and specific meaning (e.g., بردن/brdn/means “taking”). Compound verbs are created by combining an adjective or a noun with a simple verb (e.g., نارامگرتن/ər'ɑ:mgrtn/means being patient). Finally, Complex verbs, which created by add a prefix, or suffix to a simple verb [7], (e.g., تێکدان/tēkdən/means spoiling created by a prefix (no-meaning) + simple verb, بردنەو/brdnəw/created by a simple verb + a suffix (هه) means to win).

For each of these verbs, we manually found their bases (i.e., past stem) and roots (i.e., present roots), because each verb has a different structure it cannot be done by a program. All Kurdish verbs(Chawg) end with “ن/n/” letter hence, bases are created by dropping the “ن/n/” letter at the end. We replace it by an underscore. Regarding their roots, most of the verbs have different roots for past and present depending on the verb. Thus, we have multiple roots for each verb. Sometimes the verb has a root which is very far from the verb in terms of writings. We place an underscore in the places which have the possibility of adding prefix or suffix or affix.

Examples of bases are shown in Table 1.

Examples of roots are shown in Table 2.

These underscores will be replaced by pronouns and/or negation words or a special letter based on the tense and person you want to generate.

In Kurdish, the verbs(infinitive) are ends with letter “ن” as we mentioned before and before the “ن” letter one of these

TABLE 1: bases example

Verb	Base (Past stem)
بردن	برد_
نارامگرتن	نارامگرت_
تێکدان	تێکدا_

TABLE 2: Root Example

Verb	Root1	Root2
بردن	به_	بر_
نارامگرتن	نارام_گر	نارام_گیر
تێکدان	تیک_ده	تیک_در

five letters are coming (“د/d/,” “ی/i/,” “ت/t/,” “و/w/,” “ئ/ə/”). Most of the times, these letters have effect on which modal prefix/postfixes will be used. For example, if it has “و” letter before the “ن” we cannot use “وو/u:ə/” because will make the generated word have three consecutive “و” letter which is not correct in Kurdish.

3.1. Verb Types

The verbs are divided into two types (intransitive and transitive). Intransitive verb is a verb that cannot take an object (e.g., هاتن means coming). Transitive verbs take an object (eg. شستن means washing). Each type has different rules for word generation and takes a different set of bound pronouns (BP) which is shown in Table 3. Each word is manually marked which set of BP accepts.

3.2. Tenses

Future sense is gained from context or by time expressions. While the present tense is formed by adding one of the modal prefix such as “ده” or “ته” before the root of the verb and a subjective bounding pronoun at the end (modal prefix + root + Subjective bound pronoun) example, (بردن, root: به_ present simple: دهبهم. While “ده” is the modal prefix and “م” is bound pronoun for me).

There are many past tenses in Kurdish language. All of them can be formed by adding subjective BP and/or modal prefixes.

3.3. Subjective BP

Pronouns for Past tenses Past tenses are using the following subject pronouns set for transitive and intransitive verbs, see Table 3.

Pronouns for Present tenses

Present tenses are using the following subjective bound set for both transitive and intransitive verbs, see Table 4.

TABLE 3: Past bound pronouns

Person Type	Transitive		Intransitive	
	Singular	Plural	Singular	Plural
1 st Person	م	مان	م	ین
2 nd person	ت	تان	یت	ن
3 rd person	ی	نای	None	ن

TABLE 4: Singular and plural example

Person Type	Singular	Plural
1 st Person	م	ین
2 nd person	ی/یت	ن
3 rd person	ئ/ئیت	ن

Negative tenses are created by adding one of these two modal prefixed (“نە”، “نا”) with wither past stem or roots [7]. The position of the prefix is varying based on the tense you want to generate. It will be mentioned in the Rules section.

3.4. Rules

Rules of generating verbs in Kurdish vary based on verb type, tense, and negativity, thus we have to check every verb we face and specify the properties and most importantly which tense we are generating.

For most of the tenses, we have a special modal prefix and/or suffix or postfix to represent that tense. For each verb type the position of the modal prefixed is different for example, In the simple verbs, the prefixes are going to the beginning of the past stem but in complex verbs the prefix goes after the first preposition. In compound verbs, the prefix goes after a pre-word which is usually a noun or an adjective attached to a verb to create the compound verb. Sometimes the verb has more than one pre-word or preposition, thus some of the prefixes will be placed after the first pre-word and some of them (such as negative words) placed after the last preposition.

We have written approximately 94 rules to create the words. Simple verbs have 12 rules, complex verbs have 36 rules. compound verbs have 34 rules. Finally, we have 12 rules for present tenses for all types of the verbs. We will not be able to write and explain each of the rules. We have shown some of the rules for each verb type below.

3.5. Simple Verbs

Simple past: $[Past\ stem][Subjective\ BP]$ (eg. بردم/brdm/ means I took)

Negative simple past: $[Negative\ word][Subjective\ BP][past\ stem]$ (eg. نەبەرد/nəbrd/ means I did not take)

Past continues: $[Modal\ Prefix][Subjective\ BP][Past\ stem]$ (eg. دەمانبرد/dəmənbrd/ means we were taking)

3.6. Complex Verbs

Simple past (transitive): $[1^{st}\ prefix][Subjective\ BP][other\ prefixes][past\ stem]$ (eg. رابەینا/rəməɛnə/ means I brought it up)

Simple past (intransitive): $[all\ prefixes][past\ stem][Subjective\ BP]$ (eg. رابەتم/rəhətm/ means I'm used to it)

Negative simple past (transitive): $[1^{st}\ prefix][Subjective\ BP][other\ prefix][negative\ word][past\ stem]$ (eg. رانەهینا/rəməɛnə/ I did not bring it up).

3.7. Compound Verbs

Past continues (transitive): $[1^{st}\ word\ of\ past\ stem][Subjective\ BP][negative\ word\ if\ negative][modal\ prefix\ “دە”/nə/\ or\ “ئە”/ə/][rest\ of\ the\ past\ stem]$ (eg. بەکارماندەهینا/bəkərmnəɛnə/ means We were using it)

past perfect (transitive): $[1^{st}\ word\ of\ past\ stem][Subjective\ BP][negative\ word\ if\ negative][rest\ of\ the\ root][modal\ postfix\ “وە”/wə/\ or\ “ووە”/u:ə/]$ (eg. بەکارمەیناوە/bəkərmhəɛnəwə/ means I have used it)

Care must be taken when a modal prefix is added to a verb, as they may generate invalid character sequences. For example, it is possible to make three consecutive identical characters appear when a specific modal prefix is added to a specific verb. In this case, one of these characters must be removed as three consecutive identical characters in Kurdish Sorani are not allowed.

Since we have identical subjective BP in the tables for past and present tenses, sometimes we get the same word for two different people. Just like in English “you” is used for second person singular and plural. To differentiate between them we need to put it into a sentence. We have a similar pronoun which is the letter “ن” which is used in the second person plural and third person plural. Thus, the number of generated words is not equal for all of the verbs.

There is another issue while generating words, which is having two consecutive vowel letters. In this case, based on Kurdish grammar rules and depending on which vowel letter is, we had to add an extra character in between the two consecutive characters.

Furthermore, the transitive verbs also accept pronouns as objects. Thus, possibly most of the time the verbs have the

pronoun attached to them. It means that it will make the process more difficult to figure out where to put the pronoun that acts as object. This will also make the rules more complicated. For example, if you want to say “They did not take me” in English, it will be “نهيانبردم/nehæjnbrdm/” in Kurdish. The “نه” in the beginning is the negation word. The “يان” that comes after means “they”. Then, the past stem comes. Finally, the “م” at the end of the word means “me”. The position of each of these words will vary a lot depending on the verb type, tense, and negation especially in compound and complex words. For example, if we remove the negation word “they took me” it will be “برديانم/brdiænnm/” in Kurdish. Note that the “يان/iæn/” pronoun went after the past stem before the subject pronoun of “م/m/”. More examples are shown in Table 5.

4. RESULTS AND CONTRIBUTION

An enormous number of Kurdish verbs (infinitive) are collected and marked with their properties, such as verb types (simple, complex, and compound). The verbs past stem, past root, and present roots are specified. The position of pronouns and negative words is marked by replacing an underscore. This underscore will help our next steps to find where exactly each modal prefix or pronoun will be placed. Each verb is verified by a Kurdish language specialist to make sure they are available and correct. Total number of verbs is 2463. The number of verbs based on their type is shown in Table 6.

TABLE 5: Present bound pronouns

Word	Negation word	Negation word removed
نهتدمکۆلی	نه	دتمکۆلی
نهتاندەتاشین	نه	دەتاندەتاشین
نایاندەجینەوه	نا	دەیاندەجینەوه

TABLE 6: Verbs example based on their types

Verb type	Transitive	Intransitive	Total
Simple	181	175	356
Compound	1362	247	1609
Complex	357	141	498
Total	1900	563	2463

TABLE 7: Generated word examples

Verb	Some examples of generated words
/dru: stkrdn/	دروستکردن، دروستکەر، دروستکردوونە
دروستکردن	دروستکرد، ... دروستکەرت،
/trsæn/ ترسان	دەترسام، ئەدەتر سابت، ئەدەتر سان
	ئەتر سابت، ئەتر سابتیت، ... ئەتر سبت

Some examples of the verbs are shown in Table 7.

Then, a list of rules is defined. These rules cover all the possible tenses and subject persons with both positive and negative tenses. Using these rules, a list of words for each verb is generated in Fig. 1. We have generated approximately 317 words per verb. These words represent the verb for a specific subject person and possible specific object person in different tenses. These words are all the possible appearances of the verb in any text. We have gathered around 781,862 words in total including verb gerunds and negatives.

These words will be a very helpful corpus for the next research project that works on NLP on Kurdish language. Furthermore, it will help with Kurdish spell error detection and checking systems. Researchers can have a ready to go dataset that includes all the Kurdish verbs in all different tenses and persons including negative tenses. Especially all the researches and papers on stemming can have a great dataset that can verify and train their model on. It can also be a great state-of-art dataset to compare their results on.

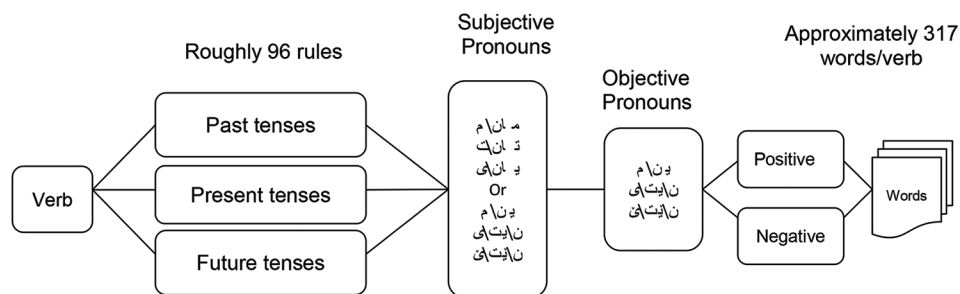


Fig. 1. The diagram of the process for the word generation.

List of the verbs that are generated in our work and the rules that we have used are available from this link in Excel format along with, all the words in this GitHub repository [19].

5. CONCLUSION

Our approach was motivated by helpful factors. We explored efficient methods to use a morphological generating tool, which is a common setting for us to construct automated translation systems and a stemmer. The number of rules for morphological transformation that must be followed. In this study, a technique that can create almost all the words from any input word was devised. After the word has been thoroughly examined, it will first be submitted, and its characteristics will be listed. Accordingly, depending on the appropriate affixes to the word supplied from the user, new inflected words are created utilizing the approach established and illustrated through this study. This study also addresses the issue, “Can inflected and derived words be created equally using the same methodology?” It was shown that, to do that, a different model based on the Root, Base and Patterns is needed as opposed to the one constructed based on the Stem and Affixes. We managed to build a large number of rules with specific suffixes and prefixes that can cover every tense, subject, and object pronouns with positive and negative states. We achieved 781,862 fully verified words that can be used for stemmers and translated. The word is publicly available for other researchers in an Excel file that mentioned in the end of the result section. For future research directions, we acknowledge that our algorithm exhibits certain complexities and could benefit from enhanced code reusability. We invite interested researchers to explore methods for reducing the number of rules and optimizing the reuse of existing ones to improve the algorithm’s speed and efficiency. In addition, although we have made a comprehensive effort to include a vast array of Kurdish verbs in our work, there remains scope for further verification and expansion. Future researchers may contribute by identifying and integrating additional Kurdish verbs that may have been overlooked in our current dataset.

REFERENCES

- [1] S. Ahmadi, “KLPT-Kurdish Language Processing Toolkit,” In: Proceedings of Second Workshop for NLP Open-Source Software (NLP-OSS), pp. 72-84.
- [2] S. Salavati and S. Ahmadi. “Building a lemmatizer and a spell-checker for Sorani Kurdish”. arXiv preprint, vol. 1809.10763 , p. 1, 2018.
- [3] D. Salih, “Kurdish Sorani Spelling Checker System,” [MA Thesis], University of Birmingham, England, 2016, 2021.
- [4] S. Ahmadi, “A formal description of Sorani Kurdish morphology”. ArXiv Preprint, vol. 2109.03942, p. 1, 2021.
- [5] F. I. Kurde de Paris. “The Kurdish Population”. 2017. Available from: <https://www.institutkurde.org/en/info/the-kurdish-population-1232551004> [Last accessed on 2023 Dec 24].
- [6] R. O. Abdulrahman and H. Hassani, “A Language Model for Spell Checking of Educational Texts in Kurdish (Sorani)”. In: Proceedings of the 1st Annual Meeting of the ELRA/ISCA Special Interest Group on Under-Resourced Languages, SIGUL 2022-Held in Conjunction with the International Conference on Language Resources and Evaluation, pp. 189-198, 2022.
- [7] H. Fatah and Z. Hamawand. “A prototype approach to Kurdish prefixes”. *International Journal on Studies in English Language and Literature*, vol. 2, pp. 37-49, 2014.
- [8] V. Cavalli-Sforza, A. Soudi, and T. Mitamura. “Arabic Morphology Generation using a Concatenative Strategy”. In: 1st Meet. North American Chapter of the Association for Computational Linguistics. NAACL 2000-co-Located with 6th Applying Natural Language Processing Conference, pp. 86-93, 2000.
- [9] R. A. Kareem. “The Syntax of Verbal Inflection in Central Kurdish”. Newcastle University, England, 2016. (Doctoral Dissertation).
- [10] S. Ahmadi. “Hunspell for Sorani Kurdish spell checking and morphological analysis”. Arxiv, vol. 2109.06374, p. 1, 2021.
- [11] A. Aqel, S. Alwadei and M. Dahab. “Building an Arabic words generator”. *International Journal of Computer Applications*, vol. 112, pp. 36-41, 2015.
- [12] D. H. Kim. “A Basic Guide to Kurdish Grammar”. Culture and Language Institute of Kurdi and Kori, Iraq, 2010.
- [13] G. Walther. “Fitting into morphological structure: Accounting for Sorani Kurdish endoclitics”. *Mediterranean Morphology Meetings*, vol. 8, pp. 299-321, 2012.
- [14] M. Naserzade, A. Mahmudi, H. Veisi, H. Hosseini, M. MohammadAmini. “CKMorph: A comprehensive morphological analyzer for Central Kurdish”. *International Journal of Digital Humanities*, vol. ???, pp. 1-46, 2023.
- [15] A. M. Saeed, T. A. Rashid, A. M. Mustafa and A. A. Agha. “An evaluation of Reber stemmer with longest match stemmer technique in Kurdish Sorani text classification. *Iran Journal of Computer Science*, vol. 1, no. 2, pp. 99-107, 2018.
- [16] A. Yoosofan, A. Rahimi, M. Rastgoo and M. M. Mojiri. “Automatic stemming of some Arabic words used in persian through morphological analysis without a dictionary”. *World Applied Sciences Journal*, vol. 8, no. 9, pp. 1078-1085, 2010.
- [17] T. M. T. Sembok and B. A. Ata. “Arabic word stemming algorithms and retrieval effectiveness”. *Lecture Notes in Engineering and Computer Science*, vol. 3, pp. 1577–1582, 2013.
- [18] N. Habash and O. Rambow. “MAGEAD: A morphological analyzer and generator for the Arabic dialects.” In: COLING/ACL 2006-21st International Conference on Computational Linguistics. 44th Annual Meeting of the Association for Computational Linguistics. vol. 1, pp. 681-688, 2006.
- [19] K. O. Aziz. “Kurdish-Morphological-Kurdish-Word, Rules and Source Code”. 2023. Available from: <https://github.com/kardoothman/kurdish-morphological-kurdish-word> [Last accessed on 2023 Feb 01].

Performance Evaluation using Spanning Tree Protocol, Rapid Spanning Tree Protocol, Per-VLAN Spanning Tree, and Multiple Spanning Tree



Rawyer Asaad Rashid¹, Dana Faiq Abd², Danyar Awat Othman¹, Hero Abdulqader¹

¹Department of Computer Science, University of Human Development, Sulaymaniyah, Kurdistan Region, Iraq

²Department of Information Technology, University of Human Development, Sulaymaniyah, Kurdistan Region, Iraq

ABSTRACT

This paper examines the concepts and practical applications of the spanning tree protocol (STP). It also covers per-VLAN spanning tree (PVST), multiple spanning tree (MST), and rapid STP (RSTP). Moreover, practical scenarios are presented to help the reader understand the concepts and implementations of these protocols. This study analyzes protocols using seven metrics. All protocols have been evaluated using these metrics in both small and big topology scenarios to obtain the best results. In addition, all metrics are mentioned in the introduction chapter, and the way used to apply tests on the metrics is described in the methodology chapter. Based on the experiments, different STPs performance are compared, including STP, RSTP, PVST, and MST. In summary, findings show that STP is easy to use and performs well overall, but it consistently has high latency issues. RSTP is suitable for small networks and has quick convergence, but it cannot handle as much load as STP. PVST performed the best in the experiments, as it demonstrated high scalability and the ability to handle a lot of pressure, although it requires strong hardware. However, MST did not perform as well as expected, as it struggled with delay problems and high jitter. In conclusion, it is recommended to use RSTP for simple networks that require fast convergence with dependable delay and capacity, or STP for networks that require good scaling and bandwidth. PVST is an excellent option for those who can afford high-performance hardware, while MST is suitable for simple networks or those with outdated hardware.

Index Terms: Spanning-Tree Protocol, Performance, Per-VLAN Spanning Tree, Rapid Spanning Tree Protocol, Multiple Spanning Tree, Convergence

1. INTRODUCTION

The second layer of the OSI model, known as the data link layer, encounters redundancy issues, notably the emergence of network loops when connecting numerous switches through

multiple paths. In addition, these challenges necessitate effective protocols to prevent loops and ensure the stability of switched networks. Moreover, the widely employed spanning tree protocol (STP) addresses this concern by implementing a spanning tree technique, eliminating loops within switches, and restoring broken links [1]. This protocol, specified in the IEEE 802.1D standard, designates a root switch and builds a topology tree to optimize the network's efficiency [2]. Finally, the root switch is chosen based on criteria such as the lowest MAC address or priority. STP ensures a loop-free topology by blocking certain links with higher path costs to the root switch [3]. Designated ports,

Access this article online

DOI: 10.21928/uhdjst.v8n1y2024.pp20-30

E-ISSN: 2521-4217

P-ISSN: 2521-4209

Copyright © 2024 Rashid, *et al.* This is an open access article distributed under the Creative Commons Attribution Non-Commercial No Derivatives License 4.0 (CC BY-NC-ND 4.0)

Corresponding author's e-mail: Rawyer Asaad Rashid, Department of Computer Science, University of Human Development, Sulaymaniyah, Kurdistan Region, Iraq. E-mail: rawyer.rashid@uhd.edu.iq

Received: 26-11-2023

Accepted: 06-01-2024

Published: 20-01-2024

root ports, and backup ports play crucial roles in determining the network's optimal configuration [4], [5]; moreover, to enhance the convergence speed of (STP), the rapid STP (RSTP) was introduced. In addition, this improved version combines several states of (STP) into a single discarding step [6], [7], significantly reducing convergence time to (30) to (50) seconds. Moreover, the port states in RSTP include disabled, blocking, listening, learning, and forwarding [2], [8]. Recognizing the limitations of a single instance (STP) for each VLAN, Cisco introduced the per-VLAN spanning tree (PVST) protocol. In addition, PVST operates as a distinct instance for each VLAN, addressing the challenge of slowed BPDU transmission [9]. Finally, the evolution of STP continues with the introduction of the multiple STP (MSTP), described in the 802.1S standard [10]. Moreover, MSTP incorporates features from both (RSTP) and VLAN protocols, reducing the number of instances and allowing for better scalability. MSTP introduces the concept of multiple spanning tree instances and regions to organize switches with similar configuration attributes [11], [12].

However, today's publications have a problem. They used only a few metrics to evaluate these protocols, similar to combining delay and convergence to evaluate a protocol. This paper attempts to assess each of the four approaches using around seven metrics. Moreover, these measurements' outputs allow for the determination of the optimal approach in every circumstance. Moreover, neither of the papers evaluated these four protocols together. The tests in this study will be STP, PVST, RSTP, and MSTP. Finally, this paper will evaluate the proposed protocols using key metrics for evaluation including:

- Performance: Measured by factors such as packet loss, jitter, bandwidth, delay, and reliability.
- Convergence: Examining STP's reaction to network changes by reconfiguring ports for forward or block states [5].
- Congestion: Assessing the capacity of links to handle data flow.
- Delay: Measuring the time frames or packets take to reach their destination [13].
- Bandwidth Utilization: Evaluating the rate at which data can flow.
- Reliability: Perform according to its specifications.
- Scalability: Ensuring flexibility for topology growth.

These metrics form the basis for a comprehensive evaluation of the protocols' effectiveness in real-world networking scenarios.

Besides, in the following sections will briefly discuss how each protocol is assessed. Moreover, the test parameters and outcomes

will be shown, also methods of measuring observations. Finally, discuss the conclusions made by the evaluators.

2. ILLUSTRATIONS OF STP, RSTP, PVST, AND MST

Figures illustrating protocols will be provided in this part so that their operation can be better understood. As can be seen, Fig. 1 (STP) represents the easiest design to comprehend and the one with the simplest loop. Finally, to shorten the path and obtain a free-loop design, one of the ports is being blocked.

Moreover, in Fig. 2, which depicts how (RSTP) operates, (RSTP) includes more ports, including backup and alternate ports. However, the concept behind STP remains the same, with the exception that RSTP converges more quickly. PVST, as depicted in Fig. 3. The root bridge for each VLAN can be a different switch. Every link is functional in PVST mode. According to VLAN 10, one of the links is blocked, in addition for VLAN 20, another link is blocked. The number (STP) instances are equal to the number of VLANs.

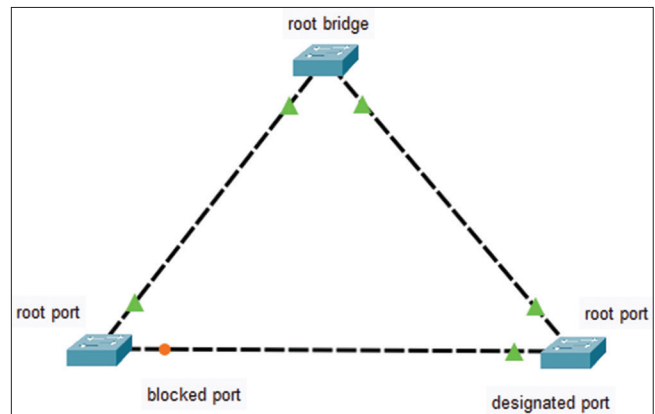


Fig. 1. An illustration of spanning tree protocol.

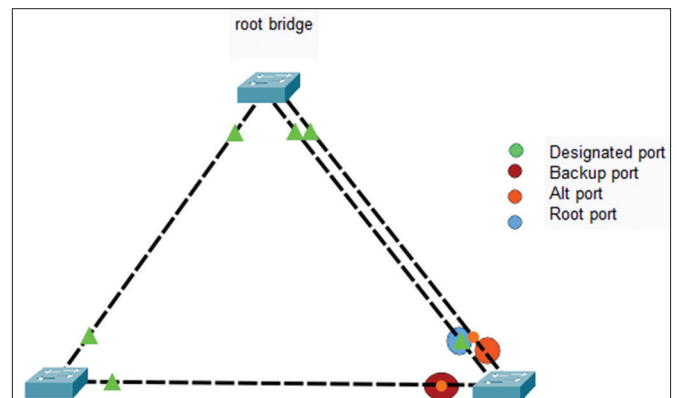


Fig. 2. An illustration of rapid spanning tree protocol.

A diagram of MST is shown in Fig. 4. Furthermore, it is well known that (MST) uses regions to divide switches with identical configurations. Moreover, the diagram makes it simple to see the regions. Those switches that have the same configurations will be in the same region.

3. LITERATURE REVIEW

The majority of papers discussing this topic only cover a small portion of the evaluation. However, the majority of the publications employed almost two evaluation protocols,

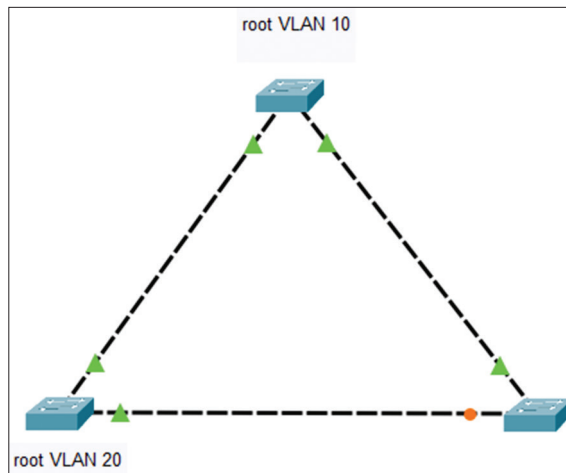


Fig. 3. An illustration of per-VLAN spanning tree.

or a limited set of metrics has been used for testing these protocols. This work attempts to assess seven metrics and four protocols using improved tools such as GNS3. Consequently, some of the papers cited in this work are old. Based on the findings of today's research, it can be stated that there are just a few different kinds of studies on the performance evaluation of free-loop algorithms. However, to describe the convergence time between (STP) and (RSTP), Sergio *et al.* (2018) conducted an environment using the (GNS3) tool. To calculate the topology's convergence time and connectivity loss, he needed a steady stream of data as can be seen in Tables 1 and 2.

In Sánchez-Herranz [14], moreover, according to Lapukhov *et al.* (2010), only under specific circumstances can (RSTP) convergence occur in less than one second, demonstrated by the tests in this paper, it cannot benefit from (RSTP's) fast convergence if the topology expands to include more than five bridges [15]. According to evaluations by Wang on various iterations of the STP protocol, PVST convergence is much slower than RSTP and MSTP, taking longer than 30 s as shown in Tables 3 and 4 [16].

In addition, ring topology and tree topology were the two different topologies that Pallos *et al.* (2007) tested (RSTP). Above all, this paper made use of the OPNET tool. The first ring implements topology. In addition, different versions are used to test (3, 4, 5, 6, and 7 bridges). The

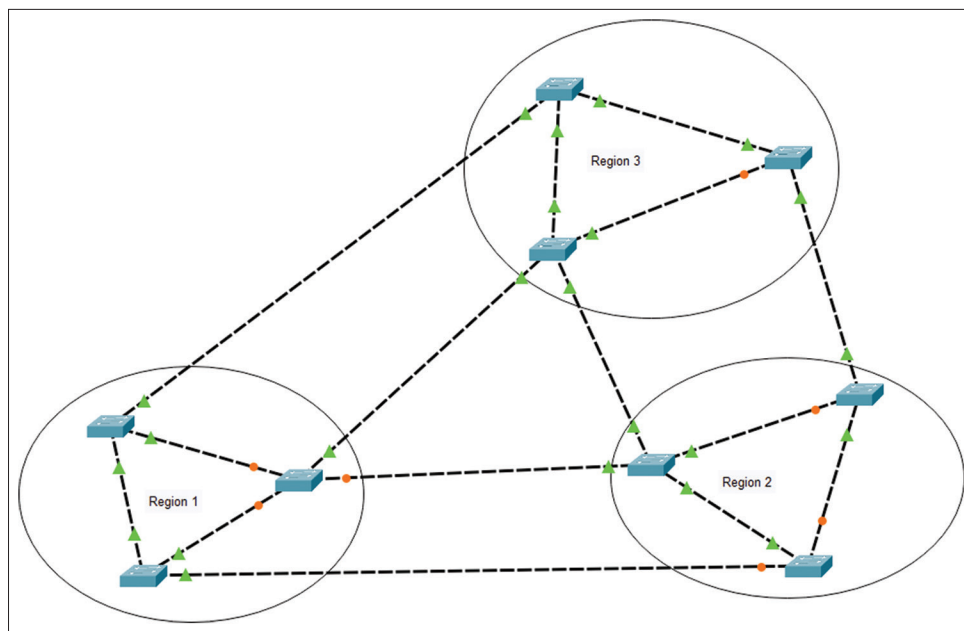


Fig. 4. An illustration of multiple spanning tree.

results demonstrate that the time for recovery increases as the number of bridges increases [17]. Moreover, according to Al-Balushi *et al.* (2012), PVST, MSTP, and RSTP are the STPs employed in this experiment. Data between an (FTP) server and a client on each (STP) mode is captured using a wire shark. The test results demonstrate that all modes may transfer data up to a maximum size of (700); however, (PVST) has captured fewer loops than (MSTP) and (RSTP). This study demonstrated that the optimal mode in terms of performance is PVST [18]. Both (RSTP) and (STP) were put to the test in various topologies by Amit noting that (STP) is more scalable and (RSTP) has a quicker convergence time but in smaller designs [19]. Furthermore, Abuguba *et al.* performed (RSTP) simulations on mesh and ring topologies

for networks with 3–30 nodes in various sizes. They found that when the number of nodes grew, message loops might also grow [20]. A work by Craiova *et al.* (2013) was released to speed up (MSTP) convergence. The configurations utilized to lower (MSTP) from 50 ms to 15 ms are as follows: Maximum age is (34); forward delay is (5), and hello timer is (4). They were able to accelerate (MSTP) and even (RSTP) convergence by using various configurations on various topologies. They only mentioned that the theoretical portion of the test was conducted; the practical portion was left out [5]. Farhan *et al.* (2019) employed a spanning tree in some cases to test load balancing on (SDN) networks. The final test, which looked at bandwidth utilization, indicated that there is not a significant difference between systems that use load balancing and those that do not. This research used common (STP) for layer-2 free loop architecture to test (SDN) with load balancing more efficiently [21]. In addition, Joseph *et al.* published a paper in 2013 about testing (STP) and (RSTP) with (OPNET) simulators. The results show that (STP) and (RSTP) both respond to connection failure in roughly 160 s, with (RSTP being somewhat faster). Furthermore, (303) seconds are required for recovery in (STP). In any case, there is not much of a difference between the two protocols. RSTP is faster, taking 3–5 s [8]. Chandan *et al.* (2014) used the port channel to implement several spanning tree research studies. The findings demonstrate that employing the port channel for (STP) has a significant impact on obtaining a faster convergence time from 56 s to around 5 s, as well as having a greater bandwidth of almost twice that of common (STP) with a single physical link as shown in Table 5.

Finally, Firmansyah *et al.* (2023), did a study on (STP) and (PVST) together using (Cisco packet tracer). For discovering convergence and overall network performance, the results show that (PVST) can provide faster convergence time and better load balancing. However, PVST needs more configuration and management compared to (STP) [23].

Above all, the main area of research right now is STP convergence. Although there are many crucial metrics to consider when assessing a network design, this paper will

TABLE 1: STP convergence time after connectivity loss

Test number	Time in second
1	44,33
2	42,92
3	47,02

From "Performance comparison of layer 2 convergence protocols. A SDN approach". STP: Spanning tree protocol

TABLE 2: RSTP convergence time after connectivity loss

Test number	Time in second
1	5.26
2	3.42
3	4.87

From "Performance comparison of layer 2 convergence protocols. A SDN approach". RSTP: Rapid spanning tree protocol

TABLE 3: MSTP convergence time

Test number	Time in second	Average
1	6.2	
2	5.7	
3	5.8	5.98
4	6.1	

From "Measurement of spanning tree performance between different protocols: Bachelor's Thesis". MSTP: Multiple spanning tree protocol

TABLE 4: RSTP convergence time

Test number	Time in second	average
1	4.3	
2	3.4	
3	4.1	4.0
3	4.3	

From "Measurement of Spanning Tree Performance Between Different Protocols: Bachelor's Thesis". RSTP: Rapid spanning tree protocol

TABLE 5: Port channel test on STP

Properties	STP with port channel	STP without port channel
Bandwidth	100 Mbps	200 Mbps
Convergence	5 s	56 s

From "Optimizing spanning tree protocol using port channel," [22]. STP: Spanning-tree protocol

examine overall (STP) modes with various topologies and determine which mode is operating most effectively in all circumstances.

4. METHODOLOGY

This study used (GNS3) tool and (vIOS2) ISO for layer-2 switches to evaluate protocols. Using the cloud built within the program and building a bridge out of (GNS3)'s (VM), the topology was connected to the internet. In addition, the connection was established to the actual network and used ping to send traffic to any DNS. Moreover, DHCP server is used to assign IP addresses to the devices. In addition, the techniques to be used to gauge the metrics during the tests must be mentioned. The decision was made by using advanced technology. Accurate data is required to make decisions. However, this cannot be obtained without a large data flow. IPERF tool is being used, which is employed to determine the network's maximum practicable bandwidth. Numerous protocols, including TCP, UDP, and SCTP with IPv4 and IPv6, are supported in IPERF tool. In addition, it returns the average of all parameters along with the bandwidth, loss, and jitter for each test. IPERF has been chosen, because it can be used as a server, a tool for creating load, and a tool for monitoring. Moreover, (IPERF) functions as the client and server idea. Once the (ISO) of (IPERF) has been imported into (GNS3), two (IPERF) devices are configured and connected to the network. As shown in the Fig. 5. It is effortless to put this into practice.

Above all, IP addresses are manually assigned to the IPERF devices after configuring the network. Although set up one of them to serve as a client and one as a server, the command to emulate a server on a device is (iperf3 -s) as shown in Fig. 6. The server then creates a port and is prepared to respond to requests.

Finally, on the client device, this command is used (iperf3 -c 192.168.1.2 -i 1 -t 30 -b 100m) as shown in Fig. 7.

(-c) denotes that this device is the client, and after that assign the server's IP address. (-i) used to receive information every second. The test's period, which in this test is 30 s, is determined by the value of (-t). The bandwidth is configured with (-b), which in this example is 100 Mb. The test's results are displayed in the Fig. 8.

In summary, the report informs that 107 Mbytes of data were transported during this test with an average

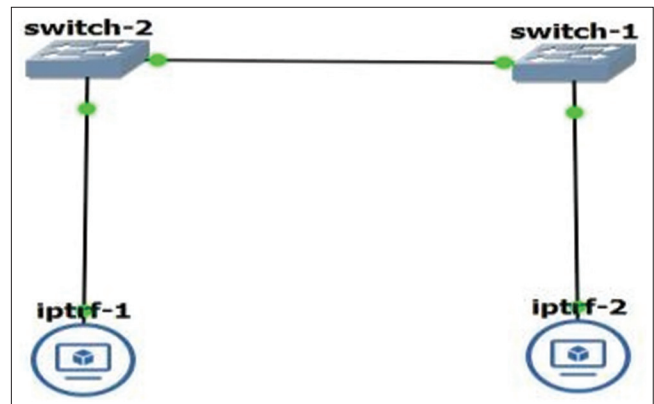


Fig. 5. Connecting IPERF servers to the network.

```
root@iperf-2:~# iperf3 -s
-----
Server Listening on 5201
-----
```

Fig. 6. iperf3 -s command for setting up the server and listening to requests.

```
root@iperf-1:~# iperf3 -c 192.168.1.2 -i 1 -t 30 -b 100m
```

Fig. 7. Command for sending packets to server from client.

bandwidth of roughly 30 Mbits/s. Because IPERF is a sophisticated tool, (-P) can send multiple client requests from various ports on the same IP. For instance, it is possible to assign (-P 10). As a result, when the test starts, the server receives requests for 10 separate devices. Moreover, using the (-u) command, which requests using (UDP) rather than (TCP), an even higher load can be created. As is well known, the network can experience a significant strain due to the use of UDP for streaming. Bandwidth, jitter, and loss on the networks can be assessed by employing (IPERF), which allows network performance decisions more effectively. Moreover, these indicators have an impact on output. In the following tests, data that are more accurate and realistic can be gathered through the utilization of appropriate methods. Finally, by evaluating the requests that fail to arrive at the desired location, other metrics, such as convergence, can be discovered. Ping command (which is a command used to ensure connectivity of two devices that use ICMP protocol) is being used with the (-t) flag to ping repeatedly see Fig. 9.

However, the average response time for a ping request is 1 s, within this time frame, there were six general failures

```

root@iptrf-1:~# iperf3 -c 192.168.1.2 -i 1 -t 30 -b 100m
Connecting to host 192.168.1.2, port 5201
[ 4] local 192.168.1.1 port 40456 connected to 192.168.1.2 port 5201
[ ID] Interval           Transfer     Bandwidth   Retr  Cwnd
[ 4]  0.00-1.00      sec    2.80 MBytes  23.4 Mbits/sec    0   144 KBytes
[ 4]  1.00-2.01      sec    4.75 MBytes  39.6 Mbits/sec   32   112 KBytes
[ 4]  2.01-3.01      sec    4.25 MBytes  35.8 Mbits/sec    2   97.6 KBytes
[ 4]  3.01-4.00      sec    4.50 MBytes  37.9 Mbits/sec    0   129 KBytes
[ 4]  4.00-5.01      sec    4.50 MBytes  37.5 Mbits/sec    3   115 KBytes
[ 4]  5.01-6.00      sec    4.38 MBytes  37.0 Mbits/sec    3   99.0 KBytes
[ 4]  6.00-10.57     sec    3.75 MBytes   6.88 Mbits/sec    0   123 KBytes
[ 4]  10.57-10.57    sec    0.00 Bytes    0.00 bits/sec    0   123 KBytes
[ 4]  10.57-10.57    sec    0.00 Bytes    0.00 bits/sec    0   123 KBytes
[ 4]  10.57-11.00    sec    1.75 MBytes  34.5 Mbits/sec    3   126 KBytes
[ 4]  11.00-12.00    sec    4.12 MBytes  34.5 Mbits/sec    0   122 KBytes
[ 4]  12.00-13.00    sec    4.00 MBytes  33.6 Mbits/sec    1   106 KBytes
[ 4]  13.00-14.00    sec    4.75 MBytes  39.9 Mbits/sec    2   93.3 KBytes
[ 4]  14.00-15.00    sec    4.00 MBytes  33.6 Mbits/sec    0   123 KBytes
[ 4]  15.00-16.00    sec    4.00 MBytes  33.5 Mbits/sec    1   107 KBytes
[ 4]  16.00-17.00    sec    3.25 MBytes  27.3 Mbits/sec    0   127 KBytes
[ 4]  17.00-18.00    sec    4.12 MBytes  34.6 Mbits/sec    3   113 KBytes
[ 4]  18.00-19.00    sec    4.25 MBytes  35.7 Mbits/sec    1   99.0 KBytes
[ 4]  19.00-20.00    sec    4.62 MBytes  38.8 Mbits/sec    0   130 KBytes
[ 4]  20.00-21.00    sec    3.88 MBytes  32.5 Mbits/sec    1   117 KBytes
[ 4]  21.00-22.00    sec    3.38 MBytes  28.3 Mbits/sec    0   137 KBytes
[ 4]  22.00-23.00    sec    3.75 MBytes  31.5 Mbits/sec    2   116 KBytes
[ 4]  23.00-24.00    sec    3.88 MBytes  32.4 Mbits/sec    1   102 KBytes
[ 4]  24.00-25.00    sec    3.12 MBytes  26.2 Mbits/sec    0   122 KBytes
[ 4]  25.00-26.00    sec    2.75 MBytes  23.1 Mbits/sec    1   105 KBytes
[ 4]  26.00-27.00    sec    4.12 MBytes  34.5 Mbits/sec    0   123 KBytes
[ 4]  27.00-28.00    sec    4.25 MBytes  35.7 Mbits/sec    1   110 KBytes
[ 4]  28.00-29.00    sec    5.50 MBytes  46.2 Mbits/sec    1   105 KBytes
[ 4]  29.00-30.00    sec    4.50 MBytes  37.7 Mbits/sec    0   133 KBytes
-----
[ ID] Interval           Transfer     Bandwidth   Retr
[ 4]  0.00-30.00      sec    107 MBytes  29.9 Mbits/sec   58
[ 4]  0.00-30.00      sec    106 MBytes  29.7 Mbits/sec
sender
receiver

```

Fig. 8. Results shown after a connection between IPEERF client and server happens.

```

C:\Users\Rawye>ping 8.8.8.8 -t

Pinging 8.8.8.8 with 32 bytes of data:
Reply from 8.8.8.8: bytes=32 time=196ms TTL=55
Reply from 8.8.8.8: bytes=32 time=108ms TTL=55
Reply from 8.8.8.8: bytes=32 time=185ms TTL=55
General failure.
General failure.
General failure.
General failure.
General failure.
General failure.
Reply from 8.8.8.8: bytes=32 time=70ms TTL=55
Reply from 8.8.8.8: bytes=32 time=120ms TTL=55
Reply from 8.8.8.8: bytes=32 time=66ms TTL=55
Reply from 8.8.8.8: bytes=32 time=63ms TTL=55
Reply from 8.8.8.8: bytes=32 time=60ms TTL=55

```

Fig. 9. Discovering convergence by calculating the time connection loss.

(requests timed out). It can be inferred from this that there was a disconnection from the internet for approximately 6 s. Convergence in STP is measured using the same methodology. The topology was manually adjusted and made a ping (-t), finally timed-out requests will be measured till the requests get a replay once more. No switch path requests were sent throughout the convergence period. This period occurred when STP rebuilt the topology (to put it simply, the internet ceased to function). To enable pinging and receive accurate data from the internet, DHCP is used to link the devices to the cloud and assign an IP address to them. Based on a comparison of the output from the small and big topologies, reliability and scalability must be determined. In addition, the final issue is congestion; a massive load must be created utilizing (UDP) and roughly 100 parallel networks. They are all making data requests at once.

5. EVALUATION

5.1. Test (STP)

Testing STP is the first test that is going to be done. Because the configuration of this protocol is the simplest. In addition, 50 parallel networks were employed. UDP protocol was used. A bandwidth of 1000 Mbits was requested for around 60 s. Moreover, to measure actual (delay) data, the network was connected to the cloud. Finally, another test was done by employing 100 parallel networks to create a massive load that lasted 100 s. In summary, (STP) can manage enormous amounts of data.

The small and large test topology is shown in Figs. 10 and 11 see Tables 6 and 7 for LAN characteristics.

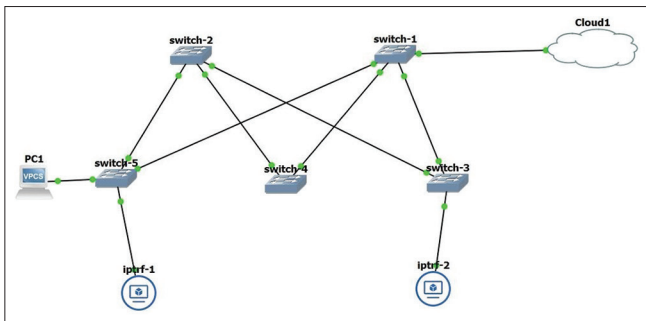


Fig. 10. Small topology.

The data measured on (STP) for both small and big topologies are shown in Table 8.

The chart demonstrates that (STP) can give an excellent result overall. The huge topology has reduced delay; 1-s change in convergence time is an excellent result. It scales very well. However, the jitter's output reveals that there has been a significant change. It is crucial to note how well 100 parallel networks performed on (STP). The only issue with (STP) is the delay and jitter, which for small networks is a little high at 146 ms.

5.2. Test (RSTP)

However, testing (RSTP) is the second test. The same (IPERF) parameters are used for (STP). Moreover, the test

TABLE 6: LAN characteristics of Figure 10

Device	LAN characteristics	Link capacity
lperfe-1	Ip: 192.168.1.1	Gigabit Ethernet
lperfe-2	Ip: 192.168.1.2	Gigabit Ethernet
PC1	DHCP	Gigabit Ethernet

TABLE 7: LAN characteristics of Figure 11

Device	LAN characteristics	Link capacity
lperfe-1	Ip: 192.168.1.1	Gigabit Ethernet
lperfe-2	Ip: 192.168.1.2	Gigabit Ethernet
PC1	DHCP	Gigabit Ethernet
PC2	DHCP	Gigabit Ethernet

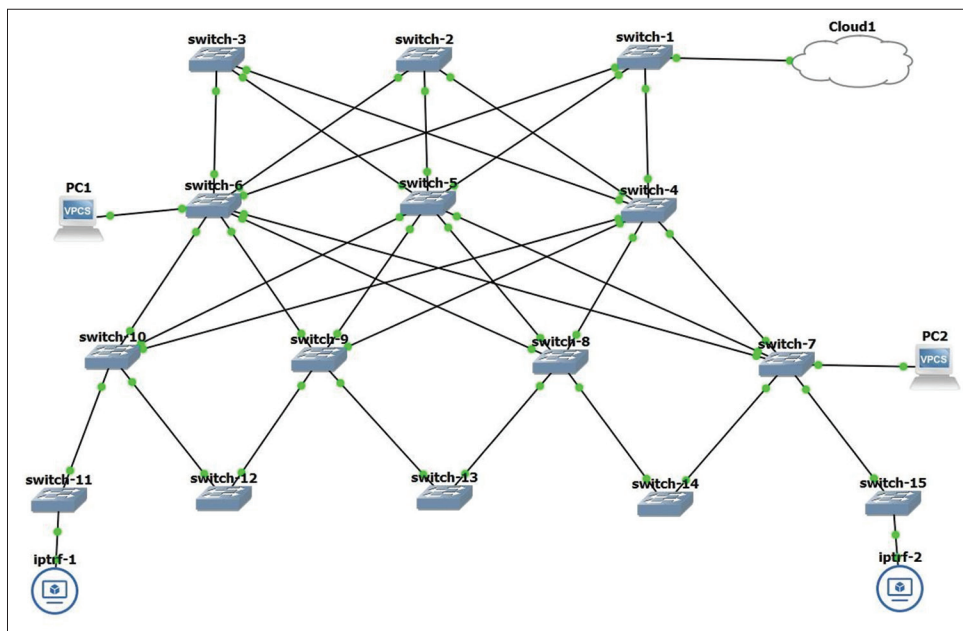


Fig. 11. Large topology.

will last 60 seconds. It has a combined bandwidth of 1000 Mbits and 50 parallel networks. Plus, the (UDP) protocol. First, the compact design was set with five switches and two (IPERF) components. In addition, the cloud-assisted in identifying (delays) in both topologies. Similar to (STP), 100 simultaneous networks are requested with a bandwidth of 1000 Mbits to detect congestion. The test was not finished since connection was lost on devices, in summary (RSTP) cannot handle that much demand because it has repeatedly lost connection.

The data measured on (RSTP) for both small and big topologies are shown in Table 9.

Table 9 shows that (RSTP) performs well in delay and convergence. However, for other metrics, such as jitter and congestion, it is arguable that (RSTP) cannot be relied on for large networks. Moreover, it can be beneficial for small networks that do not need to expand in the future. Another issue with RSTP is a connection loss, which caused it to repeatedly disconnect from the cloud while running the ping command (ping 8.8.8.8 -t). However, it did not

perform well in the congestion test. Finally, the small design transferred 143 Gigabytes of data. This amount is very good but not particularly useful due to connection loss issues.

5.3. Test (PVST)

First, PVST was set up by turning all links into trunks, except those that connected to end devices. Moreover, IPERF devices' IP addresses are assigned and configured. One of them is set to be the server and another as the client. As in STP and RSTP, the command (iperf3 -c 192.168.1.1 -I 1 -t 60 -u -b 1000m -P 50) is used.

The data measured on PVST for both small and big topologies are shown in Table 10.

These results indicate that (PVST) fared the best across all fields. Many metrics in the largetopology decreased, indicating that (PVST) has a very high degree of scalability. In summary, the delay decreased from 121 ms to 77 ms, and congestion decreased from 32 s to 26 s. Jitter increased by 1.642. Moreover, it operates best when all 100 networks are

TABLE 8: STP results

Metrics	Small topology	Large topology
Delay	146.875 MS	79.227 MS
Convergence	60 s	61 s
Reliability	Good	
Scalability	Very good	
Performance	Good	
Jitter	6.571 MS	11.738 MS
Loss	99.9915% of packets reached the destination (9819639/9820475)	99.9901% of packets reached the destination (10214613/10215625)
Congestion	Very good	
Bandwidth Utilization	127 Gigabytes transferred with an average bandwidth of 18.1 Gigabits/s*	128 Gigabytes transferred with an average bandwidth of 18.4 Gigabits/s

*50 parallel networks are used, when 18.1 is divided by 50, it gets the number of bits that y network used.

TABLE 9: RSTP results

Metrics	Small topology	Large topology
Delay	97.07 ms	88.57 ms
Convergence	19 s	23 s
Reliability	Bad (connection loss problem)	
Scalability	Bad	
Performance	Normal	
Jitter	3.844 ms	12.947 ms
Loss	99.9911% of packets reached the destination (11240599/11241598)	99.9889% of packets reached the destination (9326858/9327883)
Congestion	Very bad	
Bandwidth utilization	143 Gigabytes transferred with an average bandwidth of 20.4 Gigabits/s*	115 Gigabytes transferred with an average bandwidth of 16.4 Gigabits/s

STP: Spanning tree protocol

simultaneously requested. Given its excellent capabilities, PVST can be used for sophisticated designs and networks.

5.4. Test (MST)

In the beginning, the network was inaccessible even with switch configurations. However, MST test was conducted several times. This indicates that the network requires time

to prepare for use. The examination was extended for an additional 10–15 min. Moreover, the results of the mini and large tests are shown in Table 11. However, (delay) encountered difficulty during testing since the connection was repeatedly lost. In addition, the design went completely down while 50 parallel networks had been used. Finally, the test had to be stopped. In addition, 100 parallel requests using

TABLE 10: PVST results

Metrics	Small topology	Large topology
Delay	121.051 MS	77.214 MS
Convergence	32 s	26 s
Reliability	Very good	
Scalability	Very good	
Performance	Very good	
Jitter	6.873 MS	8.515 MS
Loss	99.9897% of packets reached the destination (10274683/10275735)	99.9910% of Packets reached the destination (10680190/10681153)
Congestion	Very good	
Bandwidth utilization	127 Gigabytes transferred with an average bandwidth of 18.1 Gigabits/s	132 Gigabytes of data transferred with an average bandwidth of 18.9 Gigabits/s

PVST: Per-VLAN spanning tree

TABLE 11: MST results

Metrics	Small topology	Large topology
Delay	143.98 ms	147.39 ms
Convergence	49 s	25 s
Reliability	Bad (good for simple topology)	
Scalability	Very bad	
Performance	Normal	
Jitter	12.424 ms	0.795 ms
Loss	99.9936% of packets reached the destination (14558717/14559654)	99.5300% of Packets reached the destination (555976/558612)
Congestion	Very bad (Gets down immediately)	
Bandwidth utilization	127 Gigabytes transferred with an average bandwidth of 18.1 Gigabits/s	6.97 Gigabytes of data transferred with an average. The bandwidth of 998 Megabits/s

MST: Multiple spanning tree

TABLE 12: STP, RSTP, PVST, and MST results

STP MODE	STP		RSTP		PVST		MST	
	Small	Large	Small	Large	Small	Large	Small	Large
Delay	146.875ms	79.227ms	97.07ms	88.57ms	121.051ms	77.214ms	143.98ms	147.39ms
Convergence	60s	61s	19s	23s	32s	26s	49s	25s
Reliability	Good		Bad		Very good		Bad	
Scalability	Very good		Bad		Very good		Very bad	
Performance	Good		Normal		Very good		Normal	
Jitter	6.571 ms	11.738 ms	3.844 ms	12.947 ms	6.873 ms	8.515 ms	12.424 ms	0.795 ms
Loss (% reached packets)	99.9915%	99.9901%	99.9911%	99.9889%	99.9897%	99.9897%	99.9936%	99.5300%
Congestion	Very good		Very bad		Very good		Very bad	
Bandwidth utilization	18.1 Gigabits/s	18.4 Gigabits/s	20.4 Gigabits/s	16.4 Gigabits/s	18.1 Gigabits/s	18.9 Gigabits/s	18.1 Gigabits/s	998 Megabits/s
Transferred (throughput)	127GB	128GB	143GB	115GB	127GB	132GB	127 GB	6.97 GB

STP: Spanning tree protocol, RSTP: Rapid spanning tree protocol, PVST: Per-VLAN spanning tree, MST: Multiple spanning tree

TCP were tested and there was no issue. In summary, UDP was used for MST with a single parallel network.

The data measured on MST for small and big topologies are shown in Table 11.

MSTs performance fell short of what was predicted in the other articles. It scales poorly and has a large delay. In addition, due to very poor congestion capacity, just one parallel network was used for all MST tests on big designs. However, using more than one network caused it to lose connectivity. The record for the worst outcome was broken by the jitter in the small network.

The data that were measured on (all modes) for both small and big topologies are shown in Table 12.

A comparison of all modes for all metrics with small and large design tests is shown in the table. According to the findings, PVST can be claimed to be in the top spot. As can be seen in the table, it had the best performance across all criteria. Moreover, STP and PVST worked best for congestion. Regarding the delay, RSTP comes in first for small topologies. Moreover, for large topologies, PVST comes in first. PVST or STP can be options if a network needs to be designed to be scalable. In addition, RSTP is recommended for throughput. However, due to the issue of connectivity loss, PVST can be helpful in that area. In terms of packet loss, all modes fared the best. The best performance, according to the statistics in the table, belongs to PVST.

6. CONCLUSION

STP, MST, PVST, and RSTP examinations produced several significant conclusions. Above all, it was discovered that each of these protocols has distinct advantages and disadvantages and that the ideal protocol to use depends on the particular needs of the network. In summary, the test results show that STP is easy to use and achieves average or even good performance overall. However, it has an issue with delay, which consistently has a high latency. On the other hand, RSTP performs well on small networks and has quick convergence, which is a benefit, but it cannot support as much load as STP. In addition, PVST performed best in the experiments. It is notable from its outputs that it can withstand a lot of pressure and is quite scalable. The only issue with PVST is that it requires strong hardware. PVST is a good option if a very high-performance network design is needed. While MST is thought of as a fairly dependable way

of operating, but sadly, MST did not perform as well as it had anticipated. It cannot handle large amounts of data and has delay problems as well as very high jitter. Finally, while no mode is 100% flawless, it is suggestible to use (RSTP) if the network is simple and has fast convergence with dependable delay and capacity. Moreover, STP can be utilized if latency is not focused on. Because it can bear pressure during irregular times and is good at scaling and bandwidth. Finally, PVST can be chosen if pricey, cutting-edge hardware can be afforded. It is incredibly high-performance and capable and serves well in every area. MST applies to both simple networks and networks with outdated or subpar hardware that cannot execute at a high level of performance.

REFERENCES

- [1] I. A. Alimi. "Bandwidth management and loop prevention in redundant networks". *The American Journal of Medicine*, vol. 2, pp. 1-12, 2016.
- [2] M. S. Guragain. "Evaluating the Future of the Spanning Tree Protocol". Sybex, United States, 2016.
- [3] F. Shahriar and J. Fan. "Performance Analysis of FHRP in a VLAN Network with STP. In: *EEE 3rd International Conference on Electronics Technology (ICET), Chengdu, China*". 2020.
- [4] G. Mirjalily. "Balanced Spanning Tree Protocol in Hierarchical NextGen Ethernet Networks". Preprint, 2022.
- [5] R. Stanica and A. Informatics. "Improving network convergence with multiple spanning tree protocol". vol. 15, no. 1, CEAI, United States, pp. 79-87, 2013.
- [6] S. Kasu, L. Hash, J. Marsh and R. Bull. "Spanning Tree Protocol". State University of New York Polytechnic Institute, New York, 2015.
- [7] J. Maia, C. A. Severiano, F. G. Guimarães, C. L. Castro, A. Lemos, J. C. F. Galindo and M. Weiss. Evolving clustering algorithm based on a mixture of typicalities for stream data mining". *Future Generation Computer Systems*, vol. 106, pp. 672-684, 2020.
- [8] J. Lu, S. Jiang and T. Xiong. "Evaluation and Comparison of Spanning Tree Protocol and Rapid Spanning Tree Protocol on Cisco Switches via OPNET". ENSC 427: Communication Networks Report, 2013.
- [9] N. Al-Balushi, R. Al-Klabani and F. Hajmohideen. "Performance evaluation using STP across layer 2 VLANs". *International Journal of Communication and Networking System*, vol. 1, pp. 1-8, 2012.
- [10] S. Kasu, L. Hash, J. Marsh and R. Bull. "Spanning Tree Protocol". State University of New York Polytechnic Institute, New York, 2015.
- [11] A. de Sousa and G. Soares. "Improving Load Balance and Minimizing Service Disruption on Ethernet Networks with IEEE 802.1 S MSTP. In: *Workshop on IP QoS and Traffic Control*". pp. 25-35, 2007.
- [12] J. Chen, X. Zheng, L. Zhang, L. Peng and X. Liu. "MSTP protocol simulation experiment based on ENSP. *Journal of Physics: Conference Series*, vol. 1486, no. 7, p. 072029, 2020.
- [13] A. Agarwal. "Limits on Interconnection Network Performance. In: *IEEE Transactions on Parallel and Distributed Systems*". vol. 2, no. 4, pp. 398-412, 1991.
- [14] S. Sánchez Herranz. "Performance Comparison of Layer 2

- Convergence Protocols. A SDN Approach*". (Master's Thesis), 2018.
- [15] P. Lapukhov. "Understanding STP and RSTP Convergence". INE Blog Documents, 2010.
- [16] Z. Wang. "Measurement of Spanning Tree Performance between Different Protocols". (Bachelor's Thesis), 2014.
- [17] R. Pallos, J. Farkas, I. Moldován and C. Lukovszki. "Performance of Rapid Spanning Tree Protocol in Access and Metro Networks, In: 2007 Second International Conference on Access Networks and Workshops". IEEE, New Jersey, pp. 1-8, 2007.
- [18] N. Al-Balushi, R. Al-Klabani and F. Hajmohideen. "Performance evaluation using STP across layer 2 VLANs". *International Journal of Communication and Networking System*, vol. 1, pp. 1-8, 2012.
- [19] B. B. Amit Kumar. "Performance evaluation of spanning tree protocol and rapid spanning tree protocol in computer networks". *IJSRD - International Journal for Scientific Research and Development*, vol. 7, no. 6, pp.214-217, 2019.
- [20] S. Abuguba, I. Moldován and C. J. B. E. Lukovszki. "Verification of RSTP Convergence and Scalability by Measurements and Simulations, In: Proceedings Broad Band Europe 2006". CISCO, United States, 2006.
- [21] F. Chahlaoui, M. R. El-Fenni and H. Dahmouni. "Performance Analysis of Load Balancing Mechanisms in SDN Networks, In: Proceedings of the 2nd International Conference on Networking, Information Systems and Security", pp. 1-8, 2019.
- [22] Y. N. Krishnan, C. N. Bhagwat and A. P. Utpat. "Optimizing Spanning Tree Protocol Using the Port Channel, In: 2014 International Conference on Electronics and Communication Systems (ICECS)", IEEE, New Jersey, pp. 1-5, 2014.
- [23] F. Firmansyah, T. A. A. Sandi, A. Fauzi and R. S. Anwar. "Analisis performa redundancy link menggunakan metode spanning tree protocol dan per VLAN spanning tree". *Jurnal Infortech*, vol. 5, no. 1, pp. 47-52, 2023.

Assessment of Health-care Professional's Knowledge Regarding the Comorbidities of Vitamin D Deficiency and its Relationship with Uterine Fibroids



Bayan Omar Sharif¹, Syamnd Mirza Abdullah², Sarwar Arif Star³, Hadeel Abdulelah Ibrahim⁴, Hawar Mardan Muhammad⁵, Zhino Raouf Ali⁶, Hussein Mustafa Hamasalih⁷

¹Department of Scientific, College of Nursing, University of Sulaimani, Kurdistan Region, Iraq, ²Department of Information Technology, Koya Technical Institute, Erbil Polytechnique University, Erbil, Iraq, ³Department of Health and Molecular Biology, Kurdistan Institution for Strategic Studies and Scientific Research, Sulaimani, Kurdistan Region, Iraq, ⁴Department of Basic Science, College of Medicine, University of Sulaimani, Kurdistan Region, Iraq, ⁵Department of Hematology, Hiwa Hospital, Sulaimani, Kurdistan Region, Iraq, ⁶Health Development and Training Center, Sulaimani, Kurdistan Region, Iraq, ⁷Department of Nursing, Smart Private Hospital, Sulaimani, Kurdistan Region, Iraq

ABSTRACT

Vitamin D deficiency is a widespread global health issue, notably prevalent in the Middle East and more severe in women. Vitamin D deficiency increases the incidence of uterine fibroids in black and white women, the most frequent benign gynecologic malignancies. This study examined health-care providers' understanding of the relationship between vitamin D insufficiency and uterine fibroid at Sulaimani Hospitals in Kurdistan, Iraq. A quantitative design, cross-sectional-descriptive study (non-probability purposive sample) of 113 female nurses and gynecologists. Data were collected using a checklist through Google Forms. The results showed that the majority of the participants were nurses (88.5%), and the remaining (11.5%) were gynecologist. Two-thirds of them work in maternity teaching hospital while others work in smart hospitals and Faruq medical cities. The results revealed that the level of knowledge was significantly associated with the position of participants and level of education ($P < 0.05$). As well, the study demonstrated that the majority of the participants were not trained regarding uterine fibroid and vitamin D deficiency. The study concluded that nearly a quarter of the health-care professionals had a medium level of knowledge, while nearly a quarter (24.8%) of them had a high level of knowledge. The study recommended to the Ministry of Health giving opportunities to health-care professionals, especially nurses, to participate in training courses, workshops, and conferences regarding the relationship between vitamin D deficiency and uterine fibroid.

Index Terms: Assessment Knowledge, Nurses, Gynecologist, Maternity Teaching Hospital, Faruq Medical City, Smart Hospital, Uterine fibroid, Vitamin D Deficiency

1. INTRODUCTION

Vitamin D is crucial for calcium balance, metabolic functions, and immune system modulation. Its deficiency is associated

with an elevated risk of non-skeletal chronic diseases such as autoimmune conditions, cardiovascular issues, and certain cancers, emphasizing its pivotal role in overall health [1].

Results of a study indicated that elevated serum vitamin D levels are strongly linked to a reduced risk of uterine fibroids (UFs), offering a promising new option for clinical treatment [2].

Vitamin D is generated in the human skin by the photochemical conversion of 7-dehydrocholesterol to cholecalciferol

Access this article online

DOI: 10.21928/uhdjst.v8n1y2024.pp31-41 E-ISSN: 2521-4217
P-ISSN: 2521-4209

Copyright © 2024 Sharif, *et al.* This is an open access article distributed under the Creative Commons Attribution Non-Commercial No Derivatives License 4.0 (CC BY-NC-ND 4.0)

Corresponding author's e-mail: Bayan O. Sharif, Department of Scientific, College of Nursing, University of Sulaimani, Kurdistan Region, Iraq. omerbayan82@gmail.com

Received: 24-10-2023

Accepted: 07-01-2024

Published: 24-01-2024

(vitamin D₃). Subsequently, vitamin D₃ undergoes metabolism to form 25-hydroxyvitamin D (25(OH)D), the primary storage and circulating form. Further transformation to the hormonal form, 1,25-dihydroxyvitamin D, occurs through hepatic and renal enzymes [3].

The worldwide prevalence of vitamin D deficiency is currently characterized as an epidemic and a significant public health concern in numerous regions. Despite the sunny conditions in the Middle East, the region continues to grapple with a high incidence of hypovitaminosis D [4].

Dietary sources of vitamin D, like fatty fish and fortified dairy products, are limited. However, the human body can synthesize vitamin D through direct exposure to sunlight's ultraviolet B radiation on the skin [5].

The role of vitamin D in the biology and therapy of uterine fibroids has been well investigated [6].

A selective progesterone modulator has received approval for short-term therapy for addressing symptomatic fibroids [7].

The common symptoms associated with leiomyomas include menorrhagia, pelvic pain or pressure, and subfertility. These symptoms vary from one patient to another and do not necessarily correlate to the size of the fibroids. Abdominal-pelvic examination may be normal if the fibroids are small, but most patients with uterine fibroids are asymptomatic and require no treatment [8].

The purpose of this study was directed at:

1. Assess the socio-demographic characteristics of the study sample.
2. Assess the level of health-care professionals' knowledge regarding the relation between vitamin D deficiency and the occurrence of uterine fibroid in Sulaimani hospitals in the Kurdistan region of Iraq.
3. To detect an association between some socio-demographic data and the level of health-care professionals' knowledge regarding the relation between vitamin D deficiency and uterine fibroid.

2. PATIENTS AND METHODS

2.1. Study Design

A quantitative design, cross-sectional-descriptive study has been implemented to assess the health-care professionals' knowledge regarding the comorbidities of vitamin D deficiency and its relationship with several diseases, especially

uterine fibroids, in Sulaimani hospitals during the period of August 10–October 15, 2021.

2.2. Administrative Approvals

Approval letters were secured from the College of Nursing/ University of Sulaimani and the Sulaimani Directorate of Health for conducting the study at Maternity Hospital, Smart Hospital, Faruq Medical City, and Bakhshin Hospital (but Bakhshin Hospital rejected participation).

2.3. Setting of the Study

The study was conducted at Maternity Teaching Hospital, Smart Hospital, and Faruq Medical City. Maternity Teaching Hospital had three types of employment (governmental, voluntary, and contract) with a mix of institute- and university-graduated nurses. Smart Hospital and Faruq Medical City were private hospitals with contract employees.

2.4. Sample of the Study

A non-probability (purposive) sample included 113 female nurses and gynecologists working in obstetric and gynecological wards.

2.5. Inclusion and Exclusion Criteria

Inclusion criteria covered all female nurses and gynecologists with all educational levels and employment types, while exclusion criteria comprised health-care providers who refused to participate, male nurses, and all doctors except gynecologists.

2.6. Study Instrument

A questionnaire, developed from a literature review, covered demographic information, questions about uterine fibroids, and vitamin D deficiency.

2.7. Validity

Content validity was established by eight experts who checked the questionnaire of this study and gave us their opinions, resulting in modifications for clarity and relevance. The final instrument was deemed valid for data collection.

2.8. Pilot Study

A pilot study was conducted with 20 health-care workers from the main study sample during the period of July 20 to August 1, 2021.

2.9. Reliability

The reliability of the knowledge determined regarding vitamin D deficiency and uterine fibroids was determined

through the use of the internal consistency (split-half) approach and the Cronbach Alpha Correlation Coefficient. Yielding a high correlation coefficient ($r = 0.81$).

2.10. Methods of Data Collection

The study selected all female nurses who work in Maternity Hospital and each department of obstetrics and gynecology in Faroq and Smart hospital, but only 113 nurses and gynecologists agreed to participate in our study. Data were collected through a Google Form sent to participants via head nurses in their respective hospitals. The collection period started from August 10 to October 15, 2021. The questionnaire, covering demographic data and knowledge about deficiency of vitamin D and uterine fibroids from health-care professionals, took approximately 10–15 min per participant. The study included 113 health-care professionals due to non-participation and dropouts several health-care professionals.

2.11. Statistical Analysis

The data were organized and coded into computer files using the statistical package of social science (SPSS), version 26. The data were performed through the computation of frequency and percentage, inferential data analysis, and the Chi-square test. The P -value is considered to be high-significant ($P < 0.01$), significant ($P < 0.05$), or non-significant ($P > 0.05$).

3. RESULTS

Table 1 revealed that all participants (100%) were female; their mean age was 32 ± 65.3 . Nearly most of the participants in the current study were nurses (88.5%), and the remaining (11.5%) were gynecologists. More than three-quarters of them worked in the Maternity Teaching Hospital (77%) while 11.9% and 7.1% worked in Smart Hospital and Faroq Medical City, respectively. 56.7% of them had more than 5 years of experience at the hospital, and 93% and 94.7% of them did not train regarding uterine fibroid and vitamin D deficiency, respectively.

Table 2 demonstrated that more than half of the participants chose the correct answer in items 1, 7, and 8, while less than half chose the false answer in all other items, but more than half did not know the answer in items 4, 5, and 6.

Table 3 showed that more than half answered correctly in item 1, while only 15.9% (11%) answered correctly in items 4 and 6, which are negative questions. Only 58.4% (69.9%) of them chose the correct answer in items 2 and 9, respectively.

Table 4 indicated that more than half of the participants chose the correct answer in items (1, 2, 3, 5.a., 5.b., 5.d., 5.e., 5.f.).

Table 5 demonstrated that more than half of the participants answered correctly on all items except item 8, which dealt with the fact that uterine fibroids do not interfere with ovulation but impair fertility.

Table 6 revealed that more than half of the participants chose the correct answer only in items 1.a., 1.I., and 4.a., and nearly a quarter of them chose the false answer in items 1.b., 1.m., 1.n., and 2.

Figure 1 showed that nearly a quarter of the health-care professionals (74.3%) had a medium level of knowledge about uterine fibroid and vitamin D deficiency, while only 24.8% of them had a high level of knowledge.

Table 7 explores that the level of knowledge was significantly associated only with the position of participants and level of education, at $P < 0.05$.

4. DISCUSSION

The purpose of the present study is to analyze the health-care professionals about the association between uterine fibroid and vitamin D insufficiency in one government and two private hospitals in Sulaimani city. The great thing is that the current study is the first to analyze the health-care providers relating about uterine fibroid and vitamin D deficiency among Kurdish employees' women in the Kurdistan area of Iraq. A study by Guo *et al.* [2] demonstrated that a significant correlation has been established between a deficiency in vitamin D and the development of leiomyomas.

Therefore, administration of vitamin D3 may decrease the size of fibroids [9]. It seems that vitamin D supplementation is an effective strategy to treat it.

Regarding socio-demographic data, the current study showed that all participants were female. More than half of them were government employees, married, nearly half of them had (1-3) children, less than a quarter of them were gynecologists, and the majority of them were nurses' staff. Among this, nearly half of the nurses graduated from the Institute of Nursing, and more than half of them had more than five years of experience at the hospital. Nearly all of them lived in urban regions. Nearly all of them did not participate in training courses regarding uterine fibroid and vitamin D deficiency and their comorbidities.

TABLE 1: Socio-demographic data

Item	Classes	Frequency	Percentage
Gender	Female	113	100
Age	22–30	43	38
	31–41	36	32
	41–50	25	22
	Up to 51	9	8
	Level of education	Secondary School of Nursing	25
	Institute of Nursing	52	46
	College of Nursing	23	20.4
	Postgraduate (M.Sc. and Ph.D.)	13	11.5
Position	Nurse	100	88.5
	Gynecologist	13	11.5
Marital status	Single	26	23
	Separated	1	0.8
	Married	86	76.2
Number of children	Zero	34	30.1
	1–3	58	51.4
	4–5	20	17.7
	More than 5	1	0.8
Residential Area	Urban	110	97.4
	Sub-Urban	2	1.8
	Rural	1	0.8
Years of Employment	1985–1991	4	3.6
	1992–1997	11	9.8
	1998–2003	30	26.6
	2004–2009	27	23.8
	2010–2015	16	14.1
	2016–2021	25	22.1
Type of Employment	Contract employee	14	12.3
	Governmental employee	72	63.8
	Voluntary employee	27	23.9
Name of Hospital	Farq medical city	8	7.1
	Maternity hospital	87	77
	Smart hospital	18	15.9
	How many years do you work in this hospital?	<1 year	24
	1–5 years	25	22.1
	More than 5 years	64	56.7
Did you do a vitamin D investigation recently	Yes	64	56.7
	No	49	43.3
Number of training courses regarding uterine fibroids	No training	105	93
	1–3	7	6.2
	>3	1	0.8
Number of training courses regarding vitamin D deficiency	No training	107	94.7
	1	5	4.5
	20	1	0.8

TABLE 2: Some items regarding age, gender, obesity and uterine fibroid

No.	Items	True	False	I don't know
1.	The incidence of pathologically diagnosed fibroids increases with age	63 (55.8)	24 (21.2)	2 (23)
2.	Myomas occur rarely before puberty and their frequency decreases with menopause	46 (40.8)	32 (28.3)	35 (30.9)
3.	The rate of hospitalization for uterine leiomyomas increases by age	48 (42.4)	36 (31.9)	29 (25.7)
4.	The risk of developing a fibroid is few in white women than in black women.	22 (19.5)	26 (23)	65 (57.5)
5.	Black women are diagnosed earlier in life, fibroids in these women are often multiple, larger and cause more severe symptoms compared to other ethnic groups	26 (23)	21 (18.6)	66 (58.4)
6.	Black women are more than two times more likely to undergo a hysterectomy	23 (20.4)	25 (22.1)	65 (57.5)
7.	Genetic is one of predisposition to leiomyomas	94 (83.1)	4 (3.6)	15 (13.3)
8.	Reduced risk of uterine fibroids has been found in those women who lost weight	73 (64.6)	31 (27.5)	9 (7.9)
9.	Visceral fat is associated with the presence of uterine fibroids, while subcutaneous fat thickness was not significantly associated with it	54 (47.8)	30 (26.6)	29 (25.6)

TABLE 3: Some items regarding reproductive factors and uterine fibroid

No.	Items	True	False	I don't know
1.	Pregnancy (high parity) is a risk factor for developing uterine fibroids	24 (21.3)	75 (66.4)	14 (12.3)
2.	Breastfeeding has been found to have little to no influence on fibroid incidence	66 (58.4)	29 (25.7)	18 (15.9)
3.	There is an inverse association between early age at menarche and fibroid incidence.	33 (29.2)	26 (23)	54 (47.8)
4.	There is a strong relation between late age at menopause and risk for fibroids	38 (33.7)	18 (15.9)	57 (50.4)
5.	Progesterone acts primarily by increasing cell responsiveness to estrogen	23 (20.4)	20 (17.7)	70 (61.9)
6.	At the fibroid level, the number of progesterone receptors is elevated.	24 (21)	12 (11)	77 (68)
7.	Polycystic ovary syndrome is associated with a higher incidence of fibroids.	48 (42.5)	27 (23.9)	38 (33.6)
8.	Both in women receiving estrogens only and in those receiving combined therapy, a correlation with the growth of fibroids is shown.	33 (29.2)	13 (11.6)	67 (59.2)
9.	The use of oral contraceptives is the risk factor for the incidence of uterine leiomyoma	79 (69.9)	18 (15.9)	16 (14.2)
10.	Hyperinsulinemia may directly or indirectly influence the development of fibroids.	42 (37.1)	25 (22.1)	46 (40.8)

TABLE 4: Some items regarding the relation between lifestyle, diet and vitamin D

No.	Items	True	False	I don't know
1.	Vitamin D is a fat-soluble vitamin.	74 (65.4)	8 (7.1)	31 (27.5)
2.	Physical inactivity is involved in fibroids development and growth.	70 (61.9)	37 (32.8)	6 (5.3)
3.	Stress is involved in fibroids development and growth.	48 (42.5)	38 (33.6)	27 (23.9)
4.	Deprivation of some diets rich in vitamin D is involved in fibroids development and growth.	60 (53.1)	28 (24.8)	25 (22.1)
5.	These foods rich in vitamin D			
5.a	Fish oil liver	96 (85)	7 (6)	10 (9)
5.b	milk and egg	104 (92)	5 (4.5)	4 (3.5)
5.c	Some fish such as: salmon, sardine, and tuna.	95 (84)	9 (8)	9 (8)
5.d	Alcohol consumption	2 (1.8)	10 (88.5)	11 (9.7)
5.e	Caffeine consumption	1 (0.8)	108 (95.5)	4 (1.7)
6.	Childhood exposure to physical, sexual, and emotional abuse seems to increase leiomyoma risk.	19 (16.8)	56 (49.6)	38 (33.6)

TABLE 5: Some statements regarding signs and symptoms of uterine fibroid

No.	Items	True	False	I don't know
1.	Uterine fibroid is a benign tumor of the uterus	65 (57.6)	34 (30)	14 (12.4)
2.	The symptoms of fibroids are depending on the location of the fibroid	76 (67)	10 (9)	27 (24)
3.	The treatment of uterine fibroid is depending on the location of it.	81 (71.7)	11 (9.7)	21 (18.6)
4.	The main causes of uterine fibroids are unknown	82 (72.6)	18 (15.9)	13 (11.5)
5.	Most women who have uterine fibroids do not have any symptoms	72 (63.8)	31 (27.4)	10 (8.8)
6.	Fibroids that occur near the uterine lining can cause heavy or painful periods, longer periods, or spotting at other times.	97 (85.9)	1 (0.9)	15 (13.2)
7.	Large fibroids may cause pelvic pain and pressure on the bladder (causing frequent urination or blocking urination)	10 (89.4)	2 (1.8)	10 (8.8)
8.	Uterine fibroids do not interfere with ovulation but impair fertility	40 (35.4)	9 (7.9)	64 (56.7)

However, knowledge is indispensable for health-care professionals, as underscored in the influential study by Sharif *et al.* [10]. This research highlights the crucial role of knowledge, especially for nurses, who, being closest to patients, play a vital part in reducing stress and anxiety through education.

However, the importance of knowledge is described in many studies; one of them is the study of Sharif *et al.* [10], which mentioned that knowledge plays a crucial role for health-care professionals in general, especially for nurses, because the nurses are the nearest person for the patients

to teach them and decrease their stress and anxiety from their diseases.

Table 2 in the current findings revealed that more than half of the participants selected the correct answer (true) in items that deal with (genetic predisposition to leiomyomas, weight loss is associated with a decreased risk of uterine fibroids in women, and uterine fibroids are linked to visceral fat, but there's no significant association with subcutaneous fat thickness. On the other hand, the same table in the present study indicated that more than half of the participants did not know the answer to the items that were explained

TABLE 6: Some facts regarding deficiency, signs and symptoms and interaction of vitamin D with some medications

No.	Items	True	False	I don't know
1. Vitamin D deficiency can cause these diseases or conditions (frequency [%])				
1.a	Insufficient vitamin D, the intestine is unable to absorb calcium and phosphorus.	80 (70.8)	5 (4.4)	28 (24.8)
1.b	Associated with autoimmune diseases	54 (47.9)	24 (21.2)	35 (30.9)
1.c	Associated with multiple sclerosis	17 (15)	11 (9.8)	85 (75.2)
1.d	Associated with hypertension	22 (19.5)	45 (39.8)	46 (40.7)
1.e	Associated with cardiovascular diseases	29 (25.7)	40 (35.4)	(38.9)
1.f	Associated with cancer	21 (18.6)	41 (36.2)	51 (45.2)
1.g	Associated with type II diabetes mellitus	30 (26.6)	38 (33.6)	45 (39.8)
1.h	Bacterial vaginosis	17 (15)	54 (47.8)	42 (37.2)
1.i	Increased risk of respiratory infection for maternal health	22 (19.5)	38 (33.6)	53 (46.9)
1.j	Increased risk of asthma for maternal health	11 (9.8)	55 (48.6)	47 (41.6)
1.k	Increased risk of schizophrenia for maternal health	18 (15.9)	43 (38.1)	52 (46)
1.l	Associated with increased risks for osteomalacia and osteoporosis	104 (92.1)	0 (0)	9 (7.9)
1.m	May lead to miscarriage	49 (43.3)	27 (23.9)	37 (32.8)
1.n	Vitamin D deficiency influenced preeclampsia and gestational diabetes mellitus.	35 (30.9)	22 (19.5)	56 (49.6)
2.	Patients with vitamin D deficiency should receive oral vitamin D2, 50,000 IU/ week for 8 weeks	43 (38.1)	23 (20.3)	47 (41.6)
3. Signs and symptoms of vitamin D toxicity				
3.a	Nausea, vomiting	75 (66.3)	10 (8.9)	28 (24.8)
3.b	Pancreatitis	32 (28.3)	15 (13.2)	66 (58.5)
3.c	Vascular calcinosis	31 (27.4)	17 (15)	65 (57.6)
4. Interaction of vitamin D supplements with some medications				
4.a	Vitamin D supplements interact with cholesterol lowering statins such as atorvastatin	24 (21.2)	11 (9.8)	78 (69)
4.b	Vitamin D supplements do not work as well if taken high-dose vitamin D supplements, Thiazide diuretics	19 (16.8)	10 (8.9)	84 (74.3)
4.c	Could raise blood calcium level too high if taking vitamin D supplements and Steroids such as prednisone (Deltasone)	27 (23.9)	4 (3.5)	82 (72.6)

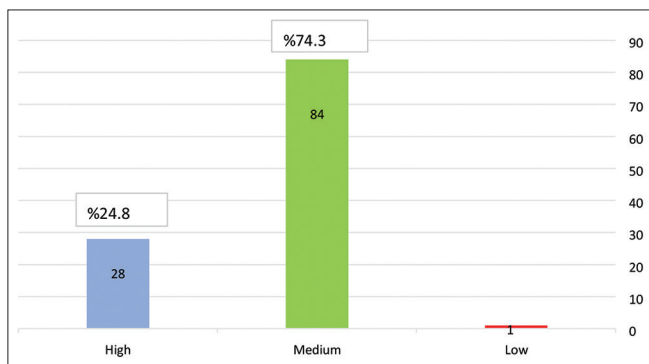


Fig. 1. Level of knowledge of the participants regarding uterine fibroid and vitamin D deficiency.

(fibroid risk is lower for white women compared to black women, black women are diagnosed with fibroids earlier, they often experience multiple, larger fibroids with more severe symptoms than other ethnic groups, and black women are over twice as likely to have a hysterectomy). Less than half of them chose the correct answer in the variables: myomas occur rarely before puberty, their frequency decreases with menopause, and the rate of hospitalization for uterine leiomyomas increases with age. Actually, women

of reproductive age have a considerably higher prevalence of uterine fibroids. This is owing to hormonal changes in females that lead to the tumor's origin. Estrogen and progesterone contribute to the progression and promotion of uterine fibroids [11]. It has increased with age during the reproductive years, reducing after menopause [12]. Especially, as noted, occur in black females [13]. Obesity is responsible for an increase in the conversion of adrenal androgens to estrogen and a lower hepatic synthesis of sex hormone-binding globulin, resulting in more unbound active estrogen. Thickness, or the expression of visceral fat, was connected with the existence of fibroids, but subcutaneous fat thickness was not substantially associated with the disease [14].

Regarding the items it deals with (there is a strong relationship between late age at menopause and risk for fibroids, and at the fibroid level, the number of progesterone receptors is elevated), less than a quarter replied properly, which is the (false) answer. More than half of them pick the correct answer in the items that are discussed (breastfeeding has been found to have little to no influence on fibroid incidence, and the use of oral contraceptives is the risk factor for the incidence of uterine leiomyoma). During the menopause

TABLE 7: Association between the level of knowledge and some socio-demographic data

Items	Classes	Knowledge level			Total	P-value
		High	Low	Medium		
Age	20–30	12	1	30	43	0.398
	31–40	12	0	23		
	41–50	6	0	20		
	>51	0	0	9		
	Total	30	1	82		
Level of education	Secondary School of Nursing	2	0	22	24	0.002
	Institute of Nursing	10	0	43		
	College of Nursing	11	1	11		
	Postgraduate (M.Sc. and Ph.D.)	7	0	6		
	Total	30	1	82		
Position	Nurse	23	0	77	100	0.001
	Gynecologist	7	1	5		
	Total	30	1	82		
Type of employment	Contract employee	4	0	10	14	0.151
	Voluntary	12	0	15		
	Government employee	14	1	57		
	Total	30	1	82		
Number of training courses regarding uterine fibroids	0	29	1	76	106	0.987
	1	1	0	4		
	2	0	0	1		
	>3	0	0	1		
	Total	30	1	82		
Number of training courses regarding vitamin D	0	28	1	73	102	0.944
	1	2	0	8		
	2	0	0	1		
	Total	30	1	82		

stage, the levels of key hormones are altered. For instance, follicle-stimulating hormone levels start to climb gradually, marking the end of reproductive years, whereas estrogen and progesterone gradually decrease [15]. According to a Chinese study by Ying *et al.* [16], which revealed that women of childbearing age with more than an equal body mass index and use of oral contraceptives are at risk of uterine leiomyoma.

Table 3 in the present study showed that less than half of the participants answered correctly regarding the items of polycystic ovary syndrome [PCOS] which is associated with a higher incidence of fibroids, both in women receiving estrogens only and in those receiving combined therapy. A correlation with the growth of fibroids is shown, but more than half of them answered correctly about the use of oral contraceptives as a risk factor for the incidence of uterine leiomyoma.

Low 25-hydroxyl vitamin D (25(OH)D) levels have been connected with endocrine disturbances in PCOS women. Moreover, vitamin D might alter the steroidogenesis of both estradiol and progesterone in healthy women, where low levels of 25(OH)D might be associated with infertility [17].

The usage of oral contraceptives and a body mass index $>25 \text{ kg/m}^2$ were the risk factors for the occurrence of uterine leiomyoma in Chinese women of reproductive age [16].

The outcomes of the current study showed that more than half of the participants chose the correct response regarding vitamin D in items that talk about (vitamin D is a fat-soluble vitamin, physical inactivity is involved in fibroids development and growth, deprivation of some diets rich in vitamin D is involved in fibroids development and growth, and foods rich with vitamin D such as fish oil, liver, milk, and eggs, some fish such as salmon, sardine, and tuna, alcohol consumption, and caffeine consumption. Whereas, less than half answered correctly concerning the involvement of stress in fibroids development and childhood exposure to physical, sexual, and emotional abuse). However, the incidence of clinical fibroids among premenopausal women is increasing due to the chronicity and severity of child and teenager physical and sexual abuse [18]. Although fewer than nearly half of them answered erroneously regarding this subject (49.6%).

Age is a crucial non-modifiable risk factor for fibroid development, with diagnoses peaking at 50 years. Myomas do not occur before puberty and decrease with menopause. The

development and growth of fibroids appear to be influenced by various modifiable risk factors, including physical inactivity, stress, and caffeine consumption. Regular exercise may protect against fibroids by lowering sex hormones, insulin, and circulating estrogen while increasing sex hormone-binding globulin levels. Women who exercise regularly have a lower risk of fibroids compared to those who don't. Stress is a potential factor in fibroids risk. Childhood abuse, including physical, sexual, and emotional abuse, increases leiomyoma risk, while supportive relationships can mitigate this. Stressful experiences are also linked to a higher body mass index and obesity [14]. Women 35 years of age in the highest risk categories of caffeinated coffee (≥ 3 cups/day) and caffeine intake (≥ 500 mg/day) were both associated with higher fibroid risk [19]. As well, a study found a positive link between event frequency and fibroid prevalence, especially in white women. Socioeconomic adjustments slightly reduced the effect. Stress intensity was correlated with fibroids in white women across all stress levels, compared to those without such experiences [20].

Concerning uterine fibroid, more than half of the participants accurately responded to variables regarding (uterine fibroid is a benign tumor of the uterus, the symptoms and treatment of fibroids are depending on the location of the fibroid, the main causes of uterine fibroids are unknown, most women who have uterine fibroids do not have any symptoms, fibroids that occur near the uterine lining can cause heavy or painful periods, longer periods, or spotting at other times, and large fibroids may cause pelvic pain and pressure on the bladder (causing frequent urination or blocking urination) but less than half of them were answered correctly regarding the item of (fibroids do not interfere with ovulation but impair fertility). The researchers returned this result to the lack of participation of health-care workers in training courses regarding uterine fibroid and vitamin D deficiency. As the current study detected, almost all of the participants did not participate in the training courses regarding vitamin D deficiency and uterine fibroid.

The present study revealed some diseases that are due to deficiency of vitamin D, such as lack of absorption of calcium and phosphorus by the intestine, autoimmune diseases, multiple sclerosis, hypertension, cardiovascular diseases, cancer, diabetes mellitus (DM), bacterial vaginosis, increased risk of respiratory infection, asthma, and schizophrenia for maternal health, osteomalacia and osteoporosis, miscarriage, preeclampsia, and gestational DM.

A study by Andersen *et al.* [21] demonstrated that there is a relationship between 25(OH)D and first-trimester

miscarriages, indicating vitamin D as a modifiable risk factor for abortion. A study indicated that vitamin D receptors are located in many different tissues, e.g., the brain, prostate, and immune system organs. Vitamin D is considered to lessen the risk of various chronic diseases, among them diabetes, cardiovascular diseases, and multiple sclerosis. Vitamin D has been proposed to reduce the incidence of breast, prostate, and colorectal cancers, presumably due to better regulation of cell differentiation, angiogenesis suppression, and apoptosis promotion [22].

Another study supported the idea that vitamin D is responsible for boosting intestinal absorption of calcium and phosphate, which is directly related to the preservation of the proper structure and function of the skeletal system. Vitamin D insufficiency is often linked to diabetes, cancer, and autoimmune illnesses [23]. Recently, vitamin D was suggested to prevent and treat autoimmune disorders such as rheumatoid arthritis, type 1 diabetes, and multiple sclerosis [24]. Vitamin D may inhibit uterine fibroid cells and reduce lesions, making it a potential anticancer agent. Vitamin D deficiency has been linked to uterine fibroids [25]. An observational British birth study found a linear connection between serum 25OHD content and a decreased risk of acute respiratory tract infection [26]. Many epidemiological studies link schizophrenia to vitamin D deficiency. In particular, two major studies linked infant vitamin D insufficiency to schizophrenia risk [27]. Vitamin D deficiency is linked to bacterial vaginosis and may explain its high racial inequality [28]. Preeclampsia women and their newborns had increased rates of 25(OH)D deficiency, while obesity did not affect levels. Obese pregnant women gave their fetuses less 25(OH)D [29]. The normal vitamin D range is 50–125 nmol/L [30]. The World Health Organization divided women into three groups based on 25-hydroxy vitamin D3 levels:

- Deficient vitamin D3: 25-hydroxy vitamin D3 < 10 ng/mL.
- Insufficient vitamin D3: 25-hydroxy vitamin D3 level 10–19.9 ng/mL.
- Vitamin D3: 25-hydroxy level ≥ 20 ng/mL: adequate [31]. Oral ergocalciferol (vitamin D2) at 50,000 IU/week for 2 months treats vitamin D insufficiency. After adjusting it, specialists recommended 800–1,000 IU of cholecalciferol (vitamin D3) from nutrition and supplements [32].

Regarding the signs and symptoms of vitamin D toxicity, which are nausea, vomiting, pancreatitis, and vascular calcinosis, more than half of the health-care professionals did not respond with the correct answers. Whereas hypercalcemia can cause acute pancreatitis if vitamin D levels

are too high [33]. Vitamin D intoxication causes nausea and vomiting [34]. Concerning the interaction of some drugs with vitamin D supplements, such as cholesterol-lowering agents such as atorvastatin, thiazide diuretics, and steroids such as prednisone, nearly three-quarters of them did not answer correctly. A study demonstrated that thiazide diuretics are used to treat blood pressure, edema, and kidney stones in hypercalciuria patients, but vitamin D supplementation may cause or worsen hypercalcemia. Prednisone, hydrocortisone, and dexamethasone are used for adrenal replacement, immunological suppression, and chemotherapy. Osteoporosis is a common corticosteroid side effect. Vitamin D metabolism changes may be a mechanism [35]. Activated and complicated, vascular calcification causes arterial and pulse wave velocity stiffness by depositing calcium in artery walls. Finally, cardiovascular illness diminishes artery elasticity and changes cardiovascular hemodynamic parameters, causing morbidity and mortality. End-stage arterial hypertension, cardiac hypertrophy, ischemic heart disease, or peripheral arterial disease dramatically increases mortality in people over 55. Calcium deposits in vessel walls are a major risk factor for severe ischemia episodes [36].

Concerning the level of knowledge of the participants regarding uterine fibroid and vitamin D deficiency, the present study showed that nearly a quarter of them had a high level of knowledge, while nearly three-quarters of them had a medium level of knowledge.

The findings were communicated to health-care professionals who did not actively participate in training courses regarding uterine fibroid and vitamin D deficiency. It's noteworthy that the predominant demographic in the data comprised nurses. However, around 25% of them had employment spans falling within the years 1998-2003, and over half had accumulated more than five years of experience in the department where they conducted vitamin D investigations.

Regarding the association between the level of knowledge and some socio-demographic data, there was no significant association between the level of knowledge and socio-demographic data except level of education and position of health-care professional (0.02, 0.02), respectively.

Nurses enhance medical teams by sharing information with patients, including discussions about expectations for quality of life. They must show understanding of patients' needs, communicate effectively using understandable language, and maintain awareness of boundaries in patient interactions [37]. The researchers identified a problem where health-care

professionals, lacking sufficient knowledge, faced challenges instructing and educating patients, resulting in complications for the patients. Therefore, this study suggests to the Ministry of Health in the Kurdistan Region of Iraq an increased focus on enhancing the scientific expertise of medical personnel. This can be achieved through their participation in training courses, seminars, workshops, and conferences, elevating their ability to provide practical and scientifically informed patient care.

5. CONCLUSION

In summary, the study showed that the risk of vitamin D deficiency leads to many comorbidities and diseases, including uterine fibroid. As well, the results of the current study indicated that nearly three-quarters of the participants had a medium level of knowledge and nearly a quarter of them had high-level knowledge, respectively, regarding the comorbidities of vitamin D deficiency and its relationship with uterine fibroids. And the level of their knowledge was only significantly associated with their position and level of education.

6. RECOMMENDATION

Health-care professionals need to participate in training courses, seminars, workshops, conferences, and booklets related to uterine fibroid and vitamin D deficiency in those hospitals that include obstetrics and gynecology departments. Collaboration is essential among health-care professionals, particularly gynecologists, who, due to their extensive knowledge and advanced studies, play a crucial role in partnering with other team members, including nurses.

7. ACKNOWLEDGMENT

The authors would like to deeply thank all participants who cooperated with this study, and the researchers would also like to deeply thank all head nurses in these three hospitals for their kind help and their facilities in achieving this study.

REFERENCES

- [1] B. Sheng, Y. Song, Y. Liu, C. Jiang and X. Zhu. "Association between vitamin D and uterine fibroids: A study protocol of an open-label, randomised controlled trial". *BMJ Open*, vol. 10, no. 11, p. e038709, 2020.
- [2] W. Guo, M. Dai, Z. Zhong, S. Zhu, G. Gong, M. Chen, J. Guo and Y. Zhang. "The association between vitamin D and uterine fibroids:

- A mendelian randomization study". *Frontiers in Genetics*, vol. 13, p. 1013192, 2022.
- [3] S. Christakos, D. V. Ajibade, P. Dhawan, A. J. Fechner and L. J. Mady. "Vitamin D: Metabolism". *Rheumatic Disease Clinics of North America*, vol. 38, no. 1, pp. 1-11, 2012.
- [4] M. Chakhtoura, M. Rahme, N. Chamoun and G. E. H. Fuleihan. "Vitamin D in the Middle East and North Africa". *Bone Reports*, vol. 8, pp. 135-146, 2018.
- [5] M. F. Holick. "Vitamin D deficiency". *The New England Journal of Medicine*, vol. 357, pp. 266-281, 2007.
- [6] M. Ciebiera, M. Włodarczyk, M. Ciebiera, K. Zaręba, K. Łukaszuk and G. Jakiel. "Vitamin D and uterine fibroids-review of the literature and novel concepts". *International Journal of Molecular Sciences*, vol. 19, p. 2051, 2018.
- [7] T. Kalampokas, M. Kamath, I. Boutas and E. Kalampokas. "Ulipristal acetate for uterine fibroids: A systematic review and meta-analysis". *Gynecological Endocrinology*, vol. 32, no. 2, pp. 91-96, 2016.
- [8] F. J. Oindiand and M. A. Mwaniki. "Uterine fibroids: Clinical presentation". In: *Leiomyoma*. IntechOpen, London, 2019.
- [9] M. Hajhashemi, M. Ansari, F. Haghollahi and B. Eslami. "The effect of vitamin D supplementation on the size of uterine leiomyoma in women with vitamin D deficiency". *Caspian Journal of Internal Medicine*, vol. 10, no. 2, p. 125, 2019.
- [10] B. O. Sharif, S. H. Sali, N. A. Sali and B. I. Salim. "Nurses' knowledge regarding cardiac catheterization at general hospital in Rania City". *Kurdistan Journal of Applied Research*, vol. 3, pp. 183-187, 2018.
- [11] E. A. Stewart, C. L. Cookson, R. A. Gandolfo and R. Schulze-Rath. "Epidemiology of uterine fibroids: A systematic review". *BJOG*, vol. 124, no. 10, pp. 1501-1512, 2017.
- [12] M. S. Drayer and W. H. Catherino. "Prevalence, morbidity, and current medical management of uterine leiomyomas". *International Journal of Gynecology and Obstetrics*, vol. 131, no. 2, pp. 117-122, 2015.
- [13] W. H. Catherino, H. M. Eltoukhi and A. Al-Hendy. "Racial and ethnic differences in the pathogenesis and clinical manifestations of uterine leiomyoma". *Seminars in Reproductive Medicine*, vol. 31, no. 5, pp. 370-379, 2013.
- [14] D. Pavone, S. Clemenza, F. Sorbi, M. Fambrini and F. Petraglia. "Epidemiology and risk factors of uterine fibroids". *Best Practice and Research Clinical Obstetrics and Gynaecology*, vol. 46, pp. 3-11, 2018.
- [15] J. L. Bacon. "The menopausal transition". *Obstetrics and Gynecology Clinics of North America*, vol. 44, no. 2, pp. 285-296, 2017.
- [16] J. Ying, D. Nie and S. Chen. "The relationship between the use of oral contraceptives and the risk of uterine leiomyoma in women of child bearing age of Han Chinese". *Pharmaceutical Bioprocessing*, vol. 6, pp. 48-52, 2018.
- [17] D. Al-Jaroudi, N. Al-Banyan, N. J. Aljohani, O. Kaddour and M. Al-Tannir. "Vitamin D deficiency among subfertile women: Case-control study". *Gynecological Endocrinology*, vol. 32, no. 4, pp. 272-275, 2016.
- [18] R. Boynton-Jarrett, J. W. Rich-Edwards, H. J. Jun, E. N. Hibert and R. J. Wright. "Abuse in childhood and risk of uterine leiomyoma: The role of emotional support in biological resiliency". *Epidemiology*, vol. 22, no. 1, pp. 6-14, 2011.
- [19] S. K. Laughlin, J. C. Schroeder and D. D. Baird. "New directions in the epidemiology of uterine fibroids". *Seminars in Reproductive Medicine*, vol. 28, no. 3, pp. 204-217, 2010.
- [20] A. I. Vines, M. Ta and D. A. Esserman. "The association between self-reported major life events and the presence of uterine fibroids". *Women's Health Issues*, vol. 20, no. 4, pp. 294-298, 2010.
- [21] L. B. Andersen, J. S. Jørgensen, T. K. Jensen, C. Dalgård, T. Barington, J. Nielsen, S. S. Beck-Nielsen, S. Husby, B. Abrahamsen, R. F. Lamont and H. T. Christesen. "Vitamin D insufficiency is associated with increased risk of first-trimester miscarriage in the Odense child cohort". *The American Journal of Clinical Nutrition*, vol. 102, no. 3, pp. 633-638, 2015.
- [22] K. F. Faridi, J. R. Lupton, S. S. Martin, M. Banach, R. Quispe, K. Kulkarni, S. R. Jones and E. D. Michos. "Vitamin D deficiency and non-lipid biomarkers of cardiovascular risk". *Archives of Medical Science*, vol. 13, no. 4, pp. 732-737, 2017.
- [23] P. Skowrońska, E. Pastuszek, W. Kuczyński, M. Jaszczol, P. Kuć, G. Jakiel, I. Woławek-Potocka and K. Łukaszuk. "The role of vitamin D in reproductive dysfunction in women-a systematic review". *Annals of Agricultural and Environmental Medicine*, vol. 23, no. 4, pp. 671-676, 2016.
- [24] B. M. Gruber-Bzura. "Vitamin D and influenza-prevention or therapy?" *International Journal of Molecular Sciences*, vol. 19, no. 8, p. 2419, 2018.
- [25] M. Ciebiera, M. Włodarczyk, A. Słabuszewska-Jóźwiak, G. Nowicka and G. Jakiel. "Influence of vitamin D and transforming growth factor β 3 serum concentrations, obesity, and family history on the risk for uterine fibroids". *Fertility and Sterility*, vol. 106, no. 7, pp. 1787-1792, 2016.
- [26] R. Bradley, J. Schloss, D. Brown, D. Celis, J. Finnell, R. Hedro, V. Honcharov, T. Pantuso, H. Peña, R. Lauche and A. Steel. "The effects of vitamin D on acute viral respiratory infections: A rapid review". *Advances in Integrative Medicine*, vol. 7, no. 4, pp. 192-202, 2020.
- [27] X. Cui, J. J. McGrath, T. H. Burne and D. W. Eyles. "Vitamin D and schizophrenia: 20 years on". *Molecular Psychiatry*, vol. 26, no. 7, pp. 2708-2720, 2021.
- [28] L. M. Bodnar, M. A. Krohn and H. N. Simhan. "Maternal vitamin D deficiency is associated with bacterial vaginosis in the first trimester of pregnancy". *The Journal of Nutrition*, vol. 139, no. 6, pp. 1157-1161, 2009.
- [29] P. Azize, F. Tahir and J. Kelsey. "Nurses' knowledge and role in the management of thalassemic patients in Sulaimania thalassemia center". *Iraqi National Journal of Nursing Specialties*, vol. 28, no. 2, pp. 59-70, 2015.
- [30] A. L. Harris. "Vitamin D deficiency and bacterial vaginosis in pregnancy". *Nursing for Women's Health*, vol. 15, no. 5, pp. 423-430, 2011.
- [31] S. W. Chang and H. C. Lee. "Vitamin D and health-the missing vitamin in humans". *Pediatrics and Neonatology*, vol. 60, no. 3, pp. 237-244, 2019.
- [32] P. Bordelon, M. V. Ghetu and R. C. Langan. "Recognition and management of vitamin D deficiency". *American Family Physician*, vol. 80, no. 8, pp. 841-846, 2009.
- [33] Z. Han, S. L. Margulies, D. Kurian and M. S. Elliott. "Vitamin D deficiency in patients with pancreatitis: Is vitamin D replacement?". *Pancreatic Disorders and Therapy*, vol. 6, p. 172, 2016.
- [34] T. Halder, R. Dastidar, S. Bhattacharya and D. Maji. "Prevalence of hashimoto's thyroiditis and its association with vitamin D deficiency in West Bengal, India". *British Journal of Medicine and Medical*

- Research*, vol. 12, pp. 1-10, 2016.
- [35] K. Robien, S. J. Oppeneer, J. A. Kelly and J. M. Hamilton-Reeves. "Drug-vitamin D interactions: A systematic review of the literature". *Nutrition in Clinical Practice*, vol. 28, no. 2, pp. 194-208, 2013.
- [36] A. Zittermann, S. S. Schleithoff and R. Koerfer. "Vitamin D and vascular calcification". *Current Opinion in Lipidology*, vol. 18, no. 1, pp. 41-46, 2007.
- [37] A. T. Khan, M. Shehmar and J. K. Gupta. "Uterine fibroids: Current perspectives". *International Journal of Women's Health*, vol. 6, pp. 95-114, 2014.

A New Approach for Software Cost Estimation with a Hybrid Tabu Search and Invasive Weed Optimization Algorithms



Hoshmen Murad Mohamedyusf¹, Hawar Othman Sharif², Mazen Ismaeel Ghareb³

¹Department of Plastic Arts, Halabja Fine Arts Institute, Halabja, Iraq, ²Department of Computer Science, College of Science, University of Sulaimani, Iraq, ³Department of Computer Science, College of Science and Technology, University of Human Development, Kurdistan Region, Iraq.

ABSTRACT

Due to the ever-increasing progress of software projects and their widespread impact on all industries, models must be designed and implemented to analyze and estimate costs and time. Until now, most of the software cost estimation (SCE) has been based on the analyst's experiences and similar projects and these models are often inaccurate and inappropriate. The project will not be finished in the specified time and will include additional costs. Algorithmic models such as COCOMO are not very accurate in SCE. They are linear and the appropriate value for effort factors is not considered. On the other hand, artificial intelligence models have made significant progress in the cost estimation modeling of software projects in the past three decades. These models determine the correct value for effort factors through iteration and training, providing a more accurate estimate compared to algorithmic models. This paper employs a hybrid model incorporating the Tabu Search (TS) algorithm and the Invasive Weed Optimization (IWO) algorithm for SCE. IWO algorithm solutions are improved using the TS algorithm. The NASA60, NASA63, NASA93, KEMERER, and MAXWELL datasets are used for the evaluation. The proposed model has been able to reduce the MMRE rate compared to the IWO algorithm and the TS algorithm. The proposed model on the NASA60, NASA63, NASA93, KEMERER, and MAXWELL datasets obtained values of MMRE of 15.43, 17.05, 28.75, 58.43, and 22.46, respectively.

Index Terms: COCOMO Model, Tabu Search Algorithm, Invasive Weed Optimization Algorithm, Software Cost Estimation, Optimization

1. INTRODUCTION

A more comprehensive examination of a project's viability and more effective management of the software development process enable development organizations to significantly reduce project risks [1], [2]. Possessing an accurate and reliable software cost estimation (SCE), especially at the beginning of software projects, is considered a crucial factor for project

success. The accurate estimation of the production SCE gives the project manager strong support for making different decisions during the software life cycle. The amount of time and effort required to develop a software project should also be known by analysts, designers, programming teams, and other software production forces [1], [3].

The project manager cannot estimate how much time, people, and other resources he will need to finish the project without a solid SCE. The project may face dangers if the diagnosis is incorrect, and it is impossible to gauge the likelihood of success [4]. Hence, metaheuristic algorithms have been employed in this article to meticulously examine the influential factors in SCE. These algorithms do not necessitate complex mathematical equations, and they

Access this article online

DOI: 10.21928/uhdjst.v8n1y2024.pp42-54

E-ISSN: 2521-4217

P-ISSN: 2521-4209

Copyright © 2024 Mohamedyusf, *et al.* This is an open access article distributed under the Creative Commons Attribution Non-Commercial No Derivatives License 4.0 (CC BY-NC-ND 4.0)

Corresponding author's e-mail: Hoshmen Murad Mohamedyusf, Department of Plastic Arts, Halabja Fine Arts Institute, Halabja, Iraq. hoshmandmorad@gmail.com

Received: 28-11-2023

Accepted: 07-01-2024

Published: 13-02-2024

address optimization problems without delving into the internal intricacies of the problem's performance [1]. These algorithms are computationally simple but powerful, and they are not limited by restrictive assumptions regarding the search space. A common approach that can be used in SCE is to use an optimal function along with an algorithmic method to find the values of the cost estimation factors that create the most optimality [29]. Still, when the dimensions of the problem become larger with the increase in the number of factors and response variables, algorithmic methods will be unable to find real solutions. Therefore, using a hybridization of Invasive Weed Optimization (IWO) [6] and Tabu Search (TS) [7] algorithms is a new methodology for optimizing SCE. Then, we will compare the effectiveness of IWO and TS algorithm with algorithmic models and we will present the best solution.

Accurate effort estimation significantly influences the outcome of software projects, determining their success or failure. Inaccurate estimations pose challenges for both companies and clients, with underestimations leading to projects exceeding planned budgets and overestimation resulting in resource wastage [8], [28]. Precision in effort estimation is crucial for risk assessment, resource allocation, and progress monitoring. Although preventing all risks in software development is often unattainable, our proposed effort estimation model can assist in mitigating risks associated with resource assignment and task scheduling. To address this issue, researchers, managers, and developers have explored various methods to enhance the accuracy of effort estimation during the early stages of software projects. For instance, managers can utilize the COCOMO model to predict the effort required at the medium level of software development. This ongoing estimation process contributes to minimizing the recurrence of risks in future endeavors.

During the past three decades, variations of methods such as COCOMO 81, COCOMO 2000, COCOMO I, and COCOMO II have been used to estimate software costs [9]. These methods are linear and do not have accurate and correct estimations. The SCE and its measurement are crucial for controlling costs in the software life cycle. One of the primary contributors to sharp increases in development and maintenance expenses is software effort estimation (SEE) (Araújo *et al.*, 2012). It is a factor that is less known in the development of software projects and cannot be easily identified or described. It is often ignored during the project planning process. In this paper, the hybridization of IWO and TS algorithms is employed to predict SCE. The margin of error can be minimized through precise measurement

and control of estimation factors. The level of collaboration needed to comprehend the program is often decided by SCE and SEE. The cost in the software development phase greatly affects the effort required to test and debug the program, modules, and subsystems. Therefore, it is necessary to provide an effective and correct model for SCE and SEE. These are the key contributions of this paper:

- In this paper, the main goal is to estimate the amount of effort factors using the hybrid model and reduce the amount of MMRE error. Usually, linear models such as COCOMO have a large amount of error and do not determine the value of the factors based on the size of the projects.
- Improvement of IWO algorithm solutions using the TS algorithm. The TS algorithm is designed to escape the trap in local optimization. It avoids recently visited solutions in the future by preserving memory (Tabu list) and leads to a more comprehensive exploration of the solution space.
- Use the TS algorithm to explore the search space and find the best answers, avoiding local optima.
- Evaluation of the hybrid model on five data sets (NASA60, NASA63, NASA93, KEMERER, and MAXWELL).

This paper's general organization is as follows: Section 2 reviews related works that use artificial intelligence algorithms in the field of SCE. The proposed model and its phases are explained in Section 3. The proposed model is assessed using various datasets in Section 4. In addition, Section 5 examines conclusions and future research.

2. RELATED WORKS

The SCE and SEE have been the subject of substantial research. Most of them done in this field have dealt with the impact of cost on software projects at the head of them is the quality and cost of the product. The attention of managers and engineers of software projects to the SCE is to control and predict the quality and productivity of the software. In this section, we discuss artificial intelligence techniques and algorithmic models that have tested and analyzed software projects. SCE and SEE models are proposed based on fuzzy C-means clustering and metaheuristic algorithms [1]. Compared to previous algorithms, the proposed algorithm has demonstrated superior results in cost prediction. The International Software Benchmarking Standards Group (ISBSG) dataset has been utilized for a linear regression model based on the criteria of relative error values [10]. The

ISBSG dataset includes 3042 software projects from different companies during the last 6 years. The correlation coefficient of factors in linear regression is calculated according to Eq. (1). In the Eq. (1), x is the independent variable, y is the dependent variable, ε is the partial error value, k is the number of variables, and α_0 and β are constant values. The act_i parameter is the actual value, est_i is the estimated value, n is the number of projects, and x is the pred value.

$$y = (\alpha_0 + \log(\prod_{i=1}^k x_i^{\alpha_i}) + \varepsilon)^\beta \quad (1)$$

$$MRE_i = \frac{|act_i - est_i|}{act_i} \times 100 \quad (2)$$

$$MMRE = \frac{1}{n} \sum_{i=1}^n MRE_i, i = 1, 2, \dots, n \quad (3)$$

$$PRED(x) = \frac{1}{n} \times \sum_{i=1}^n \begin{cases} 1, & \text{if } MRE \leq x \\ 0, & \text{otherwise} \end{cases} \quad (4)$$

In different implementations, the magnitude of relative error (MRE) has less error compared to the real data set. The optimization model of the artificial neural networks (ANN) and particle swarm optimization (PSO) derived from the optimization of the PSO and the ANN has been implemented on NASA93, COCOMO81, and MAXWELL datasets [11]. In this model, a PSO is used to train and test data in ANN. The results showed that the value of PRED (0.25) in the PSO-ANN has higher accuracy compared to other models. In addition, the classification and regression tree (CART) model is less accurate than the step-wise regression (SWR) model. Artificial bee colony (ABC)-ANN model derived from ABC algorithm and ANN has been implemented on COCOMO81, NASA93, and COCOMO_SDR datasets [12]. In the ABC-ANN model, the link function of the ABC algorithm is used to train and test the data in the ANN. The results showed that the relative error value in the ABC-ANN is less compared to COCOMO.

The hybrid chi-means model and PSO algorithm have been implemented on the COCOMO81 dataset [13]. K-means has been employed to cluster similar projects together, and the PSO algorithm has been utilized to determine effort factor values. Evaluation criteria include mean absolute relative error (MARE), variance accounted for (VAF), and variance absolute relative error (VARE). The results showed that the values of VAF, MARE, and VARE for the COCOMO model are 94.66, 17.35, and 3.72, respectively. For the Chi-means, the hybrid algorithm is equal to 95.47, 20.76, and 4.12,

respectively. Therefore, the accuracy of the hybrid algorithm is higher compared to COCOMO.

$$VAF = \left[1 - \frac{\text{var}(\text{actual}_{\text{effort}})}{\text{var}(\text{estimated}_{\text{effort}})} \right] \times 100 \quad (5)$$

$$MARE = \text{Mean} \left[\frac{\text{abs}(\text{actual}_{\text{effort}})}{\text{estimated}_{\text{effort}}} \right] \times 100 \quad (6)$$

$$VARE = \text{var} \left[\frac{\text{abs}(\text{actual}_{\text{effort}})}{\text{estimated}_{\text{effort}}} \right] \times 100 \quad (7)$$

The OCFWFLANN model is implemented by combining genetic algorithm and functional link ANN on the NASA93 dataset [14]. Genetic algorithm has been used to test and train data. The results showed that the OCFWFLANN model has a lower mean relative error value compared to functional link ANN models and SWR and CART models. In [27], a new model is implemented by hybridizing genetic algorithm and functional link ANN on the NASA93 dataset. The data have been trained and tested using a genetic algorithm. The results showed that the proposed model has a lower mean relative error value compared to functional link ANN models and SWR and CART models.

The multi-objective PSO (MPSO) model has been implemented on the COCOMO dataset [15]. This model has been utilized to determine the values of “a” and “b,” representing cost parameters. The initial stage yielded results with 20 projects, 100 iterations, and 50 particles. The second stage involved 21 projects, 100 iterations, and 50 particles. The results in the first stage showed that the MARE and PRED (0.25) in the COCOMO model are 16.13 and 20, respectively. And, in the MPSO model, it is equal to 9.01 and 24, respectively. In the second stage, the MARE and PRED (0.25) in the COCOMO model are 18.15 and 17, respectively. In the MPSO model, it is equal to 20.97 and 15, respectively.

The hybrid model of the TS algorithm and genetic algorithm has been implemented on NASA60, NASA63, and NASA93

datasets [16]. The data have been trained and tested using a genetic algorithm. The TS algorithm's factors have been optimized using a genetic algorithm. The results showed that the TS algorithm-genetic algorithm model has a lower error value compared to the genetic algorithm and the TS algorithm. A harmony search algorithm is implemented on the NASA93 dataset [17]. Finding appropriate effort factor values is the aim of the harmony search method. The proposed model's evaluation function has the same value as the MMRE. The number of program execution iterations is 5000 times. The results show that the harmony search algorithm has improved the MMRE by about 21% compared to COCOMO.

Genetic Algorithm – Bayesian Network and PSO Algorithm – Bayesian Network under Bayesian Belief Network are proposed for SCE [20]. The evaluation is done on the NASA63 data set with 15 effort factors. 40 and 20 projects have been used for training and testing data, respectively. The goal of genetic algorithm and PSO algorithm is to optimize the Bayesian belief network and reach the optimal value. The results showed that the average value of the relative error in the genetic algorithm – Bayesian network and PSO algorithm – probabilistic Bayesian network models is lower compared to COCOMO. Hybrid models of PSO algorithm – fuzzy clustering and PSO algorithm – learning automata have been proposed to estimate the SCE [18]. The evaluation is done on the NASA60 dataset. The learning automata model strategy provides the possibility for particles to achieve multiple local optima according to the reward criteria for the PSO algorithm. The trials' findings demonstrate that the hybrid model has a higher MMRE than the PSO algorithm – fuzzy clustering model.

SCE is simulated using linear regression techniques, ANN, support vector machine (SVM), and KNN [19]. The dependency of the effective qualities in SCE may be discovered using the linear regression model. The influencing elements of the hybrid model for estimation have been trained using both ant colony optimization (ACO) and the genetic test technique. Comparing the results to the COCOMO model, better outcomes have been achieved. One of the popular techniques in SCE is multi-layered ANN. The findings reveal that the multi-layer ANN has delivered a much better estimate than the COCOMO model in more than 90% of the situations. As a result, it can be said that algorithmic approaches are a strong complement to AI-based methods.

Machine learning techniques such as hybrid ANN, SVM, and genetic algorithm have been proposed for SCE [22].

Optimizing input data factors and optimizing the parameters of SVM and ANN methods are the two main goals of using genetic algorithms. *Desharnais*, NASA, COCOMO Albrecht, KEMERER, and *KotenGray* datasets are used for the evaluation. The hybrid models based on the genetic algorithm have improved significantly, according to the trials' findings across all data sets. In comparison to the SVM and multilayer ANN models, the criterion for assessing the MMRE in the hybrid models has a smaller error value. Also, the PRED criterion has higher accuracy in hybrid models. Detailed planning for the development of software projects increases efficiency and optimal use of resources and reduces time.

SCE has been analyzed using fuzzy functions. Methods employing triangular membership function, trapezoidal membership function, and Gaussian membership function have been utilized for evaluation on the NASA93 dataset [23]. The proposed method is combined with the COCOMO II model. COCOMO II model includes 17 effort factors and 5 scale factors. Evaluation and results are done on 10 projects from NASA93 dataset. The results of their experiments show that fuzzy methods have better accuracy in SCE and have a lower relative error value compared to the COCOMO II model. The combined genetic algorithm – radius function model has been proposed to estimate the cost of software projects [24]. The evaluation is done on the COCOMO81 dataset. The training and testing of the network data are considered equal to 80% and 20%, respectively. Genetic algorithm has been used to optimize the training and testing data of the basic radial function network. The results show that the average errors of relative error and mean square error in Kokomo model are equal to 2.92 and 0.0287, respectively. The average value of the relative error in the basic radial function model is equal to 0.4220 and 0.9665, respectively.

A hybrid model of genetic algorithm and fuzzy logic (GFUZZY) is presented for SCE [25]. Four hybrid data sets taken from NASA2 and COCOMO81 software projects have been used for evaluation. A new hybridization of multilayer ANN and COCOMO II has been proposed for SCE [26]. The test results demonstrate that the hybrid model is less inaccurate than the COCOMO II model. In comparison to the COCOMO II model, the COCOMO-multilayer ANN model exhibits two lower error values for the MMRE and PRED criteria. The MMRE on 63 projects using the COCOMOII model is equal to 0.58 and by the multi-layer ANN-COCOMO model is equal to 0.41. In Table 1, the models presented by researchers to SCE have been evaluated and compared.

3. PROPOSED MODEL

To SCE, the amount of effort factors should be determined based on the type of project in terms of degree, i.e., small, medium, and large. The effort aspects are highly crucial, and their quantity will determine the project’s success. Software projects necessitate the allocation of people, hardware, and software resources in production and development teams, contingent on the quantity of program code lines. If the amount of effort factors is too large, as a result, there is an incorrect estimate and the possibility of project failure due to high cost. If the amount of effort factors is too low, as a result, the project is not properly budgeted and it faces a lack of funds and is left half-finished. Therefore, the optimal value for them should be found. The best model for this is the use of metaheuristic algorithms. This algorithm can detect the optimal solution in difficult and sensitive conditions.

For some software projects, similar models and expert opinions are used, which is why the methods have two basic flaws. First, a lot of time may have been spent on

the previous project. Second, more modern tools such as advanced programming languages are used in new projects. In today’s programming languages, far fewer lines of code are required for software projects. In this article, the SCE is determined using a hybrid model utilizing the IWO and TS algorithms. NASA60, NASA63, NASA93, KEMERER, and MAXWELL datasets are used in the proposed model. The proposed model’s flowchart is displayed in Fig. 1.

The starting population in the proposed model is generated depending on the values of the effort components. To find the optimal value for the effort factors, the length of the vectors should be determined according to the software data set. For NASA60, we consider the length of vectors equal to 15 because it has 15 effort factors. We calculate the values found in the problem space in each vector and select the vector that has a minimum based on the average calculation. Other vectors for the next steps as optimal test points and their values are optimized by using different operators of the proposed model.

TABLE 1: Review of the models presented for SCE

References	Model	Data set	Function
[10]	LR	ISBSG	MRE, PRED (25)
[11]	PSO-ANN	COCOMO81, NASA93, and MAXWELL	PRED (0.25)
[12]	ABC-ANN	COCOMO81, NASA93, and COCOMO_SDR	MRE
[13]	Chi-means- PSO	COCOMO81	VAF, MARE, and VARE
[14]	OCFWFLANN	NASA93	MMRE, MDMRE, and PRED (0.25)
[27]	OCFWANN	NASA93	MMRE, MDMRE, RED (0.25)
[15]	MPSO	NASA60, NASA63, and NASA93	MMRE
[16]	Tabu-Genetic algorithm	NASA60, NASA63, and NASA93	MMRE
[17]	Harmony Search Algorithm	NASA93	MMRE
[20]	GA-Bayesian Network	NASA63	MMRE
	PSO-Bayesian Network	NASA63	MMRE
[18]	PSO-Fuzzy clustering	NASA60	MRE, MMRE
	PSO-Learning automata	NASA60	MRE, MMRE
[19]	Linear regression	NASA63	MRE
	Multilayer perceptron ANN	NASA63	MRE
	SVM	NASA63	MRE
	KNN	NASA63	MRE
[21]	Multilayer perceptron ANN	NASA63	MRE
[22]	SVM-Genetic Algorithm	NASA, COCOM, and KEMERER	PRED
	Multilayer Perceptron ANN-Genetic Algorithm	NASA, COCOM, and KEMERER	MRE
[23]	Fuzzy Logic	NASA93	MRE
[24]	Genetic algorithm and Radius Function	COCOMO 81	MMRE, MSE
[25]	Genetic Algorithm-Fuzzy Logic	NASA93	MMRE, MDMRE, and PRED (0.25)
[26]	Multilayer ANN	COCOMO	MARE, PRED (0.25)

ANN: Artificial neural network, SCE: Software cost estimation, PSO: Particle swarm optimization, SVM: Support vector machine

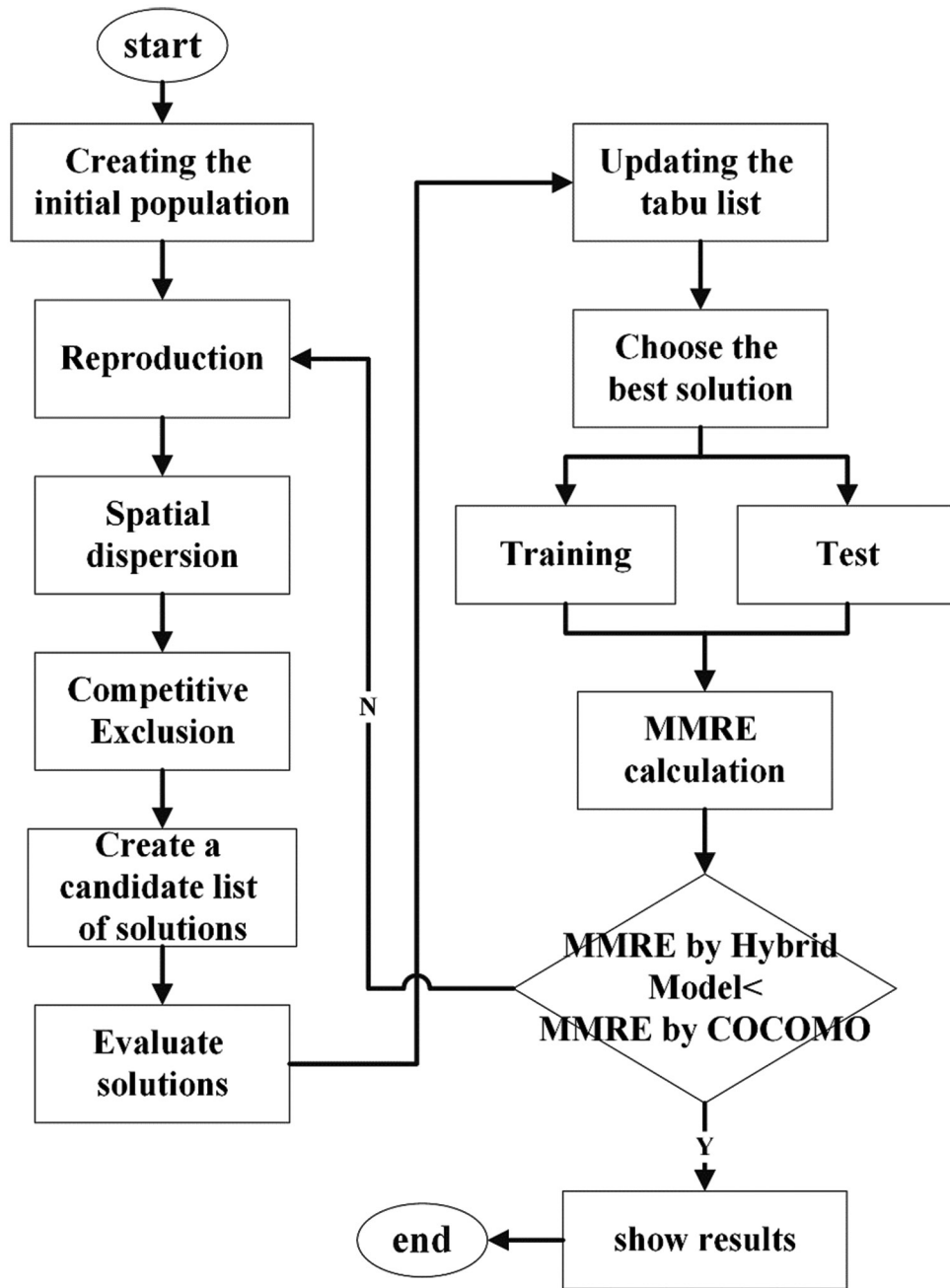


Fig. 1. Flowchart of the proposed model.

3.1. Initial Population

We create the initial population for the suggested model in the range [0.9, 1.4]. To create diversity in the initial population, optimization operations must be performed. Using the reproduction operator, we recreate the appropriate values for the initial population and then spread them over the problem environment. The new value for each effort factor is calculated according to Eq. (8). In

this equation, S_{max} and S_{min} are produced in the interval [0.9, 1.4], respectively.

$$EM_i^k = S_{max} - (S_{max} - S_{min}) \frac{f_i^k - f_{min}^k}{f_{max}^k - f_{min}^k} \quad (8)$$

In Eq. (8), the parameter f_{min}^k is the minimum colony in iteration k and f_{max}^k is the maximum colony in iteration k.

And, the parameter f_i^k is the main value of the effort factor. In each iteration, effort factors are generated in the colony, and then, the lowest and highest values are selected in each colony.

In this space, we save the optimal points close to the values of the effort factors and remove inappropriate values. Then, to optimize the solution vectors created by the IWO algorithm, we transfer them to the TS algorithm. In the TS algorithm, a list of candidate solutions is created and we choose the best solutions from among them. Solutions are chosen based on how close the values of the effort factors are to each other. The selection of solutions is done based on the proximity to the values of the effort factors. Then, we put the vectors that make the solution of the problem non-optimal in the forbidden list. With this method, optimal points can be reached at a better speed, and only the solutions that make the MMRE more optimal than the COCOMO model participate in the solution. Then, the data sets for the test and training phase are read the new values are inserted into the effort factors, and the MMRE is calculated. A fitness function is represented by the average relative error measurement. If it has a value lower than COCOMO, the result will be shown. Otherwise, the program is repeated and more optimal values are found.

3.2. Spatial Dispersion

The produced values are now dispersed at random throughout the proposed model's multidimensional space. In each step, the defined initial value ($\sigma_{initial}$) is reduced to a final value (σ_{final}). The initial value and the final value are within the range of effort factors. The number of points in the spatial distribution is defined according to Eq. (9). The goal is to guide people to the local optimal points and achieve the optimal value.

$$\sigma^k = \frac{(I_{max} - k)^n}{(I_{max} - 1)^n} (\sigma_{initial} - \sigma_{final}) + \sigma_{final} \quad (9)$$

In Eq. (9), The σ^k is the value of the standard deviation, I_{max} is the maximum number of iterations, and n is the amount of non-linearity, which is randomly generated in the range (0-1).

3.3. Update Vectors

The vectors are updated according to Eq. (10). Each vector is obtained to determine the optimal value for the effort factors based on the next value (x^{i+1}) and the predicted value (\hat{x}^i). The range of all factors in the standard range is determined by Eq. (10). Therefore, each person only explores the optimal space in the proposed model.

$$x = \left| \frac{(x^{i+1}) - (\hat{x}^i) - ((x^{i+1}) - (\hat{x}^i))}{(x^{i+1}) - (\hat{x}^i)} \right| \quad (10)$$

The solution vectors in the hybrid model contain the values of the software projects. These vectors are transformed into the optimal state based on IWO and TS operators, and their fitness is measured with each update step. If the MMRE error value is reduced, then the current solution vector is selected as the best solution and replaces the previous value of the effort factors. The combined model removes the worst solutions using the TS algorithm and places them in the forbidden list. Therefore, the agents in the search space are able to search the problem space only by following the receiving agents. As a result, the hybrid model escapes from getting stuck in the local optimum and can find the best effort values based on the size of the projects.

3.4. Evaluation Criteria

The MMRE [8] is considered a fitness function in the proposed model. The proposed model's fitness function aims to reduce relative error values when compared to the COCOMO model. Eq. (11) serves as the definition of the fitness function for the proposed model. The y parameter is equal to the real value and the \bar{y} parameter is equal to the estimated value obtained by the proposed model.

Mean Magnitude of Relative Error (MMRE) = $\frac{1}{n} \sum_{i=1}^n \left(\frac{|y_i - \bar{y}_i|}{y_i} \times 100 \right)$ (11)

Mean of Magnitude Error Relative (MMER) = $\frac{1}{n} \sum_{i=1}^n \left(\frac{|y_i - \bar{y}_i|}{y_i} \times 100 \right)$ (12)

Mean Squared Error (MSE) = $\frac{1}{n} \sum_{i=1}^n (y_i - \bar{y}_i)^2$ (13)

Root Mean Square Error (RMSE) = $\sqrt{\frac{1}{n} \sum_{i=1}^n (y_i - \bar{y}_i)^2}$ (14)

Mean Absolute Percentage

$$\text{Error (MAPE)} = \sum_{i=1}^n \left(\frac{|y_i - \hat{y}_i|}{y_i} \right) / n \times 100 \quad (15)$$

Mean of Absolute

$$\text{Errors (MAE)} = \frac{1}{n} \sum_{i=1}^n |y_i - \hat{y}_i| \quad (16)$$

Median Magnitude of Relative Error (MdMRE)=Median (MRE) (17)

The total error derived from the effort components may be calculated using Eq. (11). After optimization, the proposed model's effort components are added to the COCOMO model. The relative error value and MMRE values are calculated. A model with a lower relative error value performs better when assessing estimate criteria than a model with a greater relative error value. When compared to models with greater MMRE values, the model with a lower MMRE value performs better.

4. RESULTS AND EVALUATION

In the C# programming environment, the proposed model's performance was assessed, and the results were obtained using NASA60, NASA63, NASA93, KEMERER, and, MAXWELL data sets. There are 50 solutions in the starting population, and there are 200 iterations. The outcomes of the proposed model on various data sets are displayed in Table 2. As you can see in Table 2, the proposed model has a lower mean relative error compared to the COCOMO models, the IWO algorithm, and the TS algorithm. The proposed model cannot get stuck in local optima and finds the appropriate value for the effort factors based on the operators of the IWO algorithm and the TS algorithm (Fig. 2). The value of MDMRE on NASA60 for IWO, TS, and the proposed model is 25.89, 28.32, and 28.06, respectively.

The proposed model demonstrates superior performance with the lowest MDMRE, signifying more accurate predictions compared to IWO and TS on the NASA60 dataset. The proposed model has achieved less error due to strengthening the solutions. The value of MDMRE on NASA63 for IWO, TS, and the proposed model is 37.11, 34.23, and 33.94, respectively. The proposed model outperforms both IWO and TS by achieving the lowest MDMRE, indicating enhanced accuracy on the NASA63

dataset. The value of MDMRE on NASA93 for IWO, TS, and the proposed model is 37.85, 46.54, and 45.21, respectively. The proposed model continues to showcase improved accuracy compared to IWO and TS, as reflected in its lower MDMRE on the NASA93 dataset. The value of MDMRE on KEMERER for IWO, TS, and the proposed model is 71.75, 43.06, and 42.22, respectively. The value of MDMRE on MAXWELL for IWO, TS, and the proposed model is 46.58, 41.97, and 45.62 respectively.

In Table 2, the results of the proposed model on NASA63 are shown. The proposed model has a lower MMRE value compared to the IWO algorithm and the TS algorithm. The IWO algorithm also performs better than the TS algorithm in terms of mean relative error, mean square error, RMSE, and MAPE. The proposed model has a lower MMRE value in the NASA93 data set compared to COCOMO and the TS algorithm. The TS algorithm has a lower MMRE value compared to the IWO algorithm. In the KEMERER dataset, by comparing the proposed model with COCOMO, the proposed model has greatly reduced the MDMRE value and the MMRE value. Also, the TS algorithm has better accuracy compared to the IWO algorithm. In the MAXWELL data set, the results show that the MMRE in the proposed model is lower compared to other models. Also, the value of MAPE and MDMRE in the TS algorithm is higher compared to other models. The comparison graphs of the MMRE on the NASA60 and NASA63 datasets are displayed in Fig. 3. In comparison to existing models, the proposed model has a lower MMRE value. The MMRE value on the NASA60 dataset for IWO, TS, and the proposed model is 24.99, 23.86, and 21.93 respectively. The MMRE value on the NASA63 dataset for IWO, TS, and the proposed model is 24.01, 26.79, and 21.56 respectively.

In Fig. 4, the comparison chart of MMRE on NASA93 and KEMERER datasets is shown. In comparison to existing models, the proposed model has a lower MMRE value. The value of MMRE on the NASA93 dataset for IWO, TS, and the proposed model is 22.52, 42.79, and 38.64 respectively. The MMRE value on the KEMERER dataset for the IWO, TS, and proposed models is 112.58, 94.53, and 78.44, respectively.

The MMRE comparison graph for the MAXWELL dataset is displayed in Fig. 5. The value of MMRE on the MAXWELL dataset for IWO, TS, and the proposed model is 42.09, 33.79, and 33.25, respectively.

4.1. Iteration Based Evaluation

In Table 3, the comparison of models based on iteration is shown. Table 3 shows that the MMRE has reduced as

TABLE 2: Results of the 200 iterations of the proposed model for various data sets

Data sets	Models	MMRE	MMER	MSE	RMSE	MAPE	MAE	MDMRE
NASA60	COCOMO	29.64	40.18	31908.53	178.63	29.67	91.71	28.23
	IWO	24.99	39.46	31747.86	178.23	26.94	87.15	25.89
	TS	23.86	39.12	31669.41	177.98	26.97	86.85	28.32
	Proposed model	21.93	39.17	31257.49	176.86	26.92	86.42	28.06
NASA63	COCOMO	36.00	39.49	408448.58	639.10	102.55	210.43	37.51
	IWO	24.01	41.96	331076.69	575.39	74.01	163.46	37.11
	TS	26.79	16.95	331634.71	575.82	70.62	159.74	34.23
	Proposed model	21.56	36.51	339454.22	581.71	73.64	155.63	33.94
NASA93	COCOMO	58.50	49.05	4096.40	64.00	115.55	1137.84	48.14
	IWO	22.52	63.38	2970.93	29.87	72.43	644.46	37.85
	TS	42.79	57.98	15016.18	38.75	92.65	806.88	46.54
	Proposed model	38.64	51.19	3733.71	38.68	92.29	804.82	45.21
KEMERER	COCOMO	502.81	75.71	339382.84	1504.18	502.81	1024.08	415.09
	IWO	112.58	159.42	12619.07	290.05	112.58	168.54	71.75
	TS	94.53	133.91	10508.51	264.68	94.53	148.22	43.06
	Proposed model	78.44	190.24	12549.27	289.24	78.44	146.66	42.22
MAXWELL	COCOMO	59.92	46.26	130153.29	3607.68	59.92	2981.01	13.92
	IWO	42.09	59.38	8660.82	1019.46	92.09	2355.89	46.58
	TS	33.79	58.73	66770.25	2583.73	83.79	1287.49	41.97
	Proposed model	33.25	57.68	15023.52	387.73	92.84	809.25	45.62

IWO: Invasive Weed Optimization, TS: Tabu Search

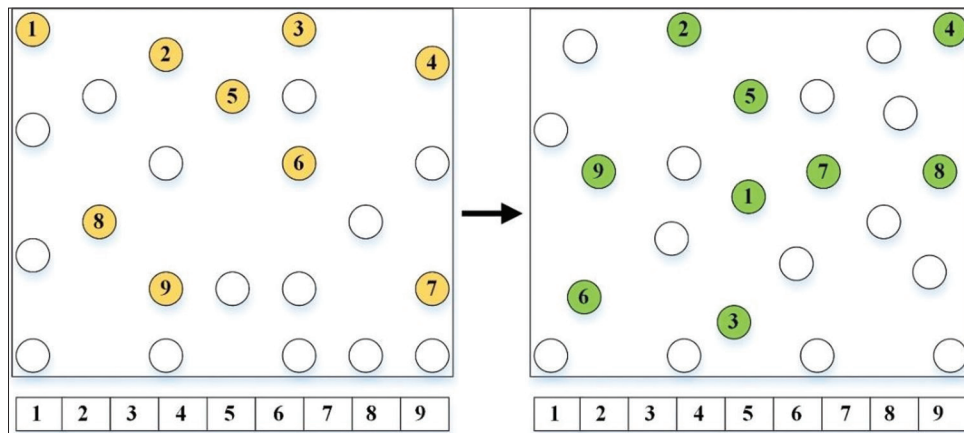


Fig. 2. Generation of optimal points for effort factors based on reproduction.

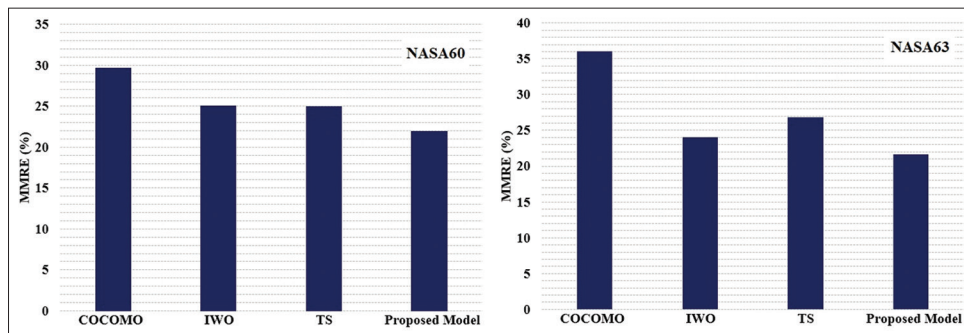


Fig. 3. MMRE comparison chart on NASA60 and NASA63 datasets.

the number of iterations has increased. The models search more points and finding the right value for the factors

is more accurate. Advanced search capability allows the algorithm to not simply settle for a local optimal solution.

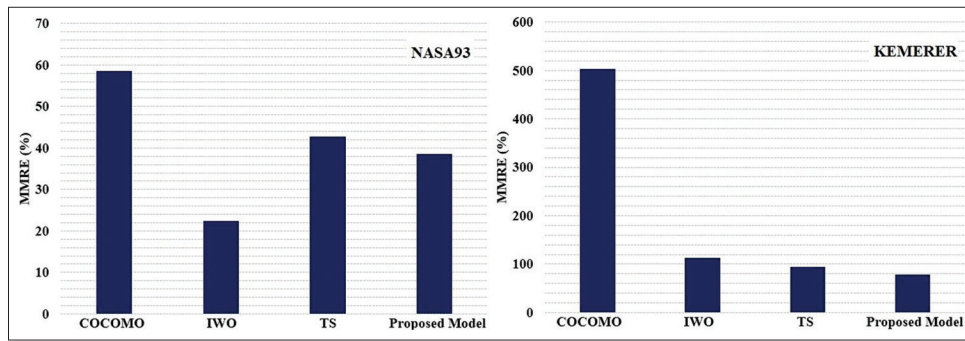


Fig. 4. Comparison chart of MMRE on NASA93 and KEMERER dataset.

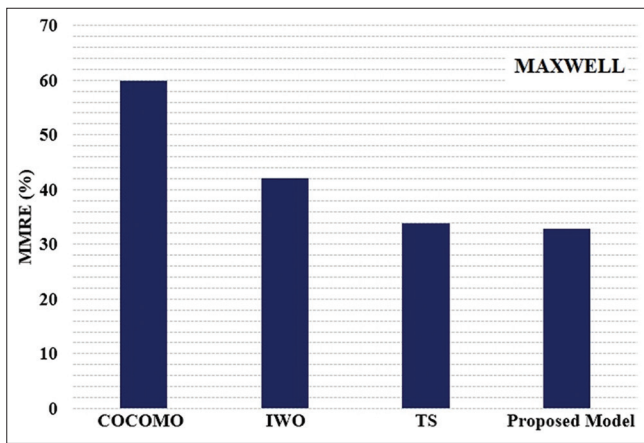


Fig. 5. MMRE comparison chart on MAXWELL dataset.

Rather, it continues to dig deeper to discover different potential solutions. By evaluating a larger number of points, the chances of finding the most appropriate and optimal solutions increase. The hybrid model is a powerful instrument for complex optimization problems as a result.

Investigations revealed that the proposed model's and the LSTM-RNN model's [29] MMRE values on NASA93 were 28.75 and 18.82, respectively. In addition, it was determined that the proposed model and the LSTM-RNN model had MMRE on MAXWELL values of 22,46 and 23,65, respectively.

4.2. Comparison and Evaluation

This section shows the comparison of the proposed model with other models. Table 4 shows that the proposed model performs better compared to other models. The percentage of training and test stages is 80 and 20, respectively. The proposed model has population diversity and avoids local optimal points. It can distinguish similar samples based on the distance index and update the banned list during the training process. The PSO-FLANN model is a technique that uses

the global optimization capabilities of PSO to fine-tune the extended functional neural network and allows it to learn complex patterns with a relatively simpler structure. The hybrid of GA and FLANN can lead to a more consistent and robust model, especially when the data have intricate and non-linear interactions. The most important advantage of the proposed model is that its computing time is less compared to models like PSO-FLANN. Also, the number of parameters of the proposed model is less compared to other models. As a result, the implementation and efficiency of the proposed model are simpler.

According to the comparative results, the proposed model has a lower error value than other models. When compared to ANN models and decision trees like CART, the proposed model's error percentage is often smaller. ANNs often require significant data for training. And sometimes, they can be prone to overfitting. In contrast, the heuristic nature of the proposed model allows it to explore the solution space more broadly and possibly converge to an optimal solution with a lower error rate. The proposed model addresses the challenge of software projects by taking advantage of the strengths of TS and IWO algorithms. The proposed model is able to generate new solutions in each iteration and can find the best values for the effort factors. Software projects are getting wider and bigger every day, and the best tool to reduce cost and error is to use meta-heuristic algorithms.

5. CONCLUSION AND FUTURE WORKS

SCE includes resources that can only be learned and implemented with practical experience. The final goal of the estimate is to be as close as possible to the realities of the project. The time needed for each stage of the project must first be estimated before determining the entire project duration can be done. In this article, the improvement of

TABLE 3: Comparison of models based on the number of iterations

Iteration	Models	MMRE				
		NASA60	NASA63	NASA93	KEMERER	MAXWELL
100	IWO	24.99	24.01	22.43	112.58	42.09
	TS	24.96	26.82	42.79	94.53	33.79
	Proposed model	21.93	21.63	38.48	78.44	32.84
200	IWO	23.14	22.48	21.06	105.56	38.15
	TS	21.65	24.80	39.74	90.52	31.49
	Proposed model	18.35	19.81	34.96	62.76	26.31
500	IWO	21.03	20.43	19.86	98.65	35.79
	TS	19.31	21.17	35.24	82.11	24.82
	Proposed model	15.43	17.05	28.75	58.34	22.46

IWO: Invasive Weed Optimization, TS: Tabu Search

TABLE 4: Comparison of the proposed model with other models

Datasets	Models	MMRE		MDMRE		PRED (0.25)	
		Train	Test	Train	Test	Train	Test
NASA60	ANN [30]	0.44	0.44	-	-	-	-
	Proposed model	0.22	0.25	0.27	0.29	0.60	0.64
NASA63	PSO-FLANN [11]	0.43	0.37	0.48	0.42	0.39	0.52
	FLANN [11]	0.45	0.38	0.49	0.47	0.35	0.49
	SWR [11]	0.34	0.35	0.42	0.44	0.52	0.50
	Proposed model	0.29	0.31	0.35	0.40	0.32	0.58
NASA93	PSO-FLANN [11]	0.49	0.34	0.44	0.45	0.39	0.50
	FLANN [11]	0.42	0.49	0.46	0.48	0.38	0.48
	SWR [11]	0.39	0.34	0.47	0.49	0.44	0.44
	OCFWFLANN [14]	0.28	0.27	0.24	0.19	0.31	0.26
	OFWFLANN [14]	0.38	0.33	0.39	0.28	0.30	0.38
	FLANN [14]	0.43	0.37	0.37	0.33	0.46	0.39
	SWR [14]	0.92	0.79	0.58	0.44	0.45	0.41
	CART [14]	0.85	0.64	0.48	0.37	0.34	0.30
	OCFWANN [27]	0.33	0.32	0.29	0.24	0.36	0.31
	OFWANN [27]	0.43	0.38	0.44	0.33	0.35	0.43
	ANN [27]	0.48	0.42	0.42	0.38	0.51	0.44
	Proposed model	0.32	0.28	0.34	0.21	0.26	0.45
MAXWELL	PSO-FLANN [11]	0.55	0.38	0.49	0.42	0.32	0.48
	FLANN [11]	0.48	0.42	0.39	0.40	0.45	0.28
	SWR [11]	0.42	0.42	0.47	0.39	0.39	0.45
	LEMABE [31]	0.47	0.48	-	-	-	-
	Proposed model	0.38	0.36	0.34	0.36	0.28	0.56

IWO: Invasive Weed Optimization, TS: Tabu Search

the IWO algorithm based on TS was used for SCE. The purpose of the TS algorithm was to optimize the effort factors and find the appropriate value for them based on the determined interval. The MMRE value for the hybrid model on NASA60, NASA63, and NASA93 is 21.93, 21.56, and 38.64, respectively. The results showed that the TS algorithm was able to improve the IWO algorithm. Also, the MMRE value for the hybrid model on KEMERER and MAXWELL was obtained as 78.44 and 33.25, respectively. According to the findings, the proposed model has a lower MMRE than both the IWO and the TS algorithms. The TS algorithm's effectiveness was superior to the IWO method in several

cases. In addition, the proposed model's MMRE was lower than that of COCOMO and other models. Project processes and stages should be prioritized and the dependencies between them should be carefully identified and all this information should be recorded in the project schedule. The dependence of different stages of the project as well as the amount of access to resources can have a significant impact on the time of the project.

The main limitations of this paper are that the proposed model has not been evaluated on the projects of an organization or a software company. Software companies

use different factors such as database programmers and computational programmers in software projects. Also, today's projects use different languages in coding, and the coding cost of each programming language is different. The second limitation is that meta-heuristic algorithms may use a specific procedure such as exploration and exploitation to find solutions, therefore, in these algorithms, there are no combined procedures such as increasing the number of layers such as ANNs.

For the work, we intend to use a combination of meta-heuristic algorithms and deep learning algorithms. Deep learning methods need to strengthen the parameters and the number of optimal layers, and these deficiencies are solved using meta-heuristic algorithms. Deep learning models, particularly neural networks, necessitate a meticulous tuning of parameters such as learning rates, regularization terms, and activation functions. Thus, determining the optimal number of layers and their configurations is a critical aspect, as an inadequate or excessive number of layers can impede the model's learning capacity or induce overfitting. To address these challenges, we propose to employ meta-heuristic algorithms. These algorithms, inspired by natural processes or optimization strategies, excel in exploring vast solution spaces and identifying optimal configurations. By leveraging the strengths of deep learning in capturing complex patterns and the optimization capabilities of meta-heuristic algorithms, we aim to develop a robust framework that excels in addressing the intricacies of diverse datasets and complex problem domains.

REFERENCES

- [1] S. K. Gouda and A. K. Mehta. "Software cost estimation model based on fuzzy C-means and improved self-adaptive differential evolution algorithm". *International Journal of Information Technology*, vol. 14, no. 4, p. 2171-2182, 2022.
- [2] S. K. Gouda and A. K. Mehta. "A self-adaptive differential evolution using a new adaption based operator for software cost estimation". *Journal of the Institution of Engineers (India): Series B*, vol. 104, no. 1, pp. 23-42, 2023.
- [3] W. Rhmann, B. Pandey and G. A. Ansari. "Software effort estimation using ensemble of hybrid search-based algorithms based on metaheuristic algorithms". *Innovations in Systems and Software Engineering*, vol. 18, pp. 1-11, 2021.
- [4] Z. A. Dizaji and F. S. Gharehchopogh. "A hybrid of ant colony optimization and chaos optimization algorithms approach for software cost estimation". *Indian Journal of Science and Technology*, vol. 8, no. 2, p. 128, 2015.
- [5] R. Mehrabian and C. Lucas. "A novel numerical optimization algorithm inspired from weed colonization". *Ecological Informatics*, vol. 1, no. 4, pp. 355-366, 2006.
- [6] B. Boehm, C. Abts and S. Chulani. "Software development cost estimation approaches-a survey". *Annals of Software Engineering*, vol. 10, no. 1-4, pp. 177-205, 2000.
- [7] O. Adalier, A. Ugur, S. Korukoglu, K. Ertas, H. Yin, P. Tino, E. Corchado, W. Byrne and X. Yao. "A New Regression Based Software Cost Estimation Model Using Power Values". In: *Proceedings of Intelligent Data Engineering and Automated Learning-IDEAL 2007: 8th International Conference, Birmingham, UK*. Springer, Germany, 2007.
- [8] T. R. Benala, K. Chinnababu, R. Mall and S. Dehuri. "A Particle Swarm Optimized Functional Link Artificial Neural Network (PSO- FLANN) in Software Cost Estimation. In: *Proceedings of the International Conference on Frontiers of Intelligent Computing: Theory and Applications (FICTA)*". Springer, Germany, 2013.
- [9] Z. H. Wani and S. Quadri. "Artificial Bee Colony-Trained Functional Link Artificial Neural Network Model for Software Cost Estimation. In: *Proceedings of Fifth International Conference on Soft Computing for Problem Solving: SocProS 2015*". vol. 2, Springer, Germany, 2016.
- [10] T. S. Sethi, C. V. Hari, B. T. Kaushal and S. Sharma. "Cluster Analysis and PSO for Software Cost Estimation. In: *Proceedings of Information Technology and Mobile Communication*. Springer, Germany, 2011.
- [11] T. R. Benala, S. Dehuri, S. C. Satapathy and S. Madhurakshara. "Genetic Algorithm for Optimizing Functional Link Artificial Neural Network based Software Cost Estimation. In: *Proceedings of the International Conference on Information Systems Design and Intelligent Applications 2012 (INDIA 2012) held in Visakhapatnam, India*". Springer, Germany, 2012.
- [12] G. S. Rao, C. V. P. Krishna and K. R. Rao. "Multi Objective Particle Swarm Optimization for Software Cost Estimation. In: *ICT and Critical Infrastructure: Proceedings of the 48th Annual Convention of Computer Society of India*". vol. 1. Springer International Publishing, Cham, 2014.
- [13] F. S. Gharehchopogh, R. Rezaii and B. Arasteh. "A New Approach by Using Tabu Search and Genetic algorithms in Software Cost Estimation. In *2015 9th International Conference on Application of Information and Communication Technologies (AICT)*". IEEE, United States, 2015.
- [14] S. S. Jafari and F. Ziaaddini. "Optimization of Software Cost Estimation Using Harmony Search Algorithm. In: *2016 1st Conference on Swarm Intelligence and Evolutionary Computation (CSIEC)*". IEEE, United States, 2016.
- [15] F. S. Gharehchopogh, L. Ebrahimi, I. Maleki and S. J. Gourabi. "A novel PSO based approach with hybrid of fuzzy C-means and learning automata in software cost estimation". *Indian Journal of Science and Technology*, vol. 7, no. 6, p. 795, 2014.
- [16] Z. A. Khalifelu and F. S. Gharehchopogh. "Comparison and evaluation of data mining techniques with algorithmic models in software cost estimation". *Procedia Technology*, vol. 1, pp. 65-71, 2012.
- [17] F. S. Gharehchopogh. "Neural Networks Application in Software Cost Estimation: A Case Study. In: *2011 International Symposium on Innovations in Intelligent Systems and Applications, Istanbul, Turkey*". IEEE, United States.
- [18] L. Oliveira, P. L. Braga, R. M. F. Lima and M. L. Cornélio. "GA-based method for feature selection and parameters optimization for machine learning regression applied to software effort estimation". *Information and Software Technology*, vol. 52, no. 11, pp. 1155-1166, 2010.
- [19] Malik, V. Pandey and A. Kaushik. "An analysis of fuzzy approaches for COCOMO II". *International Journal of Intelligent Systems and*

- Applications*, vol. 5, no. 5, p. 68, 2013.
- [20] M. Molani, A. Ghaffari and A. Jafarian. "A new approach to software project cost estimation using a hybrid model of radial basis function neural network and genetic algorithm". *Indian Journal of Science and Technology*, vol. 7, no. 6, pp. 838-843, 2014.
- [21] A. Hamdy. "Genetic fuzzy system for enhancing software estimation models". *International Journal of Modeling and Optimization*, vol. 4, no. 3, p. 227, 2014.
- [22] Attarzadeh and S. H. Ow. "Proposing A New Software Cost Estimation Model Based on Artificial Neural Networks. In: 2010 2nd International Conference on Computer Engineering and Technology". IEEE, United States, 2010.
- [23] T. R. Benala, S. Dehuri, S. Satapathy and C. S. Raghavi. "Genetic Algorithm for Optimizing Neural Network Based Software Cost Estimation. In: *Swarm, Evolutionary, and Memetic Computing*. Springer, Berlin, Heidelberg, 2011.
- [24] G. S. Rao, C. V. P. Krishna and K. R. Rao. "Multi Objective Particle Swarm Optimization for Software Cost Estimation. In: *ICT and Critical Infrastructure: Proceedings of the 48th Annual Convention of Computer Society of India*". vol. 1. Springer International Publishing, Cham, 2014.
- [25] Kaushik, N. Choudhary and P. Srivastava. "Software Cost Estimation Using LSTM-RNN. In: *Proceedings of International Conference on Artificial Intelligence and Applications: ICAIA 2020*". Springer, Germany, 2021.
- [26] N. Rankovic, D. Rankovic, M. Ivanovic and L. Lazic. "Improved effort and cost estimation model using artificial neural networks and Taguchi method with different activation functions". *Entropy (Basel)*, vol. 23, no. 7, p. 851, 2021.
- [27] M. Dashti, T. J. Gandomani, D. H. Adeg, H. Zulzalil and A. B. Sultan. "LEMABE: A novel framework to improve analogy-based software cost estimation using learnable evolution model". *PeerJ - Computer Science*, vol. 8, p. e800, 2022.

Comparative Analysis of Word Embeddings for Multiclass Cyberbullying Detection

Azhi Faraj^{1,2} and Semih Utku¹

¹Department of Computer Engineering, Faculty of Engineering, Dokuz Eylul University, Izmir, Turkey, ²Department of Information Technology, College of Commerce, Sulaimani University, Sulaymaniyah, Iraq.



ABSTRACT

Cyberbullying has emerged as a pervasive concern in modern society, particularly within social media platforms. This phenomenon encompasses employing digital communication to instill fear, threaten, harass, or harm individuals. Given the prevalence of social media in our lives, there is an escalating need for effective methods to detect and combat cyberbullying. This paper aims to explore the utilization of word embeddings and to discern the comparative effectiveness of trainable word embeddings, pre-trained word embeddings, and fine-tuned language models in multiclass cyberbullying detection. Distinguishing from previous binary classification methods, our research delves into nuanced multiclass detection. The exploration of word embeddings holds significant promise due to its ability to transform words into dense numerical vectors within a high-dimensional space. This transformation captures intricate semantic and syntactic relationships inherent in language, enabling machine learning (ML) algorithms to discern patterns that might signify cyberbullying. In contrast to previous research, this work delves beyond primary binary classification and centers on the nuanced realm of multiclass cyberbullying detection. The research employs diverse techniques, including convolutional neural networks and bidirectional long short-term memory, alongside well-known pre-trained models such as word2vec and bidirectional encoder representations from transformers (BERT). Moreover, traditional ML algorithms such as K-nearest neighbors, Random Forest, and Naïve Bayes are integrated to evaluate their performance vis-à-vis deep learning models. The findings underscore the promise of a fine-tuned BERT model on our dataset, yielding the most promising results in multiclass cyberbullying detection, and achieving the best-recorded accuracy of 85% on the dataset.

Index Terms: Cyberbullying Detection, Word Embeddings, Deep Learning, Machine Learning, Text Classification

1. INTRODUCTION

Cyberbullying involves the consistent use of electronic or digital platforms by individuals or collectives to repeatedly convey harmful or aggressive messages with the intent of causing discomfort or harm to others [1]. This encompasses actions such as sending cruel or menacing messages, sharing humiliating photos or videos, propagating gossip, or crafting fictitious profiles or websites with the purpose of

shaming an individual. Cyberbullying can lead to significant repercussions for both the target and the person engaging in it. Victims of cyberbullying may experience a range of negative effects, including feelings of sadness, anxiety, depression, and even thoughts of suicide. They may also have trouble sleeping, lose interest in activities they used to enjoy, and struggle with self-esteem [2]. Individuals engaging in cyberbullying might face serious repercussions, including disciplinary action from educational institutions or legal authorities, as well as potential legal consequences. Such actions could also negatively impact their future relationships and life opportunities. It is crucial to understand that cyberbullying is not confined to a specific age group or demographic; it can affect anyone. Although young people are commonly involved, adults are not immune to being targeted by cyberbullying [3].

Access this article online

DOI: 10.21928/uhdjst.v8n1y2024.pp55-63

E-ISSN: 2521-4217

P-ISSN: 2521-4209

Copyright © 2024 Azhi Faraj and Semih Utku. This is an open access article distributed under the Creative Commons Attribution Non-Commercial No Derivatives License 4.0 (CC BY-NC-ND 4.0)

Corresponding author's e-mail: azhi.faraj@univsul.edu.iq

Received: 19-11-2023

Accepted: 06-02-2024

Published: 20-02-2024

Automatic cyberbullying detection refers to the use of computational methods and technologies to automatically identify instances of cyberbullying in electronic communications, such as text, images, and videos.

This typically involves the utilization of natural language processing (NLP) techniques, machine learning (ML) algorithms, and other analytical approaches to analyze the content and context of electronic communications [4]. Different techniques have been put forth for automated cyberbullying identification, encompassing rule-based models, conventional ML models, and deep learning models [5]. Rule-based models depend on pre-established rule sets and lexical resources to detect instances of cyberbullying. On the other hand, conventional ML models employ algorithms such as logistic regression, decision trees, K-nearest Neighbors (KNN), and support vector machines to categorize text as either cyberbullying or not. Deep learning models, conversely, use neural networks to identify patterns in the data that indicate cyberbullying. Research on automatic cyberbullying detection has mainly focused on social media platforms such as Twitter, Instagram, and YouTube [5]. These platforms are particularly relevant for cyberbullying detection due to their popularity among young people and the large amount of user-generated content that is available for analysis.

Research in the literature has used the following features to improve the accuracy of detection [6, p. 2].

1.1. Textual Features

This includes techniques such as n-grams, skip grams, content character length, number of emoticons used, and the usage of profanity in the text.

1.2. Social Features

Refers to the attributes provided in social networks for example number of friends or followers, reactions received from posts, and additional metrics of centrality that may be derived from a graph representation (e.g., betweenness and eigenvector).

1.3. User Features

Information about the authors such as age, gender, ethnicity, and religion.

1.4. Sentiment Analysis

The polarity of the post is used to determine whether a post is cyberbullying or not.

Cyberbullying detection using word embeddings is a subject of active research in NLP [6]. Word embeddings are a

technique used to depict words within a vector space with multiple dimensions. Each dimension corresponds to a distinct semantic or syntactic aspect of the word. By mapping words to vectors, it becomes possible to use ML algorithms to automatically detect patterns in the text that may indicate bullying [7].

This paper explores the use of word embeddings for multiclass cyberbullying detection. It addresses the growing issue of cyberbullying in today's society and the need for effective methods to detect and prevent it. The study compares the performance of different word embedding techniques, including trainable word embeddings, pre-trained word embeddings, and fine-tuning language models. It goes beyond simple binary classification and focuses on multi-class detection of cyberbullying. The research employs various techniques, such as convolutional neural networks (CNN) and bidirectional long short-term memory (biLSTM), as well as popular pre-trained models such as word2vec and bidirectional encoder representations from transformers (BERT). The research contributes to the field of automatic cyberbullying detection and provides insights into the effectiveness of word embeddings for this task that follow.

This research is motivated by the urgent need to address the escalating issue of cyberbullying in the digital age, where social media platforms are intertwined with daily life. Recognizing the limitations of existing binary classification approaches in accurately detecting diverse forms of cyberbullying, this study introduces an advanced methodology that employs a combination of word embeddings and deep learning techniques. The primary contributions include the development of a multiclass detection model, which significantly improves the accuracy of cyberbullying identification compared to traditional methods. This is achieved by leveraging a fine-tuned BERT model alongside other innovative techniques such as CNN and biLSTM. The real-world impact of this work is substantial, offering tools for social media platforms and digital communities to better identify and mitigate cyberbullying, thus fostering safer online environments. Our approach not only enhances cyberbullying detection accuracy but also contributes to the broader field of digital safety and online behavioral analysis. The proposed method is particularly beneficial in social media platforms for monitoring content, in educational settings to safeguard students, and on online forums for community guideline enforcement. It also holds potential for mental health support initiatives, offering insights for targeted interventions, and can assist law enforcement in identifying and addressing severe cases. This technology aims to enhance online safety

and respect across various digital platforms, contributing to a healthier digital environment.

2. RELATED WORK

In their research, Yin *et al.* [8] have the first to explore automated recognition of cyberbullying in online environments. They collected three sets of data from three distinct online platforms to detect instances of harassment. One dataset was sourced from the Kongregate platform, whereas the other two were collected from Reddit. To classify the data, the authors used a linear kernel classification model and applied different techniques for feature extraction, including N-grams and term frequency-inverse document frequency (TF-IDF). Despite having uncertain experimental results, the study was a significant step toward further research in this field.

Researchers in Iwendi *et al.* [9] explored the effectiveness of four deep learning models – BLSTM, gated recurrent units (GRU), long short-term memory (LSTM), and recurrent neural network (RNN) – in detecting cyberbullying. They applied rigorous data pre-processing steps, including text cleaning, tokenization, stemming, lemmatization, and removal of stop words, before feeding the data into the models for prediction. Among these models, BLSTM stood out, showing higher accuracy and F1-measure scores compared to RNN, LSTM, and GRU [10] proposed a ML approach for detecting cyberbullying in text-based online communication. The authors collected a large dataset of messages from social networking sites and labeled them as either bullying or non-bullying. Subsequently, they derived a range of linguistic attributes from the messages, encompassing syntactic and semantic aspects, alongside social network characteristics. The authors employed various ML techniques, such as decision trees and support vector machines (SVMs), to categorize messages as either exhibiting bullying behavior or not.

Bozyigit *et al.* [11] collected a dataset from twitter for Turkish language and used social features to detect cyberbullying, the authors also created a web application that detects cyberbullying live. In Aizawa [12], an approach based on feature engineering was introduced for identifying multi-class cyberbullying on Twitter. The authors utilized a dataset containing 10,000 tweets that were labeled with three levels of cyberbullying severity: low, medium, and high. Initially, they employed the synthetic minority oversampling technique to oversample the underrepresented categories (low, medium, and high) by a factor of 300. Subsequently, they applied a weighted cost for misclassification in the minority categories.

On the other hand, the study outlined in Dinakar *et al.* [13] utilized deep learning architectures to investigate the performance of various deep learning algorithms (LSTM, BiLSTM, RNN, and GRU) in terms of their effectiveness for identifying antisocial behavior. The researchers performed empirical assessments to measure how well the algorithms work in recognizing antisocial behavior. [14] utilized a dataset collected from twitter with 16K records, they applied TF-IDF, task-specific embeddings to detect hate speech that was categorized to sexist, racist, or none comments, the authors reported an F1-score of 0.93.

In Agrawal and Awekar [15], the authors used YouTube comments data that they used TF-IDF and a collection of profane words then applied Naïve bayes, SVM, J48, and JRip to detect three types of cyberbullying, namely, sexuality, race, and intelligence that they achieved a maximum accuracy of 80.20% on sexuality cyberbullying. [16] used char-n grams, word n-grams as features on Wikipedia dataset that they applied Logistic Regression and Multilayer Perceptron to categorize whether the comments included personal attacks or not.

In Wulczyn *et al.* [17], the authors examined various content characteristics, such as the use of first- and second-person pronouns, as well as the presence of vulgar language. They found that these factors indeed served as markers for cyberbullying.

The study [18] involves the utilization of a deep learning algorithm in conjunction with fuzzy logic to analyze 47,733 comments from Twitter, obtained from Kaggle. The methodology includes processing these comments using Keras embeddings and classifying them with a four-layer LSTM network. The application of fuzzy logic then aids in determining the severity of the flagged cyberbullying comments.

A comparable method was employed in Agrawal and Awekar [15], where researchers mainly focused on content attributes such as racist language and profanity. Another interdisciplinary study, discussed in Mikolov *et al.* [19], approached the issue from both computer science and human behavior perspectives. In their proposed technique, the researchers extensively analyzed content features, including URLs and hashtags. Surprisingly, they observed that 64 of the tweets contained external links, and 74.2% included hashtags, but these two aspects were not indicative of bullying. Similarly, [20] continued to explore cyberbullying detection through a content-based lens, introducing new elements like emoticons and a hieroglyph dictionary. They evaluated their approach using various ML algorithms, including SVM and J48, with SVM achieving the highest accuracy rate of 81%.

Another approach in the literature about tackling cyberbullying issue has been using transformer-based models such as BERT [21], BERT-m [21], [22], DistilBERT, and IndicBERT [23]. Hybridizing various deep learning models, including Simple RNN [14], LSTM, BiLSTM [14], GRU [24], and CNN [25].

Dinakar *et al.* [13] Deep neural networks were utilized on three different datasets (Formspring, Twitter, Wikipedia), the authors in Badjatiya *et al.* [16] used basic word embeddings and language models including RoBERTa, XLNET, and ALBERT to detect cyberbullying. They evaluated their approach on a dataset of 10,000 tweets and found that the best-performing word embedding method is RoBERTa, which achieves an accuracy of 93.2%.

3. MATERIALS AND METHODS

Fig. 1 shows the proposed methodology of this research; in the following subsections, we discuss each part of the methodology.

3.1. The Dataset

The dataset has been prepared by [26] that contain 47,692 records distributed approximately equally amongst six classes as shown in figure 2, namely, not cyberbullying, religion, gender, ethnicity, age, and other. The dataset has been collected from the twitter social network. The dataset offers the opportunity to establish a multiclassification model for

forecasting cyberbullying types, develop a binary classification model to identify potentially harmful tweets, or investigate the words and patterns linked with each form of cyberbullying. Fig. 1 shows sample distribution per type.

3.2. Text Preprocessing

In the preprocessing phase, the following actions shown in Fig. 3 were performed to clean and transform the text before further analysis or modeling.

3.2.1. Remove links

This is the initial cleaning step where any hyperlinks contained in the text are removed. Links may not contribute to the analysis of the text's content, especially when the goal is to understand linguistic patterns or sentiment.

3.2.2. Clean non-alphabetical characters

At this stage, the text is further cleaned by removing any characters that are not part of the alphabet. This typically includes punctuation, numerical digits, symbols, and any other non-letter characters. This step helps in focusing the analysis on words only.

3.2.3. Convert text to lowercase

Converting all text to lowercase is a standard normalization technique that helps in maintaining consistency throughout the dataset. It ensures that the same word in different cases (e.g., "Word" vs. "word") is treated as identical during analysis.

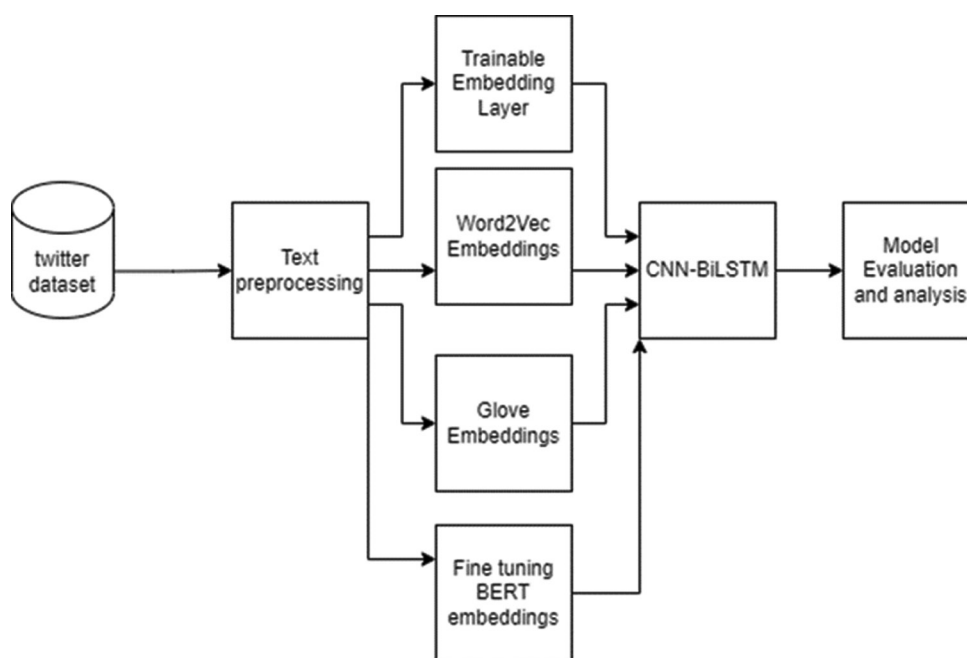


Fig. 1. Proposed methodology.

3.2.4. Tokenize

Tokenization is the process of splitting the text into individual terms or words. This is a crucial step because most language processing methods work at the word level.

3.2.5. Remove stop words

Common words such as “the,” “is,” and “in,” which appear frequently and have little lexical content, are removed in this step. By eliminating these, the data are distilled, focusing on the more meaningful content words.

3.2.6. Stemming

Stemming algorithms work by cutting off the end or the beginning of the word, considering a list of common prefixes and suffixes that can be found in an inflected word. This process reduces words to their root form, which helps in generalizing different forms of the same word (e.g., “running,” “ran,” “runs” all become “run”).

Although text preprocessing steps can impact the original meaning of tweets to some extent yet their importance in reducing noise and shifting focus on the most meaningful words remains crucial. While stop words (such as “the” and “is”) are often grammatically essential, they usually carry little semantic weight. The subsequent word embedding stage effectively captures the deeper semantic and syntactic

relationships between the remaining words. Therefore, although some nuances may be lost, this trade-off is a necessary part of optimizing the model for efficiently detecting patterns indicative of cyberbullying.

3.3. Word Embeddings

It represents a method employed within the field of (NLP) and ML. They involve representing words as dense numerical vectors within a multi-dimensional space. These vectors grasp both the semantic (meaning-related) and syntactic (grammar-related) associations amongst words, which are learned from how the words are used together in a large collection of text [19]. Word embeddings allow machines to understand and process language more effectively by capturing the meaning and associations of words in a numerical format which can be effortlessly utilized as input for various ML algorithms. In recent years, word embeddings have gained extensive usage in a variety of text classification and information retrieval tasks [19]. In this research, several different embeddings have been compared.

3.3.1. Trainable embedding

To establish a baseline, we create an embedding layer with the vocabulary size (100,000), the dimensionality of the dense vector representation (8), and the length of the input sequences (input-length=50), which is randomly initialized and trainable. This implies that the baseline does not utilize pre-existing embeddings but instead learns them from scratch alongside other model parameters. Consequently, this approach allows us to examine how performance is affected by either training word embeddings from scratch or using pre-trained ones.

3.3.2. Word2Vec

Mikolov *et al.* [27] is a neural network-based approach for learning word embeddings. It employs a neural network consisting of two layers to predict a target word, given the context of neighboring words (Referred to as the “continuous bag-of-words” model) or to forecast a context of neighboring words given a target word (referred to as the “skip-gram” model). The embeddings learned by the model are the weights of the input layer, which can be used as a dense representation

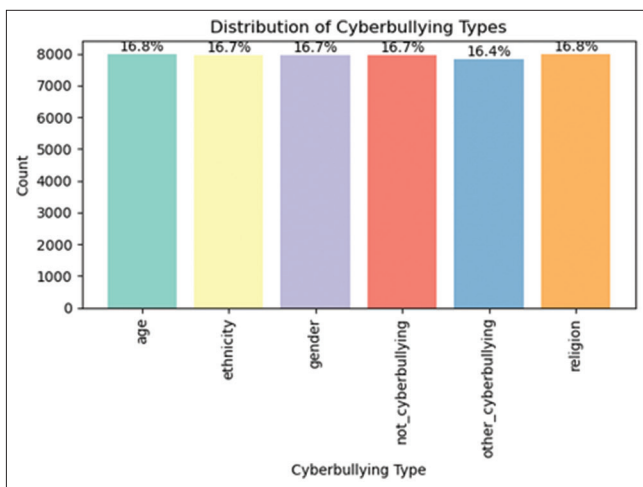


Fig. 2. Sample distribution amongst classes.

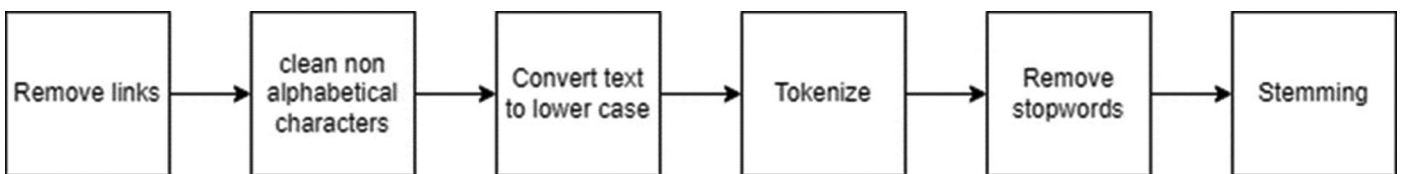


Fig. 3. Preprocessing steps taken.

of words in a high-dimensional space. The model contains 300-dimensional vectors for 3 million words and phrases.

3.3.3. Global vectors for word representation (GloVe)

Pennington *et al.* [28] have a model that learns word embeddings through a matrix factorization technique. It operates on the co-occurrence matrix of words in a corpus, which is a symmetric matrix where each element (i, j) represents the frequency at which word i and word j co-occur within the same context. GloVe factorizes this matrix into two lower-dimensional matrices, which are used as the word embeddings. This method also enables keeping track of the relationship between the words. We used glove-twitter-100, which is trained on 2B tweets, 27B tokens, 1.2M vocab, uncased.

3.3.4. BERT

Devlin *et al.* [29] constitutes a model rooted in the transformer architecture, which acquires profound bidirectional representations by jointly considering both preceding and succeeding context across all layers. Through pre-training on an extensive text corpus, it employs masked language modeling, wherein certain input words are replaced with a (MASK) token. Subsequently, the model is trained to predict the original words, enabling it to discern contextual associations between terms. BERT's effectiveness spans a diverse array of natural language understanding tasks, and it presently enjoys widespread utilization in NLP endeavors. In this study, we opted for the bert-base-uncased version, featuring 12 layers and 12 attention heads.

Each embedding method has its own unique characteristics, and it's crucial to understand the feature vectors they provide, whether used individually or in combination. In the text classification workflow, the embedding layer applies one or more pre-trained embeddings to create word representations for the downstream encoder, denoted as e . In our approach, we use CNN-BiLSTM to transform the embedded vectors $\langle x_0, x_1, x_2, \dots, x_n \rangle$ into a single sequence representation, summarized as O , that is, $O = e^{(x_0, x_1, x_2)}$. Once encoded, O is then passed to a fully connected layer denoted as f to produce logits across all labels: $g = f(O)$.

In the case of multi-label classification, we calculate the probability using the sigmoid function:

$$P(l_i | s) = \text{sigmoid}(g_i)$$

Here, the label l_i is assigned to the training example s if the estimated probability exceeds 0.5.

3.4. Classification (CNN-BiLSTM)

Following the embedding layer is a bidirectional layer encapsulating an LSTM layer which is depicted in Fig. 4. The LSTM is a type of RNN designed for sequential data processing. The bidirectional wrapper enables the LSTM to process input in the forward and backward directions simultaneously. Moreover, the LSTM layer is configured to return the full sequence.

Subsequently, a convolution1D layer is added, primarily used for one-dimensional convolution applied to sequential data, such as text. The layer requires three parameters: The number of filters (32), the kernel size (8), and the activation function employed (ReLU). To perform global max pooling on temporal data, the model incorporates a GlobalMaxPool1D layer, thereby extracting the maximum value across all time steps. To flatten the input, a Flatten layer is introduced, which reshapes the multidimensional output into a one-dimensional vector.

Next, a Dense layer with 128 neurons and a ReLU activation function is appended. A dense layer represents a regular layer of neurons within the neural network, with each neuron receiving input from all neurons in the preceding layer, establishing dense connections.

To combat overfitting, a Dropout layer with a dropout rate of 0.2 is included. Dropout serves as a regularization technique by randomly deactivating a fraction of input units during the forward pass. The final layer added is a dense layer consisting of 6 neurons and employing a SoftMax activation function. This layer is tasked with producing the probabilities linked to the input's membership within each of the six classes. The model is ultimately compiled with the sparse categorical cross-entropy loss function, the Adamax optimizer, and accuracy as the evaluation metric.

4. RESULTS AND DISCUSSION

This section presents the findings of our experiments, where we utilized deep learning models to create a cyberbullying detection system (CDS). The purpose of the CDS was to detect and categorize instances of linguistic cyberbullying into multiple classes. Regarding the choice of the word embeddings used in our experiments, pre-trained word embeddings performed better than trainable word embeddings.

In this investigation, we assessed the efficacy of a proposed

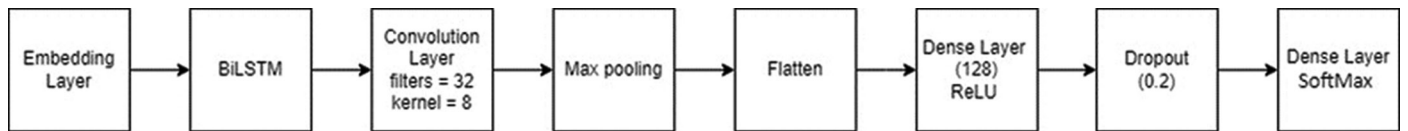


Fig. 4. Convolutional neural networks-bidirectional long short-term memory model.

model by utilizing various evaluation metrics to gauge its capacity for distinguishing the six classes of cyberbullying. The following commonly used evaluation criteria are employed to gauge the effectiveness of cyberbullying classifiers for social media networks:

- Accuracy (equation 1): This measures the ratio of correctly identified instances to all cases and is frequently employed to evaluate the performance of cyberbullying prediction models.

$$Accuracy = \frac{TP + TN}{TP + TN + FP + FN} \# \quad (1)$$

- Precision (equation 2): Precision determines the percentage of relevant tweets among tweets classified as both true positives and false positives for a given category.

$$Precision = \frac{TP}{TP + FP} \# \quad (2)$$

- Recall (equation 3): This metric assesses the proportion of relevant tweets that are correctly identified out of all relevant tweets.

$$Recall = \frac{TP}{TP + FN} \# \quad (3)$$

- F-measure (equation 4): The F-measure offers a unified metric that considers both recall and precision, providing a balanced assessment of both aspects.

$$F1 = \frac{2 * Precision * Recall}{Precision + Recall} = \frac{2 * TP}{2 * TP + FP + FN} \# \quad (4)$$

However, since the dataset is balanced these metrics produced similar numbers; therefore, we report the accuracy of each embedding in (Fig. 5). The bar chart visualization of the results showed that fine-tuning BERT achieved the highest accuracy of 85%, indicating its effectiveness in identifying instances of cyberbullying. Glove and Word2Vec followed closely behind with accuracies of 82% and 81.31%, respectively, showcasing their strong performance as well. The Trainable model, which represents a non-trained approach to word embeddings, achieved an accuracy of 80.2%. We used a batch size of 32

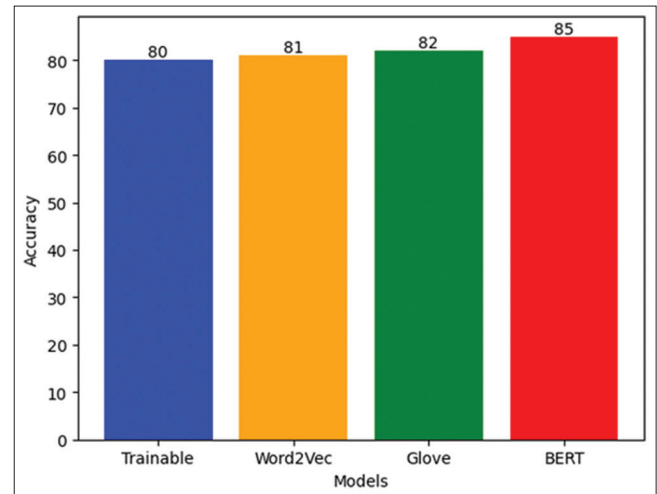


Fig. 5. Accuracy of different word embeddings for the convolutional neural networks-bidirectional long short-term memory model.

and ran the model for six epochs.

Regarding the individual classes of cyberbullying, the two classes of other cyberbullying and non-cyberbullying recorded worse results in all the experiments (Fig. 6) show the accuracy, precision, recall, and F1-score of BERT model. In an attempt to further increase model performance, [30] have used a modified version of this dataset where the other cyberbullying class has been removed from the dataset.

To further investigate the results achieved with our proposed method, we conducted tests using several classical ML algorithms, as shown in Fig. 7: Logistic Regression, KNN, Random Forest, and Naïve Bayes. The data underwent the same preprocessing steps, as described in Fig. 3. Subsequently, we applied the TF-IDF vectorizer to extract features and reduce the dimensionality of the vocabulary.

TF-IDF stands as a numerical metric utilized in information retrieval and text mining. Its purpose is to gauge the significance of a term within a specific document or an entire collection [12]. For our experiments, we allocated 20% of the dataset for testing and used the remaining 80% for training.

For logistic regression, we set the maximum iteration to 300 and chose lbfgs as the solver. As for KNN, we selected

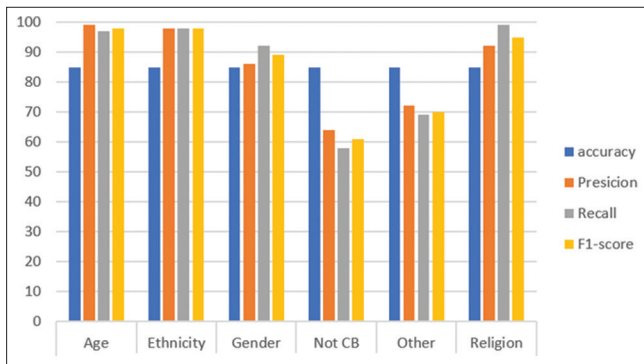


Fig. 6. Bidirectional encoder representations from transformers metrics for the six classes of the dataset.

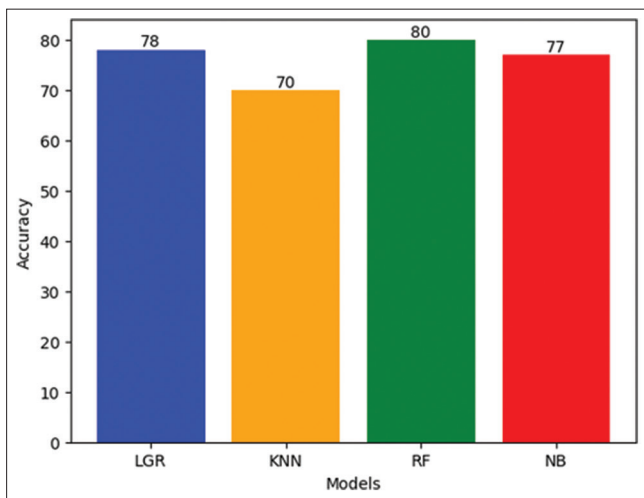


Fig. 7. Accuracy of baseline models.

$k=3$ and used uniform weights. In the case of random forest, we specified a maximum depth of 100. All other hyperparameters were set to the default values provided by the sklearn library [31].

5. CONCLUSION AND FUTURE WORK

This research article focuses on the application of word embeddings for multiclass cyberbullying detection. The study compares the performance of trainable word embeddings, pre-trained word embeddings, and fine-tuning language models using various techniques and models such as CNN and biLSTM, as well as word2vec and BERT.

The research goes beyond simple binary classification and instead focuses on multi-class detection of cyberbullying. By

employing a dataset collected from Twitter, the study explores the effectiveness of different word embedding techniques in detecting cyberbullying types such as religion, gender, ethnicity, age, and others. The preprocessing phase includes actions such as removing links, cleaning text, tokenization, removing stop words, and stemming.

The results indicate that fine-tuning the BERT model on the dataset yields the most promising results. The proposed CNN-BiLSTM model, incorporating word embeddings and deep learning techniques, demonstrates effectiveness in classifying and detecting cyberbullying instances.

In the future, it is important to focus on domain adaptation and transfer learning for cyberbullying detection. Researchers should investigate techniques for adapting models to different social media platforms or domains. Exploring transfer learning approaches that leverage knowledge from related tasks or domains can enhance the performance of cyberbullying detection models. Creating cross-domain datasets will enable the evaluation of domain adaptation and transfer learning techniques in realistic settings. In addition, developing knowledge distillation methods can facilitate the transfer of knowledge to smaller, more efficient models. Real-world evaluations are crucial to measure the effectiveness of domain adaptation and transfer learning techniques, considering variations in data distribution, biases, and user behaviors. By enhancing the generalizability of cyberbullying detection models, we can better address the challenges across diverse platforms and user contexts.

The findings can aid in the development of more accurate and efficient methods for identifying and preventing cyberbullying, particularly in the context of social media platforms.

REFERENCES

- [1] R. S. Tokunaga. "Following you home from school: A critical review and synthesis of research on cyberbullying victimization". *Computers in Human Behavior*, vol. 26, no. 3, pp. 277-287, 2010.
- [2] K. Hellfeldt, L. López-Romero and H. Andershed. "Cyberbullying and psychological well-being in young adolescence: The potential protective mediation effects of social support from family, friends, and teachers". *International Journal of Environmental Research and Public Health*, vol. 17, no. 1, p. 45, 2020.
- [3] K. Rudnicki, H. Vandebosch, P. Voué and K. Poels. "Systematic review of determinants and consequences of bystander interventions in online hate and cyberbullying among adults". *Behaviour and Information Technology*, vol. 42, no. 5, pp. 527-544, 2023.
- [4] H. Rosa, N. Pereira, R. Ribeiro, P. Ferreira, J. Carvalho, S.

- Oliveira, L. Coheur, P. Paulino, A. V. Simão and I. Trancoso. "Automatic cyberbullying detection: A systematic review". *Computers in Human Behavior*, vol. 93, pp. 333-345, 2019.
- [5] F. Elsafoory, S. Katsigiannis, Z. Pervez and N. Ramzan. "When the timeline meets the pipeline: A survey on automated cyberbullying detection". *IEEE Access*, vol. 9, pp. 103541-103563, 2021.
- [6] D. Yin, Z. Xue, L. Hong, B. D. Davison, A. Kontostathis and L. Edwards. "Detection of harassment on web 2.0". *Proceedings of the Content Analysis in the Web*, vol. 2, pp. 1-7, 2009.
- [7] F. Almeida and G. Xexéo. "Word Embeddings: A Survey". arXiv, 2023. Available from: <https://arxiv.org/abs/1901.09069> [Last accessed on 2023 Nov 13].
- [8] D. Yin, Z. Xue and L. Hong. "Detection of Harassment on Web 2.0". In: *Proceedings of the Content Analysis in the WEB*, vol. 2, pp. 1-7, 2009.
- [9] C. Iwendi, G. Srivastava, S. Khan and P. K. R. Maddikunta. "Cyberbullying detection solutions based on deep learning architectures". *Multimedia Systems*, vol. 29, no. 3, pp. 1839-1852, 2023.
- [10] B. A. Talpur and D. O'Sullivan. "Multi-class imbalance in text classification: A feature engineering approach to detect cyberbullying in twitter". *Informatics*, vol. 7, p. 52, 2020.
- [11] A. Bozyiğit, S. Utku and E. Nasibov. "Cyberbullying detection: Utilizing social media features". *Expert Systems with Applications*, vol. 179, p. 115001, 2021.
- [12] A. Aizawa. "An information-theoretic perspective of tf-idf measures". *Information Processing and Management*, vol. 39, no. 1, pp. 45-65, 2003.
- [13] K. Dinakar, R. Reichart and H. Lieberman. "Modeling the Detection of Textual Cyberbullying". In: *Proceedings of the International AAAI Conference on Web and Social Media*, pp. 11-17, 2011. Available from: <https://ojs.aaai.org/index.php/icwsm/article/view/14209> [Last accessed on 2023 Nov 13].
- [14] A. Dewani, M. A. Memon and S. Bhatti. "Cyberbullying detection: Advanced preprocessing techniques and deep learning architecture for Roman Urdu data". *Journal of Big Data*, vol. 8, no. 1, p. 160, 2021.
- [15] S. Agrawal and A. Awekar. Deep learning for detecting cyberbullying across multiple social media platforms. In: G. Pasi, B. Piwowarski, L. Azzopardi and A. Hanbury, Eds. "Advances in Information Retrieval. Lecture Notes in Computer Science". vol. 10772. Springer International Publishing, Cham, pp. 141-153, 2018.
- [16] P. Badjatiya, S. Gupta, M. Gupta and V. Varma. "Deep Learning for Hate Speech Detection in Tweets". In: *Proceedings of the 26th International Conference on World Wide Web Companion-WWW '17 Companion*. ACM Press, Perth, Australia, 2017, pp. 759-760.
- [17] E. Wulczyn, N. Thain and L. Dixon. "Ex Machina: Personal Attacks Seen at Scale". In: *Proceedings of the 26th International Conference on World Wide Web*. International World Wide Web Conferences Steering Committee, Perth Australia, pp. 1391-1399, 2017.
- [18] M. H. Obaid, S. K. Guirguis and S. M. Elkaffas. "Cyberbullying detection and severity determination model". *IEEE Access*, vol. 11, pp. 97391-97399, 2023.
- [19] T. Mikolov, W. Yih and G. Zweig. "Linguistic Regularities in Continuous Space Word Representations". In: *Proceedings of the 2013 Conference of the North American Chapter of the Association for Computational Linguistics: Human Language Technologies*, pp. 746-751, 2013. Available from: <https://aclanthology.org/n13-1090.pdf> [Last accessed on 2024 Jan 10].
- [20] C. Wang, P. Nulty and D. Lillis. "A Comparative Study on Word Embeddings in Deep Learning for Text Classification". In: *Proceedings of the 4th International Conference on Natural Language Processing and Information Retrieval*. ACM, Seoul Republic of Korea, pp. 37-46, 2020.
- [21] M. Das, S. Banerjee and P. Saha. "Abusive and Threatening Language Detection in Urdu Using Boosting based and BERT based Models: A Comparative Approach". arXiv, 2021. Available from: <https://arxiv.org/abs/2111.14830> [Last accessed on 2024 Jan 10].
- [22] S. Gaikwad, T. Ranasinghe, M. Zampieri and C. M. Homan. "Cross-lingual Offensive Language Identification for Low Resource Languages: The Case of Marathi". arXiv, 2021. Available from: <https://arxiv.org/abs/2109.03552> [Last accessed on 2024 Jan 10].
- [23] D. Saha, N. Paharia, D. Chakraborty, P. Saha and A. Mukherjee. "Hate-Alert@DravidianLangTech-EACL2021: Ensembling Strategies for Transformer-based Offensive Language Detection". arXiv, 2021.
- [24] A. M. Ishmam and S. Sharmin. "Hateful Speech Detection in Public Facebook Pages for the Bengali Language". In: *2019 18th IEEE International Conference on Machine Learning and Applications (ICMLA)*, IEEE, pp. 555-560, 2019.
- [25] R. Cao, R. K. W. Lee and T. A. Hoang. "DeepHate: Hate Speech Detection Via Multi-Faceted Text Representations". In: *12th ACM Conference on Web Science*. ACM, Southampton United Kingdom, pp. 11-20, 2020.
- [26] J. Wang, K. Fu and C. T. Lu. "Sosnet: A Graph Convolutional Network Approach to Fine-grained Cyberbullying Detection". In: *2020 IEEE International Conference on Big Data (Big Data)*, IEEE, pp. 1699-1708, 2020.
- [27] T. Mikolov, I. Sutskever, K. Chen, G. S. Corrado and J. Dean. "Distributed Representations of Words and Phrases and Their Compositionality". In: *Advances in Neural Information Processing Systems*. vol. 26, 2013. Available from: [Last accessed on 2024 Jan 10].
- [28] J. Pennington, R. Socher and C. D. Manning. "Glove: Global Vectors for Word Representation". In: *Proceedings of the 2014 Conference on Empirical Methods in Natural Language Processing (EMNLP)*, pp. 1532-1543, 2014.
- [29] J. Devlin, M. W. Chang, K. Lee and K. Toutanova. "BERT: Pre-training of Deep Bidirectional Transformers for Language Understanding". arXiv, 2019. Available from: <https://arxiv.org/abs/1810.04805> [Last accessed on 2024 Jan 10].
- [30] T. H. Aldhyani, M. H. Al-Adhaileh and S. N. Alsubari. "Cyberbullying identification system based deep learning algorithms". *Electronics*, vol. 11, no. 20, p. 3273, 2022.
- [31] F. Pedregosa, G. Varoquaux, A. Gramfort, V. Michel, B. Thirion, O. Grisel, M. Blondel, P. Prettenhofer, R. Weiss, V. Dubourg, J. Vanderplas,... and E. Duchesnay. "Scikit-learn: Machine learning in python". *Journal of Machine Learning Research*, vol. 12, pp. 2825-2830, 2011.

Iraqi Kurd or Arab Male Authenticity Detection Based on Facial Feature



Bnar Abdulsalam Abdulrahman¹, Nama Ezzaalddin Mustafa²

¹Department of Computer, School of Science, Komar University of Science and Technology, Sulaymaniyah, Iraq,

²Department of Computer Science, School of Science and Engineering, University of Kurdistan-Hewler, Erbil, Iraq

ABSTRACT

As an inherent human characteristic, ethnicity plays a fundamental and critical role in biometric identification. On the other hand, the human face is the core of man's identity, and facts such as age and race are often extrapolated automatically from the face. The objective is to utilize computer technologies to identify and categorize ethnic groups based on facial features. Convolutional neural networks (CNN), which can automatically identify underlying patterns from data, excel at learning image features and have shown state-of-the-art performance in several visual recognition challenges, such as ethnicity detection. Although the automated classification of traits such as age, gender, and ethnicity is a well-researched topic, Iraqi ethnic groupings have not yet been addressed. This study seeks to tackle the challenge of predicting the ethnicity of Iraqi male individuals based on their facial traits for the two largest ethnic groups, the Arabs, and the Kurds. Male Iraqi Kurds and Arabs were each represented by 260 image samples. The dataset underwent a diverse array of preprocessing and data enhancement techniques, including image resizing, isolation, gamma correction, and contrast stretching. Moreover, to augment the dataset and expand its diversity, various techniques such as brightness adjustment, rotation, horizontal flip, and grayscale augmentations were systematically applied, effectively increasing the overall number of images, and enriching the dataset for improved model performance. Face images of Kurds and Arabs were classified using the Faster region-based CNN (RCNN) approach of deep learning. Due to insufficient data in the dataset, we propose employing transfer learning to extract features using several pre-trained models. Specifically, we examined EfficientNetB4, ResNet-50, SqueezeNet, VGG16, and MobileNetV2, resulting in accuracies of 96.73%, 94.91%, 93.39%, 92.48%, and 90.32%, accompanied by corresponding precision values of 0.86, 0.81, 0.80, 0.70, and 0.69, respectively. It is essential to emphasize that the following inference speeds – VGG16 (4.5 ms), ResNet-50 (4.6 ms), SqueezeNet (3.8 ms), MobileNetV2 (3.7 ms), and EfficientNet-B4 (16 ms) – represent the computing times needed for each backbone. Moreover, to achieve a harmonious trade-off between precision and the time required for inference, we chose ResNet-50 as the foundational framework for our model aimed at classifying ethnicity. The study also acknowledges limitations such as the availability and diversity of the dataset. Nevertheless, despite these limitations, it provides valuable perspectives on the automated prediction of Iraqi male ethnicity through facial features, presenting potential applications in various domains. The findings contribute to the broader conversation surrounding biometric identification and ethnic categorization, underscoring the importance of ongoing research and heightened awareness of the inherent limitations associated with such studies.

Index Terms: Faster Region-based Convolutional Neural Network, Convolutional Neural Networks, Detection, Iraq, Ethnicity

Access this article online

DOI:10.21928/uhdjst.v8n1y2024.pp64-77

E-ISSN: 2521-4217

P-ISSN: 2521-4209

Copyright © 2024 Abdulrahman and Mustafa. This is an open access article distributed under the Creative Commons Attribution Non-Commercial No Derivatives License 4.0 (CC BY-NC-ND 4.0)

1. INTRODUCTION

Biometric recognition, particularly facial recognition, plays a pivotal role in various domains such as surveillance, advertising, human-computer interaction (HCI), and social media profiling. Ethnicity is a vital component in biometric

Corresponding author's e-mail: Bnar Abdulsalam Abdulrahman, Komar University of Science and Computer Department, School of Science, Komar University of Science and Technology, Sulaymaniyah, Iraq. E-mail:bnar.abdulsalam@komar.edu.iq)

Received: 19-12-2023

Accepted: 18-02-2024

Published: 03-03-2024

recognition. Classifying individuals by race, nationality, and ethnicity substantially affects HCI, surveillance, and military contexts. Improving understanding of ethnicity has the potential to dramatically accelerate the development of inclusive and culturally sensitive technology in the field of HCI. Designing user interfaces that recognize and adapt to a wide range of ethnic origins makes technology more accessible to a greater range of users. This understanding extends to facial recognition systems, making them more accurate and sensitive to cultural differences. Precise classification of ethnic groups can also lead to advances in surveillance and security applications, such as border control, customs inspections, and public safety measures. In military situations, proper ethnicity identification is critical for information gathering and developing efficient communication strategies [1].

Continually shifting populations reshape the collective identities of regions, nations, and races. Even though it is complex, categorizing individuals by race and ethnicity has aided national censuses and national security in many nations. The classification process is also an important topic in social science, and it is helpful in studies of health care, education, and socioeconomic status [2]. It is economically significant in market research, especially in multiethnic nations.

Iraq is among the nations with the most significant number of ethnic groups. The current demographics of Iraq reveal a multiethnic, multicultural nation sharing the same landmass. According to World Bank statistics, Iraq's population is around 43 million and comprises several ethnic groups [3]. Arabs and Kurds are the majority, while Christians, Turkmen, Assyrians, and Yezidis are the minority. According to estimates, 75–80% of the population is Arab, while 15–20% is Kurdish [4]. Figs. 1 and 2 visually represent the main ethno-religious groups in Iraq and showcase individuals in their traditional attire, respectively.

In recent years, studying racial and ethnic groupings based on facial images has become a vital face recognition issue [2]. Faces provide a great deal of information, including identification, gender, age, ethnicity, expression, *et cetera*. Consequently, there has been a rise in interest in automated face ethnicity classification, and various methods have been created. In an uncontrolled context, it is not easy to properly and efficiently distinguish different races based merely on a human face. Face images must contain racial sensitivity for classification to be effective. These distinctive features may be categorized into chromatic/skin tone and local and global characteristics [5]. Due to the uniformity of skin color

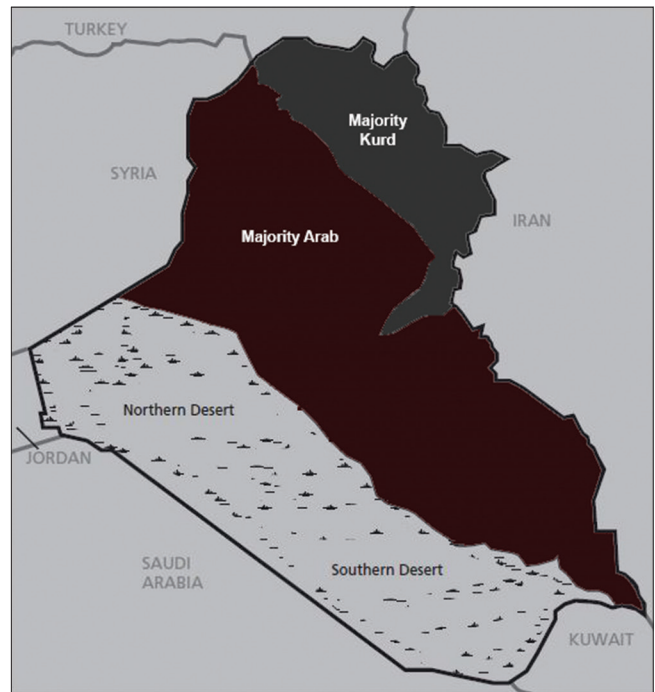


Fig. 1. Main ethnoreligious groups in Iraq.



Fig. 2. Kurdish and Arabs in traditional dress.

between races and the variability of lighting conditions in everyday life, skin tone cannot be used to identify persons on its own. The addition of local or global descriptors may enhance the accuracy of categorization.

Humans have an innate aptitude for facial recognition, enhanced by cultural and cognitive processes, which permits the human visual system to comprehend familiar faces quickly and effectively. Genes, environment, culture, and other variables frequently impact facial characteristics [6].

Nevertheless, the genes of a particular ethnic group are rarely unique and may contain DNA pieces from various ethnic groups. As a result, there may be facial resemblance across various races. It is vital to utilize cognitive and perceptual intelligence while examining the facial traits of people of

different races. This means being able to see subtle variations influenced by genetics, environment, and cultural factors. In addition, the application of advanced technologies and intelligent algorithms contributes to the accurate analysis of facial features.

Considering the previously mentioned aspects, this research aims to construct a system for classifying males within Iraq's principal ethnic groups – namely, the Arabs and Kurds. Nonetheless, distinguishing between Kurds and Arabs based solely on ethnic traits poses significant challenges. Fig. 3 underscores this difficulty, revealing that individuals from these two ethnic groups often share similarities in facial features, including skeletal structure, eye color, nose size, and eye size. The primary distinguishing features, as highlighted in Fig. 4, include skin color and lip shape. However, it is important to note that there are instances where the differentiation based on skin tone and lip shape becomes challenging as well due to occasional similarities between the two groups. While skin color may initially appear to be a significant distinguishing factor, the presence of color variations within the same ethnic group complicates the categorization process based solely on this characteristic. Consequently, the manual extraction of features becomes a complex task.

To overcome these challenges, this research leverages deep learning techniques [7], specifically convolutional neural networks (CNN), to develop a model capable of distinguishing between Kurds and Arabs effectively.

Meanwhile, it is not easy to build a deep learning model without data, which is required for models to gain experience and the capacity to make predictions based on the provided data. Training datasets must be provided to the learning algorithm for deep learning models to learn how to do various tasks, followed by testing and validation datasets to ensure the model processes the data successfully. The quality of its training data hampers every deep learning technique [8]. Due to this and the fact that, as far as is known, there are no current datasets for ethnicity identification in Iraq, this study aimed to provide a suitable dataset to address this issue.

2. RELATED WORKS

Face ethnic identification has gained prominence during the last decade. Numerous research has been conducted to manually extract racial face features through a range of traditional machine learning approaches, and recently,



Fig. 3. Kurdish and Arab facial characteristics.



Fig. 4. Kurdish and Arab face characteristics differ from each other.

the efficient and speedy methods of the deep learning methodology have been used for end-to-end facial detection.

Starting with the traditional approach, one of these researchers, Lin *et al.* 2006 [9], introduced a method for analyzing face images, combining the Gabor filter to extract key facial features, AdaBoost learning to select a series of simple classifiers, and Support Vector Machine (SVM) classifier to recognize the face images. The system has been implemented on the FERET dataset, which focuses on human face images. This approach detects Mongoloid, Caucasian, and African ethnicity classifications. This study demonstrated remarkable accuracy in the identification of

gender, ethnicity, and age from facial images. Notably, it attained an accuracy of 91.58% for females and 90.40% for males, 89.05% for individuals of yellow ethnicity and 89.28% for those of white ethnicity, and 91.77% for younger age groups and 90.32% for older age groups. These results underscore the system's effectiveness in the realm of facial recognition.

Following that on the FERET dataset, Manesh *et al.* 2010 [10] offered a two-class ethnicity categorization for Asian and non-Asian images. The approach assesses the confidence of distinct face areas by applying a modified Golden ratio mask followed by an SVM classifier on facial characteristics such as the eyes, nose, and mouth rather than the whole image. Ensuring that facial patches are in a consistent position for comparison is deemed crucial in face processing. The algorithm they introduced yielded a notable accuracy of 94% on the dataset.

Furthermore, Xie *et al.* [11] proposed a technique for classifying ethnicity on massive face datasets using Kernel Class-dependent Feature Analysis (KCFA) and color-based facial traits. It targets the periorbital region as opposed to the whole face. The experiment used both public and self-collected datasets. Their proposed method exhibits remarkable accuracy, achieving an impressive rate of around 96% in classifying individuals into three distinct ethnic categories: Caucasian, African American, and Asian.

Moving further to the deep learning approach, Wang *et al.* 2016 [7] provide a unique solution to the issue of ethnicity classification using Deep Convolution Neural Networks (DCNN) to extract and categorize characteristics concurrently. Their proposed strategy undergoes rigorous testing across three scenarios: The classification of White and Black, Chinese and Non-Chinese, and Han, Uyghur, and Non-Chinese individuals. The evaluation is conducted using several widely recognized face image databases, including MORPH-II, CASIA-PEAL, and CASIA-WebFace. The outcome of this study illustrates the effectiveness of the suggested method compared to the previous approaches. Nevertheless, the trained model exhibits limited generalization capability when confronted with diverse factors, such as variations in illumination and head pose. Moreover, Srinivas *et al.* 2017 [12] investigated the fine-grained ethnic categorization of the Eastern Asia population. They introduce a new dataset Wild East Asian Face (WEAFD) Dataset that contains seven ethnic groups (Chinese, Filipino, Indonesian, Japanese, Korean, Malaysian, and Vietnamese). This dataset is well suited for performing

age, gender, and detailed ethnicity classification tasks. They used CNN to obtain baseline data for the WEAFD. The findings show that determining a person's precise ethnicity is the hardest challenge, followed by determining their age and gender. Furthermore, Masood, *et al.* 2018 [13] utilized a CNN and Artificial Neural Network (ANN) in the FERET dataset to predict three ethnicities: Mongolian, Caucasian, and Negro. Both experiments successfully addressed the task of ethnicity classification. The CNN model outperformed the ANN approach, achieving an impressive accuracy of 98.6%, whereas the ANN approach yielded a comparatively lower accuracy of 82.4%. Recently, Belcar *et al.* 2022 [14] provided an overview of recent advancements in ethnicity classification with an emphasis on CNNs and suggested a novel approach for ethnicity classification utilizing just the central portion of the face and CNN. They used the UTKFace and FairFace datasets, for categorizing (White, Black, Latin, Indian, Middle Eastern, East Asian, and Southeast Asian). In their study, they ascertained that the area encompassing the nose and eyes holds the most significant concentration of visual data, playing a pivotal role in achieving successful ethnicity classification.

Furthermore, Chen *et al.* 2016 [15] used a K-nearest neighbor technique, an SVM classifier, a two-layer neural network, and a CNN to train a classifier to predict Chinese, Japanese, and Korean. Before being put into various learning techniques, the face images were first cropped and augmented. CNN had the highest accuracy rate, at 89.2%. However, the CNN displayed overfitting on new images, suggesting that more varied data and GPU utilization are required for improved outcomes in the future.

Besides this, some studies employed a hybrid strategy, Heng *et al.* 2018 [16] present a hybrid supervised learning strategy for performing ethnicity categorization that utilizes both the power of CNN and the abundant network-obtained information. A supervised hybrid SVM learning method is designed to train the combined feature vectors for ethnicity classification. A dataset including Bangladeshi, Chinese, and Indian ethnic groups is used to test the effectiveness of the suggested technique, which obtained an overall accuracy of 95.2%.

Likewise, Aina *et al.* 2022 [17] created a CNN model for identifying the ethnicity of Nigerians based on face images using transfer learning methods and VGG-16 architecture. The model's evaluation was conducted using a dataset comprising images of Nigerian ethnic groups, namely Yoruba, Hausa, and Igbo, achieving an impressive accuracy

of 92.86%. The research demonstrated that their novel model excels in tasks related to ethnicity classification, particularly when confronted with an exceptionally limited and imbalanced dataset.

3. METHODOLOGY

Several steps comprise the approach outlined in this study. Since no dataset existed for Iraq-specific identification of Arab and Kurdish ethnicity, it was required to create one. A collection of 130 images was assembled for each ethnic group, resulting in a combined dataset of 260 images. While collecting images, male Kurds and Arabs aged 18–70 were observed.

3.1. Pre-Processing

Due to variations in lighting and camera characteristics, the images require to be adjusted before further processing. To address this, the dataset underwent the following preprocessing methods:

- Image resizing is conducted since it alters the size of the images and, if necessary, stretches them to a more suitable pixel-by-pixel size. That will help optimize both training time and computational power. Furthermore, a consistent input size is required by several models, most notably CNNs, necessitating image resizing to ensure accurate processing of inputs.
- Item isolation, which is the ability to isolate an object inside a frame. In other words, implementing this process on the dataset amplifies the intensity of facial features while diminishing the intensity of non-facial elements. After this treatment, only the facial portion of the image is retained [18]. We adopt this approach because our study exclusively focuses on the facial region, which, in turn, plays a pivotal role in achieving enhanced accuracy in our findings.
- Gamma adjustment is employed to enhance visibility in high and low-light conditions by modifying brightness. A gamma value exceeding one results in darker images, while a value less than one produces brighter images. Following the determination of the average intensity level in the region, a new gamma value is selected for optimization [19]. Fig. 5 demonstrates the need to control unnecessary amplification in initially bright images and illuminate each image based on its actual brightness. We incorporate this approach into the dataset to guarantee perceptual uniformity and consistent picture quality throughout the entire set, given the critical role of

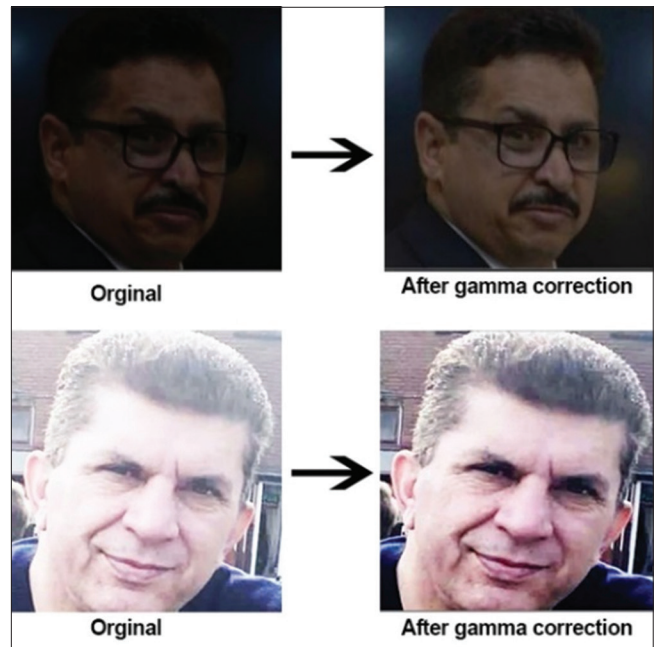


Fig. 5. Correction of images using gamma.

constant brightness and contrast in object recognition tasks.

- Contrast stretching is an image enhancement technique that attempts to improve the contrast in an image by “stretching” the range of intensity values it contains to span a desired range of values [19]. Some of the images in our collection have insufficient or excessive contrast; thus, preprocessing the image contrast is advantageous. This is used because contrast preprocessing makes edges more visible by amplifying the contrasts between surrounding pixels; it also enhances normalization and line identification under various lighting situations and makes the data simpler for recognition models to understand. The image in Fig. 6 depicts the various preprocessing techniques applied to the dataset.

3.2. Data Augmentation

In addition, following preprocessing, data augmentation techniques are used to enhance the number of training samples and minimize overfitting. The following techniques have been applied to the dataset:

- The first augmentation technique applied is brightness to make the model more adaptable to lighting and camera settings, which alters the brightness of the images by randomly darkening and brightening the average intensity channel [20]. The intensity level is a representation of how light or dark each pixel is in the image.

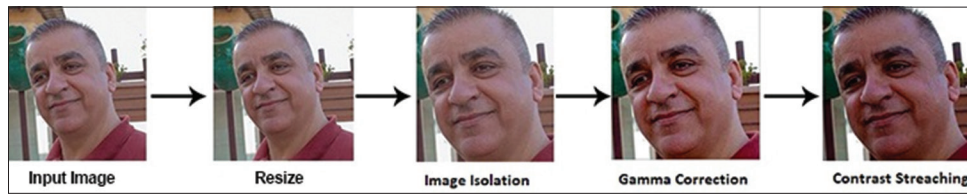


Fig. 6. Preprocessing techniques employed.

- Furthermore, rotation augmentation is incorporated, which is a crucial upgrade since it modifies the angles at which objects appear in the training dataset; this will introduce variety to rotations and make the model more resistant to camera roll. This strategy may increase diversity to prevent a model from retaining training data and becoming camera orientation insensitive. Along with adding a horizontal flip to make the model face orientation insensitive [20].
- Finally, the grayscale augmentation approach is employed to include grayscale and RGB images in the training set [21]; hence, our model will not rely on skin color to differentiate Arab and Kurdish males since Kurds often have lighter skin than Arabs.



Fig. 7. Augmentation techniques applied.

Fig. 7 illustrates the application of augmentation techniques to our dataset, leading to a growth in the training set size to 1,093 images. Adhering to best practices, data augmentation was exclusively performed on the training set, while the test set and validation set retained only the original, non-augmented data. In addition to integrating data augmentation methods during the preprocessing phase, we systematically evaluated their impact on the model’s performance using thorough validation and testing protocols. Our aim was to confirm that these augmentation techniques not only enriched the variety within the training dataset but also translated into heightened generalization and resilience when assessing the model. The findings offered valuable insights into the model’s generalization capabilities and the real-world effectiveness of the augmentation strategies in unfamiliar scenarios.

3.3. Faster RCNN

This research investigates the accuracy and speed of inference provided by Faster RCNN, a neural network that achieves exceptional levels of both efficiency and accuracy for image classification applications.

This algorithm is one of the most well-known object detection architectures based on convolution neural networks (CNN). The architecture of the model comprises the network backbone, the region proposal network (RPN), and the fast RCNN algorithm, an older version of this method, as shown in Fig. 8

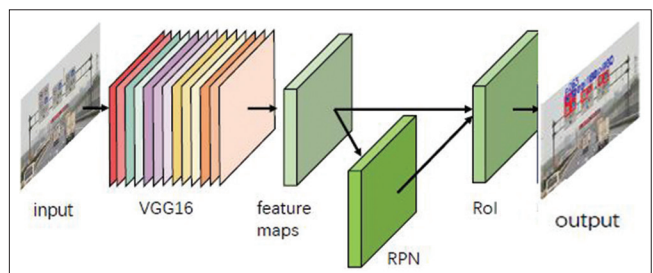


Fig. 8. Faster RCNN Algorithm [24].

- **Backbone Network:** The backbone is a feature extraction network with pre-trained deep neural network architectures. This network is usually pre-trained on extensive datasets, specifically designed for tasks such as image classification. The backbone operates by producing high-resolution feature maps, effectively capturing hierarchical features from the input image.

- **Region Proposal Network (RPN):** The RPN is responsible for suggesting potential regions within the image where objects could potentially exist. It predicts a classification score and bounding boxes which are dual predictions: Estimating the probability of an object's presence in a proposed region and determining the coordinates for a bounding box encapsulating that object. To achieve this, the network employs predetermined anchor boxes, pre-defined boxes with various scales, and aspect ratios on the images. These anchor boxes serve as the basis for generating region proposals, tiny portions of an image. The classification score determines whether all anchors contain an object. The bounding box regressions are used to identify the anchors' items accurately. In addition, to address the issue posed by the varying sizes of region proposals, a technique called Region of Interest Pooling (ROI pooling) is employed. ROI pooling ensures the generation of fixed-size feature maps, streamlining the processing for subsequent layers. This strategy overcomes the limitations linked to fully connected layers, thereby improving the model's capability to effectively handle regions of interest with different sizes.
- **Fast RCNN:** The last part of the architecture takes high-resolution feature maps from the network backbone and region proposals from the region proposal network. Moreover, by employing ROI pooling, the model acquires fixed-size feature maps for each region proposal. Subsequently, these fixed-size feature maps are inputted into fully connected layers to produce SoftMax scores for each class and revised bounding boxes for region proposals [22].

3.3.1. Backbone Networks

The selection of an appropriate network will directly impact the accuracy of the model for feature extraction. Numerous networks have been suggested and have become well-known pre-trained networks used for Deep Learning (DL) models in any AI endeavor. These networks are used for feature extraction or as backbones at the beginning of any DL model. A backbone is a well-established network that has been taught for several previous jobs and exhibits its efficacy. Commonly used backbones include VGG16, ResNet-50, SqueezeNet, MobileNetv2, and EfficientNet-B4. This study examines these currently common backbones to see which one provides a superior outcome when used with faster RCNN for ethnicity categorization.

3.3.1.1. VGG16

VGG16, one of the CNN algorithms, is one of the most advanced computer vision models. The 16 in VGG16

represents 16 weighted layers. There are 21 layers, consisting of 13 convolutional layers, five Max Pooling layers, and three dense layers, but only 16 weight layers (learnable parameters layer). VGG16 accepts 224 by 244 input tensors with three RGB channels. In place of a considerable number of hyper-parameters, VGG16 focuses on convolution layers of 3×3 filters with stride one and always uses the same padding and MaxPool layers of 2×2 filters with stride 2. The convolution and max pool layers are organized appropriately throughout the whole design. Conv-1 layer has 64 filters, Conv-2 contains 128 filters, Conv-3 contains 256 filters, and Conv 4 and Conv 5 have 512 filters. In addition, a stack of convolutional layers is followed by three fully connected (FC) layers: The first two have 4096 channels each, while the third does classification and has 1000 channels (one for each class). Soft-max layer is the last layer [23]. Fig. 9 illustrates the design of VGG16.

The rationale behind choosing VGG16 as the backbone stems from its simplicity and effectiveness in architecture and proven success in various computer vision tasks with its deep 16-layer structures, utilization of small 3×3 convolutional filter, and consistent filters, VGG16 emerges as a dependable choice for feature extraction tasks.

3.3.1.2. ResNet-50

ResNet-50 is a CNN with 50 layers (48 convolutional layers, one MaxPool layer, and one intermediate pool layer). ResNet50, like VGG16, accepts input tensors of sizes 224 and 244 with three RGB channels.

As seen in Fig. 10, ResNet's design includes convolution with a kernel size of 7×7 and 64 different kernels, each of which has a stride size of 2. Afterward, there is a maximum pooling size of 2 strides. In the second convolution, there is a $1 \times 1,64$ kernel, then a $3 \times 3,64$ kernel, and finally a $1 \times 1,256$ kernel; these three layers are repeated three times, resulting in a total of nine layers. Following that, there is a kernel of $1 \times 1,128$, then a kernel of $3 \times 3,128$, and lastly, a kernel of $1 \times 1,512$. This procedure is done four times for a total of twelve layers. In addition, there is a kernel of 1×1256 and two different kernels of $3 \times 3,256$ and $1 \times 1,1024$, and this pattern is repeated six times for a total of 18 layers. And then again, a $1 \times 1,512$ kernel followed by two additional instances of $3 \times 3,512$ and $1 \times 1,2048$, repeated three times to produce a total of nine layers. After that, there is an average pool, which concludes with a wholly linked layer having 1000 nodes and, in the end, a SoftMax function [23].

ResNet-50 is a widely adopted backbone due to its ability to manage deeper networks through residual connections

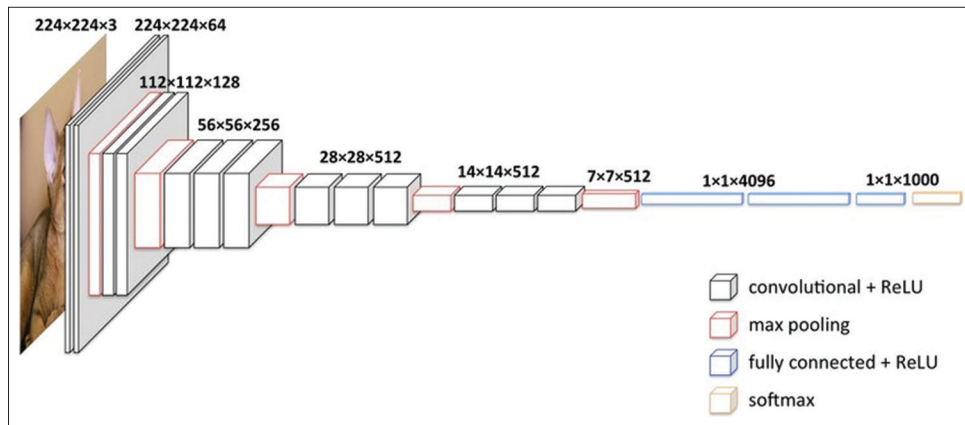


Fig. 9. The architecture of VGG-16 [28].

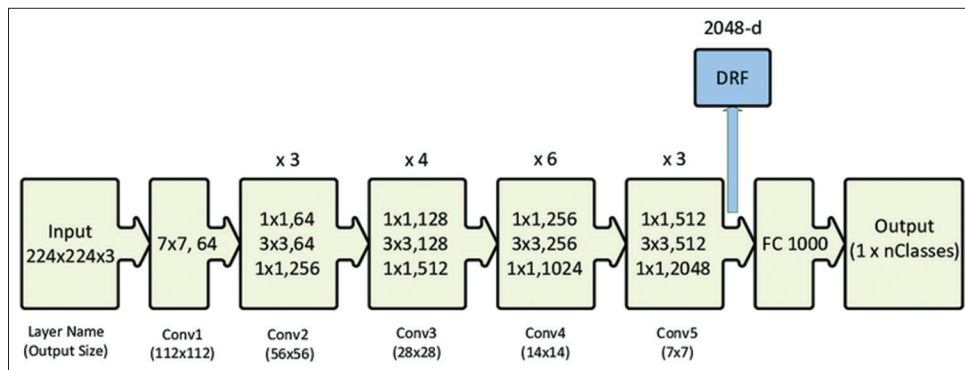


Fig. 10. The architecture of ResNet-50 [22].

and residual blocks. These features address the vanishing gradient problem, enabling the training of exceptionally deep networks and minimizing issues associated with vanishing gradients, making ResNet-50 a reliable option for object detection.

3.3.1.3. SqueezeNet1

SqueezeNet is a deep neural architecture that involves a “squeezed” network for training image classification models. The goal of inventing SqueezeNet was to construct a smaller neural network with fewer parameters (therefore requiring fewer calculations, less memory, and a shorter inference time) that can readily fit into memory devices and be communicated over a computer network with cutting-edge precision [24].

The primary goal of the work was to discover CNN architectures with minimal parameters and competitive accuracy. Therefore, they developed these strategies for improved implementation; they substituted 3 × 3 filters with 1 × 1 filters and used squeeze layers to reduce the number of input channels to 3 × 3 filters, so they deliberately reduced the

number of parameters in a CNN while aiming to maintain accuracy. In addition, they down-sampled late in the network such that the activation maps of the convolution layers are large. Here, the theory is that more great activation maps (due to delayed down sampling) may lead to better classification accuracy, everything else remaining equal, and thus will optimize classification accuracy on a restricted parameter allocation.

This model has an image input size of 227 × 227. It consists of convolution layers to extract features, fire modules consisting of a squeeze convolution layer (1×1 filters alone) feeding into an expanded convolution layer with a mixture of 1 × 1 and 3 × 3 convolution filters. Thus, the number of inputs is restricted to 1 × 1, resulting in dimension reduction (limited number of channels). Finally, there are pooling layers for performing down-sampling [24]. Fig. 11 depicts the architectural design of SqueezeNet.

SqueezeNet is chosen for its lightweight design, making it ideal for limited computational resources. It achieves similar

performance as larger models with fewer parameters, and its use of 1×1 convolutions reduces parameter count while maintaining expressive capabilities.

3.3.1.4. MobileNet-v2

MobileNet-v2 is a CNN that has been purposefully developed to function optimally in resource-limited and mobile contexts. This model allows any input size more than 32×32 , and the system's performance is improved for images with larger dimensions. In addition, it has 53 layers of convolution, each of which is either a 1×1 convolution or a 3×3 depth-wise convolution. This model uses two distinct blocks: A residual block with a stride of 1 and a block with a stride of 2 used for downsizing. In addition, there are three layers for each kind of block: The first layer is a 1×1 convolution using the ReLU6 algorithm, the second layer is the depth-wise convolution, and the third layer is another 1×1 convolution, but this time without any non-linearities [25]. Fig. 12 depicts an illustration of the architecture of MobileNet-v2.

MobileNetv2 is chosen for its optimal performance on mobile and edge devices, balancing model size, and accuracy. It optimizes computational resources, using inverted residuals and linear bottlenecks while maintaining accuracy.

3.3.1.5. EfficientNet-B4

Constructing neural networks that use convolutional layers require a specific amount of time and resources. When more resources are available, these networks are built later to achieve better degrees of precision. In which the intuition behind the networks is that if the input image is larger, the network needs more layers to increase the receptive field and more channels to capture more fine-grained patterns on the larger image. The network can get away with fewer layers and channels if the input image is smaller [26]. The traditional conventional approaches to model scaling are random; models are scaled in the direction of depth or width. This approach of randomly scaling models requires a substantial amount of manual tuning in addition to person-hours, and the result is frequently either insignificant or nonexistent performance increases. On the other hand, EfficientNet suggested scaling up CNN models to achieve more accuracy and efficiency in a manner far more virtuous using a compound coefficient that scales each dimension consistently using a specified set of scaling coefficients. The concept is to scale with a constant ratio to achieve a balanced relationship between the image's width, depth, and resolution [26].

The architecture of EfficientNet, as shown in Fig. 13, uses a mobile inverted bottleneck convolution, which is quite like

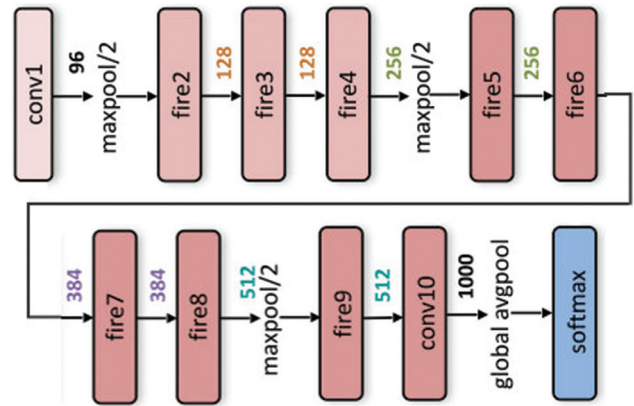


Fig. 11. The architecture of SqueezeNet [29].

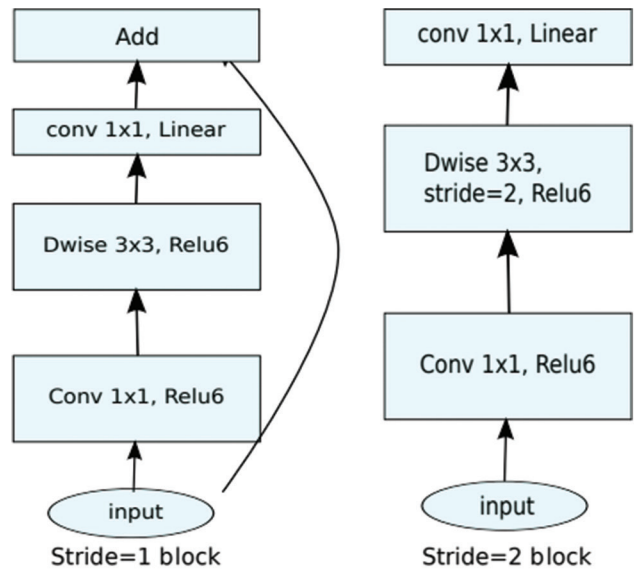


Fig. 12. The architecture of MobileNet-v2 [25].

MobileNet V2 but is much more complex due to the rise in FLOPS. To create the family of EfficientNet, this basic model is expanded to its full extent [27]. In addition, this model takes input images of shapes 224×224 .

The decision to choose EfficientNet models is grounded in their recognized efficiency, achieved through simultaneous scaling of the model's depth, width, and resolution. Specifically, EfficientNet-B4 is selected for its adept balance between model size and performance. This model introduces a compound scaling method, which efficiently adjusts the model's dimensions, contributing to improved accuracy.

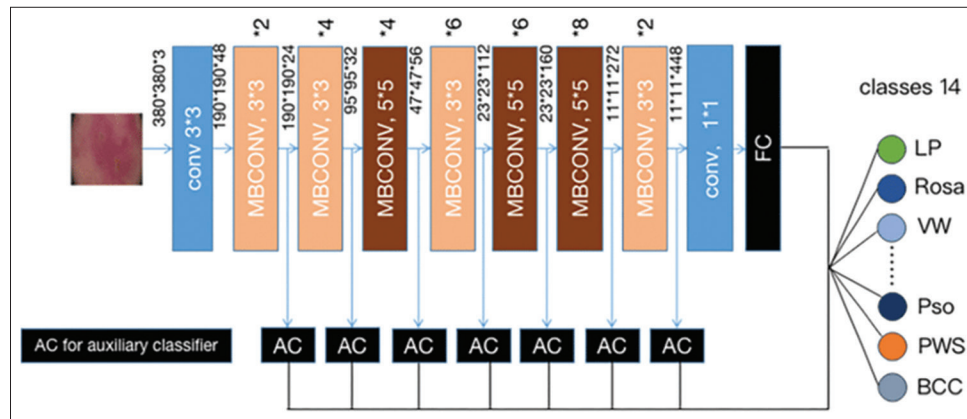


Fig. 13. The architecture of EfficientNet-B4 [30].

4. EXPERIMENTAL RESULTS

In this section, we will begin by describing the dataset partitioning utilized in the study, and then, we will present the findings for Faster RCNN. We have decided to use faster R-CNN as an object detector due to its widespread application and highly accurate object detection that has been reported for various applications. We trained the model using five different backbones, namely VGG16, ResNet-50, SqueezeNet, MobileNetv2, and EfficientNet-B4, to determine whether increased layer depth and model complexity had a positive impact on the detector's overall performance.

4.1. Splitting the Dataset

Since there are no pre-defined established criteria for separating a dataset, researchers often consider the size of the dataset as one of the splitting parameters. Splitting the dataset is required for unbiased evaluation of prediction performance and is often performed to prevent overfitting [25]. We have tried partitioning the dataset to avoid biased results or false impressions. The ratio for the training set is 0.7 to ensure that the model has sufficient data to learn. In addition, 0.2 is specified for the validation set to guarantee that it will lead to accurate model tuning. The remaining 0.1 is reserved for the test set to know how the model would perform on unseen data.

The dataset contains 260 images, each 130 for one of the Kurdish and Arab ethnicities. After splitting and applying data augmentation techniques, there are 1093 images in the training set, 52 in the validation, and 27 in the test set.

4.2. Training and Testing Phases

At first, several hyperparameters were examined in an effort to optimize the Faster R-CNN model's performance.

The model fine-tuning procedure uses a systematic approach with the dual goals of reducing validation losses and enhancing training accuracy. The initial stage in the process was selecting appropriate learning rates according to the architectures that are being used. For VGG16, ResNet-50, and EfficientNet-B4 backbones, the best performance was obtained at a learning rate of 0.001. On the other hand, networks such as SqueezeNet and MobileNetv2 performed better when their learning rate was set to 0.01. In addition, another crucial aspect of the fine-tuning procedure was the thoughtful selection of the batch size. After a thorough investigation of various batch sizes, it was found that 64 was the optimal batch size for the best results. This choice brought computational efficiency and model performance into a perfect balance.

Determining the maximum number of iterations was a crucial choice that determined how well the model worked. This value was first set at 60,000 iterations and was dynamically adjusted. The number of iterations was raised in situations when the validation accuracy indicated improvement. On the other hand, the number of iterations was reduced if overfitting was found. By ensuring that the model was trained for the ideal amount of time, this adaptive technique reduced the likelihood of both underfitting and overfitting.

We carried out iterative trials with hyperparameters, learning from the model's performance on both training and validation sets, with the goal of having the optimum fine-tuning procedure. For optimal performance, this iterative refinement aimed to match the Faster R-CNN model with the particulars of the task and dataset.

Regarding the results, the following points elucidate the key outcomes attained in terms of both accuracy and inference time on our dataset:

- EfficientNet-B4: Achieved the highest accuracy, but with the slowest inference time.

- MobileNetv2: Provided faster inference, but at the cost of the lowest accuracy.
- ResNet-50: Balanced accuracy, with a reasonable inference time.

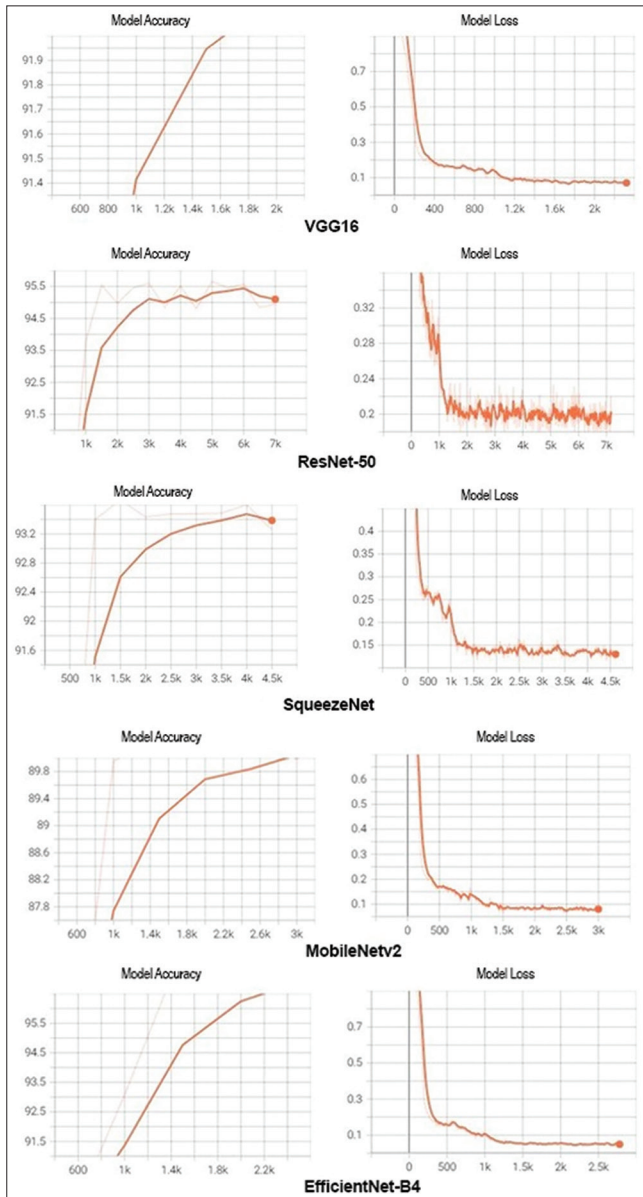


Fig. 14. Training and validation loss and accuracy metrics resulted from Faster RCNN with different backbones.

The findings are shown in Table 1 when a separate backbone was used as a feature extraction network for the Faster RCNN. Fig. 14 displays the training loss and accuracy learning curves for each of the five backbones used in this research.

As seen from Table 1, our model attained more accuracy when using EfficientNet-B4, with an average mAP of 96.73%; however, its inference time is very sluggish compared to that of other networks since it takes 16 ms to identify a single image. Although Faster RCNN employing MobileNetv2 fared better, with an average inference speed of 3.7 ms, the accuracy is relatively poor compared to other backbones, which had an accuracy of 90.32%. On the other hand, when it comes to the problem of ethnicity categorization, it is preferable to have a model that combines high accuracy with a short inference time. Because of this, the model which makes use of ResNet-50 will be used to address the issue of ethnicity classification in Iraq. This model has a maximum accuracy percentage of 94.91% and an operating time of 4.6 ms for classifying a single image.

The decision to adopt ResNet-50 as the definitive model for ethnicity categorization in our study was reached after a thorough evaluation considering practical factors for real-world deployment, such as:

- This study emphasizes the inherent trade-offs in ethnicity categorization between achieving high accuracy and guaranteeing fast inference times. A fine balance between inference time and accuracy is important in situations when prompt decision-making is required, especially for safety checks, and similar applications.
- Likewise, the importance of minimal inference time cannot be emphasized in real-time deployment scenarios when quick judgments are required. ResNet-50 manages to keep a realistic balance by offering remarkable accuracy without sacrificing comparatively quick inference times.

TABLE 1: Results of faster RCNN with different backbones

Backbone	Arab (%)	Kurd (%)	Total Accuracy (%)	Prec.	Rec.	F ₁	Inf. Time (ms)	Training Time
VGG16	91.95	93	92.48	0.70	0.90	0.79	4.5 ms	2 h 5 min 10 s
ResNet-50	92.95	96.88	94.91	0.81	0.90	0.84	4.6 ms	1 h 31 min 5 s
SqueezeNet	90.01	96.77	93.39	0.80	0.91	0.85	3.8 ms	40 min 25 s
MobileNetv2	86.2	94.45	90.32	0.69	0.89	0.78	3.7 ms	1 h 51 min 30 s
EfficientNet-B4	95.61	97.84	96.73	0.86	0.92	0.89	16 ms	3 h 2 min 31 s

- It underscores the challenges associated with inaccurately categorizing male Arab and Kurdish individuals due to facial similarities. Nevertheless, it also demonstrates the commendable performance of ResNet-50 in effectively addressing intricate ethnicity classification issues, rendering it a viable choice for practical applications.

A thorough assessment of several factors, such as accuracy, inference time, interpretability of the model, robustness, and ease of deployment, helped determine the choice of ResNet-50. Because of its shown effectiveness in image classification tasks and the substantial support it receives in the literature, its adoption is strongly validated. The consistent results obtained on our dataset further validate the appropriateness of choosing this backbone architecture.

Figure 15 depicts some ethnicity classification results with a high degree of accuracy, as when the skin tone and facial characteristics are distinct, the model will perform nicely and accurately detect and categorize them.

However, it is crucial to recognize the limitations of our model when evaluating its efficacy, especially in scenarios where Arab males share physical attributes with Kurds. For instance, Arabs with fair skin and Kurds with dark skin, along with other facial features, pose a significant challenge to the model. This similarity may lead to a decrease in accuracy or, in certain cases, result in misclassification, where individuals are mistakenly classified as belonging to the opposing ethnicity. A visual representation of various instances of this complex scenario can be found in Fig. 16.



Fig.15. Detecting Arabs and Kurds accurately by the model.

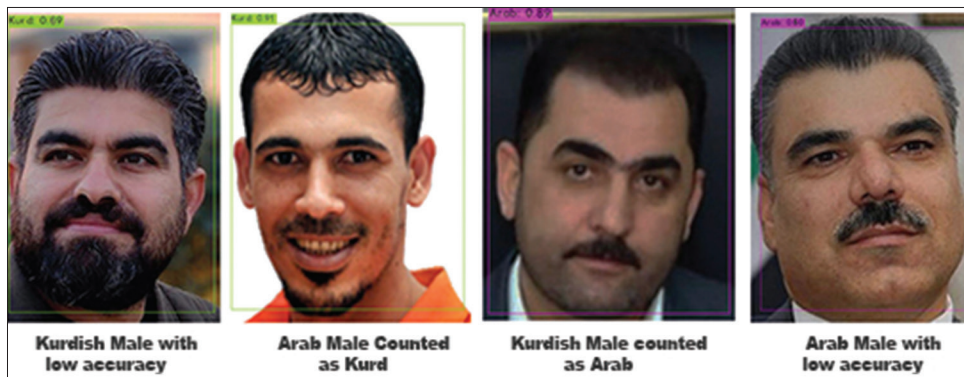


Fig. 16. Examples of the wrong classification by the model

The model's vulnerability to physical characteristics, especially those tied to appearance, raises concerns about the accuracy of ethnicity categorization. This highlights the necessity for a nuanced strategy that surpasses simplistic traits. Furthermore, there is a crucial demand for a more extensive dataset, recognizing the inherent richness and diversity within Arab and Kurdish ethnic groups. There's apprehension that the current model might not fully grasp the entire spectrum of their diversity, underscoring the urgency for a more comprehensive dataset. Augmenting the dataset to accurately reflect the varied traits within each ethnic group holds the promise of substantially enhancing the model's performance. In addition, the quality and format of the training data significantly impact how well the model performs. Any bias in the data may lead to incorrect classifications, particularly when dealing with similar-looking groups. A detailed analysis of the representativeness and quality of the training data is required to address these constraints.

On the other hand, a significant challenge lies in the model's inability to factor in historical and cultural variables, particularly those related to ethnicity. A more holistic approach is essential, one that considers language patterns and cultural context. Integrating these elements during the model's training phase holds the potential to improve accuracy and reduce misclassifications. Emphasizing the importance of incorporating language nuances and cultural context becomes pivotal in addressing this limitation and elevating the overall performance of the model.

5. CONCLUSIONS

Our study has introduced a robust CNN-based approach for predicting the Kurdish/Arab ethnicity of males in Iraq based on facial images. Our work has important implications across diverse fields such as HCI, face recognition, biometric-based recognition, surveillance, and military.

In the absence of an Iraqi ethnicity dataset, we generated a comprehensive dataset. Our advanced CNN model, faster RCNN, leverages different feature extraction models, including VGG16, ResNet-50, SqueezeNet, MobileNetv2, and EfficientNet-B4.

Regarding accuracy assessment, Faster RCNN with EfficientNet reached the highest accuracy by achieving an average mAP of 96.73%. Remarkably, MobileNetv2 showcased the swiftest operational speed, at a rapid 3.7 ms. Thus, considering the balance between accuracy and

inference time, we selected the algorithm with ResNet-50 backbone as the optimal model for ethnicity classification attaining a noteworthy accuracy of 94.91% and a processing time of 4.6 ms.

Future research should focus on creating a more comprehensive dataset that includes a diverse range of gender identities. Although this study focuses on the largest ethnic groups in Iraq, the Kurds, and Arabs, there is potential to broaden its coverage to include all ethnicities in the country. Recognizing potential data biases, particularly in the complicated context of Iraq, is critical for broadening the study to minimize any negative effects on real-world applications. The significance of this research relies on ensuring that the produced technology is not only useful but also adaptable beyond a binary ethnicity categorization. This versatility is necessary for dealing with the region's broad and nuanced ethnic environment. Furthermore, future research should investigate the larger social and ethical implications of facial recognition technology for detecting ethnicity in Iraq. This necessitates a comprehensive and responsible approach to the development and deployment of such systems, as well as an in-depth knowledge of their social impact.

REFERENCES

- [1] M. Smith and S. Miller. "The ethical application of biometric facial recognition technology". *Ai and Society*, vol. 37, pp. 167-175, 2022.
- [2] N. Narang and T. Bourlai. "Gender and Ethnicity Classification Using Deep Learning in Heterogeneous Face Recognition. In: *International Conference on Biometrics (ICB)*". IEEE, Piscataway, pp. 1-8, 2016.
- [3] TWB. "The World Bank, World Bank Open Data", 2023. Available from: <https://data.worldbank.org>
- [4] EUAA. "Religious and Ethnic Minorities, and Stateless Persons". European Union Agency for Asylum, Grand Harbour, 2021. Available from: <https://euaa.europa.eu/country-guidance-iraq-2021/215-religious-and-ethnic-minorities-and-stateless-persons> [Last accessed on 2023 Jan 02]
- [5] M. Jmal, W. S. Mseddi, R. Attia and A. Youssef. "Classification of Human Skin Color and its Application to Face Recognition. In: *MMEDIA 2014: The Sixth International Conference on Advances in Multimedia*". IARIA, 2014.
- [6] S. Richmond, L. J. Howe, S. Lewis, E. Stergiakouli and A. Zhurov. "Facial genetics: A brief overview". *Frontiers in Genetics*, vol. 9, p. 462, 2018.
- [7] W. Wang, F. He, and Q. Zhao. "Facial Ethnicity Classification with Deep Convolutional Neural Networks. In: *Chinese Conference on Biometric Recognition*". Springer, Berlin, pp. 176-185, 2016.
- [8] C. Janiesch, P. Zscheck and K. Heinrich. "Machine learning and deep learning". *Electronic Markets*, vol. 31, no. 3, pp. 685-695, 2021.
- [9] H. Lin, H. Lu and L. Zhang. "A New Automatic Recognition System of Gender, Age and Ethnicity. In: *Congress on Intelligent Control*

- and Automation". vol. 2, no. 3, pp. 9988-9991, 2006.
- [10] F. S. Manesh, M. Ghahramani and Y. P. Tan. "Facial Part Displacement Effect on Template-based Gender and Ethnicity Classification. In: *Proceedings of 11th International Conference on Control Automation Robotics and Vision (ICARCV)*". Singapore, pp. 1644-1649, 2010.
- [11] Y. Xie, K. Luu and M. Savvides. "A Robust Approach to Facial Ethnicity Classification on Large Scale Face Databases. In: *IEEE Fifth International Conference on Biometrics: Theory, Applications and Systems*". IEEE, Piscataway, pp. 143-149, 2012.
- [12] N. Srinivas, H. Atwal, D. C. Rose, G. Mahalingam, K. Ricanek and D. S. Bolme. "Age, Gender, and Fine-grained Ethnicity Prediction Using Convolutional Neural Networks for the EAST Asian Face Dataset. In: *2017 12th IEEE International Conference on Automatic Face and Gesture Recognition (FG 2017)*". pp. 953-960, 2017.
- [13] S. Masood, S. Gupta, A. Wajid, S. Gupta and M. Ahmed. Prediction of human ethnicity from facial images using neural networks. In: "Data Engineering and Intelligent Computing". Springer, Berlin, pp. 217-226, 2018.
- [14] D. Belcar, P. Grd and I. Tomičić. "Automatic ethnicity classification from middle part of the face using convolutional neural networks". *Informatics*, vol. 9, no. 1, p. 18, 2022.
- [15] H. Chen, Y. Deng and S. Zhang. "Where am I from?-East Asian Ethnicity Classification from Facial Recognition". Project study in Stanford University, San Francisco, 2016.
- [16] Z. Heng, M. Dipu and K. H. Yap. "Hybrid Supervised Deep Learning for Ethnicity Classification Using Face Images. *IEEE.2018, International Symposium on Circuits and Systems (ISCAS)*". Florence, Italy, pp. 1-5, 2018.
- [17] S. Aina, M. O. Adeniji, A. R. Lawal and A. I. Oluwaranti. "Development of a convolutional neural network-based ethnicity classification model from facial images". *International Journal of Innovative Science and Research Technology*, vol. 7, no. 4, pp. 1216-1221, 2022.
- [18] Roboflow. "New Feature: Isolate Objects", 2021. Available from: <https://blog.roboflow.com/isolate-objects> [Last accessed on 2025 Jan 25].
- [19] S. Rahman, M. M. Rahman, M. Abdullah-Al-Wadud, G. D. Al-Quaderi and M. Shoyaib. "An adaptive gamma correction for image enhancement". *EURASIP Journal on Image and Video Processing*, vol. 2016, no. 1, p. 35, 2016.
- [20] OpenGenus. "Data Augmentation Techniques, Computing Expertise and Legacy", 2019. Available from: <https://iq.opengenus.org/data-augmentation> [Last accessed on 2023 Jan 25].
- [21] J. Wang and S. Lee. "Data augmentation methods applying grayscale images for convolutional neural networks in machine vision". *Applied Sciences*, vol. 11, no. 15, p. 6721, 2021.
- [22] A. Mahmood, A. G. Ospina, M. Bennamoun, S. An, F. Sohel, F. Boussaid, R. Hovey, R. B. Fisher and G. A. Kendrick. "Automatic hierarchical classification of kelps using deep residual features". *Sensors*, vol. 20, no. 2, p. 447, 2020.
- [23] D. Theckedath and R. R. Sedamkar. "Detecting affect states using VGG16, ResNet50 and SE-ResNet50 networks". *SN Computer Science*, vol. 1, pp. 1-7, 2020.
- [24] F. N. landola, S. Han, M. W. Moskewicz, K. Ashraf, W. J. Dally and K. Keutzer. "SqueezeNet: AlexNet-level accuracy with 50x fewer parameters and and <0.5MB model size". [arXiv preprint] arXiv:1602.07360, 2016.
- [25] M. Sandler, A. Howard, M. Zhu, A. Zhmoginov and L. C. Chen. "Mobilenetv2: Inverted Residuals and Linear Bottlenecks. In: *Proceedings of the IEEE Conference on Computer Vision and Pattern Recognition*". pp. 4510-4520, 2018.
- [26] M. Tan and O. Le. "Efficientnet: Rethinking Model Scaling for Convolutional Neural Networks. In: *International Conference on Machine Learning*". pp. 6105-6114, 2019.
- [27] A. Shahid. "EfficientNet: Scaling of Convolutional Neural Networks Done Right Medium", 2020. Available from: <https://towardsdatascience.com/efficientnet-scaling-of-convolutional-neural-networks-done-right-3fde32aef8ff> [Last accessed on 2023 Feb 03].
- [28] B. Shi, R. Hou, M. A. Mazurowski, L. J. Grimm, Y. Ren, J. R. Marks, L. M. King, C. C. Maley, E. S. Hwang and J. Y. Lo. "Learning Better Deep Features for the Prediction of Occult Invasive Disease in Ductal Carcinoma in Situ through Transfer Learnin. In: *Proceedings of the SPIE Medical Imaging 2018: Computer-Aided Diagnosis*". vol. 10575, pp. 620-625, 2018.
- [29] T. H. B. Nguyen, E. Park, E., X. Cui, V. H. Nguyen and H. Kim. "fPADnet: Small and efficient convolutional neural network for presentation attack detection". *Sensors*, vol. 18, no. 8, p. 2532, 2018.
- [30] C. Y. Zhu, Y. K. Wang, H. P. Chen, K. L. Gao, C. Shu, J. C. Wang, L. F. Yan, Y. G. Yang, F. Y. Xie and J. Liu. "A deep learning-based framework for diagnosing multiple skin diseases in a clinical environment". *Frontiers in Medicine*, vol. 8, p. 626369, 2021.

Blood storage impacts on the hematological indices of healthy subjects and patients with iron-deficiency anemia and beta-thalassemia – A comparative study



Mudhafar Mohamed M. Saeed

Department of Anesthesia, Sulaimani Technical Institute, Sulaimani Polytechnic University, Sulaimani, Kurdistan Region, IRAQ

ABSTRACT

Background: There are scientific evidence confirmed specific changes in blood cell counts, reducing the efficacy and feasibly the safeness of blood transmission when storing blood at 4°C for 5 weeks or more.

Objectives: The study aimed to investigate the effects of stored blood obtained from healthy subjects and patients with anemia due to iron deficiency and beta-thalassemia, on hematological indices.

Materials and Methods: A total of 37 participants, consisting of 14 healthy subjects, 13 patients with iron-deficiency anemia, and 10 patients with beta-thalassemia minor, were recruited from Hiwa Hospital between November 2021 and July 2022. Blood samples were obtained from the participants and stored at 4°C for 5 weeks. Hematological indices, including red cell distribution, platelet distribution width, and mean platelet volume, were determined using a hematology analyzer at weekly intervals.

Results: Blood storage caused significantly increased mean values of hematological indices among healthy subjects as well as among patients with iron-deficiency anemia and beta-thalassemia, although the pattern of changes was differed.

Conclusions: The storage of whole blood significantly increased hematological indices, showing variations in both healthy subjects and patients with iron-deficiency anemia and beta-thalassemia. The pattern of raise in these hematological indices is specific to iron-deficiency anemia and thalassemia when compared with healthy subjects.

Index Terms: Blood Storage, Iron-deficiency Anemia, Thalassemia, Hematological Indices

1. INTRODUCTION

Blood preservation at 4°C for a few weeks may compromise the safety and efficacy of the stored blood as a therapeutic

intervention for managing patients experiencing blood loss, as blood platelets maintain their functionality when stored in whole blood at 4°C for up to 15 days [1]. Similarly, a separate investigation revealed that the aggregation capacity of blood platelets remains unaffected when the entire blood is stored at 20°C for up to 21 days [2]. Utilizing filtration before storage led to a reduction in white blood cells and the preservation of blood platelet function by eliminating bioactive substances derived from white cells [3]. The storage of whole blood from individuals with sickle cell anemia for 5 weeks resulted in a noteworthy increase in the lymphocyte-to-neutrophil ratio [4].

Access this article online

DOI: 10.21928/uhdjst.v8n1y2024.pp78-83

E-ISSN: 2521-4217

P-ISSN: 2521-4209

Copyright © 2024 Mudhafar Saeed. This is an open access article distributed under the Creative Commons Attribution Non-Commercial No Derivatives License 4.0 (CC BY-NC-ND 4.0)

Corresponding author's e-mail: Mudhafar Mohamed M.Saeed , PhD. Clinical Biochemistry, Lecturer, Department of Anesthesia, Sulaimani Technical Institute, Sulaimani Polytechnic University, Sulaimani, Kurdistan Region, IRAQ. E-mail: Mudhafer.saeed@spu.edu.iq

Received: 09-12-2023

Accepted: 17-02-2024

Published: 10-03-2024

Furthermore, while blood storage does not significantly alter the deformability index of red cells, it does bring about a significant change in red distribution width [5]. In terms of cell counts, non-leukoreduction blood storage for 5 weeks at $4 \pm 2^\circ\text{C}$ significantly decreased white cell and platelet counts, elevated echinocytes, and maintained an unchanged lymphocyte count during storage [6]. Various hematological indices, such as red distribution width, mean platelet volume, platelet distribution width, neutrophil-to-lymphocyte ratio, and platelet-to-lymphocyte ratio, serve as biomarkers for diverse medical conditions, including inflammation, cardiovascular events, and chronic diseases like diabetes mellitus [7], [8], [9], [10]. Transfusion of 7-day stored blood in transfusion-dependent thalassemic patients associated with an increase in hematological and biochemical markers related to RBC lysis and inflammation [11]. Consequently, exploring the impact of blood storage derived from healthy individuals, as well as those with anemia due to iron deficiency or beta-thalassemia, on these hematological indices is the main goal for the current study.

2. MATERIALS AND METHODS

The current work was carried out in the Department of Pharmacy at the Technical Institute of Sulaimani, Sulaimani Polytechnic University, Kurdistan Region of Iraq. Participants were recruited from Hiwa Hospital in Sulaimani, from November 2021 to July 2022. Inclusion criteria comprised individuals diagnosed with iron-deficiency anemia, those with beta-thalassemia minor, and healthy subjects who designated as negative controls. A total of 14 healthy subjects (median age 34 years), 13 patients with iron-deficiency anemia (median age 37 years), and 10 patients with beta-thalassemia (median age 31 years) were included in the study. Exclusion criteria encompassed individuals who had received a blood transfusion within 4 weeks of the study, those employing non-steroidal and steroidal anti-inflammatory agents, anabolic drugs, pregnant, and breast-feeding women. Iron-deficiency anemia diagnosis was confirmed by a hemoglobin level $<12\text{ g/dL}$, serum ferritin $<30\text{ ng/ml}$, and the presence of microcytic hypochromic red cells with anisocytosis and poikilocytosis. Beta-thalassemia patients were diagnosed through hemoglobin electrophoresis, revealing low hemoglobin A and elevated percentages of HbA2 and HbF, with hospital attendance for investigation.

Approximately 15 ml of fresh blood were drawn through venipuncture from each participant and distributed into six tubes containing anticoagulant (ethylenediaminetetraacetic

acid). The samples were stored at 4°C for 5 weeks for the determination of hematological indices on a weekly basis, in addition to baseline data. The hematological indices, including mean red cell width distribution, mean platelet volume, and platelet width distribution, were measured using Beckman Coulter hematology analyzer (United State).

2.1. Statistical Analysis

The results are expressed as a number, median, and mean \pm standard deviation (SD). The data were analyzed by one-way analysis of variance (ANOVA) using SPSS version 22 (IBM-compatible). P-value ≤ 0.05 is a cut-off value of significant difference.

3. RESULTS

Table 1 illustrates significant alteration of the hematological indices that occurred after whole blood stored at 4°C for 35 days. From the current study, a significant increase of the RDW from the 2nd week to the 5th week as well as a significant fluctuation of PDW from the 1st to the 5th week were observed, while the platelet indices started from the 1st week to the 4th weeks, and retained non-significantly differed from the pre-storage values [Table 1].

It was observed that there were no significant changes in (RDW) and (MPV) following the storage of whole blood at 4°C for 35 days among patients with iron-deficiency anemia. However, a significant elevation was observed in platelet distribution width (PDW) from the 1st to the 5th week. Non-significant changes were noticed in RDW and MPV during various periods of whole blood storage [Table 2].

Significant elevation was recorded in the RDW value after storing the whole blood for beta-thalassemia patients at 4°C during the 2nd and the 3rd weeks of storage. Similarly, significant increase in the PDW and MPV from 1st to 5th week of whole blood stored at 4°C . Non-significant increment of the PDW was observed only after 2 weeks of storage [Table 3].

It was noticed that the mean plot from RDW of beta-thalassemia patients is approximately similar to that of healthy subjects, while the mean plot of patients with iron-deficiency anemia showed a bimodal increment in RDW [Fig. 1a-c].

It was reported that the mean plots of PDW from iron-deficiency anemia patients and beta-thalassemia patients were

TABLE 1: Effect of whole blood storage on the hematological indices in the healthy subjects (n=14)

Storage duration	RDW	P-value compared with pre-storage	PDW	P-value compared with pre-storage	MPV	P-value compared with pre-storage
Pre-storage	13.2±0.70		12.5±1.9		10.3±0.84	
Week 1	13.3±0.82	1.000	15.9±2.82	0.049	11.9±1.12	0.002
Week 2	15.8±1.33	<0.001	17.4±3.08	<0.001	12.1±1.16	<0.001
Week 3	17.1±0.96	<0.001	16.6±3.43	0.006	11.8±1.05	0.003
Week 4	17.3±0.95	<0.001	16.0±3.04	0.033	11.5±0.89	0.037
Week 5	16.9±0.89	<0.001	14.8±3.20	0.591	11.0±1.05	1.000
P value	<0.001		0.001		0.001	
F value	54.43		4.781		5.966	

The results are expressed as mean±SD. P value was calculated using one-way ANOVA. Comparison between pre-storage and post-storage blood was done by *post hoc* Bonferroni test.

RDW: red distribution width, PDW: platelet distribution width, MPV: mean platelet volume

TABLE 2. Effect of whole blood storage on the hematological indices in patients with iron-deficiency anemia (n=13)

Storage duration	RDW	P-value compared with pre-storage	PDW	P-value compared with pre-storage	MPV	P-value compared with pre-storage
Pre-storage	15.9±3.45		9.9±1.93		9.0±1.13	
Week 1	16.4±3.69	1.000	13.7±1.84	<0.001	12.9±5.36	1.000
Week 2	17.9±3.47	1.000	13.3±2.58	0.001	10.8±1.19	1.000
Week 3	17.7±3.51	1.000	14.3±2.01	<0.001	18.6±27.8	0.575
Week 4	18.1±3.01	1.000	15.4±1.92	<0.001	11.4±0.67	1.000
Week 5	17.6±3.10	1.000	13.8±1.88	<0.001	10.7±0.82	1.000
P value	0.514		<0.001		0.373	
F value	0.857		10.541		1.090	

The results are expressed as mean±SD. P value was calculated using one-way ANOVA. Comparison between pre-storage and post-storage blood was done by *post hoc* Bonferroni test.

RDW: red distribution width, PDW: platelet distribution width, MPV: mean platelet volume

TABLE 3. Effect of whole blood storage on the hematological indices in patients with thalassemia hereditary anemia (n=10)

Storage duration	RDW	P-value compared with pre-storage	PDW	P-value compared with pre-storage	MPV	P-value compared with pre-storage
Pre-storage	17.0±3.20		11.0±0.89		9.0±0.94	
Week 1	19.6±2.70	1.000	16.1±1.51	0.006	12.0±0.44	<0.001
Week 2	21.5±3.88	0.087	14.0±0.94	0.404	11.7±0.34	<0.001
Week 3	22.3±4.18	0.020	18.1±4.58	<0.001	12.2±1.17	<0.001
Week 4	22.0±3.62	0.037	15.3±4.33	0.037	11.4±0.90	<0.001
Week 5	21.5±3.50	0.095	15.6±3.14	0.016	11.3±0.80	<0.001
P value	0.011		<0.001		<0.001	
F value	3.30		6.233		20.193	

The results are expressed as mean±SD. P value was calculated using one-way ANOVA. Comparison between pre-storage and post-storage blood was done by *post hoc* Bonferroni test.

RDW: red distribution width, PDW: platelet distribution width, MPV: mean platelet volume

approximately similar, whereas they were differed from the corresponding plot of healthy subjects [Fig. 2a-c].

It was concluded that the mean plot of MPV of beta-thalassemia patients has a peak value of MPV increment after 3 weeks of whole blood storage of, which was similar to the corresponding plot of iron-deficiency anemia. The plots of MPV of patients with iron-deficiency anemia and

beta-thalassemia were differed from the corresponding plot of healthy subjects [Fig. 3a-c].

4. DISCUSSION

The results of this study highlighted important findings, including the effects of whole blood storage on the

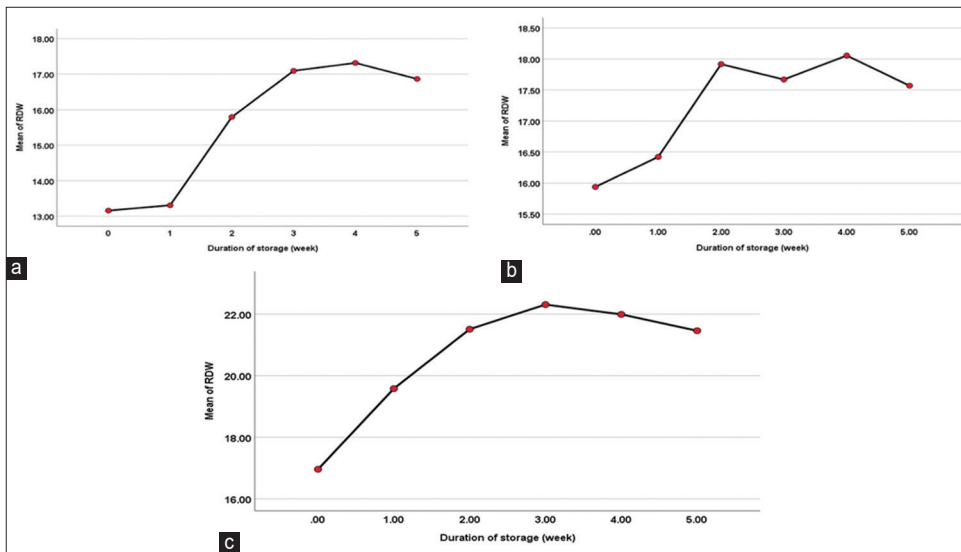


Fig. 1. The mean plot of the red distribution width (coefficient variation %) after storing whole blood, obtained from health subjects (above), patients with iron-deficiency anemia (middle), and patients with thalassemia hereditary anemia, at 4°C for 5 weeks.

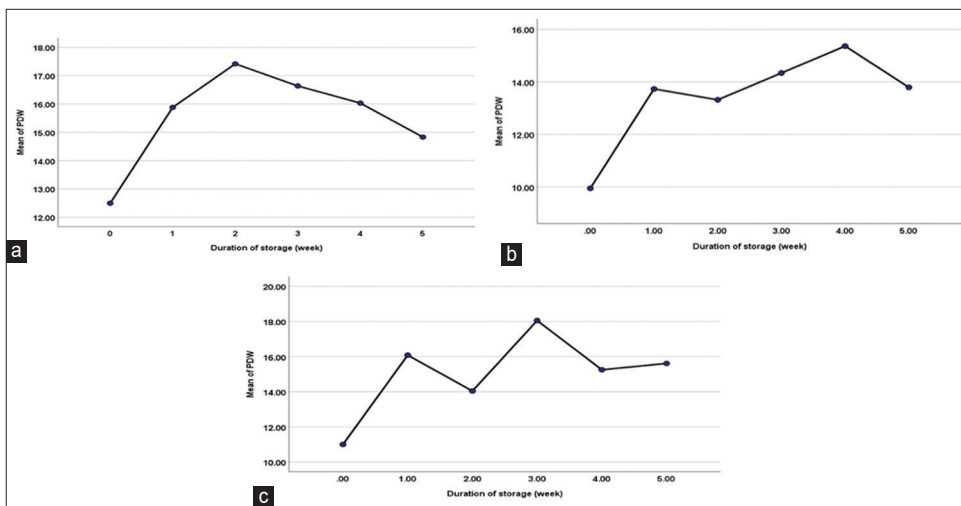


Fig. 2. The mean plot of the platelet distribution width (%) after storing whole blood, obtained from health subjects (above), patients with iron-deficiency anemia (middle), and patients with thalassemia hereditary anemia, at 4°C for 5 weeks.

hematological indices extended to red cell diseases, in addition to the duration of the storage. The baseline mean value of RDW of healthy subjects was less than the corresponding means of iron-deficiency anemia and beta-thalassemia patients. This finding agreed with the results reported by Aulakh *et al.* in 2009 who observed that the mean \pm SD of RDW among iron-deficiency anemia was $18.37 \pm 2.22\%$ compared with $16.55 \pm 1.51\%$ of the interrelated value of healthiness [12]. The differences between the mean values of iron-deficiency anemia and beta-thalassemia patients were parallel to the results of

other studies [13]. Patients with iron-deficiency anemia have a higher mean value of MPV, and there was an inverse relationship with serum iron level [14]. Storage of the whole blood at 4°C caused an increase in the mean values of the RDW, PDW, and MPV among healthy subjects. Storage temperature played an important role in the RDW, PDW, and MPV as reported by Daves *et al.* who found that storage of the blood samples in different temperatures for short period showed variability in these parameters [15]. The pathological red cell as with iron-deficiency anemia and beta-thalassemia exerts an additional effect on the

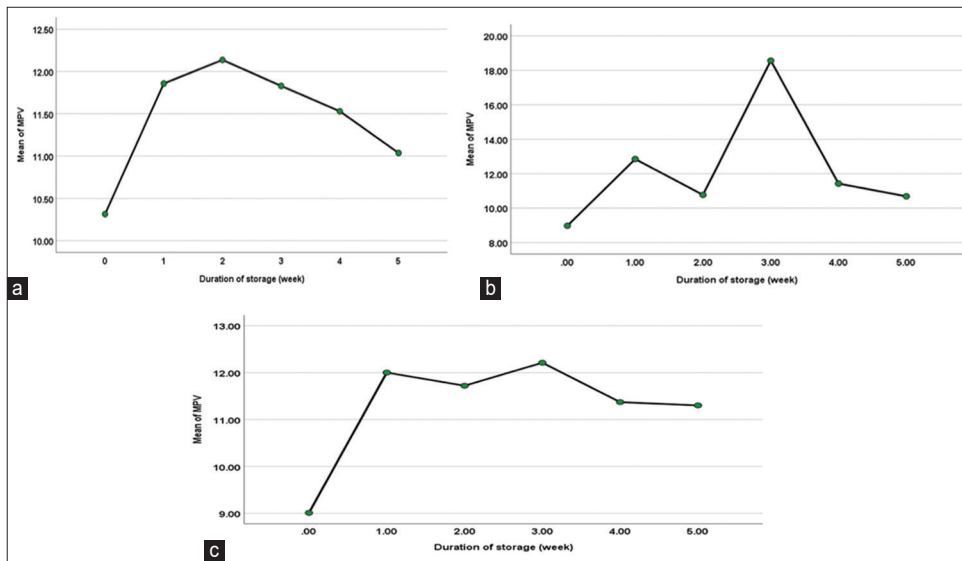


Fig. 3. The mean plot of the mean platelet volume (fL) after storing whole blood, obtained from health subjects (above), patients with iron-deficiency anemia (middle), and patients with thalassemia hereditary anemia, at 4°C for 5 weeks.

changes in the RDW, PDW, and MPV, which were the fundamental results of the current study. Low serum iron and ferritin levels among iron-deficiency anemia can explain the increment of RDW during storage, as the microcytic hypochromic red cells tend to show anisocytosis and changes in the red cell shapes [16], although it does not explain our results with thalassemia patients whereas the serum iron is usually high. Red cells of thalassemia patients were characterized by the presence of a higher percentage of anisocytosis with greater morphological alterations, which explained their tendency to have a higher RDW [17]. Patients with thalassemia showed significantly higher values of platelet indices whether at pre-storage or during storage phases due to that the blood platelets of those patients were in a state of activation, i.e., the higher rate of changing their shape and size, which increased by cold temperature [18]. The strength of this study is involving two clinical conditions characterized by microcytic anemia: One of them with iron deficiency and the other with iron overload (thalassemia), which showed different mean plots, which indicating the iron status plays a role in the determination of hematological indices values.

In conclusion, the storage of whole blood significantly caused elevation in the hematological indices with some variations among healthy subjects and patients with iron-deficiency anemia as well as beta-thalassemia. Mean plots of RDW, PDW, and MPV were specific for iron-deficiency anemia and thalassemia compared with the healthy subjects.

REFERENCES

- [1] P. C. Spinella, H. F. Pidcock, G. Strandenes, T. Hervig, A. Fisher, D. Jenkins, M. Yazer, J. Stubbs, A. Murdock, A. Sailliol, P. M. Ness and A. P. Cap. "Whole blood for hemostatic resuscitation of major bleeding". *Transfusion*, vol. 56, no. Suppl 2, pp. S190-S202, 2016.
- [2] S. Sperling, P. J. Vinholt, U. Sprogøe, M. H. Yazer, H. Frederiksen and C. Nielsen. "The effects of storage on platelet function in different blood products". *Hematology*, vol. 24, no. 1, pp. 89-96, 2019.
- [3] M. R. Wirtz, J. Jurgens, C. J. Zuurbier, J. J. T. H. Roelofs, P. C. Spinella, J. A. Muszynski, J. Carel Goslings and N. P. Juffermans. "Washing or filtering of blood products does not improve outcome in a rat model of trauma and multiple transfusion". *Transfusion*, vol. 59, pp. 134-145, 2019.
- [4] E. Aninagyei, E. T. Doku, P. Adu, A. Egyir-Yawson and D. O. Acheampong. "Storage related haematological and biochemical changes in *Plasmodium falciparum* infected and sickle cell trait donor blood". *BMC Hematology*, vol. 18, p. 30, 2018.
- [5] Y. Zheng, J. Chen, T. Cui, N. Shehata, C. Wang and Y. Sun. "Characterization of red blood cell deformability change during blood storage". *Lab on a Chip*, vol. 14, no. 3, pp. 577-583, 2014.
- [6] E. Spada, R. Perego, L. Baggiani and D. Proverbio. "Haematological and morphological evaluation of feline whole blood units collected for transfusion purposes". *Journal of Feline Medicine and Surgery*, vol. 21, no. 8, pp. 732-740, 2019.
- [7] A. Y. Gasparyan, L. Ayvazyan, D. P. Mikhailidis and G. D. Kitas. "Mean platelet volume: A link between thrombosis and inflammation?" *Current Pharmaceutical Design*, vol. 17, no. 1, pp. 47-58, 2011.
- [8] F. Zaccardi, B. Rocca, D. Pitocco, L. Tanese, A. Rizzi and G. Ghirlanda. "Platelet mean volume, distribution width, and count in type 2 diabetes, impaired fasting glucose, and metabolic syndrome: A meta-analysis". *Diabetes Metabolism Research and Reviews*, vol. 31, no. 4, pp. 402-410, 2015.
- [9] M. Orak, Y. Karakoç, M. Ustundag, Y. Yildirim, M. K. Celen and

- C. Güloğlu. "An investigation of the effects of the mean platelet volume, platelet distribution width, platelet/lymphocyte ratio, and platelet counts on mortality in patents with sepsis who applied to the emergency department". *Nigerian Journal of Clinical Practice*, vol. 21, no. 5, pp. 667-671, 2018.
- [10] X. Wu, B. Cai, Z. Su, Y. Li, J. Xu, R. Deng and L. Wang. "Aspartate transaminase to platelet ratio index and gamma-glutamyl transpeptidase-to-platelet ratio outweigh fibrosis index based on four factors and red cell distribution width-platelet ratio in diagnosing liver fibrosis and inflammation in chronic hepatitis B". *Journal of Clinical Laboratory Analysis*, vol. 32, no. 4, p. e22341, 2018.
- [11] U. Naeem, N. Baseer, M. T. M. Khan, M. Hassan, M. Haris and Y. M. Yousafzai. "Effects of transfusion of stored blood in patients with transfusion-dependent thalassemia". *American Journal of Blood Research*, vol. 11, no. 6, pp. 592-599, 2021.
- [12] R. Aulakh, I. Sohi, T. Singh and N. Kakkar. "Red cell distribution width (RDW) in the diagnosis of iron deficiency with microcytic hypochromic anemia". *Indian Journal of Pediatrics*, vol. 76, no. 3, pp. 265-268, 2009.
- [13] J. J. M. L. Hoffmann, E. Urrechaga and E. Aguirre. "Discriminant indices for distinguishing thalassemia and iron deficiency in patients with microcytic anemia: A meta-analysis". *Clinical Chemistry and Laboratory Medicine*, vol. 53, no. 12, pp. 1883-1894, 2015.
- [14] M. J. Park, P. W. Park, Y. H. Seo, K. H. Kim, S. H. Park, J. H. Jeong and J. Y. Ahn. "The relationship between iron parameters and platelet parameters in women with iron deficiency anemia and thrombocytosis". *Platelets*, vol. 24, no. 5, pp. 348-351, 2013.
- [15] M. Daves, E. M. Zagler, R. Cemin, F. Gnech, A. Joos, S. Platzgummer and G. Lippi. "Sample stability for complete blood cell count using the Sysmex XN haematological analyser". *Blood Transfusion*, vol. 13, no. 4, pp. 576-582, 2015.
- [16] M. D. Akkermans, L. Uijterschout, M. Nuijsink, D. M. Hendriks, J. B. van Goudoever and F. Brus. "Red blood cell distribution width is not a reliable biomarker for low iron stores in children with cystic fibrosis". *Pediatric Hematology and Oncology*, vol. 34, no. 1, pp. 10-16, 2017.
- [17] A. Vayá, R. Alis, M. Suescún, L. Rivera, J. Murado, M. Romagnoli, E. Solá and A. Hernandez-Mijares. "Association of erythrocyte deformability with red blood cell distribution width in metabolic diseases and thalassemia trait". *Clinical Hemorheology and Microcirculation*, vol. 61, no. 3, pp. 407-415, 2015.
- [18] S. Karmakar, D. Banerjee and A. Chakrabarti. "Platelet proteomics in thalassemia: Factors responsible for hypercoagulation". *Proteomics Clinical Applications*, vol. 10, no. 3, pp. 239-247, 2016.

Enhancing COVID-19 Detection Accuracy: Optimal Gene Combinations, Kit Performance, and Reliable Detection Intervals



Dara A. Tahir¹, Sehand Kamaludeen Arif²

^{1,2}Department of Biology, University of Sulaimani, Al sulaimaniyah, Iraq

ABSTRACT

A significant challenge and threat to public health have been created by the COVID-19 pandemic for the entire global population. The study aimed to compare the SARS-CoV-2 RNA detection capabilities of available primers and probes to identify the most reliable, efficient, and affordable method. From 200 previously detected samples of SARS CoV-2, 94 samples were selected randomly and used for the optimization of our primers and probes. We compared our results with two kits that have been approved by the health authority. In addition, we evaluated the detectability of each gene. The study compared the diagnostic performance of different gene combinations for COVID-19 detection using kits A and B and a novel approach combining *RdRp*, *N*, and *E* genes. Results showed that the combined approach exhibited superior discriminatory power, particularly with the inclusion of the *E* gene, boasting area under the curve (AUC) values of 83.3%, 79.1%, and 93.7% for the respective genes. Kit B, with *Orf1ab* and *N* genes, outperformed Kit A (*RdRp* and *S* genes), with AUC values of 81.2% and 90.6% versus 80.2% and 75%, respectively. The chart representation highlighted gene detection frequencies across various cycle threshold (Ct) ranges, demonstrating robust identification within the 20.1–30 Ct range across all kits and genes, emphasizing the reliability of detection within specific intervals. Combining *RdRp*, *N*, and *E* genes showed the highest accuracy for COVID-19 diagnosis, particularly with the *E* gene. Detection was most reliable within the 20.1–30 Ct range across all gene combinations and kits.

Index Terms: SARS-CoV-2, *RdRp* Gene, *E* Gene, *N* Genes, Kit Comparison

1. INTRODUCTION

Coronaviruses cause various illnesses from common colds to severe diseases such as syndrome coronavirus 2 (SARS-CoV) and COVID-19. These viruses carry a single-stranded RNA genome ranging from 26 to 32 kb. They are classified into four genera – Alpha, Beta, Gamma, and Delta, and they infect both humans and animals, with around 30 species

found across human, mammal, and bird samples. Human coronaviruses fall into alpha and beta species [1]. Following 229E, NL63, OC43, HKU1, Middle East Respiratory Syndrome (MERS)-CoV, and the initial SARS-CoV outbreaks, SARS-CoV-2 marks the eighth known coronavirus to impact human populations [2].

The SARS-CoV outbreak in 2002–2003 stemmed from class B beta-coronaviruses originating from bats, whereas the MERS resulted from a class C beta-coronavirus linked to camels in 2012 and beyond [3]. The pneumonia case identified in Wuhan, China, in late December 2019, initially attributed to a coronavirus due to respiratory symptoms, was designated as severe acute respiratory SARS-CoV-2 by the World Health Organization [4], [5].

Access this article online

DOI: 10.21928/uhdjst.v8n1y2024.pp84-92

E-ISSN: 2521-4217

P-ISSN: 2521-4209

Copyright © 2024 Tahir and Arif. This is an open access article distributed under the Creative Commons Attribution Non-Commercial No Derivatives License 4.0 (CC BY-NC-ND 4.0)

Corresponding author's e-mail: Dr. Sehand Kamaludeen Arif, Department of Biology, University of Sulaimani, Al sulaimaniyah, Iraq.
E-mail: sehand.arif@univsul.edu.iq

Received: 07/12/2023

Accepted: 20/12/2023

Published: 11/03/2024

The novel virus' genomic sequence is 96.2% identical to that of the bat. In Wuhan, China, researchers discovered the SARS-related coronavirus (SARSrCoV; RaTG13), which contains a genome that is not entirely identical to either the SARS-CoV (about 79%) or the MERS-CoV (about 50%) genomes [6], [7].

Developing specific primers and probes in regions with minimal similarity to other viruses is crucial to avoid misidentification of SARS-CoV-2 [8]. As the most sensitive and specific assay, real-time reverse transcription-quantitative polymerase chain reaction (RT-qPCR) is the "gold standard" diagnostic technique for the detection of SARS-CoV-2 infection [9].

SARS-CoV-2 displays the typical genome organization of the β -coronaviruses. There are 14 functional open reading frames in the genome, including two noncoding regions at each end and other areas that code for structural, accessory, and nonstructural proteins [10].

This study aims to detect SARS-CoV-2 using various probes and primers that target different genes (such as *RdRp*, *E*, and *N* genes) through reverse transcription real-time and conventional PCR assays. The goal is to compare the efficacy of these primers/probes in detecting SARS-CoV-2 RNA and identify the most accurate, speedy, and cost-effective detection method.

2. MATERIALS AND METHODS

2.1. Sample Collection

Between September 2020 and September 2021, ninety-four samples were selected randomly from a total of 200 samples (Nasopharyngeal swabs) of SARS-CoV-2 previously gathered by Shahid Tahir Ali Wali Bag laboratory in Sulaimani City/Iraqi Kurdistan Region. The (94) selected samples were used for optimization of our primers and probes and for comparing the obtained results with two available kits (AddMedi/South Korea and AeHealth/UK) proved by health authority and evaluation of detectability of each gene.

2.2. RNA Extraction

RNA extractions were carried out using an Addprep viral nucleic acid extraction kit according to the manufacturer's protocol (AddBio Company/South Korea).

2.3. Storage of the RNA

To avoid degradation, eluted RNA was stored at -80°C after the RNA extraction process was completed.

2.4. Designing of primers and Probes for RT-qPCR

Based on the sequencing analysis, four sets of primers and probes were designed as follows: One set of forward primers, reverse primer, and dual modified fluorescence probe for each of *RdRp*, *N*, *E*, and *GAPDH* gene for internal control detection. Amplicons were selected for *RdRp*, *N*, and *E* genes by Primer-BLAST, which were (110, 110, and 80 bp), respectively, and *in silico* analyzed using NCBI Primer BLAST to exclude miss annealing with other respiratory viruses. *In silico* predictions also demonstrated that those primers do not bind to non-specific targets for human, bacterial, fungal, and apicomplexan.

The lyophilized form of primers and probes was produced by a humanized genomic Macrogen company from South Korea (Tables 1 and 2).

2.5. RT-qPCR Procedure

Samples containing RNA were subjected to a reverse transcription step to convert RNA into cDNA using reverse transcriptase enzymes. The reaction mixes, containing the designed primers, probes, nucleotides, and specialized polymerase enzymes, were prepared and inserted into the (applied biosystems RT-qPCR) instrument. The instrument cycled through denaturation, annealing, and extension stages, amplifying the target sequences exponentially. Fluorescence emitted during each cycle was monitored, with the software recording and analyzing the signal, determining the initial amount of viral genetic material present in the samples based

TABLE 1: Primers and probes for real-time polymerase chain reaction (*RdRp*, *N*, *E* gene)

Genes	Primers and probes
RdRp F	TTGATTGTTACGATGGTGGCT
RdRp R	CATAATAAAGTCTAGCCTTACCCCA
RdRp-Probe	FAM- GGTTGTTGACGATGACTTGGTTAGCA-BHQ
N F	ATTCGTGGTGGTGACGGTAA
N R	ATGCCGTCTTTGTTAGCACC
N Probe	HEX-GGGAAGTCCAGCTTCTGGCCC-BHQ
E F	ACTTCTTTTCTTGCCTTCGTGGT
E R	GCAGCAGTACGCACACAATC
E Probe	ROX- AGCGCAGTAAGGATGGCTAGTGT -BHQ

TABLE 2: Primers and probes for real-time polymerase chain reaction (internal control GAPDH)

Internal control GAPDH	
IC F	GGTGAAGGTCGGAGTCAACG
IC R	TGAAGGGGTCATTGATGGCAA
IC Probe	Cy5- CTGGTGACCAGGCGCCCAAT-BHQ

on the Ct values. Results were interpreted by comparing Ct values against known standards or controls to ascertain the presence and approximate quantity of SARS-CoV-2 genetic material in the samples.

2.6. Statistical Analysis

Statistical analysis was conducted using two software programs: IBM SPSS (Version 26) and RStudio (Version 1.1.463). These programs were employed to perform various statistical tests (area under the curve [AUC], z – test, and P -value) and analyses, ensuring a comprehensive and rigorous approach to data analysis.

2.7. AUC

AUC refers to the graphical representation of a receiver operating characteristic (ROC) curve. In this context, it reflects the assay's ability to distinguish between positive and negative samples based on Ct values. A higher AUC value indicates better discrimination between these samples, signifying the test's accuracy in correctly identifying the presence or absence of SARS-CoV-2 genetic material. This statistical measure helps assess the overall performance and reliability of the PCR assay by quantifying its ability to differentiate between infected and non-infected samples based on Ct values, contributing crucial insights into the assay's diagnostic potential.

Z-test: Z-values represent the number of standard deviations; a data point is from the mean. In this case, the more negative the Z-value, the lower the Ct value, indicating higher viral RNA levels or better detection sensitivity.

P-value: The low P -values indicate high statistical significance. It suggests strong evidence against the null hypothesis, reinforcing the reliability of the observed differences.

3. RESULTS

3.1. Detectability of Primers and Probes in Clinical Samples

Out of 200 previously identified SARS-CoV-2 samples, 94 were randomly chosen for the optimization of our primers and probes. The obtained findings were compared with two health authority-endorsed kits to evaluate the detectability of each gene: Kit A with CE and IVD certificate from South Korea with detection channel HEX (RdRp gene) and FAM (S gene), while Kit B with CE and IVD certificate from United Kingdom with detection channel FAM (ORF1ab gene) and VIC (N gene) and the current designed primers as well as probes FAM (RdRp), HEX (N), ROX (E), and CY5 (IPC).

Kit A, which consists of RdRp and S genes, demonstrated an AUC of 80.2% and 75%, respectively. This indicated that Kit A's performance, as measured by the AUC, is 80.2% for one gene and 75% for the other. The AUC value served as a metric for the ability of this kit to distinguish between positive and negative COVID-19 samples. Higher AUC values generally indicated better discriminatory power.

In contrast, Kit B, comprising the Orf1ab and N genes, exhibited AUC values of 81.2% and 90.6%. These AUC values suggested that Kit B is quite effective, with the first gene achieving an AUC of 81.2% and the second gene reaching an even higher AUC of 90.6%. The higher AUC for the N gene in Kit B may indicate its higher accuracy in diagnosing COVID-19 cases. The approach of the current study, which combines the RdRp, N, and E genes, achieved the AUC values of 83.3%, 79.1%, and 93.7%, respectively. These AUC values demonstrated the effectiveness of this approach when using different gene combinations. The AUC of 93.7% for the E gene suggested that it may be a particularly valuable component for COVID-19 diagnosis within this approach.

To visualize the data and facilitate a more comprehensive understanding, the information is presented in a bar chart (Fig. 1).

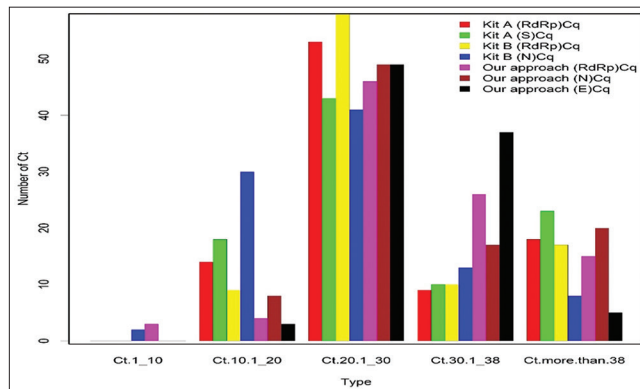


Fig. 1: The X-axis of the chart represents the number of samples tested, while the y-axis indicates the Ct values. Ct values are often used in polymerase chain reaction tests and indicate the number of amplification cycles required to detect a specific gene target in a sample. Gene detection across Ct value ranges in various test kits. The bar chart visually presents gene detection within specific Ct value ranges across different test kits and methodologies, it's important to note that the statistical significance of differences in detection rates was assessed separately through appropriate statistical tests. These tests, including but not limited to t-tests, ANOVA, or non-parametric equivalents, were conducted to evaluate the significance of differences in detection rates between the various gene targets across different kits and methodologies. The results of these statistical analyses provide quantitative insights into the observed differences in detection rates, complementing the visual representation provided by the bar chart. Ct: Cycle Threshold.

The chart allows for a visual comparison of how the AUC values for Kit A, Kit B, and the current approach with various gene combinations vary with the number of samples tested and their corresponding Ct values. This comprehensive comparison of kits and gene combinations could be useful in making informed decisions about which testing method may be the most suitable for COVID-19 diagnosis, taking into account both accuracy and scalability based on the number of samples. It appeared that the current approach with three genes (RdRp, N, and E) showed the highest AUC values, which are 83.3%, 79.1%, and 93.7%, respectively. These AUC values are indicative of the accuracy and discriminatory power of the diagnostic method.

Comparatively, Kit B, which combines Orf1ab and N genes, has AUC values of 81.2% and 90.6%. Kit A, with RdRp and S genes, has AUC values of 80.2% and 75%. Based on these AUC values alone, it appeared that the current approach with three genes was the most effective in diagnosing COVID-19, especially when the E gene is included which appeared to contribute significantly to the accuracy of the test, as reflected in its higher AUC value of 93.7%.

In the comparison between kits with two genes (Kit A and Kit B), Kit B, with AUC values of 81.2% and 90.6%, seemed to be more effective than Kit A, which has AUC values of 80.2% and 75%.

The Ct value ranges are color coded to depict the distribution of gene detection levels. Notably, the range of 20.1–30 exhibits the highest frequency of gene detection across all kits and genes, indicating consistent and reliable identification within this Ct range. The chart highlights the varying detection levels among different genes and kits, emphasizing the robustness of detection within specific Ct value intervals.

The Z-test results indicate significant differences ($P < 0.0001$) among gene targets tested within Kit A, B, and our approach. The E gene exhibits the lowest Z-value of -1.49 , followed closely by the N gene (kit B) with a Z-value of -1.46 . These findings suggest that E gene demonstrates the highest sensitivity in detecting COVID-19.

4. DISCUSSION

Since the first record of the coronavirus disease 2019 (COVID-19) pandemic, real-time RT-qPCR laboratory testing to identify severe acute respiratory SARS-CoV-2 has been crucial in limiting the spread of the virus [11]. The

World Health Organization developed and made a number of RT-qPCR assays accessible to the general public not long after the viral genome sequences became available. The E gene, RdRp gene, ORF1ab gene, and N gene are only a few of the target genes within the viral genome that was used to select the primer and probe sequences for these experiments. Based on these primer and probe sequences, numerous commercial and laboratory-developed tests for SARS-CoV-2 detection were created. Several mutational events have resulted from the widespread sustained person-to-person transmission of SARS-CoV-2, some of which may alter the sensitivity and specificity of existing PCR assays [12]. The gold standard for diagnosing COVID-19 is rRT-PCR, but it has been noted that false-positive and false-negative samples may cause issues. Regarding which of the goals is most important for diagnosis, there are differing viewpoints. Testing with three targets is more expensive and time-consuming than testing with two targets. The conclusion drawn from our study is based on a comparative analysis of two different assay methods: one that detects N and RdRp genes (utilizing commercial kits) and another that detects N, E, and RdRp genes (our manual 3-gene method). While it's true that the comparison involves a 3-gene method versus a 2-gene method, the primary focus is on evaluating the sensitivity difference between these two approaches rather than a direct comparison of equal gene sets. Our conclusion is derived from the observation that the assay detecting N, E, and RdRp genes consistently yielded more positive detections across the tested samples compared to the assay detecting only N and RdRp genes. This difference in sensitivity forms the basis of our conclusion that the 3-gene assay is more sensitive than the 2-gene assay.

Barjaktarović *et al.* revealed that the new variations of SARS-CoV-2 are continuously found since it is an RNA virus that mutates more frequently than DNA viruses. Sequences that are less mutable are the focus of diagnostic testing. Yet, it has been discovered that mutations in the N gene and the RdRp gene increase the possibility of false-negative results, reduce test sensitivity, and result in diagnostic errors [13]. Because of the E gene's high stability, it is possible to develop new mRNA vaccines against illnesses caused by newer SARS-CoV-2 strains. Moreover, known coronaviruses have highly conserved E and M gene sequences. They are less likely to experience mutations than the S gene, making the E gene a suitable diagnostic target with a high level of specificity. It is vital to use diagnostic tests that target less changeable genes to identify people infected with present and future variations of the SARS-CoV-2 virus since new SARS-CoV-2 variants are continually developing and complicating COVID-19 testing [13].

The quantitation cycle, which is the primary outcome of qPCR, is the cycle in which fluorescence can be observed. Lower Ct values indicate higher starting copy numbers of the target. This is the fundamental tenet of the quantitative strategy offered by real-time PCR. Previous researchers have recorded comparisons of the effectiveness of various commercial PCR kits for the RT-qPCR diagnosis of SARS-CoV-2 [14], [15], [16], [17].

Lu *et al.* in 2020, compared and evaluated the effectiveness of Sansure and BioGerm, which are both commonly used in Liuzhou people's Hospital in Guangxi, China, and had corresponding effectiveness levels of 80 and 94% [8]. On the other hand, Eberle *et al.* in 2021 examined nine RT-qPCR kits that were being utilized in the German city of Bavaria to diagnose viruses. Most of them achieved sensitivity levels of 90–100%, however, two kits claimed efficacy levels of 49% (Fast Track Diagnostics Kit) or 62% (Wells Bio, Inc.) with the greatest proportion of false negatives. Hence, when it comes to the identification of viral variations, kits with more than one target gene are less likely to produce false negative results than tests with a single genetic target [18], [19].

These studies recommended evaluating the effectiveness of commercial RT-qPCR kits used locally to analyze COVID-19. In fact, a poor SARS-CoV-2 diagnosis could encourage the future spread of this and other infectious diseases. No standardization, comparison, or efficacy investigations using commercial RT-qPCR kits used in the mass diagnosis of local SARS-CoV-2 or the detection of developing variants have been reported for Sulaimani, the city with a high number of PCR tests performed per thousand residents.

The current study announces the first clinical validations and comparison of two commercially available RT-qPCR Kits for detecting SARS-CoV-2 Kit A and Kit B to primers and probes we designed. For the detection of SARS-CoV-2 genes and diagnosis, the Ct and the relative fluorescence units acquired from their RT-qPCR reactions exhibited significant disparities in the total RNA volume. These differences were significant because they significantly affected the detection of COVID-19-positive cases.

The evaluation of different testing kits and gene combinations in the context of COVID-19 diagnostics, as measured by AUC values, offered crucial insights into their accuracy and discriminatory power [20]. AUC values, representing the ability to distinguish between positive and negative COVID-19 samples, showcased varying performance among

the tested kits and gene combinations. Notably, higher AUC values typically indicated better discriminatory ability, serving as a fundamental metric for assessing the efficacy of these diagnostic methods. Comparing Kit A and Kit B revealed intriguing nuances in their performance. While Kit A demonstrated AUC values of 80.2% for RdRp and 75% for the *S* gene, Kit B exhibited a relatively higher accuracy, with AUC values of 81.2% for Orf1ab and an impressive 90.6% for the *N* gene. This comparison suggested that Kit B, particularly the *N* gene within it, displayed a superior capacity in accurately diagnosing COVID-19 cases compared to Kit A.

The findings of this study underscore the pivotal role of gene selection in optimizing the accuracy of COVID-19 diagnosis. Our results revealed compelling evidence supporting the superior performance of the combined *RdRp*, *N*, and *E* genes, showcasing robust discriminatory power with notable area under the curve (AUC) values. Particularly striking was the outstanding 93.7% AUC value for the *E* gene within this multi-gene approach, surpassing individual gene performances within both Kit A and Kit B. The statistically significant differences ($p < 0.0001$) observed in AUC values among these genes signal the potential for the *E* gene as a cornerstone in enhancing diagnostic precision, suggesting its superiority over RdRp and *N* genes in our tested context. The remarkably high AUC for the *E* gene highlights its promise as a key component in amplifying the reliability and accuracy of COVID-19 diagnosis, offering a potential avenue for refining

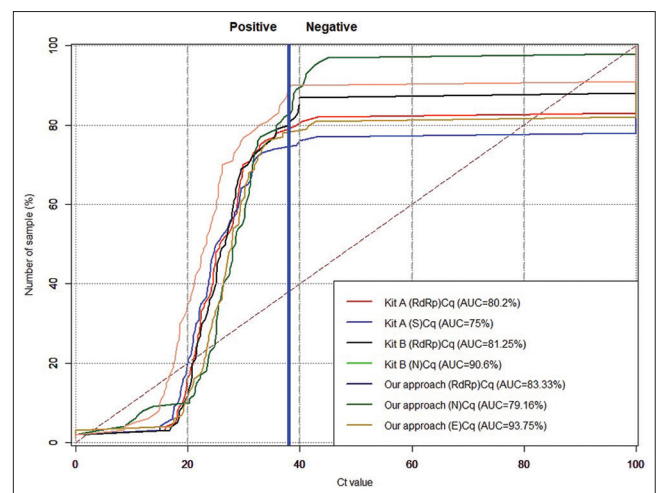


Fig. 2. Line graph shows the performance of different testing kits and our approach using specific genes evaluated in the context of COVID-19 diagnostics. The assessment is based on the calculation of the area under the curve values, which are a common measure of the accuracy of diagnostic tests. The comparison involved three different sets of genes: Kit A (RdRp and S), Kit B (Orf1ab and N), and our approach combining RdRp, N, and E genes.

Sample NO.	Kit A						Kit B						Our approach											
	RdRp			S			Orf1ab			N			RdRp			N			E			IC		
	RFU	Cq	RFU	RFU	Cq	RFU	RFU	Cq	RFU	RFU	Cq	RFU	RFU	Cq	RFU	RFU	Cq	RFU	RFU	Cq	RFU	RFU	Cq	
1	1130	21.06	3546	19.95	898	21.58	837	16.77	92.3	24.95	198	23.01	1072	24.27	145	26.02								
2	1921	24.66	5395	24	1006	25.06	955	22.71	115	9.57	49.4	33.99	276	33.72	182	27.18								
3	1753	15.92	5351	14.95	975	16.77	1045	10.43	121	28.63	184	29.15	845	29.15	159	28.30								
4	1602	20.49	4719	19.67	1059	20.82	960	18.19	2.79	45.00	0.81	0.0	67.3	37.40	196	29.36								
5	1755	27.50	3699	26.61	978	28.08	925	25.22	107	30.01	205	27.15	919	26.86	134	29.29								
6	0.92	0.0	-2.00	0.0	259	39.91	544	36.43	94.6	23.39	235	21.20	1334	22.44	184	25.14								
7	1754	18.12	4612	17.31	981	18.55	862.	16.18	108	27.80	209	26.16	867	28.38	178	27.05								
8	1513	28.26	2637	27.32	994	28.58	947	24.05	95.8	23.56	206	26.29	1054	26.67	192	26.05								
9	1847	19.32	4032	18.52	873	20.86	792	15.07	102	26.12	208	24.39	1041	25.24	217	28.60								
10	1671	26.76	2721	26.06	1031	26.79	954	23.37	2.69	21.14	243	17.62	1451	19.22	224	25.11								
11	2053	24.55	3636	24.03	663	26.77	517	25.53	113	24.94	277	23.56	1485	24.71	152	25.01								
12	1957	20.54	4240	19.89	1193	20.81	1110	18.48	136	30.18	217	29.45	725	30.51	162	31.14								
13	1988	19.83	4786	18.82	1147	19.62	1028	15.30	86.4	23.35	246	20.14	1435	21.87	199	26.59								
14	1669	28.87	1736	29.02	1063	28.31	1016	25.51	109	25.17	94.0	29.24	1300	25.07	131	27.25								
15	1925	21.79	4122	21.07	1037	22.31	966	19.11	113	28.01	231	26.39	1096	27.86	168.	26.45								
16	1750	17.77	4576	16.08	978	18.17	873	12.90	121	29.03	226	27.02	879	29.05	277	27.14								
17	1632	24.13	3066	23.53	986	23.86	929	18.67	98	23.66	257	19.73	1394	22.26	142	27.99								
18	1811	22.90	3537	22.21	1011	23.38	979	21.05	6.90	31.02	216	28.06	719	30.41	232	28.41								
19	1999	25.71	3266	25.06	1233	25.86	1154	20.61	101	21.42	277	20.84	1818	21.07	190	23.09								
20	2339	19.58	5366	18.70	1185	20.33	1093	15.86	-2.24	34.36	-2.86	0.0	40.2	42.05	169	27.10								
21	1948	21.82	4173	21.09	1094	22.29	979	18.09	127	30.31	191	29.41	785	30.31	219	25.60								
22	747	35.60	260	39.95	689	35.83	949	32.01	99.6	25.83	258	24.04	1327	24.33	142	29.22								
23	1896	25.07	3396	24.28	1238	25.21	1099	22.91	99.7	20.29	265	17.01	1698	18.75	165	24.08								
24	845	33.82	349	35.39	908	33.65	944	29.52	1.79	11.95	9.19	41.07	582	30.93	135	28.51								
25	1690	21.09	3806	20.15	1107	21.45	1046	17.80	89.8	23.82	240	22.10	1272	23.55	324	23.72								
26	1589	29.75	1876	29.35	1073	29.51	1040	25.19	87.3	31.29	183	30.21	631	31.30	219	27.16								
27	1.59	0.0	-1.1	0.0	503	39.75	730	36.98	1.76	40.97	-1.84	18.98	68.4	37.84	581	25.54								
28	1.08	0.0	-1.48	0.0	-1.86	0.0	-2.15	0.0	95.4	4.19	-0.22	0.0	165	34.99	161	30.93								
29	1966	24.60	3313	24.15	1157	24.87	1114	22.26	113	28.03	230	26.89	1214	27.37	216	24.76								
30	1.06	0.0	1.91	0.0	309	39.65	655	36.33	2.78	43.60	6.30	42.82	116	36.07	179	27.79								
31	2032	22.29	4164	21.46	1080	22.36	1001	19.72	112	25.07	277	24.46	1475	25.64	162	26.05								
32	1458	28.99	1758	28.36	936	29.00	928	26.14	120	30.50	147	30.65	633	31.43	200	25.55								
33	1492	21.21	2884	20.80	844	20.82	789	16.63	97.9	24.66	229	22.57	1241	23.56	181	26.29								
34	1891	22.19	4145	21.23	1090	21.74	1017	18.50	123	25.15	277	23.37	1475	24.51	198	25.02								
35	1.38	0.0	1.41	0.0	0.69	0.0	-1.06	0.0	1.71	40.80	0.69	0.0	60.0	37.89	464	27.07								
36	2003	25.63	3467	24.82	1101	25.85	1021	22.45	137	27.53	273	26.67	1097	28.22	345	25.91								
37	1781	28.82	2346	28.21	1207	28.89	1145	25.21	126	31.02	208	29.63	757	30.56	356	25.12								
38	2106	18.11	5228	17.44	1203	18.52	1072	15.12	87.3	21.59	286	19.52	1739	20.26	156	25.30								
39	2059	24.53	3967	23.44	1114	24.58	1002	19.84	133	27.35	296	24.23	1269	26.18	335	26.25								
40	317	39.34	104	0.0	799	35.76	868	31.21	-1.76	32.94	2.21	0.0	108	36.13	459	25.31								
41	700	35.85	271	39.36	756	34.65	855	30.09	12.4	38.38	4.22	0.0	146	34.97	256	29.20								
42	2036	23.03	3750	22.37	1038	23.53	995	20.05	119	25.17	275	24.83	1460	25.60	233	26.31								
43	1272	32.86	826	33.20	1029	32.98	1033	29.28	54.8	32.46	59.7	33.80	376	33.10	597	25.34								
44	2104	16.27	5392	15.01	1128	17.09	1207	8.81	100.4	20.39	300	17.60	1883	18.81	192	24.92								
45	67.4	0.0	1.72	0.0	0.23	0.0	-1.08	0.0	-0.42	38.96	2.77	0.0	14.5	0.0	165	30.45								
46	2012	19.77	4664	19.09	1103	20.08	1032	17.15	111	25.25	294	22.84	1607	23.86	206	25.78								
47	2056	19.11	5007	18.33	1182	19.45	1093	15.78	87.1	23.96	283	20.36	1634	21.52	139	27.22								

(Contd...)

Sample NO.	Kit A						Kit B						Our approach											
	RdRp			S			Orf1ab			N			RdRp			N			E			IC		
	RFU	Cq	RFU	RFU	Cq	RFU	RFU	Cq	RFU	RFU	Cq	RFU	RFU	Cq	RFU	RFU	Cq	RFU	RFU	Cq	RFU	RFU	Cq	
48	1903	21.77	4077	20.60	21.90	947	17.94	91.7	25.54	253	22.79	1308	24.77	185	25.97									
49	1640	21.39	3407	20.69	21.59	844	17.77	98.4	25.47	229	23.40	1158	24.56	136	26.60									
50	1424	29.15	1180	29.26	29.36	1061	25.80	117	0.0	103	32.49	428	32.74	164	29.36									
51	2273	19.87	4874	19.18	20.55	1061	17.53	131	25.22	304	23.74	1622	24.49	203	24.50									
52	1578	29.85	1533	29.53	28.55	1194	26.23	78.5	32.47	68	33.07	375	33.23	180	28.76									
53	2079	24.58	3584	23.83	25.31	989	22.18	126	28.47	245	27.35	1085	28.07	205	25.68									
54	2056	18.53	4769	17.61	19.03	970	13.97	114	21.40	293	19.32	1673	21.27	179	26.07									
55	1247	32.74	205	43.00	32.20	952	28.85	5.59	38.65	106	32.45	352	33.31	162	28.61									
56	1223	31.24	954	31.62	31.17	898	28.28	89.2	32.17	98.4	31.92	415	32.58	259	27.94									
57	1576	22.46	3061	22.06	23.09	935	20.75	110	26.41	236	26.09	1234	25.59	177	25.36									
58	1.47	0.0	3.88	0.0	0.0	532	37.91	125	11.22	1.99	0.0	8.21	0.0	168	29.71									
59	113	0.0	2.35	0.0	0.0	-0.05	0.0	-0.03	41.94	6.38	41.66	102	36.37	525	24.55									
60	2057	19.60	4748	18.77	20.13	990	16.16	108	22.27	291	21.04	1647	21.68	448	24.04									
61	1234	31.47	1037	31.38	0.0	-0.20	0.0	8.68	36.69	31.1	33.21	283	33.79	338	23.38									
62	1848	29.80	155	0.0	1072	27.24	24.79	124	31.58	269	28.12	918	29.34	140	29.88									
63	165	0.0	9.70	0.0	354	37.98	552	-1.04	35.88	0.26	0.0	79.9	36.84	345	26.30									
64	1175	28.87	2106	29.46	903	28.60	897	112	30.17	172	30.25	649	30.84	193	28.66									
65	1222	26.04	3071	25.64	26.12	884	21.19	132	28.60	242	26.20	1064	27.16	208	26.26									
66	1.27	0.0	-1.91	0.0	391	39.92	410	70.4	38.75	1.40	0.0	100	36.13	555	24.84									
67	1448	29.00	1455	31.79	27.11	1184	24.34	161	29.77	269	29.07	944	29.59	137	30.23									
68	1.88	0.0	1.25	0.0	-9.08	0.0	794	0.85	10.63	-0.07	0.0	13.7	0.0	359	26.83									
69	1649	28.15	1648	30.69	1084	26.95	1097	23.82	31.28	290	26.77	975	28.87	203	29.38									
70	1714	25.08	3728	24.14	1003	25.19	967	126	26.20	275	25.47	1253	26.61	428	25.03									
71	1488	29.42	1023	31.56	1048	28.20	1081	129	31.23	259	29.13	846	30.22	186	29.43									
72	1117	31.73	1328	31.43	979	31.48	959	76.6	13.80	113	31.88	418	32.59	482	25.62									
73	1257	29.34	1580	31.15	865	27.88	903	96.5	30.24	235	27.98	814	29.70	134	28.76									
74	1703	18.01	4162	17.34	889	18.35	867	-0.16	22.23	302	19.34	1713	20.36	265	26.19									
75	1919	24.89	3410	24.50	981	25.29	984	145	28.07	262	27.77	1230	27.64	223	26.46									
76	206	43.13	4.88	0.0	451	39.19	895	5.77	41.06	0.21	0.0	69.6	37.30	461	25.89									
77	1763	22.26	3425	22.08	1004	25.13	977	20.60	39.42	132	30.85	588	31.75	165	26.69									
78	0.74	0.0	-1.41	0.0	335	38.30	399	-1.05	35.89	-0.24	0.0	74.3	37.18	628	23.74									
79	5.16	0.0	0.10	0.0	345	39.81	424	0.13	8.79	-1.21	0.0	107	35.75	379	26.48									
80	1926	22.17	4031	21.43	982	24.35	950	121	26.78	250	23.84	1212	26.20	254	23.68									
81	1509	22.40	2956	22.04	877	22.55	902	115	28.04	229	25.31	1005	26.43	137	29.04									
82	0.34	0.0	-0.21	0.0	0.80	0.0	-1.15	3.92	42.57	0.63	0.0	8.32	0.0	108	31.93									
83	2059	23.44	3822	23.04	1018	23.93	977	21.28	25.94	283	24.94	1308	26.49	221	24.78									
84	1941	25.07	3380	24.74	1048	25.46	1013	92.7	31.64	128	30.89	813	30.24	149	27.59									
85	311	40.46	3.26	0.0	-1.36	0.0	1.82	-2.30	30.79	5.54	0.0	84.3	36.83	190	28.56									
86	1946	20.33	4277	19.76	1159	20.72	1148	129	28.70	265	26.38	1157	27.08	162	28.15									
87	1656	29.10	1957	28.96	1029	29.23	1033	100	31.98	152	30.38	690	31.03	190	27.79									
88	1592	28.04	2383	27.52	1112	27.77	1168	103	31.29	206	36.98	821	29.78	165	27.71									
89	578	37.92	30.0	0.0	419	35.54	654	2.69	40.54	17.9	0.0	174	34.53	144	28.73									
90	126	0.0	0.57	0.0	0.42	0.0	99.3	99.9	38.91	0.91	27.90	150	34.75	219	28.84									
91	1493	29.88	947.2	32.45	956	27.91	970	112	31.69	255	27.20	828	29.62	215	29.06									
92	2012	23.87	3812	23.39	966	23.65	964	122	27.62	245	30.20	1136	27.75	158	28.27									
93	1777	27.81	2716	27.17	1038	27.45	1028	94.6	31.83	181	23.28	725	30.59	132	29.46									
94	2102	21.47	4567	20.93	997	21.42	990	110	25.39	280	36.98	1390	24.98	133	27.40									
95	2.69	0.0	0.40	0.0	2.23	0.0	0.60	5.52	38.65	4.61	0.0	95.9	35.96	225	30.1									
96	1973	24.29	3786	23.80	750	30.65	561	6.58	38.17	-0.80	27.90	114.8	35.85	44.3	36.84									

testing strategies and elevating diagnostic efficacy (Fig. 2). The bar chart provided a clear overview of gene detection across various Ct value ranges for different genes tested using multiple kits (Kit A, Kit B) and a distinct approach. It vividly showed the frequency of gene detection within each Ct range, presenting a color-coded comparison across kits and genes. One striking observation was the consistency in gene detection within the 20.1–30 Ct range, which emerged as the most reliable across all kits and genes. This range consistently exhibited the highest frequency of gene detection, implying a robust and dependable identification within this specific Ct interval. Moreover, the chart highlighted the disparities in detection levels among different genes and kits. It underscored the importance of considering both the gene being targeted and the testing methodology, as they influence the detection efficacy within specific Ct value intervals (Fig. 1).

The Z-values reflect the deviation from the mean and indicate the sensitivity of each target in detection. Lower Z-values suggest a higher abundance or greater ease of detection. Notably, the E gene Ct stands out with the lowest Z-value of -1.49 , followed closely by Kit B N Ct with a Z-value of -1.46 . These values imply a potentially heightened sensitivity for detecting COVID-19 viral RNA in these specific gene regions. Moreover, all recorded *P*-values are extremely low (0.00001), signaling strong statistical significance. This suggests substantial evidence against the null hypothesis and underscores the reliability of the observed differences in sensitivity among gene targets.

The practical implications of these findings extend to the clinical realm of COVID-19 diagnostics. The superiority of the current approach suggested a promising avenue for enhancing accuracy in detecting COVID-19 cases, particularly emphasizing the significance of incorporating the E gene in diagnostic methodologies. The insights gained from this study advocate for the critical consideration of gene combinations in optimizing diagnostic accuracy, potentially influencing decision-making in clinical settings.

Despite the significance of these findings, there are inherent limitations that warrant consideration. Factors such as sample size, variations in testing methodologies, or specific population characteristics might have influenced the observed results. Therefore, future research endeavors should focus on expanding sample sizes, validating findings in diverse populations, as well as exploring additional gene combinations to further solidify these findings and translate them into clinically applicable solutions.

In conclusion, the assessment of AUC values among different testing kits and gene combinations elucidated a hierarchy of effectiveness in COVID-19 diagnostics. This approach, particularly with the inclusion of the E gene, emerges as a highly promising diagnostic method with enhanced accuracy, laying a foundation for improved COVID-19 testing methodologies and potentially contributing to more effective disease management strategies. The most dependable detection occurred within the 20.1–30 Ct range across various gene combinations and testing kits.

5. ACKNOWLEDGMENTS

We would like to thank the Kurdistan Regional Government, the Ministry of Higher Education and Scientific Research as well as the Presidency of Sulaimani University.

6. ETHICS APPROVAL

The study was approved by the Ethics Committee of the Biology Department, College of Science, University of Sulaimai (protocol code UoS-Sci-Bio 0010/September/19/2023)

7. CONFLICTS OF INTERESTS

The authors declared that they have no competing interests.

8. AUTHOR CONTRIBUTIONS

Conceptualization, S.A.; methodology, S.A. and D.A.; software, Z.H.; validation, S.A., D.A., and Z.H.; formal analysis, D.A. and Z.H.; investigation, D.A.; resources, D.A and Z.H.; data curation, S.A.; writing—original draft preparation, D.A.; writing—review and editing, S.A and Z.H.; visualization, D.A.; supervision, S.A. All authors have read and agreed to the published version of the manuscript.

9. FUNDING

This research received no external funding.

REFERENCES

- [1] Y. Chen, Q. Liu and D. Guo. "Emerging coronaviruses: Genome structure, replication, and pathogenesis". *Journal of Medical Virology*, vol. 92, no. 4, pp. 418-423, 2020.

- [2] R. A. Khailany, M. Safdar and M. Ozaslan. "Genomic characterization of a novel SARS-CoV-2". *Gene Reports*, vol. 19, p. 100682, 2020.
- [3] M. J. Loeffelholz and Y. W. Tang. "Laboratory diagnosis of emerging human coronavirus infections-the state of the art". *Emerging Microbes and Infections*, vol. 9, no. 1, pp. 747-756, 2020.
- [4] A. E. Gorbalenya and S. C. Baker. "The species severe acute respiratory syndrome-related coronavirus: classifying 2019-nCoV and naming it SARS-CoV-2". *Nature Microbiology*, vol. 5, no. 4, pp. 536-544, 2020.
- [5] C. Sohrawi, Z. Alsafi, N. O'Neill, M. Khan, A. Kerwan, A. Al-Jabir, C. Iosifidis and R. Agha. "World health organization declares global emergency: A review of the 2019 novel coronavirus (COVID-19)". *International Journal of Surgery*, vol. 76, no. 1, pp. 71-76, 2020.
- [6] S. U. Rehman, L. Shafique, A. Ihsan and Q. Liu. "Evolutionary trajectory for the emergence of novel coronavirus SARS-CoV-2". *Pathogens*, vol. 9, no. 3, p. 240, 2020.
- [7] L. T. Phan, T. V. Nguyen, Q. C. Luong, T. V. Nguyen, H. T. Nguyen, H. Q. Le, T. T. Nguyen, T. M. Cao and Q. D. Pham. "Importation and human-to-human transmission of a novel coronavirus in Vietnam". *New England Journal of Medicine*, vol. 382, no. 9, pp. 872-874, 2020.
- [8] R. Lu, X. Zhao, J. Li, P. Niu, B. Yang, H. Wu, W. Wang, H. Song, B. Huang., & N. Zhu. "Genomic characterisation and epidemiology of 2019 novel coronavirus: Implications for virus origins and receptor binding". *The Lancet*, vol. 395, no. 10224, pp. 565-574, 2020.
- [9] A. Banko, G. Petrovic, D. Miljanovic, A. Loncar, M. Vukcevic, D. Despot and A. Cirkovic. "Comparison and sensitivity evaluation of three different commercial real-time quantitative PCR Kits for SARS-CoV-2 detection". *Viruses*, vol. 13, no. 7, p. 1321, 2021.
- [10] Y. Lu, L. Li, S. Ren, X. Liu, L. Zhang, W. Li and H. Yu. "Comparison of the diagnostic efficacy between two PCR test kits for SARS-CoV-2 nucleic acid detection". *Journal of Clinical Laboratory Analysis*, vol. 34, no. 10, p. e23554, 2020.
- [11] V. M. Corman, O. Landt, M. Kaiser, R. Molenkamp, A. Meijer, D. K. Chu and T. Bleicker. "Detection of 2019 novel coronavirus (2019-nCoV) by real-time RT-PCR". *Eurosurveillance*, vol. 25, no. 3, p. 2000045, 2020.
- [12] M. Y. Wang, R. Zhao, L. J. Gao, X. F. Gao, D. P. Wang and J. M. Cao. "SARS-CoV-2: Structure, biology, and structure-based therapeutics development". *Frontiers in Cellular and Infection Microbiology*, vol. 10, pp. 587269, 2020.
- [13] I. Barjaktarović, M. Y. Wang, R. Zhao, L. J. Gao, X. F. Gao, D. P. Wang and J. M. Cao. "Diagnosing COVID-19: Diagnostic importance of detecting E gene of the SARS-CoV-2 genome". *Future Virology*, vol. 18, no. 1, pp. 31-38, 2023.
- [14] P. B. Van Kasteren, B. Van der Veer, S. Van Den Brink and L. Wijsman. "Comparison of commercial RT-PCR diagnostic kits for COVID-19". *Journal of Clinical Virology*, vol. 128, p. 104412.
- [15] Z. Iglói, M. Leven, Z. A. K. Abou-Nouar and B. Weller B. "Comparison of commercial realtime reverse transcription PCR assays for the detection of SARS-CoV-2". *Journal of Clinical Virology*, vol. 129, p. 104510, 2020.
- [16] A. Tastanova, C. I. Stoffel, A. Dzung, P. F. Cheng, E. Bellini, P. Johansen, A. Duda, S. Nobbe, R. Lienhard, P. P. Bosshard and M. P. Levesque. "A comparative study of real-time RT-PCR-based SARS-CoV-2 detection methods and its application to human-derived and surface swabbed material". *The Journal of Molecular Diagnostics*, vol. 23, no. 7, pp. 796-804, 2021.
- [17] J. Zhao, Y. Zhang and B. Cao. "Comparison of the performance of Six SARS-CoV-2 nucleic acid detection kit in positive samples using RT-PCR". *Journal of Clinical Chemistry and Laboratory Medicine*, vol. 4, no. 3, p. 170, 2021.
- [18] U. Eberle, C. Wimmer, I. Huber, A. Neubauer-Juric, G. Valenza and N. Ackermann, A. Sing and Bavarian SARS-CoV-2-Public Health Laboratory Team. "Comparison of nine different commercially available molecular assays for detection of SARS-CoV-2 RNA". *European Journal of Clinical Microbiology and Infectious Diseases*, vol. 40, pp.1303-1308, 2021.
- [19] D. Kalita and S. Deka. "Effectiveness of different gene-target strategies for SARS-CoV-2 screening by RT-PCR and other modalities". *Journal of Medical Diagnostic Methods*, vol. 9, no. 4, p. 298, 2020.
- [20] C. Hernández, C. Florez, S. Castañeda, N. Ballesteros, D. Martínez, A. Castillo, M. Muñoz, S. Gomez, A. Rico, L. Pardo, A. Paniz-Mondolfi and J. D. Ramírez. "Evaluation of the diagnostic performance of nine commercial RT-PCR kits for the detection of SARS-CoV-2 in Colombia". *Journal of Medical Virology*, vol. 93, no. 9, pp. 5618-5622, 2021.

The Reality of Extension Works in the Directorate of Agricultural Extension and Agricultural Research In Kurdistan Region of Iraq



Ahmed Sajid Hameed

Department of Horticulture, College of Agricultural Engineering Sciences, Raparin University, Kurdistan Region, Iraq

ABSTRACT

The study aims to identify the reality of extension works in the Directorate of Agricultural Extension and Agricultural Researches in the Kurdistan region of Iraq, and the study area included all governorates of the Kurdistan Region of Iraq (Germian, Erbil, Sulaymaniyah, Dohuk). The research community included all workers in agricultural extension, agricultural research, and agricultural directorates in all governorates, there were 215 respondents. The sample of the respondents includes (71) representing 33% of the population, taken by a simple random sampling method. The data were collected through personal interviews; questionnaire was prepared for this purpose. To confirm the validity, the questionnaire was reviewed by some experts. In general, the reality of extension work was described by the respondents (extension workers and agricultural engineers working in the Agricultural Research and Extension Directorate) as weak. Conducting training courses for agricultural extension workers regarding methods and methods of communication to work with farmers, emphasizing the importance and necessity of linking and coordinating between agricultural extension and education (universities) to graduate a qualified agricultural guide. Cooperation with other research agencies that work on producing and generating agricultural scientific information and practices approved by the Ministry of Agriculture.

Index Terms: The extension work, Directorate of Research and Agricultural Extension

1. INTRODUCTION

The agricultural sector is considered one of the most important productive sectors in the economy of most countries in general, and the developing ones in particular [1]. Agriculture plays a fundamental role in raising the economic and social level of farmers and constitutes a major source of national income, and a field

for the work of the vast majority of the population of countries around the globe [2].

The agricultural sector in the Kurdistan Region plays an important role in the region's economy, as it is responsible for achieving self-accumulation to develop itself and to secure a profuse used in the development of other sectors, in addition to providing food consumption requirements for all citizens and employing a lot of the workers [3].

The agricultural sector undertakes the following contributions:[4]

The contribution of agriculture to production local, the contribution of agriculture to the agri-food industries, as it

Access this article online

DOI: 10.21928/uhdjst.v8n1y2024.pp93-98 E-ISSN: 2521-4217
P-ISSN: 2521-4209

Copyright © 2024 Ahmed Sajid Hameed. This is an open access article distributed under the Creative Commons Attribution Non-Commercial No Derivatives License 4.0 (CC BY-NC-ND 4.0)

Corresponding author's e-mail: Ahmed Sajid Hameed, MS.c. Agricultural extension and education, Assist lecturer, Horticulture Department, College of Agricultural Engineering Sciences, Raparin University, Kurdistan Region, Iraq. E-mail: ahmad.sajid@uor.edu.krd

Received: 04-08-2023

Accepted: 08-03-2024

Published: 04-04-2024

works to secure the raw materials needed for it, and it also supplies agricultural industries factories with the raw materials needed for them, as is the case in tobacco, spinning and weaving factories, and others [1].

Since its inception, agricultural extension has had a role in bringing about agricultural and rural development, as it contributes to raising the economic efficiency of agricultural production through education and training activities and the transfer of technological information, which leads to improve agricultural production, increasing farmers' incomes, and improving working conditions and economic conditions for agricultural workers. Countries of the world adopt it, expand its scope, use it, and secure its requirements to perform its functions in the best way [5].

The agricultural extension plays an important role in documenting the relationship between the technical of agriculture and farmers [5], as its mission is to simplify and transmit information and scientific research results and include them in extension programs, and use various extension methods and means to reach farmers adopt modern agricultural methods, and work to increase production, raise farm incomes, and improve the economic and social level of farmers [6].

The extension is responsible for the process of disseminating modern agricultural ideas and practices by transmitting research results to farmers in a simple and applicable way, persuading and teaching them to put them into practice in accordance with their conditions to achieve high productivity, raise the economic level, and adapt to new changes [7].

The importance of the research is evidenced by the basic roles; the agricultural extension apparatus plays in the process of economic development, as the extension process depends on the guide as a crucial element in field extension activities, and a main tool for the delivery of extension services to farmers, and the transfer of their needs and desires to the concerned authorities to address them and find solutions to them. This requires that extension workers, including extension agents, have certain characteristics, to be able to work with farmers successfully [1], [2], [3], [4], [5].

The extension programs are considered an essential and important element in the extension process (extension work), and to be able to assess his work and the extent to which he

is able to perform his mission to the fullest, it is necessary to study the reality of the extension work [8].

The following are some defines about of research:

defines it as "an informal educational service performed outside of school for the purpose of training and influencing farmers and their families." This is for the purpose of adopting improved means in agricultural production, both plant and animal, as well as in marketing, farm management, and soil conservation [9], [10].

The extension planning "Is group from the works or the process which it has been by limiting of the extension program exclusion steps and from within the work the commissions inside the agricultural extension and the farmers" [11], [12].

Definition of implementing agricultural extension work: "It is carrying out all the steps that were written in the planning process for agricultural extension work." [13].

Define the extension evaluation: "Is the judgment on activity or value the extension program according to standards limited perceptible results" [14], [15].

Therefore, the research came to answer the following questions:

1. What is the reality of the extension work in the field of (planning, implementation, and evaluation process)?
2. What are the most important problems facing agricultural extension work?

The study aims to focus on the following is identified:

1. Identify the reality of the extension work (the process of planning, implementation, and evaluation).
2. Identify the problems facing the extension work.

2. RESEARCH METHOD

Research method: In the field, this research follows that the descriptive approach was used in the process of collecting data from the respondents (agricultural extension workers) because it is considered an appropriate method for obtaining data. This method is considered one of the branches of the curriculum and descriptive in social research [6].

Research population: The field survey was conducted in four regions: (Garmian, Erbil, Sulaymaniyah, and Dohuk). The

research included all agricultural extension specialists working at the General Authority for Agricultural Research and Extension and its branches, and the number of the research community reached 215 female agricultural extension workers [Table 1].

Research sample: Sample of the respondents includes (71) representing 33% of the population, taken by a simple random sampling method as shown in Table 1.

2.1. Data Collection

The questionnaire removal was prepared for the sake of collecting data, and the questionnaire consisted of two parts; the first part related to the reality of the indicative work: as a scale was prepared to measure the reality of the extension work and it consisted of three levels (weak 1, medium 2, good 3), and the second part concerned the main problems facing the extension work.

Building the scale: A tripartite scale was prepared to identify each of them (the reality of the planning process, the implementation process, and the evaluation process of extension work). The number of items for each topic of the reality of extension work was 10 items and the range of each topic was 1–30. This scale contains three levels (weak level with a score of 1–10, medium level with a score of 11–20, good level with a score of 21–30).

The face validity and content validity of the questionnaire were measured by presenting it to a group of experts in the field of agricultural extension. The initial test (pre-test) was conducted in July 2014 on a sample of 14 individuals. To measure the validity of the questionnaire, the questionnaire was distributed to a group of fig farmers (from outside the research sample), using the Pearson equation to obtain reliability and validity values of 0.71 and 0.84 degrees, respectively.

The data collection process was conducted from the respondents in the governorates, districts, and sub-districts

TABLE 1: Show the population and study sample of the respondents

No.	City	Population	The percentage	Sample
1	Germian	19	33	6
2	Sulaymaniyah	122	33	40
3	Erbil	41	33	14
4	Dohuk	33	33	11
Total	-----	215	-----	71

Source: Ministry of Agriculture - Kurdistan Region, Iraq 2014.

of the Kurdistan Region, using the questionnaire form and the personal interview, for the period between August 11, 2014, and September 12, 2014, when 71 forms were collected.

After the completion of data collection, unpacking, and classification, it was analyzed using the Statistical Analysis Program (SPSS) for the social sciences.

3. RESULTS AND DISCUSSION

1. Identifying the reality of extension work (planning, implementation, and evaluation process):

The General Directorate of Agricultural Research and Extension carries out the planning, implementation, and evaluation process for all extension activities and works in cooperation with other agricultural departments and branches affiliated with the General Directorate of Agricultural Research and Extension in all governorates of the region.

Table 2 shows the reality of the extension work (the planning process), which includes a set of topics of the planning process for extension work that was covered by the study. The results of the study showed the percentages of this process (the planning process), which are as follows:

1. The percentage of the weak level ranges between 77 and 35%.
2. The percentage of the medium level ranges between 31 and 16%.
3. The percentage of good levels ranges between 34 and 7%.

It used in conclusion from Table 2 is that more than half of the respondents (extension workers and agricultural engineers working in the Agricultural Research and Extension Directorate) described the reality of the extension work (the planning process) as weak.

Table 3 shows the reality of the extension work (implementation process), which includes a set of stages or topics of the implementation process of the extension work which were covered by the study and the results of the study showed the percentages of this process (implementation process), which are as follows:

1. The percentage of the weak level ranges between 84 and 49%.
2. The percentage of the medium level ranges between 44 and 16%.

TABLE 2: The reality of the extension work (planning process)

No.	Items	Frequency	%	The level
1.	Putting extension work plans by specialists	38	54	Weak
		20	28	Medium
		13	18	Good
2.	Flexibility in the work plan	25	35	Weak
		22	31	Medium
		24	34	Good
3.	Method of developing a work plan	46	65	Weak
		12	17	Medium
		13	18	Good
4.	The basis for the approved work plan	30	42	Weak
		21	30	Medium
		20	28	Good
5.	Calculate work plan costs	41	58	Weak
		15	21	Medium
		15	21	Good
6.	Limits of the work plan	39	55	Weak
		14	20	Medium
		18	25	Good
7.	Effectiveness of the work plan	49	69	Weak
		14	20	Medium
		8	11	Good
8.	Following the work plan	50	70	Weak
		11	16	Medium
		10	14	Good
9.	Suitable for the work plan with the needs of farmers	37	52	Weak
		21	30	Medium
		13	18	Good
10.	Existence of a work plan evaluation process	55	77	Weak
		11	16	Medium
		5	7	Good

3. The percentage of good levels ranges between 16 and 0%.

It used in conclusion from Table 3 is that more than half of the respondents (extension workers and agricultural engineers working in the Agricultural Research and Extension Directorate) described the reality of the extension work (implementation process) as weak.

Table 4 shows the reality of the extension work (the evaluation process), which includes a group of stages or topics of the evaluation process for the extension work that was covered by the study, and the results of the study showed the percentages of this process (evaluation process), which are as follows:

1. The percentage of the weak level ranges between 33 and 48%.
2. The percentage of the medium level ranges between 12 and 34%.
3. The percentage of good level ranges between 4 and 12%.

It used in conclusion from Table 4 is that more than half of the respondents (extension workers and agricultural

TABLE 3: The reality of the extension work (implementation process)

No.	Items	Frequency	%	The level
1.	The implementation of the extension work is carried out by specialists	41	58	Weak
		20	28	Medium
		10	14	Good
2.	Implement the principle of flexibility in the extension work	37	52	Weak
		23	32	Medium
		11	16	Good
3.	Using educational methods suitable with the needs of farmers	45	63	Weak
		15	21	Medium
		11	16	Good
4.	The implementation of the extension work be within the financial, material, and human capabilities	35	49	Weak
		26	37	Medium
		10	14	Good
5.	Conducting the following process for the implementation of the extension work	60	84	Weak
		11	16	Medium
		0	0	Good
6.	The implementation process is suitable to achieve the aims	41	58	Weak
		15	21	Medium
		15	21	Good
7.	The effectiveness of the extension work implementation process	38	54	Weak
		23	32	Medium
		10	14	Good
8.	Process of implementation extension work is within the limits of needs and objectives	40	56	Weak
		20	28	Medium
		11	16	Good
9.	The process of implementation of the extension work was carried out within the limited time	39	55	Weak
		26	37	Medium
		6	8	Good
10.	Conducting the evaluation process for the extension work carried out	35	49	Weak
		31	44	Medium
		5	7	Good

engineers working in the Agricultural Research and Extension Directorate) described the reality of the extension work (evaluation process) as weak.

In general, it can be concluded from the tables with numbers 2–3–4 that the reality of extension work was described by the respondents (extension workers and agricultural engineers working in the Agricultural Research and Extension Directorate) as weak, and this weakness may be attributed to the reality of the work to the following reasons:

1. The littleness of specialized agricultural extension staff who plan, implement, and evaluate extension work.
2. Littleness of experienced employees in the Agricultural Research and Extension Directorate in the field of extension work.
3. Weakness or no training courses in the field of extension work for employees of the Agricultural Research and

TABLE 4: The reality of the extension work (evaluation process)

No.	Items	Frequency	%	The level
1.	Evaluation of extension work plan and implementation	47	47	Weak
		17	17	Medium
		7	7	Good
2.	Flexibility evaluation in extension work during the planning and implementation	47	47	Weak
		15	15	Medium
		9	9	Good
3.	Evaluation of educational methods with the needs of farmers in the extension work	33	33	Weak
		34	34	Medium
		4	4	Good
4.	Evaluation of the financial, material, and human capabilities used in the extension work	36	36	Weak
		31	31	Medium
		4	4	Good
5.	Evaluating the following process for the extension work	48	48	Weak
		12	12	Medium
		11	11	Good
6.	Evaluation of the effectiveness of the planning and implementation process of the extension work	36	36	Weak
		26	26	Medium
		9	9	Good
7.	The extension work evaluation was within the limits of needs and aims	39	39	Weak
		20	20	Medium
		12	12	Good
8.	Evaluation of the implementation of the extension work was conducted within the specified time	39	39	Weak
		26	26	Medium
		6	6	Good
9.	Evaluation of the aims which it achieved through the implementation of the extension work	44	44	Weak
		16	16	Medium
		11	11	Good
10.	Evaluation of the behavioral changes after implementation of the extension work	47	47	Weak
		13	13	Medium
		11	11	Good

TABLE 5: The percentages of the most important problems facing the reality of extension work

No.	The problem	Frequency	%
1.	Weakness of cooperation between the Agricultural Scientific Research and the Agricultural Research and Extension Directorate	70	98.5
2.	Weakness in agricultural marketing, low prices	70	98.5
3.	Unavailability of money and moral incentives	69	97.1
4.	Unavailability of transportation	66	92.9
5.	Weakness relationship between the farmer and the agricultural guide	64	90.1
6.	Small size and dispersion of agricultural holdings	63	88.7
7.	Unavailability of tools and extension agents	61	85.9
8.	Unavailability of specialized technical staff	59	83

agricultural techniques.

- Unavailability of specialized technical staff and the overlapping and abundance of agricultural extension workers.
- Unavailability of money and moral incentives to encourage extension work.
- Weakness of cooperation between the agricultural scientific research and the Agricultural Research and Extension Directorate on a permanent and continuous basis, and this leads to a delay in the arrival of the results of the agricultural scientific research to the farmers.
- Weakness relationship between the farmer and the agricultural extension, the lack of response of most farmers to attending the extension seminars, and their lack of conviction in modern technology.
- Weakness agricultural marketing, low prices for agricultural products, and high prices for production inputs compared to the poor income of farmers.
- Small size and dispersion of agricultural holdings, which make it difficult to apply extension programs to them.

Extension Directorate.

- Identify the problems in the extension work.

A group of the most important technical and administrative problems that the extension work suffers from has been identified or recognized, and the problems Table 5:

- Unavailability of transportation means.
- Unavailability of tools and extension agents such as CD, agricultural films, and television, and the unavailability of extension fields that are used in the process of educating farmers, and thus persuading farmers of modern

4. CONCLUSIONS AND RECOMMENDATIONS

- Littleness of extension staff specialized in agricultural extension, as the General Directorate of Agricultural Research and Extension suffers from it.
- Littleness of experience for workers in the General Directorate of Agricultural Research and Extension in agricultural extension work, i.e., in (planning, implementing, and evaluating) agricultural extension work.

3. Littleness or no participation of workers in the General Directorate of Agricultural Research and Extension in training courses in the field of agricultural extension outside and within the region.
4. Conducting training courses for agricultural extension workers regarding methods and methods of communication to work with farmers.
5. Emphasizing the importance and necessity of linking and coordinating between agricultural extension and education (universities) to graduate a qualified agricultural guide.
6. Cooperation with other research agencies that work on producing and generating agricultural scientific information and practices approved by the Ministry of Agriculture and recommended for use by farmers, as the agricultural guide is the link with the farmer.

REFERENCES

- [1] S. Sultan. "The preferred guiding methods for farmers in Al-Hariq Governorate in the Kingdom of Saudi Arabia for Agricultural Sciences". *The Journal of Animal and Plant*, vol. 7, no. 1, pp.20-33, 2008.
- [2] T. M. Salih and N. Abdullah. "The reality of using extension methods by workers in agricultural extension in Nineveh Governorate and its relationship to some variables". *Al-Rafidain Agriculture Journal*, vol. 39, no. 2, 2011.
- [3] A. Khalidi. "The reality of agricultural extension workers in Tartous". *Tishreen University Journal of Scientific Studies and Research*, vol. 29, no. 2, pp. 55-68, 2011.
- [4] A. A. Hassan. "*The Reality of the Extension Activities of the Extension Centers in the Governorates of Duhok, Erbil and Sulaymaniyah, and the Obstacles in Performing their Educational Role*". PhD Dissertation, University of Mosul, Iraq, 2007.
- [5] A. Hafeez, I. Muhammad and H. Bahi. "*Methods of Scientific Research and Statistical Analysis in the Educational, Psychological and Mathematical Fields*". Dar Al-Kuttab for Printing and Publishing, Saudi Arabia, 2000.
- [6] A. G. Zijp and W. Byerlee. "*Rural Extension and Advisory Services*". World Bank, Washington, 2004.
- [7] J. R. Feder and G. Andeson. "*Rural Extension Services*". World Bank, Washington, 2003.
- [8] J. R. Feder, G. Willett and A. G. Zijp. "*Improving Agricultural Extension. A Reference Manual*". FAO Rome; 1997.
- [9] R. M. Ismail. "The reality of the extension planning process in the Baghdad agricultural directorate". *Iraqi Journal of Agricultural Sciences*, vol. 44, no. 6, pp. 719-728, 2013.
- [10] N. Riad. "*Fundamentals of Modern Agricultural Extension*". University of Damascus, Syria, 2002.
- [11] W. Peterson. "*Method for Planning Effective Linkages*". ISNAR, Netherlands, 2004.
- [12] R. Ramirez. "*Understanding Farmers' Communication Networks: Combining PRA with Agricultural Knowledge Systems Analysis*". Gatekeeper Series No. 66. IIED, London, 2003.
- [13] W. Rivera and M. K. Qamar. "*Agricultural and Rural Extension Worldwide: Options for Institutional Reform in the Developing Countries*". FAO, Rome, p. 12, 2001.
- [14] H. Subhi. "*Some Factors Affecting the Performance of Extension Agents in some Governorates of the Arab Republic of Egypt*". PhD Dissertation, Cairo University, Egypt, 1994.
- [15] W. G. Hubbard and L. R. Sandman. "*Using Diffusion of Innovation Concepts for Improved Program Evaluation Extension, A Reference Manual*". FAO, Rome, 2007.

Using the Cuckoo Optimization to Initialize the Harmony Memory in Harmony Search Algorithm to Find New Hybrid (CSHS) Algorithm



Fariaa Abdalmajeed Hameed^{1,2}, Kanar R. Tariq^{1,2}, Harith Raad Hasan^{1,2}, Riyam Alaa Johni³

¹Technical College of Informatics, Sulaimani Polytechnic University (SPU), Sulaimani, Iraq, ²Department of Software Engineering, Faculty of Engineering and Computer Science, Qaiwan International University (QIU), Sulaymaniyah, Iraq, ³Department of Computer Science, Kurdistan Technical Institute (KTI), Sulaymaniyah, Iraq.

ABSTRACT

The current paper seeks to present a hybrid harmony search algorithm, using CS and HS. The proposed algorithm takes advantage of using a method to initialize the harmony memory (HM) with the help of the cuckoo search optimization algorithm. The HS algorithm is inspired by the method used by musicians to create and enhance harmony in music. It follows 3 main principles of pitch adjustment (PA), HM consideration (HMC), and random selection (RS). The performance of HS can be affected by its poor accuracy in optimization and speed of convergence, 2 main issues with it. However, to improve the HS algorithm, Cuckoo search can be used as it can do a local search using one parameter only, other than the size of the population, making it work more efficiently. This current method has been tested for its validity and efficiency in performance by being implemented on many international standard optimization problems. The results confirm the fact that the performance of the currently proposed algorithm is better and more efficient in finding solutions compared to HS and other algorithms.

Index Terms: Optimization, Cuckoo Search, Harmony Search Algorithm, Harmony Memory, Hybrid Algorithm

1. INTRODUCTION

Many meta-heuristic search algorithms have been developed over the past decades and have proven useful in solving various optimization problems in technical fields. Such as genetic algorithm-simulated annealing, ant colony optimization, particle swarm optimization, bee algorithm, firefly algorithm [1], bat inspired approach (BIA) [2]. The main reasons metaheuristic algorithms are more popular among researchers than traditional optimization techniques, such as gradient-based techniques are algorithmic simplicity, ease of implementation, and versatility of solutions [3].

However, when solving some complex optimization problems, such as discrete structure optimization [4], water supply network construction [5], and vehicle routing problems [6]. Conventional optimization algorithms cannot provide reasonable and accurate solutions in a limited time.

In this article, we combine two metaheuristic algorithms, Harmony Search (HS) and Cuckoo Search Optimizer (CS), to produce a hybrid CSHS algorithm. Comparing eight benchmark optimization problems of the proposed algorithm with standard Cuckoo Search CS, Bat Algorithm BA, and standard Harmony Search HS, we find that CSHS performs better on most benchmark optimization problems than other algorithms where HS is prone to local minima. To alleviate this drawback, CS [7] can be used to perform local searches more efficiently.

In the last few years, various meta-heuristic algorithms have been created, and these algorithms have successfully

Access this article online

DOI: 10.21928/uhdjst.v8n1y2024.pp99-107

E-ISSN: 2521-4217

P-ISSN: 2521-4209

Copyright © 2024 Hameed, *et al.* This is an open access article distributed under the Creative Commons Attribution Non-Commercial No Derivatives License 4.0 (CC BY-NC-ND 4.0)

Corresponding author's e-mail: fariaa.hameed@spu.edu.iq

Received: 05-02-2024

Accepted: 19-03-2024

Published: 07-04-2024

settled problems related to optimization in different technical areas. These algorithms include genetic algorithm simulated annealing, particle swarm optimization, bee algorithm, ant colony optimization, firefly algorithm [1], bat inspired approach (BIA) [2]. There are a few reasons why metaheuristic algorithms are preferred over traditional optimization techniques. The metaheuristic algorithms are simple, and they can be easily applied. Furthermore, they provide comprehensive solutions that can be adapted to many different situations. When it comes to more complicated optimization problems such as vehicle routing problems, metaheuristic algorithms can provide reasonable solutions, while conventional algorithms cannot provide precise and logical solutions in a short time.

This article seeks to take advantage of using both Cuckoo Search and HS Optimizer to create a hybrid CSHS algorithm. Comparing eight benchmark optimization problems of the proposed algorithm with standard CS, standard BA, and standard HS, we find that CSHS performs better on most benchmark optimization problems than other algorithms where HS is prone to local minima. To alleviate this drawback, CS [7] can be used to perform local searches more efficiently.

2. METAHEURISTIC ALGORITHMS

2.1. Harmony Search (HS) Algorithm

The Harmony Search (HS) algorithm was recently introduced by Geem *et al.* It is believed to be a powerful population-based metaheuristic algorithm [8]. This search algorithm is influenced by what musicians do to achieve harmonic state through repeatedly adjusting their instruments' pitch. This algorithm takes the advantage of being simple as it does not need some information like the gradient of the objective function.

However, the HS may have slower convergence rates than other optimization techniques, especially in complicated and high-dimensional search spaces. This can have an influence on both the algorithm's performance and efficiency. Fine-tuning factors such as harmony memory (HM) size, pitch adjustment rate, and bandwidth can be difficult to determine and may need extensive trial and error in a number of problem areas.

HS was originally created to solve continuous optimization challenges. Adapting it to address discrete or combinatorial optimization problems may need additional techniques or adjustments. Furthermore, the quality of the initial HM can dramatically impact the algorithm's effectiveness.

In this optimization process, there are 3 factors: harmonic memory (HM), pitch adjustment rate (PAR), and distance bandwidth (BW). Besides these 3 factors, the size of the HM and the number of improvisations (NI) are considered factors. Having been randomly generated, the primary population of harmony vectors is stored in HM. Later, new harmony candidates are generated using all the solutions in the HM. This is done by the memory consideration rule, pitch adjustment rule, and random reinitialization. In the end, the new candidate harmony is compared to the worst harmony vectors to update the HM. If the worst harmonic vector is better than the worst harmonic vector in HM, it is replaced by a new candidate vector. This is repeated until the desired criteria are achieved. Basically, the HM algorithm includes 3 fundamental stages: initialization, harmony vector improvisation, and HM update. All these stages are elaborated on as follows [9]:

Step1. Initialize the optimization problem and algorithm parameters.

Step2. Initialize the HM.

Step3. Improvise a new harmony from the HM.

Step4. Update the HM.

Step5. Repeat Steps 3 and 4 until the termination criterion is satisfied. Figs. 1 and 2 show the Harmony Search flowchart and pseudocode, respectively.

2.2. Cuckoo Search (CS)

The new metaheuristic algorithm called Cuckoo Search (CS) is intended to solve optimization-related problems that align with the cuckoo species' distinctive parasitic behavior, predatory flight behavior, and fruit fly. However, CS, like any algorithm, has restrictions, such as requiring several parameters, such as the cuckoo population size, the chance of egg laying, and the step size for random walks. These parameter choices might have an impact on the algorithm's performance, thus obtaining the best values may necessitate some tinkering. Furthermore, balancing exploration and exploitation is a prevalent problem in optimization algorithms. The basic Cuckoo Search algorithm may not completely use historical data or previous iterations to steer the search. Improved memory and learning techniques may be required to improve the algorithm's performance.

In particular, each egg in CS represents a new solution; the cuckoo's flight determines its walking steps, and the objective is to replace an unsuccessful solution in the nest with an optimal and better one. That is, an egg is in every nest. The technique can be extended to more complicated scenarios in which there are numerous eggs in each nest (and thus numerous solutions). For instance, equation (1) below is used

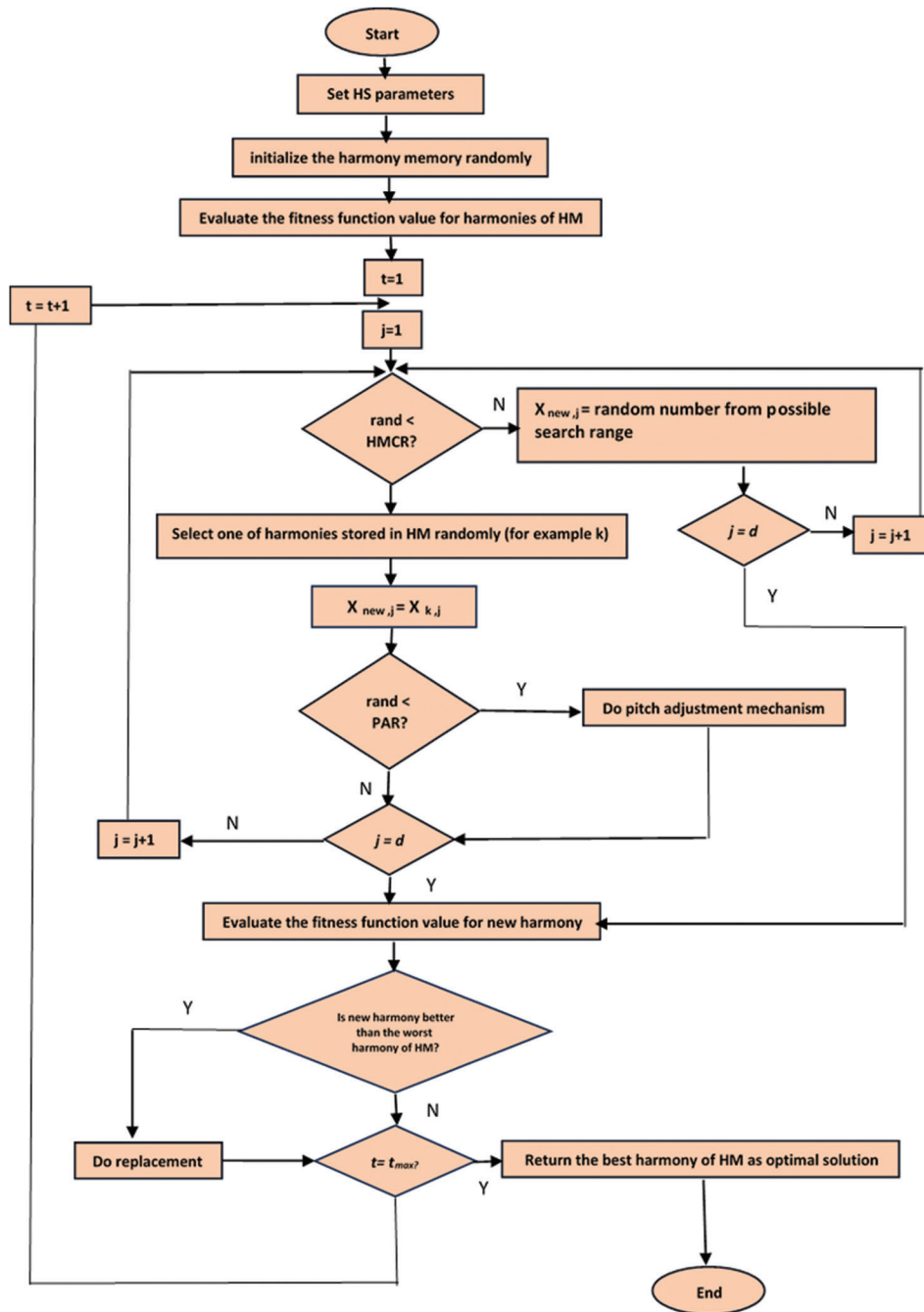


Fig. 1. Flow chart of the harmony search algorithm.

to carry out the Levy flight when creating a new solution $x(t+1)$ for Cuckoo I.

$$X_i^{(t+1)} = X_i^{(t)} + \beta \oplus Le^{yy}(\lambda) \quad (1)$$

The step size associated with the problem scales under examination is represented by $\alpha > 0$ in equation (1) above;

in most circumstances, $\alpha = 1$ can be utilized. The product \oplus denotes entry-wise multiplications, whose product is comparable to the PSO; however, because the length of the step is greater in the long run, the random walk-through Levy flight performs better in terms of search step exploration. Equation (2) essentially depicts a random walk that is provided by the Levy flights:

```

Pseudo code of the Harmony Search algorithm (HSA)
Begin;
Define objective function  $f(x)$ ,  $x=(x_1, x_2, \dots, x_d)^T$ 
Define Harmony Memory Considering rate (HMCR)
Define Pitch adjusting rate (PAR) and other parameters
Generate Harmony Memory with random harmonies
while ( $t < \text{max number of iterations}$ )
  while ( $i \leq \text{number of variables}$ )
    if ( $\text{rand} < \text{HMCR}$ ),
      Choose a value from HM for the variable  $i$ 
      if ( $\text{rand} < \text{PAR}$ ),
        Adjust the value by adding certain amount
      end if
    else
      Choose a random value
    end if
  end while
  Accept the New Harmony (solution) if better
end while
Find the current best solution
end
    
```

Fig. 2. Pseudocode of the harmony search algorithm.

$$Le^y \left(\gg \right) \sim u = t^{-\lambda}, (1 < \lambda \leq 3) \tag{2}$$

The above equation (2) is an infinite variance, having an infinite mean. Figs. 3 and 4 demonstrate the flowchart and the pseudocode of Cuckoo Search.

3. PROPOSED METHOD

Efficiency has turned into an indispensable desired quality in today's world. Therefore, almost all manufacturers strive to gain the highest efficiency possible. As a result, optimization is now valued and wanted more than ever. The ultimate goal is to seek the optimal values of some decision variables to achieve the best solutions to deal with some optimization problems. Instead of using the traditional method of creating and initializing the population of harmony vectors at random and storing them in the HM, the proposed method uses Cuckoo Search, which offers both local and global search to find the best solution. Thus, local solutions are maintained thanks to the harmony search algorithm's HM and pitch adjustment rate. The steps that follow introduce the key steps. Step 1: Initialize the optimization problem and algorithm parameters.

Step 2: Using CS to Initialize the HM.

Step 3: Improvise a new harmony from the HM.

Step 4: Update the HM.

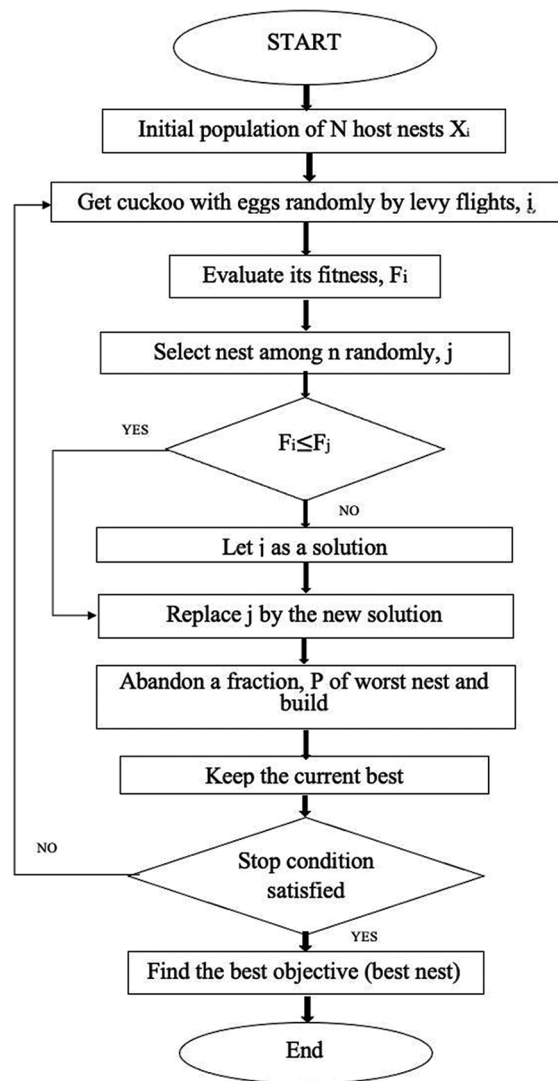


Fig. 3. Cuckoo algorithm flowchart [10].

Step 5: Repeat Steps 3 and 4 until the termination criterion is satisfied.

Figs. 5 and 6 show the CSHS flowchart and pseudocode.

4. EXPERIMENTAL SETUP AND RESULT

4.1. Experimental Setup

In this part, the studies that were carried out to determine and evaluate the performance of the proposed hybrid harmony algorithm and its variations are described for several analytical benchmark functions. Where it is applied to 8 minimization and maximization standard benchmark functions [11] as detailed in Table 1, Dimension (n) and Range are the feasible

bound of function, respectively. To have a balanced outcome, all the possible methods are used in a computer equipped with a Windows 10 OS, an Intel(R) Core (TM) i5-8350U CPU @ 1.70GHz 1.90 GHz, and Python used as a programming language.

```

Objective function  $f(X), X = (f(x_1, x_2, \dots, x_d))^T$ 
Generate initial population of  $n$  host nests  $X_i$  ( $i=1, 2, \dots, n$ )
While  $t < Max\_iterations$  do
    Get a cuckoo randomly by Levy flights
    Evaluate its quality/ fitness  $F_i$ 
    Choose a nest among  $n$  (say,  $j$ ) randomly
    If  $F_i > F_j$  then
        replace  $j$  by the new solution;
    End If
    A fraction ( $Pa$ ) of worse nests are abandoned and
    new ones are built;
    Keep the best solutions
    Rank the solutions and find the current best
End While
Postprocess results and visualization
    
```

Fig. 4. Pseudocode of the Cuckoo search algorithm

TABLE 1: Numerical benchmark functions		
Test function	Dimension (n)	Range
F1	30	[-100, 100]
F2	3	[-5.12, 5.12]
F3	2	[-32.768, 32.768]
F4	10	[-30,30]
F5	2	[-500, 500]
F6	2	[-100, 100]
F7	3	[-5.12, 5.12]
F8	2	[-1.28, 1.28]

TABLE 2: Summarize results for all benchmarks

Benchmark	n		HS	CS	BA	CSHS
F1	30	max	4.8265	78	8.365	0.74979
		min	0.0123	0.0000462	0.6124	0.66048
F2	3	max	1.45501	0	1.2301	12.0736
		min	0	0	0	0.01733
F3	2	max	0.650521303	6.91E-01	0.521303	2.6489
		min	6.1303E-19	6.50E-19	6.103E-15	0.025
F4	10	max	-0.418 e005	-0.418 e005	-0.418 e005	-0.409 e005
		min	-0.418 e005	-0.358 e005	-0.418 e005	-0.398 e005
F5	2	max	-837.965	-595.2761	-887.900	-429.42
		min	-837.9657	-710.327	-337.9657	-837.946
F6	2	max	1.7147	0.0298	1.847	0.96028
		min	0.2	0.00064	0.2	0.018245
F7	3	max	0.97989	1.7147	0.93389	1.2358
		min	0.000511	0.2	0.000511	0.0099
F8	2	max	-0.802-1	-0.265	-0.692	-0.0002
		min		-0.38	-1	-0.231

1. SpShpere (n variables) (F1):

$$SP_n(x) = \sum_{i=1}^n x_i^2 \tag{3}$$

2. Rastrigin's Function (F2):

$$f(x) = 10n + \sum_{i=1}^n [x_i^2 - 10 \cos(2\pi x_i)] \tag{4}$$

3. Ackley's Function (F3):

$$f(x) = -a * \exp \left(-b * \sqrt{\frac{1}{n} \sum_{i=1}^n x_i^2} \right) - \exp \left(\frac{1}{n} \sum_{i=1}^n \cos(c x_i) \right) + a + \exp(1) \tag{5}$$

Where:

a= 20

b = 0.2

c = 2*π

4. Rn Rosen Brock (F4):

$$f(x) = \sum_{i=1}^{n-1} [100(x_{i+1} - x_i^2)^2 + (1 + x_i)^2] \tag{6}$$

5. Schwefel's function (F5)

$$f(x) = \sum_{i=1}^n [-x_i \sin(\sqrt{|x_i|})] \tag{7}$$

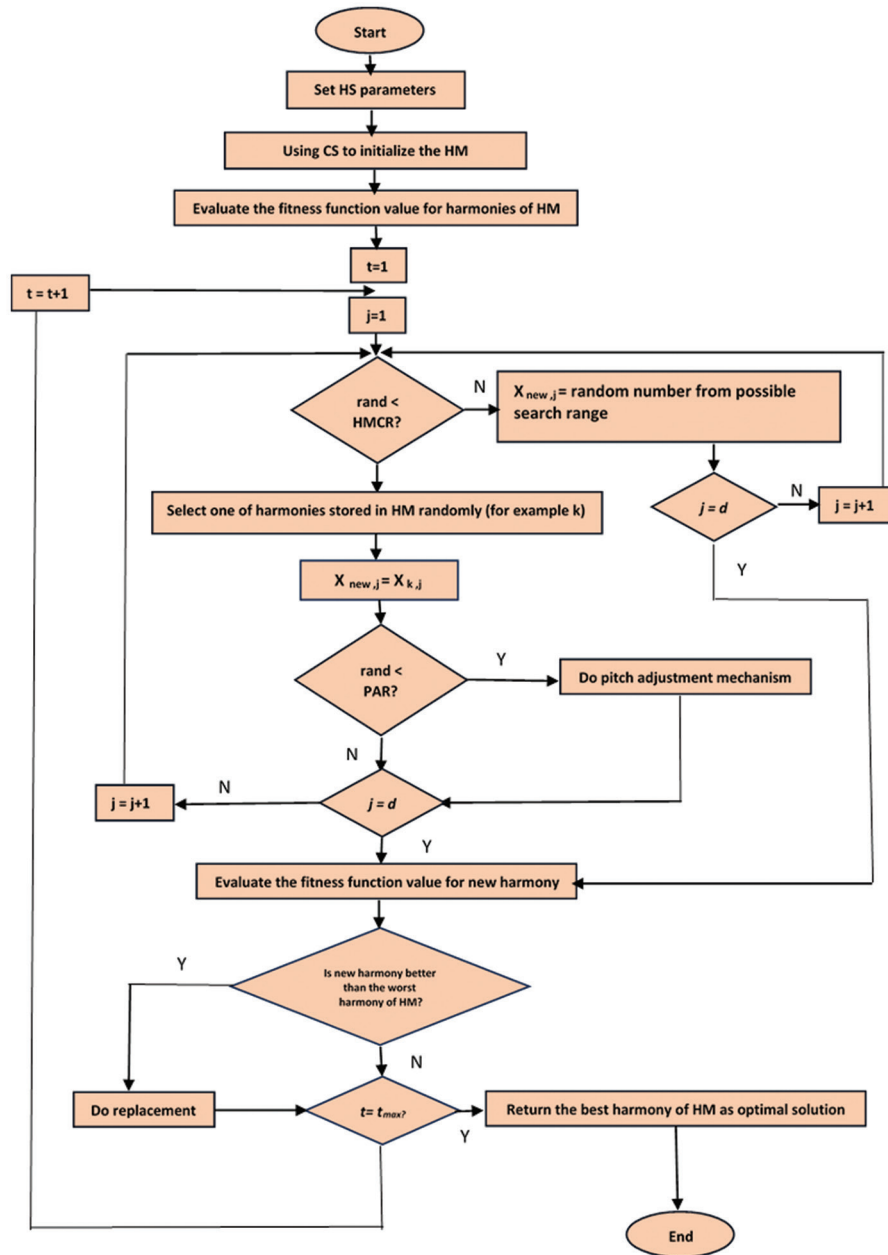


Fig. 5. CSHS flowchart.

6. Step Function (F6)

$$f(x) = \sum_{i=1}^n (x_i + 0.5)^2.$$

7. Generalized Restraining's Function (F7)

$$f(x) = \sum_{i=1}^n [x_i^2 - 10 \cos(2\pi x_i) + 10] \quad (9)$$

8. Quadric (F8)

$$f(x) = \sum_{i=1}^n i x_i^4 + random(0,1) \quad (10)$$

4.2. Experimental Result

The performance of CSHS on 8 benchmark functions is compared to 3 other approaches called BA, CS [12], HS [13], [14] to verify its performance. The results of the

TABLE 3: The average of the best value on F2 benchmark function with the iterations 2000,3000,4000,5000

Function	Iteration	HS	CS	BA	CSHS	Time CS	Time HS	Time BA	Time CSHS
F2	2000	0.633	1.45501	0.161	0.8930	0.124	0.141	0.311	0.281
	3000	0.786	0.00106	0.7729	0.095	0.188	0.188	0.138	0.359
	4000	0.161	0	0.143	0.261	0.218	0.219	0.2106	0.421
	5000	0.775	0	0.5626	0.318	0.218	0.218	0.205	0.483

TABLE 4: The average of the best value on F3 benchmark function with the iterations 2000,3000,4000,5000

Function	Iteration	HS	CS	BA	CSHS	Time CS	Time HS	Time BA	Time CSHS
F3	2000	6.50503E-1	6.50303E-1	4.418 e005	0.67566	0.171	0.171	0.141	0.312
	3000	6.51303E-19	6.3303E-1	3.418 e005	0.3746	0.187	0.218	0.188	0.39
	4000	6.591303E-19	6.91303E-1	4.418 e005	0.0280	0.234	0.218	0.219	0.452
	5000	6.1303E-19	6.34903E-1	6.418 e005	0.025	0.266	0.266	0.218	0.468

TABLE 5: The average of the best value on F4 benchmark function with the iterations 2000,3000,4000,5000

Function	Iteration	HS	CS	BA	CSHS	Time CS	Time HS	Time BA	Time CSHS
F4	2000	-0.418 e005	-0.411 e005	-0.413 e005	-0.412 e005	0.156	0.071	0.155	0.112
	3000	-0.418 e005	-0.362 e005	-0.315 e005	-0.415 e005	0.171	0.203	0.218	0.359
	4000	-0.418 e005	-0.362 e005	-0.417 e005	-0.415 e005	0.171	0.203	0.218	0.359
	5000	-0.418 e005	-0.362 e005	-0.615 e005	-0.415 e005	0.249	0.218	0.266	0.421

TABLE 6: The average of the best value on F5 benchmark function with the iterations 2000,3000,4000,5000

Function	Iteration	HS	CS	BA	CSHS	Time CS	Time HS	Time BA	Time CSHS
F5	2000	-837.9657745	-595.2761	-395.761	-837.246	0.156	0.171	0.124	0.312
	3000	-837.965	-684.648	-954.648	-837.842	0.187	0.172	0.188	0.375
	4000	-837.965	-623.720	-603.70	-837.884	0.218	0.219	0.218	0.405
	5000	-837.965	-699.914	-749.14	-837.798	0.266	0.234	0.218	0.437

TABLE 7: The average of the best value on F6 benchmark function with the iterations 2000,3000,4000,5000

Function	Iteration	HS	CS	BA	CSHS	Time CS	Time HS	Time BA	Time CSHS
F6	2000	0.20	0.0055	0.84	0.2662	0.141	0.187	0.134	0.214
	3000	0.37	0.0298	0.9052	0.0692	0.156	0.188	0.103	0.172
	4000	0.84	0.00064	0.75	0.9052	0.187	0.172	0.298	0.374
	5000	0.75	0.00155	0.0298	0.4888	0.203	0.218	0.234	0.39

TABLE 8: The average of the best value on F7 benchmark function with the iterations 2000,3000,4000,5000

Function	Iteration	HS	CS	BA	CSHS	Time CS	Time HS	Time BA	Time CSHS
F7	2000	0.131	0.20	0.122	0.6351	0.172	0.156	0.311	0.228
	3000	0.142	0.39	0.192	0.00990	0.187	0.203	0.138	0.043
	4000	0.187	0.54	0.387	0.01149	0.218	0.218	0.2106	0.39
	5000	0.203	0.95	0.293	0.0526	0.25	0.219	0.205	0.468

TABLE 9: The average of the best value on F8 benchmark function with the iterations 2000,3000,4000,5000

Function	Iteration	HS	CS	BA	CSHS	Time CS	Time HS	Time BA	Time CSHS
F8	2000	-1	-0.299	-0.262	-0.153	0.0452	0.03355	0.228	0.078
	3000	-1	-0.362	-0.310	-0.231	0.06865	0.0484	0.033	0.1162
	4000	-0.802	-0.340	-0.680	-0.0002	0.0905	0.0655	0.039	0.1498
	5000	-0.802	-0.380	-0.802	-0.0003	0.11235	0.07955	0.468	0.18565

TABLE 10: The average of the best value on F1 benchmark function with the iterations 2000,3000,4000,5000

Function	Iteration	HS	CS	BA	CSHS	Time CS	Time HS	Time BA	Time CSHS
F1	2000	3.727	0.87	0.5626	0.71727	0.11	0.078	0.1638	0.56005
	3000	0.5626	0.08	0.29	0.69163	0.1638	0.11465	0.2106	0.8502
	4000	2.9317	0.29	0.69143	0.68829	0.2106	0.1529	0.0708	1.0975
	5000	1.3834	0.78	0.5626	0.69143	0.26205	0.1903	0.31465	1.40325

```

Pseudocode of the HSCS
Begin;
Define objective function  $f(x)$ ,  $x=(x_1, x_2, \dots, x_d)^T$ 
Define Harmony Memory Considering rate(HMCR)
Define Pitch adjusting rate (PAR) and other parameters.
Generate Harmony Memory with the Cuckoo Search algorithm
Begin;
Generate initial population of  $n$  host nests  $X_i$  ( $i=1,2,\dots,n$ )
While  $t < \text{Max\_iterations}$  do
    Get a cuckoo randomly by Levy flights
    Evaluate it's quality/fitness  $F_i$ 
    Choose a nest among  $n$  (say,  $j$ ) randomly
    If  $F_i > F_j$  then
        replace  $j$  with the new solution;
    End if
    A fraction ( $Pa$ ) of worse nests are abandoned and new ones are built;
    Keep the best solutions
    Rank the solutions and find the current best
End while
Postprocess results and visualization
//End generation of the Harmony Memory
while ( $t < \text{max number of iterations}$ )
    while ( $i < \text{number of variables}$ )
        if ( $\text{rand} < \text{HMCR}$ )
            Choose a value from HM for the variable  $i$ 
            if ( $\text{rand} < \text{PAR}$ ),
                Adjust the value by adding a certain amount
            end if
        else choose a random value
        end if
    end while
    Accept the new harmony (solution) if better
end while
Find the current best solution
end
    
```

Fig. 6. Pseudocode of the HSCS algorithm.

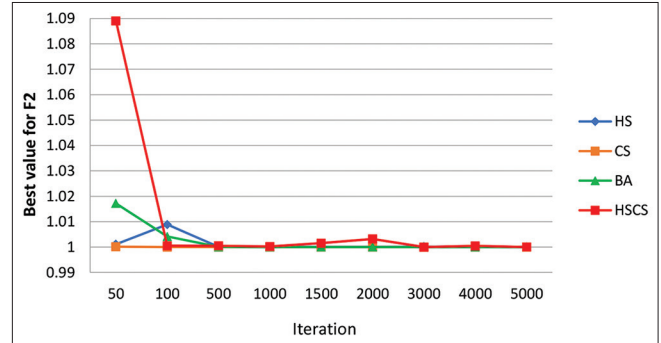


Fig. 8. The Performance of HS, CS, BA, HSCS on test function F2.

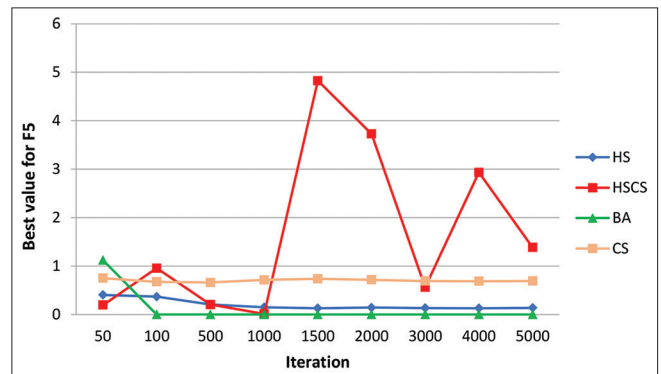


Fig. 9. The Performance of HS, CS, BA, HSCS on test function F5.

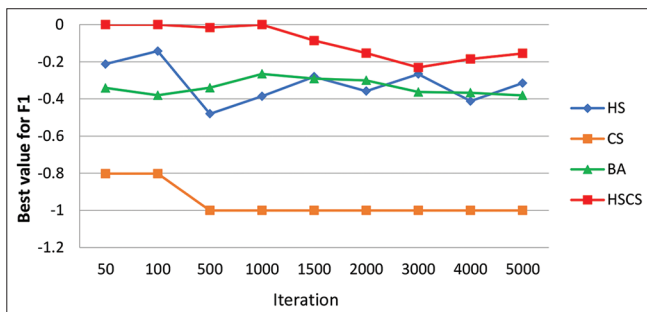


Fig. 7. The Performance of HS, CS, BA, HSCS on test function F1.

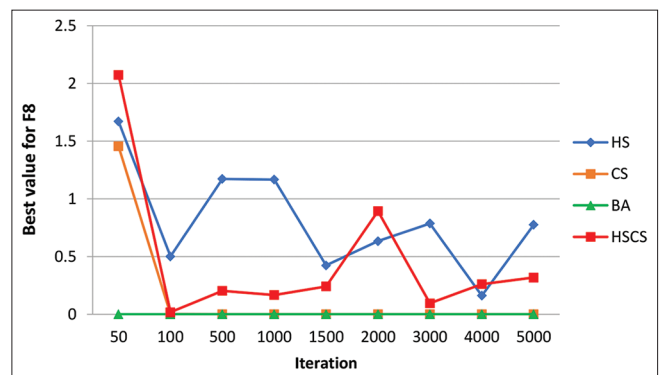


Fig. 10. The Performance of HS, CS, BA, HSCS on test function F8.

benchmark functions used in this experiment are illustrated in Table 2. Here, n shows the function dimension and \min and \max represent minimum value and maximum value, respectively.

This research considers the time component in addition to all the information displayed in Tables 2-10, where different

numbers of iterations have been applied to the optimization methods.

In addition, the most representative convergence curves are provided (Figs. 7-10). The values in the figures represent the average functional optimum, with being the true value. From Fig. 7, we can see that HSCS is better at finding solutions than any other method, especially in F1, F2, F5, and F8.

5. CONCLUSION

The CSHS algorithm outperformed the other three classical optimization algorithms, CS, BA, and HS, in terms of obtaining the best value or minimum values in the majority of the benchmark functions, as can be seen from the tables above and Table 2's results. This is because the proposed algorithm completed local searches more quickly than the other two classical algorithms. The primary advantage of Cuckoo Search is that it requires relatively few parameters – just one, the probability function – and the population size. In comparison to other metaheuristic algorithms, this makes the Cuckoo search algorithm highly straightforward and efficient. It enhances the process by merging HS and CS.

ACKNOWLEDGMENT

The authors would like to acknowledge the Sulaimani Polytechnic University, Qaiwan International University, and Kurdistan Technical Institute for their financial support of this research. Thanks also go to the reviewers of this paper for their constructive comments.

DATA AVAILABILITY

All data included in this study are available on request by contact with the corresponding author.

CONFLICTS OF INTEREST

The authors declare that there are no conflicts of interest regarding the publication of this paper.

REFERENCES

- [1] X. S. Yang. "Nature-inspired Metaheuristic Algorithms". Luniver Press, United Kingdom, 2010. Available from: <https://books.google.iq/books> [Last accessed on 2024 Feb 05].
- [2] X. S. Yang. A new metaheuristic bat-inspired algorithm. In: "Nature Inspired Cooperative Strategies for Optimization (NICSO 2010)". Springer, Berlin, Heidelberg, pp. 65-74, 2010.
- [3] X. S. Yang. "Nature-inspired metaheuristic algorithms: Success and new challenges". *Journal of Computer Engineering and Information Technology*, vol. 1, pp. 1-3, 2012.
- [4] K. S. Lee, Z. W. Geem, S. Lee and K. Bae. "The harmony search heuristic algorithm for discrete structural optimization". *Engineering Optimization*, vol. 37, no. 7, pp. 663-684, 2005.
- [5] Z. W. Geem. "Optimal cost design of water distribution networks using harmony search". *Engineering Optimization*, vol. 38, no. 3, pp. 259-277, 2006.
- [6] Z. W. Geem, K. S. Lee and Y. Park. "Application of harmony search to vehicle routing". *American Journal of Applied Sciences*, vol. 2, no. 12, pp. 1552-1557, 2005.
- [7] R. G. Babukartik and P. Dhavachelvan. "Hybrid algorithm using the advantage of ACO and Cuckoo search for job scheduling". *International Journal of Information Technology Convergence and Services*, vol. 2, no. 4, pp. 25-34, 2012.
- [8] Z. W. Geem, J. H. Kim and G. V. Loganathan. "A new heuristic optimization algorithm: Harmony search". *Simulation*, vol. 76, no. 2, pp. 60-68, 2001.
- [9] K. S. Lee and Z. W. Geem. "A new meta-heuristic algorithm for continuous engineering optimization: Harmony search theory and practice". *Computer Methods in Applied Mechanics and Engineering*, vol. 194, no. 36, pp. 3902-3933, 2005.
- [10] M. Shehab, A. T. Khader and M. A. Al-Betar. "A survey on applications and variants of the cuckoo search algorithm". *Applied Soft Computing*, vol. 61, pp. 1041-1059, 2017.
- [11] "Evolutionary Programming Made Faster". IEEE Xplore. Available from: <https://ieeexplore.ieee.org/abstract/document/771163> [Last accessed on 2024 Feb 04].
- [12] X. S. Yang and S. Deb. "Cuckoo Search Via Lévy Flights". IEEE Xplore, 2009. Available from: <https://ieeexplore.ieee.org/document/5393690> [Last accessed on 2024 Feb 04].
- [13] J. H. Kim and Z. W. Geem. "Harmony Search Algorithm: Proceedings of the 2nd International Conference on Harmony Search Algorithm (ICHSA2015)". Springer, Berlin, 2015. Available from: <https://books.google.iq/books> [Last accessed on 2024 Feb 05].
- [14] Y. Feng, G. G. Wang and X. Z. Gao. "A novel hybrid Cuckoo search algorithm with global harmony search for 0-1 knapsack problems". *International Journal of Computational Intelligence Systems*, vol. 9, no. 6, pp. 1174-1190, 2016.

Training Needs of Farmers in the Field of Fig Fruit Breeding in Rania District: Sulaymaniyah Governorate and Relationship with Some Variables



Ahmed Sajid Hameed

Department of Horticulture, College of Agricultural Engineering Sciences, Raparin University, Kurdistan Region, IRAQ

ABSTRACT

The study aimed to identify the training needs of the farmers in the field of fig fruit breeding and to determine the relationship between training needs and some variables. The study area included Rania District in Sulaymaniyah Governorate. The research population involved 5205 farmers. The research sample was 104 respondents who were taken using a simple random sampling method, representing 2% of the study population. The research included 20 villages that were included in the research. Data were collected through the questionnaire and personal interviews. The results showed that more than 74% of fig farmers were between (medium and high levels) in need of training in their field of work, and the average training need reached 53.25°. The results showed that there is a statistically significant relationship between the training need and the economic level and the number of years working in the field of fig breeding. The study also showed that there is no significant relationship between the training need and (the area used for raising figs). The study recommended that the responsible authorities increase extension services and activities (such as seminars, training courses, and extension magazines) to increase farmers' skills and thus increase production.

Index Terms: Training needs, Fig fruit farmers, Fig plant breeding.

1. INTRODUCTION

Figs (Latin: *Ficus carica*), which is a seasonal fruit tree, is cultivated in West Asia and the Middle East, but its habitat extends from Turkey to northern India and is spread in the Mediterranean countries. It reached southern California in 1759 [1]. Figs provide the human body with vitamins, minerals, and fiber. They contain a large proportion of sugar and major mineral salts, such as calcium, phosphorous,

and vitamin C and have health benefits such as getting rid of acne and pimples, preventing constipation, high blood pressure and protecting against prostate cancer [2]. Fig fruit is famous and favorite throughout history. It is a fruit that has been appreciated since ancient times in its dry and greenish form, and it is grown in several regions, such as Palestine, Persia, Iraq, Syria, Jordan, Lebanon, Libya, Saudi Arabia, and the Sultanate of Oman. Warm and temperate, it is called (in English: *Ficus Caria*) [3], [4]. The main compound found in figs is dextrose, which is 50% of the fig composition - vitamins A, B, and C - containing high levels of iron, calcium, potassium, and copper salts - which gives high calories. Hence, every 100 g of green figs gives 70 calories, and dry figs give the same weight 270 calories [5]. The fig plant is an evergreen perennial that includes many genera and species, some of which are eaten - such as parchment and

Access this article online

DOI: 10.21928/uhdjst.v8n1y2024.pp108-114

E-ISSN: 2521-4217

P-ISSN: 2521-4209

Copyright © 2024 Hameed. This is an open access article distributed under the Creative Commons Attribution Non-Commercial No Derivatives License 4.0 (CC BY-NC-ND 4.0)

Corresponding author's e-mail: Ahmed Sajid Hameed, M.Sc. Agricultural extension and education, Assist lecturer, Department of Horticulture, College of Agricultural Engineering Sciences, Raparin University, Kurdistan Region, IRAQ. E-mail: ahmad.sajid@uor.edu.krd

Received: 04-08-2023

Accepted: 22-03-2024

Published: 09-04-2024

sycamore figs - which contain many proteins, carbohydrates, vitamins, minerals, and digestive enzymes [5]. Figs are one of the most water-rich summer fruits and are delicious in taste [6]. They are not eaten unless ripe, unlike some other fruits whose acid is eaten. It is rich in minerals, fresh, and dried. Figs are classified as a member of the Moraceae family and its fruits ripen in the summer. Figs are grown in various regions of the world, but its fertile crescent is located in the Levant and Iraq, and it is grown in regions with relatively warm winters that are not exposed to frost [7]. Furthermore, some types of it grow in rocky areas [8]. It comes to Saudi Arabia and the Gulf from various regions, but modern farms in the south and north of the kingdom supply the market with large quantities of it. Figs are varieties of it: the Esmeralda, the American, the common, and the wild, known as the fig stallion. It also has small, delicious varieties that grow in the Taif and southern regions, and it is called "hamat" there [9]. Medical uses and benefits: there are several uses and benefits of figs, including the manufacture of syrups, soothes the skin, softens it and removes pimples, removes the problems of colds and colds and their effects on the nose and throat - Figs are used on dental abscesses, gum infections, tumors in the mouth and others. It strengthens the liver and activates it and removes the enlargement of the spleen. Among the benefits of fig fruits are strengthen the kidneys, increasing blood circulation activity, and treating chest diseases, coughs, asthma, and infections [10]. It prevents the pooling of water in the heart, lungs and body that results by gently reducing pressure, and preventing bleeding - the brain and blood circulation in it activates so the brain functions in a better way, especially if it is eaten with materials rich in phosphorous such as nuts, almonds, pistachios and pine nuts - treats circulatory diseases in the brain such as phlegm and tremor Blotting - treats skin diseases such as vitiligo - treats gout diseases and works to excrete uric acid salts from the body through urine and through sweating. It treats joint diseases and pain [11]. Figs treat mental illnesses, calm nerves, remove anxiety, fear, frustration, and tension. Figs are an important source for strengthening and stimulating sexual energy for men and women, similar to strawberry and blueberry [8].

According to the data contained in the census, there is a variation in the annual production of figs, as production reached 24,418 tons of figs in 2017, and increased to 28,872 tons in 2018, then decreased in 2019 to 19531 tons, then increased in 2020–27,558 tons (Ministry of Agriculture - Kurdistan Region 2020).

The local product of figs is not sufficient to meet local needs, and for this reason, about 24,000 tons of figs are

imported annually from abroad, and during the past 5 years, 93,112 tons of figs were imported from Iran, Syria, Egypt, and southern Iraq to the Kurdistan Region (Ministry of Agriculture - Kurdistan Region 2019).

This difference in the quantity of production is due to several reasons:

1. Diseases that affect fig plants.
2. Insects that infect fig plants.
3. Training needs in fig plant breeding.

Hence, the idea of the current research is to study the training needs of fig farmers in managing the fig plant and the relationship between the training needs of farmers and some of their personal variables.

Accordingly, the current research is devoted to identifying the training needs of fig fruit farmers in fig plant breeding, and this research focuses on the following questions:

1. What is the level of training needs of fig fruit farmers in the field of fig breeding?
2. What is the relationship between the level of training needs of farmers and some of the following personal variables: (The economic level of the farmers, the area used to grow figs and how many years number worked in growing the fig plant)?

1.1. Research Aims

1. Determine the level of training needs of fig fruit farmers in the field of fig breeding.
2. Determine the relationship between the level of training needs of farmers and some of the following personal variables (the economic level of the farmers, the area used to grow figs and how many years number worked in growing the fig plant).

1.2. Research Hypothesis

There is no significant correlation between the training needs of fig fruit farmers and (the economic level of the farmers, the area used to grow figs, and how many years number worked in growing the fig plant).

2. RESEARCH METHODS

2.1. Research Method

The descriptive approach was used to conduct the current research [12], [13], which aims to uncover the studied reality by accessing data that identify the training needs of fig fruit farmers and in everything related to fig plant breeding.

2.2. Search Area

The research included farmers located within the Rania Agriculture Division located within the borders of Sulaymaniyah Governorate. This division was chosen to conduct the research because the number of fig farmers in it was large, reaching 5205 farmers.

2.3. Research and Sample Community

The number of agricultural villages reached 57 villages. The number of villages that were included in the research reached 20 villages, i.e., 37 villages were excluded due to the small number of farmers in them, as shown in Table 1.

The research included all fig farmers who own agricultural lands and are officially registered with the Agricultural Division in Rania district. A proportional random sample was selected from the community of farmers who were actually included in the research 5205 farmers with a ratio of 2% of fig fruit farmers were taken due to their large number. The sample of farmers who were included in the research reached 104 farmers, as shown in Table 1.

2.4. Prepare the Training Needs Scale

The researcher prepared a measure of the training needs of fig fruit farmers after reviewing the scientific literature in the field of (fig fruit farmers) and surveying the opinions of experts and specialists in this field [14].

The scale included two parts, as follows:

Part One: It includes a number of questions that are believed to be related to the personal variables of fig farmers, which are related to their training needs regarding dealing with the fig plant, and these variables are:

- The economic level of the farmers.
- The area used to grow figs.
- How many years number worked in growing the fig plant.

These variables were identified after field follow-up of the researcher in the target area, reviewing the relevant literature, and reviewing studies related to training needs [15].

Part Two: The researcher developed a measure of training needs in the field of fig cultivation according to the scientific literature and took the opinions of a group of specialists in horticulture and gardening engineering.

Two fields of research were identified and included 20 items as follows:

TABLE 1: The research population and sample

No.	Name of the village	The number of farmers	The ratio (%)	The sample
1	Sarkabkan	365	2	7
2	Dollaraqa	187	2	4
3	Charqorna	405	2	8
4	Shaedafaqeer	118	2	2
5	Boskeen	646	2	12
6	Qorago	243	2	5
7	Darband	188	2	4
8	Toopao	392	2	7
9	Qroocha	476	2	9
10	Golak	151	2	3
11	Grrjaan	582	2	11
12	Sarkhma	125	2	3
13	Qamtaraan	150	2	3
14	Astreelan	104	2	2
15	Galegolán	102	2	2
16	Kanemaran	281	2	6
17	Grdetle	222	2	4
18	Zangaranga	142	2	3
19	Cholea – Namrood	226	2	5
20	Garmkadaal	200	2	4
Sum		5205	2	104

- The field of managing the fig plant, which includes 13 items.
- The field of fig plant diseases includes 7 items.

2.5. Validity Measure

For the purpose of examining the validity of the questionnaire, the questionnaire form was presented to agricultural extension and education experts to ensure that the questionnaire questions measured the training needs of fig farmers. As for measuring the validity of the content, it was measured by presenting the questionnaire to experts in the field of horticulture.

2.6. Measurement of Reliability and Validity Factor

Pre-test of the questionnaire form was conducted on August 16, 2020, to measure the validity and validity of the questionnaire and using the half-segmentation equation of (person) to obtain the stability and then the root of the reliability degree to obtain the degree of validity, and their value was 0.86, 0.927° and straight.

2.7. Data Collection

The process of collecting data from farmers in the two areas within the borders of Sulaymaniyah Governorate - Raparin District (Rania district) was carried out through the questionnaire form and the personal interview and recording of their answers for the period between June 9, 2020, and October 25, 2020, where 104 were collected forms.

2.8. Statistical Methods

After data were collected, unpacked, and tabulated, it was analyzed using the Social Sciences Statistical Analysis Software (SPSS).

3. RESULTS AND DISCUSSION

The first aim:

1. Determine the level of training needs of fig fruit farmers in the field of fig breeding.
2. Measuring the training need for fig fruit farmers in the field of fig breeding:

Table 2 concludes that the level of training needed for fig farmers is described as medium and tends to be high because 74% of farmers fall into this category, and the degree of training needed ranges between 51 and 100°, and the average degree of training needed is 53.25°.

The higher the score a farmer obtains through the questionnaire form, the more this means that farmers need training courses in their field of work.

This may be due to several reasons, the most important of which are the following:

- Through direct observation during the data collection process, it has been observed that farmers do not wish to read the manuals that are being distributed through extension agents.
- Through direct observation during the data collection process, it was noted that farmers do not wish to visit the Agricultural Extension Department in the event of an injury.

The second aim:

The second objective of the study: To identify the relationship between the training needs for fig fruit farmers and some personal variables that were dealt with in the study as follows (the economic level of farmers, the area

used to grow the fig plant, years number worked in growing the fig plant).

1. The economic level

To describe the economic level of the fig fruit farmer, the farmers were divided into three income levels (low level, medium level, high level). The highest percentage was for the average economic level and reached 77%, followed by 13% for the low economic level, and finally 10% for the high economic level, as shown in Table 3.

To determine the type of correlation between the training need and the economic level, the simple correlation equation (Pearson) was used and its value was found to be 0.295°. This indicates the existence of a positive correlation to verify the significance. For this relationship, the (t) test was used, the calculated value of which was 2.039°, and when compared to the tabular value (t) of 1.982°, this means that it is significant at the probability level of 0.05. Therefore, the hypothesis that there is a correlation between the training needs of fig fruit farmers and the economic level was accepted.

This can be explained by the existence of a significant correlation between fig growers and the economic level, which is that farmers at the medium - and high-income levels have an acceptable income and want to increase their income, and this positively affects their interest in the need or participation in training courses for raising fig trees.

Table 3 shows the economic level of fig farmers, their number and percentage, the average training need for each category, and the relationship between the economic level and the training need for farmers.

Table 5 shows the number of years of work in the field of fig cultivation, the number of farmers and their percentages, the average training need for each category, and the relationship between the number of years of work in the field of fig cultivation and the training needed for farmers.

2. The area is growing fig

To describe the area used to grow the fig plant, farmers were divided into 3 categories according to the cultivated area and the extent of each category 9 dunums, starting from 1 to 10 dunums and ending with 21–30 dunums. The number of farmers and the percentages for each category were calculated as shown in Table 4, and it appeared that the highest cultivated area in the field of fig cultivation was 30 dunums and the least cultivated area was 1 donum, and the

TABLE 2: Distribution of fig farmers according to the categories of degrees of training need

No	Categories of training needs degrees	Level of training needs	Frequency	Percentage	Average training needs
1	(21–50)	Low	25	26	40
2	(51–70)	Medium	35	36	62
3	(71–100)	High	40	38	79
Total			104	100	53.25

X=53.25, SD=11.7, N=104

highest percentage was 96% within a category 1–10 dunums, followed by 2% for each of the remaining two categories.

To find the type of correlational relationship between the training need and the area used to grow the fig plant, a simple correlation equation (Pearson) was used, and it was found that its value - 0.181 score indicates the existence of a correlation between them, and to verify the significance of this relationship, a t-test was used. Its calculated value is 0.101° and when compared with the tabular value of (t) of 1.982°, which means that it is a non-significant relationship. Therefore, we reject the research hypothesis, which states that there is a significant relationship between the training need and the area used to grow fig plants, and accept the statistical hypothesis which states that there is a non-significant relationship between the training need and the area used to grow fig plants.

The explanation for this is that the cultivated area does not significantly affect the need of fig growers to participate in

training courses in their field of work. In other words, the greater the area planted with fig trees, the more it will have a very weak effect on the need for training courses.

Table 4 shows the area used to grow the fig plant, the number of farmers and their percentages, the average training need for each category, and a test of the relationship between the area used to grow the fig plant and the training need for farmers.

3. Years number worked in growing the fig plant:

To describe the number of years of work in the field of fig cultivation, farmers were divided into 3 categories according to the number of years of work in the field of fig cultivation, and the range of each category is 19 years, starting from 1 to 20 years and ending with 41–60 years. The number of farmers and the percentages for each category are calculated as shown in Table 5, where the highest percentage of years of work in fig cultivation reached 82% for the first category, 1–20 years, followed

TABLE 3: The relationship between the economic level and the training need of farmers

No	The economic level	Number of farmers	%To Farmers	Average training needs for each category	Correlation	Calculated (t)	Tabular (t)
1	Low	14	13	37.7	0.295	2.039	1.982
2	Medium	80	77	37.2			
3	High	10	10	33.1			
	SUM	104	100				

Tabular (T) value 1.982 at the probability level 0.05

TABLE 4: The relationship between the area used for growing figs and the training needs of farmers

No	Categories of cultivated area in pomegranate	Number of farmers	% To farmers	Average training needs for each category	correlation	Calculated (t)	tabular (t)
1	(1–10)	85	82	88.6	- 0.181	0.101	1.982
2	(11–20)	12	11	76.4			
3	(21–30)	7	7	77.3			
	SUM	104	100				

Tabular (T) value 1.982 at the probability level 0.05

TABLE 5: The relationship between the number of years working in the field of fig cultivation and the training needs of farmers

No.	Number of years of work in the field of pomegranate cultivation	Number of farmers	% To farmers	Average training needs for each category	Correlation	Calculated (t)	tabular (t)
1	(1–20)	85	82	66.1	0.221	2.138	1.982
2	(21–40)	10	10	67.8			
3	(41–60)	9	9	65.5			
	Sum	104	100				

Tabular (T) value 1.982 at the probability level 0.05

by 8% of years of work in fig cultivation for the other two categories.

To determine the type of correlation between the training need and the number of years working in the field of fig cultivation, the simple correlation equation (Pearson) was used, and its value was found to be 0.221° , which indicates the existence of a relationship. Correlation: To confirm the importance of this relationship, the (t) test was used, whose calculated value was 2.138° , and when compared to the tabulated value of (t) of 1.982° . This means that this relationship is significant at the probability level of 0.05. Therefore, the research hypothesis was accepted, which states that there is a significant relationship between the number of years of work in the field of fig cultivation and the training needed.

This result can be explained by the fact that fig farmers' experience in their work increases with the increase in the number of years of work, and thus, the need to participate in training courses increases to gain experience in their field of work and thus increase income.

Table 5 shows the number of years of work in the field of fig cultivation, the number of farmers and their percentages, the average training need for each category, and the relationship between the number of years of work in the field of fig cultivation and the training needed for farmers.

3. CONCLUSIONS

1. The results of the study showed that the training needed for fig farmers ranges from the average level to the very high level. From this, it was concluded that the agricultural educational extension services provided to fig farmers are diminished.
2. It appeared that there is a significant relationship between the training need and both the economic level and the number of years of work in the field of fig breeding. We conclude from this that the higher the economic level and the greater the number of years of work for the farmer, the greater the training need to learn about everything that has been developed in the field of fig breeding and thus we get to increase production, it appeared that there is a non-significant relationship between the training need and the area used in raising figs. This means that the area used in raising figs has no effect on the training needs of the farmers.

3.1. Recommendations

1. Given the general increase in the training need for fig farmers in their field of work, and the close relationship between the training need, the economic level and the number of years of work in the field of fig cultivation for them, the researcher recommends intensifying extension activities and services such as seminars, training courses, and the public that is accompanied by a government effort to raise the educational level of the fig farmers, so that they can understand the science brought about by the scientific revolution in the field of fig cultivation.
2. Given the high training needs of pomegranate farmers in the fields of fig plant disease control and fig cultivation management, it is recommended to focus on activities and extension services (seminars, training courses, and the public) in the first place in areas with a high and therefore minimal training need.

REFERENCES

- [1] P. Alfrey. "All You Need to Know about Figs-Ficus Carica". Permaculture Magazine, Petersfield, 2019.
- [2] J. Carroll. "Fig Types: Different Types of Figs Trees for The Garden". Gardening Knows How, Dar Al-Kuttab Publishing, Bedford, 2009.
- [3] M. E. Kislev, A. Hartmann and O. Bar-Yosef. "Early domesticated fig in the Jordan Valley". *Science*, vol. 312, no. 5778, pp. 1372-1374, 2007.
- [4] J. Dixon, A. Gulliver and D. Gibbon. "Global Farming Systems Study: Challenges and Priorities to 2030". World Bank, FAO, Rome, 2001.
- [5] V. P. Vikas and S. C. Bhangale and V. R. Patil. "Evaluation of anti-pyretic potential of *Ficus carica* leaves". *International Journal of Pharmaceutical Sciences Review and Research*, vol. 2, no. 2, pp. 151-155, 2013.
- [6] M. Hayek. "Encyclopedia of Medicinal Plants (in Arabic, English, French, German, and Latin)". Library of Lebanon Publishers, Beirut, 2001.
- [7] W. J. Ma, Y. Q. Peng, D. R. Yang and J. M. Guan. "Coevolution of Reproductive Characteristics in Three Dioecious Fig Species and their Pollinator Wasps". Academic Press, New York, 2009.
- [8] F. N. Briggs and P. F. Konwles. "Introduction to Plant Breeding". Reinhold, New York, 2000.
- [9] S. Lev-Yadun, G. Ne'eman, S. Abbo, and M. A. Flaishman. "Early domesticated fig in the Jordan Valley". *Science*, vol. 314, no. 5806, p. 1683, 2006.
- [10] D. J. Cotter and J. N. Walker. "Climate-Humidity for Fig Cultivation". Freeman, Dallas, 1999.
- [11] W. B. Enderud and J. E. Saleeb. "The Fig, *Ficus carica* Linnaeus: Its Biology, History, Culture, and Utilization". Jurupa Mountains, USA, 2013.
- [12] M. A. Al-Younis. "Social Statistics". University of Baghdad, Baghdad, 1999.
- [13] M. Khairy. "Statistics in Psychological, Educational and Social

- Research*". Faculty of Arts, Ain Shams University, Abbassia, 2001.
- [14] A. Abas. "*Principles of Statistics in Education and Psychology*". Al-Aqsa Library, Pakistan, 2002.
- [15] A. F. Khalil. "*Training Needs for Agricultural Extension Workers in Northern Iraq*". Master's Thesis. University of Mosul, Iraq, 2007.

Assessment of Symptoms of Depression and Anxiety among Menopause Women in Sulaimani City, Kurdistan: Cross-sectional Study



Araz Mohammed Abdulkarim¹, Mahabat Hassan Saeed², Akam Mustafa Hassan^{3*}

¹Department of Psychiatric and Mental Health Nursing, College of Nursing, University of Sulaimani, City of Sulaimani, Iraq, ²Department of Maternal Neonate Nursing, College of Nursing, University of Sulaimani, City of Sulaimani, Iraq, ³Department of Anaesthesia, College of Health and Medical Technology, Sulaimani Polytechnic University, City of Sulaimani, Iraq

ABSTRACT

Menopause represents a pivotal developmental juncture in a woman's life, characterized by a spectrum of physiological alterations and the potential emergence of depressive symptomatology. The manifestation of anxiety and depression during the menopausal phase is intricate and influenced by a confluence of biological, social, and psychological determinants. This study aims to assess depression and anxiety among menopausal women while elucidating their associations with various sociodemographic attributes. A cross-sectional study was executed at the Ali Kamal Consultation Center, encompassing 126 menopausal women. Data compilation utilized a structured questionnaire encompassing sections on sociodemographic particulars, menopausal symptoms, and the Hospital Anxiety and Depression Scale. Statistical analysis employing SPSS version 25 encompassed frequency and percentage along with Chi-square tests. A substantial proportion of women (72.5%) reported prevalent anxiety, with a noteworthy 74.2% exhibiting discernible signs of depression. Sociodemographic determinants, including age and age at marriage, body mass index, and marital status, exhibited robust associations with anxiety and depression. The prevalence of depression and anxiety symptoms in menopausal women underscores the imperative for targeted interventions. Sociodemographic variables emerged as pivotal determinants influencing the likelihood of developing these psychological symptoms. Notably, occupation and place of residence exhibited no statistically significant correlations.

Index Terms: Menopause, Depression, Anxiety

1. INTRODUCTION

Menopause represents a significant transitional phase in a woman's life, marked by both physical and emotional changes that can profoundly impact well-being. Among

the various challenges faced during this period, depression and anxiety emerge as prevalent psychological concerns affecting menopausal women [1], [2]. The ramifications of these mental health issues extend beyond the individual, influencing overall quality of life, social interactions, productivity, and self-esteem. Recognizing the prevalence and identifying risk factors associated with depression and anxiety in menopausal women in Iraq is crucial [1], [3]. Depression and anxiety, as highlighted in previous research [2], emerge as prevalent challenges during menopause, impacting various facets of women's lives. The ramifications of these mental health issues extend beyond the individual,

Access this article online

DOI: 10.21928/uhdjst.v8n1y2024.pp115-121

E-ISSN: 2521-4217

P-ISSN: 2521-4209

Copyright © 2024 Abdulkarim, et al. This is an open access article distributed under the Creative Commons Attribution Non-Commercial No Derivatives License 4.0 (CC BY-NC-ND 4.0)

Corresponding author's e-mail: araz.abdulkarim@univsul.edu.iq

Received: 03-01-2024

Accepted: 12-03-2024

Published: 21-04-2024

influencing overall quality of life, social interactions, productivity, and self-esteem. Recognizing the prevalence and identifying risk factors associated with depression and anxiety in menopausal women in Iraq is crucial [1], [3]. The etiology of depression and anxiety during menopause encompasses hormonal fluctuations, stressors, and socio-cultural influences [4]. Therefore, a comprehensive understanding of their prevalence and associated risks is essential for providing effective healthcare to women in Iraq during this life stage. Menopause entails various consequences, including vasomotor symptoms, atrophy in the general and urinary tracts, osteoporosis, cardiovascular risks, cognitive decline, and psychological changes such as depression and anxiety [5], [6]. The interplay of biological, social, and psychological factors during this stage contributes to the vulnerability of women, with studies indicating a substantial prevalence of depression (18–41.8%) and anxiety (7–25%) in pre- and post-menopausal women [7], [8].

Depression, ranging from transient negative mood states to clinically defined disorders causing significant distress, and anxiety-related disorders manifesting as panic attacks or generalized worry pose significant challenges to women's mental health [9], [10]. These conditions, as highlighted by researchers, not only lead to risky behaviors but are also strongly correlated with diminished quality of life [11]. In addition, menopausal symptoms are factors that contribute to anxiety and depression [12].

This study centers on the Ali Kamal Health Center in Sulaymaniyah City, a pivotal healthcare institution serving women in the region. Focusing on this center allows for a nuanced examination of depression and anxiety prevalence among menopausal women attending this facility. Different instruments were used to assess mood during menopause in previous studies, such as the depression and anxiety stress scale [13]. The Patient Hospital Questionnaire-9 [14]. However, in this study, we used the Hospital Anxiety and Depression Scale. This scale is used to detect the emotional symptoms of anxiety and depression and was used in previous studies [12], [15].

The study aims to assess depression and anxiety and explore their association with socio-demographic characteristics in menopausal women in Sulaymaniyah City, Kurdistan, Iraq. The outcomes of this research are poised to offer valuable insights into the mental health landscape of menopausal women, guiding the development of targeted interventions to enhance their well-being in Iraq.

2. MATERIAL AND METHODS

2.1. Design

The qualitative, cross-sectional study was conducted at the Ali Kamal consultation center, a facility of the general teaching hospital in Sulaymaniyah City, Iraq, Kurdistan, and the period of data collection started from November 2022 until February 2023.

2.2. Study Sample

Non-probability: a purposive sample size of 126 menopausal women attending Ali Kamal Health Center for the check-up.

2.3. Inclusion and Exclusion Criteria

Women had to meet certain criteria to be included in the study: being between the ages of 50 and 60, reaching menopause naturally (as opposed to undergoing hysterectomy and surgery), having gone more than a year without having their period, and agreeing to participate in the study. Women under 50 who suffer from psychological conditions and cannot participate in interviews were excluded.

2.4. Data Tools

A questionnaire was developed for data collection and composed of three sections. The first section related to sociodemographic characteristics included age, age at marriage, educational level, occupation, marital status, residential area, height and weight, and age at menarche. The second section is related to menopause symptoms, which include forgetfulness, vaginal dryness, no sexual desire, lethargy, hot flashes, hair loss, shortsightedness, weight gain, sweating, skin dryness, urine leakage, and sleep disturbance. The third section, measured through the hospital anxiety scale by Zigmond and Snaith [16], which is a standard tool used for detecting anxiety and depression in non-psychiatric individuals, has been used in many pieces of research with good reliability and validity [7], [12]. Its 14 items were rated on a 4-point ranging from 0 to 3.

The scale comprised seven items to assess depression, five of which are marks for anhedonia (an inability to experience pleasure), and two concern appearance and feelings of slowing down. Seven items assess anxiety; two assess automatic anxiety (panic and butterflies in the stomach); and the other five assess tension and restlessness. The questionnaire was translated into the Kurdish language through a forward-backward procedure.

2.5. Validity and Reliability of the Study Instrument

The validity of the questionnaire is determined through a panel of experts in related fields. For the reliability of the

questionnaire, a pilot study was carried out at the Ali-Kamal Health Center on a sample of ten women selected from the October 8–20, 2022, interviewed by the researcher to determine the reliability and clarity of the questionnaire and to estimate the average time required for data collection. The result of a pilot study showed that the items were clear and understood, and the time required was from 30 to 60 min for each respondent. The internal consistency of the instrument was determined through the computation of the interclass correlation coefficient, and the result of the reliability was ($r = 0.84, P < 0.01$), which was a statistically adequate level of internal consistency. The sample of the pilot study was not included in the original sample of the study.

2.6. Data Collection

The data were collected through a face-to-face interview method conducted with each participant to fill out the questionnaire.

2.7. Data Analysis

The data were analyzed using a Statistical Package for the Social Science, SPSS version 25 software. The descriptive statistics include frequencies, percentages, mean, and forecast standard deviation. The inferential statistics, including the

Chi-square (2X) test and Fisher’s exact test, were used to analyze the data; a *P*-value of 0.05 was used as the cut-off for statistical significance and 0.001 for high statistical significance.

3. RESULTS

As seen in Table 1, women between the ages of 44 and 53 comprised the majority of participants in this study (69.1%), and most were married. In this study, 47.4% of the study samples were overweight according to body mass index (BMI). Regarding education level, more participants (32.5%) were only primary school educated. In this study, 51.7% of the women worked as stay-at-home mothers. Finally, almost all participants were from the city center.

TABLE 1: Demographic characteristics of the participants

Variables	Frequency	Percentage
Age		
50–54	83	69.1
55–60	37	30.9
Marital status		
Married	96	58.6
Unmarried	18	37.5
Widow	2	3.8
Divorce	4	
Body mass index		
Normal	35	30.2
Overweight	55	47.4
Obese	24	20.7
Extreme obese	2	1.7
Occupation		
Housewife	62	51.7
Employed	58	48.3
Level of education		
Illiterate	8	6.7
Primary educated	39	32.5
Secondary educated	35	29.2
Institute graduated	28	23.3
College and post-graduated	10	8.3
Residency		
Urban	119	99.2
Suburban	1	0.8
Total	120	100

TABLE 2: Signs and symptoms of the patients

Variable	Signs and symptoms	
	Frequency	Percentage
Forgetfulness		
Yes	104	86.7
No	16	13.3
Vaginal dryness		
Yes	101	84.2
Not	19	15.8
No sexual desire		
Yes	99	82.5
Not	21	17.5
Lethargy		
Yes	102	85
Not	18	15
Hot flushes		
Yes	99	82.5
Not	21	17.5
Hair loss		
Yes	96	80
No	24	20
Short-sighted		
Yes	93	77.5
Not	26	21.7
Weight gain		
Yes	92	76.7
Not	28	23.3
Excessive sweating		
Yes	99	82.5
Not	21	17.5
Skin dryness		
Yes	98	81.7
Not	22	18.3
Urine leakage		
Yes	88	73.3
No	32	26.7
Sleep disturbance		
Yes	96	80
No	24	20
Total	120	100

Overall data on signs and symptoms of pregnancy reveals that the majority of participants have menopausal signs and symptoms, as shown in the Table 2.

The table delineates the frequency and percentage distribution of various signs and symptoms reported by the patients. The most prevalent symptom is forgetfulness, with 86.7% of patients experiencing it. Vaginal dryness is reported by 84.2% of patients, followed by a lack of sexual desire in 82.5% of cases. The table provides a comprehensive overview of the occurrence of diverse symptoms among the surveyed patients.

Table 3 provides an assessment of anxiety among the patients based on various statements. The majority of respondents reported feeling tense or wound up most of the time (72.5%). In addition, a significant proportion experienced worrying thoughts a great deal of the time (62.5%) and reported feeling quite badly or very definitely that something awful was about to happen (60%). The table comprehensively outlines the frequency and percentage distribution of anxiety levels across different statements, offering insights into the prevalence of anxiety symptoms among the surveyed patients.

TABLE 3: Anxiety profile of the patients

Items	Frequency	Percentage
1. I feel tense or wound up		
From time to time, occasionally	12	10
A lot of the time	21	17.5
Most of the time	87	72.5
2. I get a sort of freighted feeling as if something awful is about to happen		
A little, but it doesn't worry me	10	8.3
Yes, but not too badly	38	31.7
Very definitely and quite badly	72	60
3. Worrying thoughts go through my mind		
From time to time, but not too often	5	4.2
A lot of the time	40	33.3
A great deal of the time	75	62.5
4. I can sit at ease and feel relaxed		
Usually	5	4.2
Not Often	41	34.2
Not at all	74	61.7
Total	120	100
5. I get a sort of freighted feeling like but terrified in the stomach		
Occasionally	5	4.2
Quiet Often	45	37.5
Very often	70	58.3
6. I feel restless as i have to be on the move		
Not very much	6	5
Quite a lot	32	26.7
Very much indeed	82	68.3
7. I get sudden feelings of panic		
Not very often	7	5.8
Quiet often	36	30
Very often indeed	77	64.2
Total	120	100

Table 5 presents the association between anxiety-related questions and various sociodemographic variables, indicated by the corresponding p-values. The p-values signify the level of significance for each relationship. Lower P-values generally suggest a more significant association. For instance, in the context of age and question 4 (“I can sit at ease and feel relaxed”), a P-value of 0.0 indicates a statistically significant association. This table serves as a valuable reference for understanding the relationships between anxiety symptoms and sociodemographic factors within the studied population.

Table 6 illustrates the association between depression-related questions and various sociodemographic variables, denoted by the corresponding P-values. The P-values indicate the level of significance for each association. Lower P-values generally signify a more significant association. For instance, in the context of age and question 2 (“I can laugh and see the funny side of things”), a P-value of 0.022 indicates a statistically

TABLE 4: Depression scale of the patients by frequency and percentage

Items	Frequency	Percentage
1. I still enjoy the things I used to enjoy		
Not quite so much	4	3.3
Only a little	27	22.5
Hardly at all	89	74.2
2. I can laugh and see the funny side of things		
As much as I always could	7	5.8
Not quite so much now	8	6.7
Definitely not so much now	30	25
Not at all	75	62.5
3. I feel cheerful		
Most of the time	4	3.3
Sometimes	17	14.2
Not often	40	33.3
Not at all	59	49.2
4. I feel as if I am slowed down		
Not at all	1	0.8
Sometimes	3	2.5
Very often	46	38.3
Nearly all the time	70	58.3
5. I have lost interests in my appearance		
I take just as much care as ever	5	4.2
I may not take quite as much care	3	2.5
I don't take as much care as I should	29	24.2
Definitely	83	69.2
6. I look forward with enjoyment to things		
As much as I ever did	4	3.3
Rather less than I used to	10	8.3
Definitely less than I used to	31	25.8
Hardly at all	75	62.5
7. I can enjoy a good book or radio or TV program		
Sometimes	3	2.5
Not often	50	41.7
Very seldom	67	55.8
Total	120	100

TABLE 5: Association between a demographic characteristic of the patients and anxiety

Demographic variable	Anxiety questions (P-value)						
	1. I feel tense or wound up	2. I get a sort of freighted feeling as if something awful is about to happen	3. Worrying thoughts go through my mind	4. I can sit at ease and feel relaxed	5. I get a sort of freighted feeling like but terrifies in the stomach	6. I feel restless as I have to be on the move	7. I get sudden feelings of panic
Age	0.4	0.1	0.9	0.0	0.2	0.4	0.6
BMI	0.5	0.4	0.6	0.4	0.0	0.7	0.3
Occupation	0.2	0.6	0.2	0.7	0.4	0.6	0.4
Education level	0.1	0.7	0.6	0.001	0.001	0.3	0.8
Residency	0.6	0.001	0.03	0.5	0.4	0.5	0.5
Marital status	0.02	0.001	0.2	0.0	0.2	0.4	0.3

BMI: Body mass index

TABLE 6: Association between a demographic characteristic of the patients and depression

Demographic variables	Depression (P-value)						
	1. I still enjoy the things I used to enjoy	2. I can laugh and see the funny side of things	3. I feel cheerful	4. I feel as if I am slowed down	5. I have lost interests in my appearance	6. I look forward with enjoyment to things	7. I can enjoy a good book or radio or TV program
Age	0.53	0.022	0.03	0.931	0.187	0.034	0.46
Age at marriage	0.367	0.026	0.182	0.744	0.426	0.094	0.592
BMI	0.619	0.548	0.51	0.116	0.0	0.841	0.269
Occupation	0.087	0.77	0.332	0.294	0.077	0.572	0.007
Education level	0.012	0.294	0.041	0.09	0.251	0.001	0.64
Residency	0.579	0.607	0.734	0.44	0.574	0.547	0.396
Marital status	0.039	0.697	0.007	0.911	0.589	0.217	0.681

BMI: Body mass index

significant association. This table provides valuable insights into the relationships between depression symptoms and sociodemographic factors within the studied population.

In Table 4 the data shows how depressed the participants were; the majority (74.2%) of the women appeared unhappy. More than half (62.5) of the study samples did not have any ability to laugh or find humor in situations. 49.2% of the participants said they did not feel happy at all. Nearly all of the respondents (58.3%) felt slowed down most of the time. More than half of the female population (69.2%) firmly believes that their interest in women's looks has diminished. More than half of the women (55.8%) very rarely enjoy listening to or watching an excellent book or radio show.

4. DISCUSSION OF THE RESULTS

The temporal intricacies of a woman's reproductive phase, marked by the decline in ovarian function, render

it challenging to pinpoint a definitive age for menopause initiation. Consistent with the study by Ahlawat *et al.* (2019), our research focused on women aged 50 to 54, constituting 69.1% of the participants. Our findings indicate that 47.4% of the study sample was classified as overweight, potentially attributed to age-related changes, reduced physical activity, and a sedentary lifestyle. While consistent with [17], discrepancies with [18] are discussed, considering regional variations in race, ethnicity, and biological characteristics.

The prevalence of menopausal symptoms and indications in our study aligns with the hormonal changes inherent in the menopausal transition, affecting diverse biological systems. Notably, despite most participants having completed only primary school, education emerges as a potential modifier, contradicting [19] findings on the positive correlation between education and the quality of life of menopausal women. Our study resonates with [20], [21], reporting prevalent menopausal symptoms among participants aged 50–54. Discrepancies with [22] are acknowledged,

considering potential regional variations in cultural and biological characteristics.

The prevalence of nervousness reported by 72.5% of participants during menopause suggests potential anxiety symptoms accompanying or preceding depression. Contrary to Kravitz *et al.* (2014) [23], our findings emphasize the impact of environmental stressors during the midlife transition. The vulnerability to depression during the menopause transition is underscored by a recent study, indicating a high percentage (74.2%) of women reporting dissatisfaction or depression. This vulnerability, heightened during perimenopause, necessitates attention to potentially reversible psychological conditions, given the increased risks for osteoporosis and cardiovascular disease in post-menopausal women.

Risk factors for depressive mood during the menopause transition, such as poor sleep, stressful life events, unemployment, and a higher BMI, align with existing literature, emphasizing the multifactorial nature of depression during this period. Educational attainment and non-white-collar occupations are highlighted as sociodemographic risk factors, consistent with previous studies. Anxiety, another prevalent symptom during the menopause transition, demonstrates associations with sociodemographic characteristics, except for occupation status. This finding diverges from studies among teachers and healthcare workers, emphasizing the nuanced role of occupation-related stress in exacerbating menopausal symptoms.

5. CONCLUSION

Our study aims to assess depression and anxiety symptoms among menopausal women, with age and age at marriage, BMI, and marital status emerging as significant sociodemographic factors influencing the likelihood of developing these symptoms. The absence of associations with occupation and place of residence underscores the complexity of these psychological manifestations. The study recommends the implementation of counseling and nursing management to mitigate the prevalence of anxiety and depression among menopausal women.

6. ACKNOWLEDGMENT

Gratitude is extended to all study participants for their involvement. Special recognition is given to the administration of the Ali Kamal Health Center for their invaluable support and cooperation in facilitating the collection of research data.

7. ETHICAL CONSIDERATIONS

The research adhered to ethical standards, with a clear articulation of its purpose and the requisite permissions secured. Approval was obtained from the Scientific Committee of the Psychiatric Mental Health Nursing Department at the College of Nursing and the Ethical Committee at the College of Medicine at the University of Sulaymaniyah. Further authorization from the General Health Director was acquired to conduct the study at Ali Kamal Health Centre. Prior to their participation, participants were fully informed about the research objectives, and verbal informed consent was obtained.

8. CONFLICTS OF INTERESTS

The authors declare the absence of any conflicts of interest.

9. FUNDING

The study was financially supported through author fees.

REFERENCES

- [1] P. Ahlawat, M. M. Singh, S. Garg and Y. M. Mala. "Prevalence of depression and its association with sociodemographic factors in post-menopausal women in an urban resettlement colony of Delhi". *Journal of Mid-life Health*, vol. 10, no. 1, p. 33, 2019.
- [2] M. Nobahar, Z. Hydarinia-Naieni and R. Ghorbani. "The prevalence of depression, anxiety, and stress and their association with vitamin D and estrogen levels in postmenopausal women in Semnan". *Middle East Journal of Rehabilitation and Health Studies*, vol. 6, no. 4, e91953, 2019.
- [3] W. A. Rocca, L. G. Rocca, C. Y. Smith, E. Kapoor, S. S. Faubion and E. A. Stewart, "Frequency and type of premature or early menopause in a geographically defined American population". *Maturitas*, vol. 170, pp. 22-30, 2023.
- [4] F. A. Yilmaz and D. Avci. "The relationship between personality traits, menopausal symptoms, and marital adjustment". *Health Care for Women International*, vol. 43, no. 10-11, pp. 1142-1157, 2020.
- [5] D. H. Barlow. "Continuing progress on vasomotor symptoms". *Menopause*, vol. 30, no. 3, pp. 235-236, 2023.
- [6] R. A. Andrews, B. John and D. Lancaster. "Symptom monitoring improves physical and emotional outcomes during menopause: A randomized controlled trial". *Menopause*, vol. 30, no. 3, pp. 267-274, 2023.
- [7] T. Tangen and T. Mykletun. "Depression and anxiety through the climacteric period: An epidemiological study (HUNT-II)". *Journal of Psychosomatic Obstetrics & Gynecology*, vol. 29, no. 2, pp. 125-131, 2019.
- [8] C. Zhang, Y. Xue, H. Zhao, X. Zheng, R. Zhu, Y. Du, J. Zheng and

- T. Yang. "Prevalence and related influencing factors of depressive symptoms among empty-nest elderly in Shanxi, China". *Journal of Affective Disorders*, vol. 245, pp. 750-756, 2019.
- [9] C. Schiweck, D. Piette, D. Berckmans, S. Claes and E. Vrieze. "Heart rate and high frequency heart rate variability during stress as biomarker for clinical depression: A systematic review". *Psychological Medicine*, vol. 49, no. 2, pp. 200-211, 2019.
- [10] D. H. Barlow and K. K. Ellard. "Anxiety and related disorders". *General Psychology*, vol. FA18, no. 178, 179-240, 2018.
- [11] C. J. Gibson, Y. Li, A. J. Huang, T. Rife and K. H. Seal. "Menopausal symptoms and higher risk opioid prescribing in a national sample of women veterans with chronic pain". *Journal of General Internal Medicine*, vol. 34, pp. 2159-2166, 2019.
- [12] A. Nawaz, S. F. Iqbal, A. Fatima and A. Ahmad. "Anxiety and depression and its risk factors among post-menopausal women-hospitals based study". *Pakistan Journal of Medical Research*, vol. 59, no. 4, pp. 130-134, 2020.
- [13] A. Bener, D. Saleh, N. M. Bakir and A. Bhugra. "Depression, anxiety, and stress symptoms in menopausal Arab women: Shedding more light on a complex relationship". *Annals of Medical and Health Sciences Research*, vol. 6, no. 4, pp. 224-231, 2016.
- [14] J. Ford, F. Thomas, R. Byng and R. McCabe. "Use of the patient health questionnaire (PHQ-9) in practice: Interactions between patients and physicians". *Qualitative Health Research*, vol. 30, no. 13, pp. 2146-2159, 2020.
- [15] N. Barghandan, N. Dolatkah, F. Eslamian, N. Ghafarifar and M. Hashemian. "Association of depression, anxiety and menopausal-related symptoms with demographic, anthropometric and body composition indices in healthy postmenopausal women". *BMC Womens Health*, vol. 21, no. 1, p. 192, 2021.
- [16] A. S. Zigmund and R. P. Snaith. "The hospital anxiety and depression scale". *Acta Psychiatrica Scandinavica*, vol. 67, no. 6, pp. 361-370, 1983.
- [17] J. T. T. Gonçalves, M. F. F. Silveira, M. C. C. Campos and L. H. R. Costa. "Overweight and obesity and factors associated with menopause". *Ciência and Saúde Coletiva*, vol. 21, pp. 1145-1156, 2016.
- [18] S. Koo, Y. Ahn, J. Y. Lim, J. Cho and H. Y. Park. "Obesity associates with vasomotor symptoms in postmenopause but with physical symptoms in perimenopause: A cross-sectional study". *BMC Womens Health*, vol. 17, no. 1, pp. 126, 2017.
- [19] J. E. Blumel, C. Castelo-Branco, L. Binfa, G. Gramegna, X. Tacla, B. Aracena, M. A. Cumsille and A. Sanjuan. "Quality of life after menopause: A population study". *Maturitas*, vol. 34, no. 1, pp. 17-23, 2000.
- [20] P. Monteleone, G. Mascagni, A. Giannini, A. R. Genazzani and T. Simoncini. "Symptoms of menopause-global prevalence, physiology and implications". *Nature Reviews Endocrinology*, vol. 14, no. 4, pp. 199-215, 2018.
- [21] E. Yisma, N. Eshetu, S. Ly and B. Dessalegn, "Prevalence and severity of menopause symptoms among perimenopausal and post-menopausal women aged 30-49 years in Gulele sub-city of Addis Ababa, Ethiopia". *BMC Womens Health*, vol. 17, pp. 24, 2017.
- [22] P. Nkwo and H. Onah. "Positive attitude to menopause and improved quality of life among Igbo women in Nigeria". *International Journal of Gynecology and Obstetrics*, vol. 103, no. 1, pp. 71-72, 2008.
- [23] H. M. Kravitz, L. L. Schott, H. Joffe, J. M. Cyranowski and J. T. Bromberger, "Do anxiety symptoms predict major depressive disorder in midlife women? The Study of Women's Health Across the Nation (SWAN) Mental Health Study (MHS)". *Psychological Medicine*, vol. 44, no. 12, pp. 2593-2602, 2014.
- [24] P. K. Srikanteswara, J. D. Cheluvaiiah, J. B. Agadi and K. Nagaraj. "The relationship between nerve conduction study and clinical grading of carpal tunnel syndrome". vol. 10, pp. 13-18, 2016.

Efficient Breast Cancer Dataset Analysis Based on Adaptive Classifiers



Thikra Ali Kareem¹, Muzhir Shaban Al-Ani², Salwa Mohammed Nejres³

¹Imam Ja'afar Al-Sadiq University, Salah Al-Din, Dijail, ²Department of Information Technology, College of Science and Technology, University of Human Development, Sulaymaniyah, KRG, Iraq, ³Ministry of Higher Education and Scientific Research, Baghdad, Iraq.

ABSTRACT

Many algorithms have been used to diagnose diseases, with some demonstrating good performance while others have not met expectations. Making correct decisions with the minimal possible errors is of the highest priority when diagnosing diseases. Breast cancer, being a prevalent and widespread disease, emphasizes the importance of early detection. Accurate decision-making regarding breast cancer is crucial for early treatment and achieving favorable outcomes. The percentage split evaluation approach was employed, comparing performance metrics such as precision, recall, and f1-score. Kernel Naïve Bayes achieved 100% precision in the percentage split method for breast cancer, while the Coarse Gaussian support vector machines achieved 97.2% precision in classifying breast cancer in 4-fold cross-validation.

Index Terms: Breast cancer, Adaptive classifiers, Performance measures, Percentage split evaluation technique, Healthcare analysis.

1. INTRODUCTION

The development of the Internet and its containment of a vast amount of data, coupled with the emergence of large data volumes generated by social media, has made data today exceptionally massive. This necessitates new approaches for its transfer, processing, and analysis, collectively known as big data. This data may be unstructured, semi-structured, or structured, benefiting various sectors such as societal, business, industry, agriculture, education, and healthcare [1], [2].

The internet of things (IoT) contains a huge number of sensors connecting to other systems and devices, producing

extensive data that requires novel analytical methods, particularly wireless sensor networks, as the data source [3], [4].

Given the immense volume of data, traditional database systems are inadequate for storing, handling, and analyzing such quantities. The concept of big data involves large-scale processes for identifying and interpreting information into new insights. While the term “big data” has long been in use, its prominence surged following the rise of social media [5], [6]. The exponential growth of data worldwide, characterized by vast volume, high speed, and diverse types, demands an infrastructure capable of simultaneous processing and storage. Cloud computing offers on-demand computing resources that can be quickly configured, provisioned, and released as per users' needs, making it accessible to individuals and organizations alike [7], [8].

In data analysis, starting from processing, cleaning, and filtering, correct data retrieval is essential to perform the necessary analysis. Analyzing and calculating metrics such as maximum, minimum, and standard deviation using relevant tools are

Access this article online

DOI:10.21928/uhdjst.v8n1y2024.pp122-128 E-ISSN: 2521-4217
P-ISSN: 2521-4209

Copyright © 2024 Kareem, *et al.* This is an open access article distributed under the Creative Commons Attribution Non-Commercial No Derivatives License 4.0 (CC BY-NC-ND 4.0)

Corresponding author's e-mail: Department of Information Technology, College of Science and Technology, University of Human Development, Sulaymaniyah, KRG, Iraq. Email: muzhir.al-ani@uhd.edu.iq

Received: 06-02-2024

Accepted: 06-04-2024

Published: 25-04-2024

crucial for obtaining accurate results. Optimal analysis follows proper steps to ensure accuracy and reliability [9], [10]. Smart cities can utilize distributed stream processing frameworks for real-time data processing, a practical application in addition to their current IoT adoption. Choosing a suitable framework for smart city data analytics requires a comprehensive understanding of target application features [11], [12].

Big data analysis employs various analytical methods depending on the data's nature, aiming to extract insights. These methods include statistical analysis, correlation analysis, and regression analysis [13], [14]. The aim of the proposed approach is to develop an effective algorithm for disease prediction by employing classification approaches to address health-care issues during diagnosis and achieve efficient performance results.

2. LITERATURE REVIEW

Babar *et al.* proposed a health-care architecture based on energy harvesting analysis of health monitoring devices. The proposed architecture consists of three layers. Consistent datasets were verified on Hadoop server to validate the proposed design based on the threshold value. The goal of this research is to make smart decisions and deal with events. The analysis shows that the proposed design has great potential in the field of smart health [15].

Singh and Yassine utilized IoT and big data analytics to create energy management strategies to manage home energy effectively and efficiently. They proposed a unified architecture that enables creative activities to process massive amounts of granular energy use data in close to real-time. The complexity and resource requirements of data processing, storage, and classification analysis in close to real-time are addressed by proposing an IoT big data analysis system that uses fog computing [16].

Shah *et al.* proposed a new design and philosophy for the disaster-resistant smart city. Together, the Hadoop ecosystem and Spark form a powerful system environment that allows for real-time and offline analysis. System efficiency is evaluated in terms of processing time and throughput. The aim of this research is to add to the body of knowledge and guide future research on the design and implementation of disaster-resilient smart cities based on this system and the IoT. This strategy can lead to immediate and effective situational awareness, which can help mitigate the effects of the disaster [17].

Syed *et al.* proposed a new smart healthcare framework to monitor the physical activity of older individuals using the Internet of Medical Things and intelligent machine learning algorithms for quick analysis, decision-making and better treatment suggestions. Hadoop MapReduce algorithms are used to handle massive amounts of data in parallel. The aim of this study is to predict the physical activity of respondents to help them live a healthier lifestyle. This study provides an excellent option for detecting physical activity and monitoring the health of elderly people remotely [18].

Li introduced a fog-assisted IoT-based intelligent and real-time health-care information processing system. In this system, minimal latency and large amounts of data generated by IoT sensors are offloaded to the fog cloud for data analysis and processing. The data then are processed and stored in a central cloud system using Hadoop and Apache Spark in order to process and analyze. The proposed compression strategy results in a 60% reduction in the amount of data in this system, in addition, for real-time data analytics; it offers a fog-powered approach with a big data environment [19].

Hadi *et al.* presented a multidisciplinary approach to e-health care, priority, big data analytics, and radio resource optimization in a multi-tier 5G network. They used a combined system including three machine learning algorithms (naïve Bayesian classifier, logistic regression, and decision tree) to evaluate historical outpatient stroke medical data and signals from IoT sensors attached to the body to predict the probability of an impending stroke. Two optimization approaches, namely, the weighted sum rate maximization approach and the proportional fairness approach, are presented to achieve this goal. The proposed methods improved the average signal-to-noise ratio and proportional fairness [20].

Ge *et al.* demonstrated a system that collects data from sensors and used deep learning to evaluate and monitor patients' health data to predict disease and provide timely alerts in this work. Extensive analysis and experimental data are provided to show that the proposed strategy was safe and effective. When a patient uploads their health information, the system allows for precise access and confirmed deletion [21].

Lv *et al.* developed the theory of fuzzy function-based mean clustering algorithm using K-means and fuzzy theory in big data analysis technology. The results indicated that when the effective propagation probability was 100% and the value was between 0.01 and 0.05, it was close to the true result and has the least data delay. This study showed that using big data analysis techniques to enhance electric vehicle transportation

networks can significantly reduce network data transmission performance delay and adjust the route to effectively stop the spread of congestion [22].

Kaya *et al.* studied priority of speed and accuracy in health data and aimed to detect anomalies at the edge of IoT for effective management of big data. The data stream for age, gender, height, time, temperature, and weight is used in the analysis through applied Naïve Bayes, neural network, logistic regression, and random forest algorithms. The experimental results compared speed and accuracy and obtaining logistic regression (LR) algorithm provides great success in the IoT system. Machine learning (ML) algorithms are suitable for the IoT edge because they can make timely and efficient decisions in the health-care sector [23].

Ahmed *et al.* designed an approach based on neural networks, which aimed to diagnose and predict the epidemic. This model provided descriptive, diagnostic, predictive, and prescriptive analysis using big data analytics. This model was used to predict COVID-19 within the creation of a health monitoring platform. The results of the neural network-based model were also compared with the results of other machine learning methods. The neural network-based algorithm achieves high percentage accuracy without using any computationally expensive deep learning-based methodology [24].

Qin *et al.* used big data analytics to implement the multimedia-assisted student-centered learning model, which addresses critical policies to help educational institutions achieve this transformation in a more systematic way by clarifying teachers' instruction. When compared to alternative technologies, simulation results indicate that the proposed model improves student attention (97.3%), efficiency

(90.1%), student retention rate (97.5%), engagement (98.2%), and learning outcomes (95.3%) [25].

3. DATA SET

The University, of Wisconsin, (USA) provided this breast cancer database. This dataset consists of 699, instance and 10, attributes, the target (class): (two for benign and four for malignant). The dataset contains (458) benign, class and (241) malignant class so that the data of dataset are imbalanced data. The description attributes with its values about this dataset can be summarized as follows:

Sample code number, clump thickness (1–10), uniformity, of cell size (1–10), uniformity of cell shape (1–10), marginal adhesion (1–10), single, epithelial cell size (1–10), bare nuclei (1–10), bland chromatin (1–10), normal chromatin (1–10), mitoses (1–10), and class (two for benign and four for malignant).

4. PROPOSED APPROACH

The dataset including information about the situation of patients, then will be processed using prediction approach such as Kernel Naive Bayes, Linear support vector machine (SVM), Coarse Tree, K-Nearest Neighbors, Cosine KNN, Coarse Gaussian SVMs and Fine Tree. Then, the performance of the algorithms will be evaluated using a suitable evaluation model such as k-fold cross-validation and percentage split approaches. The proposed approach includes many parts as shown in Fig. 1.

1. Breast cancer dataset: Including preparing and organizing the dataset to be accessible by the next step.

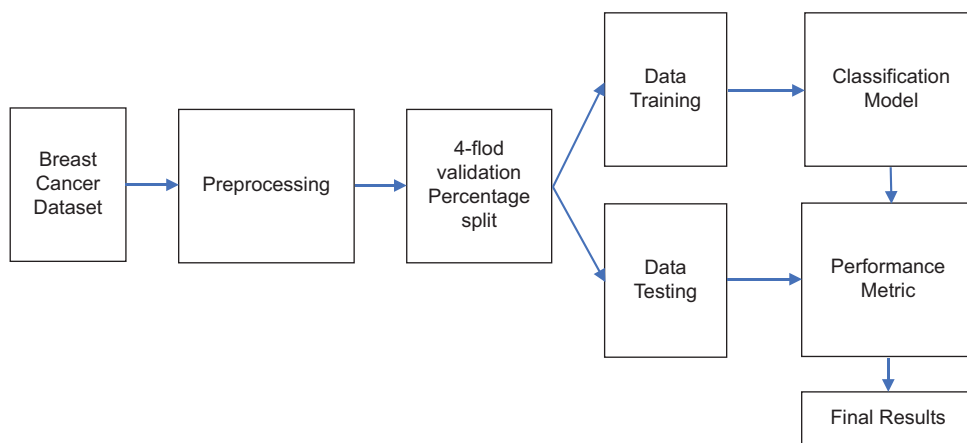


Fig. 1. Proposed approach for breast cancer dataset.

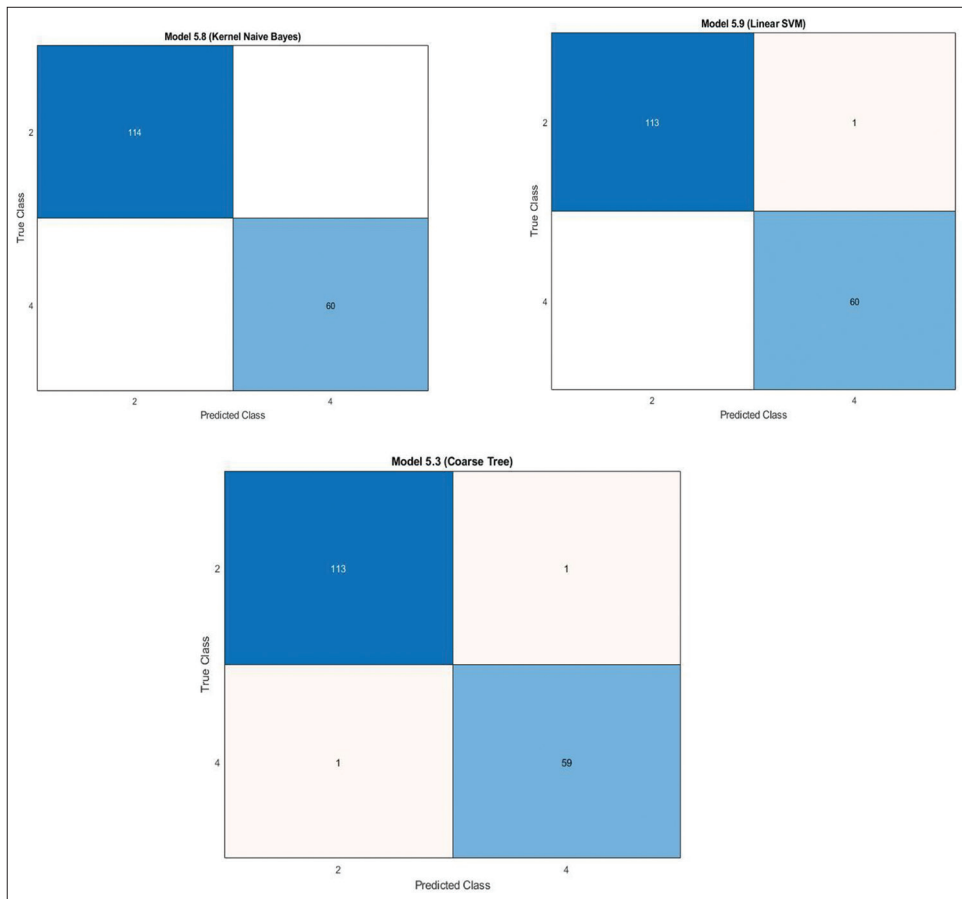


Fig. 2. Confusion matrix of breast cancer (percentage split).

- Data preprocessing: include three parts: outlier detection, missing values and normalization which can perform by using many functions provided with MATLAB classification learner.
- Feature selection: It is the process of choosing the essential variables to improve accuracy. The important and affected features that are required to increase accuracy are chosen in this work.
- Data splitting: Breast cancer dataset was divided into: training and test sets using 4-fold validation and percentage split. This splits randomly with 25% held out for testing and 75% for the training.
- Machine learning models: Coarse DT has few leaves and distinguishes between classes with coarse distinctions and a maximum of four splits, Linear SVM, Kernel Naïve Bayes for percentage split and Fine Tree, Cosine KNN, Coarse Gaussian SVM and Subspace KNN for 4-fold cross validation in breast cancer dataset.

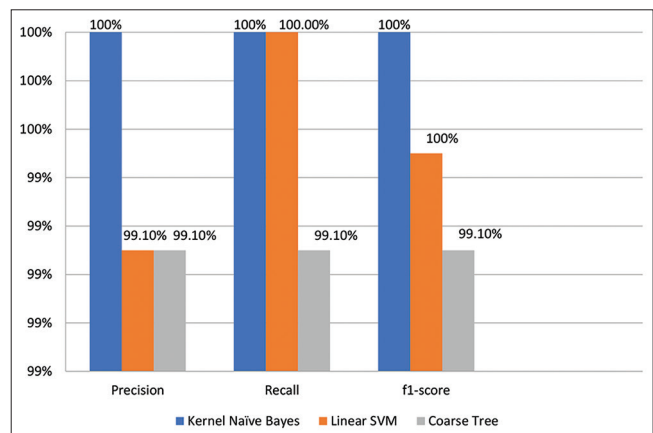


Fig. 3. Comparison of kernel NB, linear support vector machine, coarse tree algorithms.

5. DISCUSSION AND ANALYSIS

The of breast cancer confusion matrix is implemented in the case of percentage split which is used to calculate different

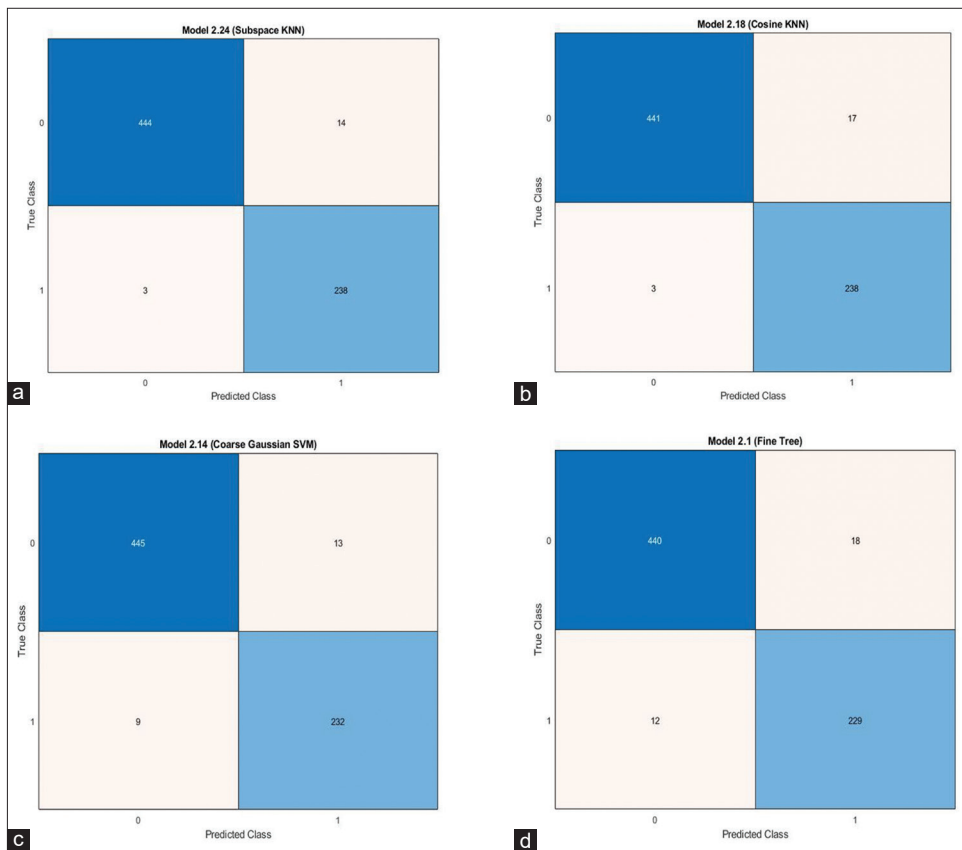


Fig. 4. Confusion matrix of breast cancer (4-fold cross validation).

performance metrics such as precision, Recall and f1-score as shown in Fig. 2.

The precision, recall and f1-score are measured for Kernel Naïve Bayes, Linear SVM, coarse tree classifiers respectively. Fig. 3 shows the performance comparison values of Kernel Naïve Bayes, Linear SVM, and Coarse Tree classifier algorithms in case of percentage split.

In this work, different classifier algorithms are applied on breast cancer dataset. The Kernel Naïve Bayes is adapted to classify the breast cancer and the outcomes of the experimented results are compared the precision, recall and f1-score of many classifier algorithms like Coarse Tree and Linear SVM. So that the obtained results are 100% for all precision, recall and f1- score for Kernel Naïve Bayes approach.

Applying different classification algorithms on breast cancer dataset leading that the subspace KNN is adapted to classify the breast cancer in case of 4-fold cross validation. Fig. 4

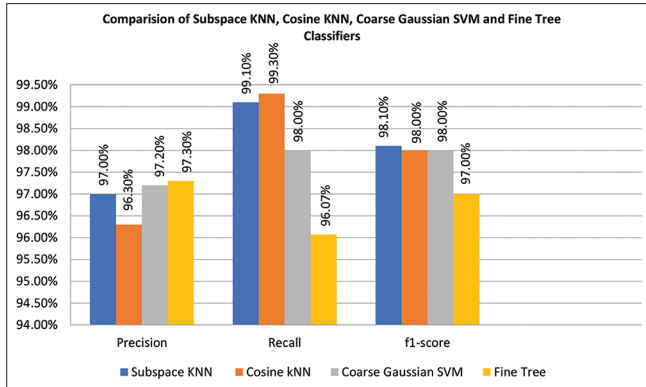
shows the confusion matrix which used to compute the different performance metrics such as accuracy, sensitivity, specificity and f-measure.

Precision, recall, and f1-score are measured for Subspace KNN, Cosine KNN, Coarse Gaussian SVM and Fine Tree classifiers. Fig. 5 shows the performance comparison values of Subspace KNN, Cosine KNN, Coarse Gaussian SVM and Fine Tree classifier algorithms in case of 4-fold cross validation. This figure indicated a better performance in case of subspace KNN compared to other algorithms.

Table 1 shows the outcomes of the proposed approach compared with other studies that used this dataset. The classification algorithms used in this study show that the obtained performance is 100% for precision, recall, and f1-score compared to reference [7]. In addition, the performance is 97.2%, 99.1%, and 98.1% for precision, recall, and f1-score compared to reference [8].

TABLE 1: Results are compared to previous results in breast cancer dataset

This study	Other study	Method	Accuracy (%)	Precision (%)	Recall (%)	F1-score (%)
Applying percentage split evaluation technique	Dhanya <i>et al.</i> [7]	Used ensemble techniques	97.86	-	-	-
Applying 4-fold cross validation	Classification via applied approach		-	100	100	100
	Bayrak <i>et al.</i> [8]	Used support vector machine technique		96	95.7	-
	Classification via applied approach			97.2	99.1	98.1

**Fig. 5.** Metrics of breast cancer (4-fold cross validation).

6. CONCLUSIONS

Efficient big data analytical approaches and machine learning algorithms are utilized for accurate prediction and decision making. So that different machine learning algorithms are being implemented for predicting breast cancer. The machine learning techniques are using comparisons based on important performance metrics such as precision, recall, and f1-score. Machine learning (disease prediction) is a suitable technique that assists in the early detection of disease, may aid practitioners in diagnosis decision-making, and also gives accurate predictions. Many machine learning algorithms applied on Wisconsin breast cancer (WBC) dataset that generate best performance accuracy for diagnosis and prediction the WBC dataset, in which the Kernel Naïve Bayes gives 100% as precision in percentage split method, the Coarse Gaussian SVM is adapted to classify the breast cancer in case of 4-fold cross validation which gives 97.2% as precision.

REFERENCES

[1] P. Raj, T. Poongodi, B. Balusamy and N. Khari. "The Internet of Things and Big Data Analytics Integrated Platform and Industry Use Cases". 1st ed. Routledge, United Kingdom, 2020.

[2] L. Wang and R. Jones. "Big data analytics in cyber security: Network traffic and attacks". *Journal of Computer Information*

Systems, vol. 61, pp. 1-8, 2020.

- [3] Z. A. Dagdeviren and O. Dagdeviren. "BICOT: Big data analysis approaches for clustering cloud based IOT systems". *European Journal of Science and Technology*, vol. Special Issue 26, pp. 395-400, 2021.
- [4] K. Ding and P. Jiang. "RFID-based production data analysis in an IoT-enabled smart Job-shop". *IEEE/CAA Journal of Automatica Sinica*, vol. 5, no.1, pp. 128-138, 2018.
- [5] S. Sawalha and G. Al-Naymat. "Towards an efficient big data management schema for IoT". *Journal of King Saud University-Computer and Information Science*, vol. 34, pp. 7803-7818, 2021.
- [6] N. Arhab, M. Oussalah and M. S. Jahan. "Social media analysis of car parking behavior using similarity based clustering". *Journal of Big Data*, vol. 9, p. 74, 2022.
- [7] R. Sharma, D. K. Sharma, D. Bhatt and B. Thai Pham. "Big Data Analysis for Green Computing Concepts and Applications". 1st ed. Routledge, United Kingdom, 2022.
- [8] H. Nasiri, S. Nasehi and M. Goudarzi. "Evaluation of distribute stream processing framework for IOT applications in smart cities". *Journal of Big Data*, vol. 6, p. 52, 2019.
- [9] F. Ullah, H. Naeem, S. Jabbar, S. Khalid, M. A. Latif, F. Al-Turjman and L. Mostarda. "Cyber security threats detection in internet of things using deep learning approach". *IEEE Access*, vol. 7, pp. 124379-124389, 2019.
- [10] A. K. Sangaiah, A. Thangavelu and V. M. Sundaram. "Cognitive Computing for Big Data Systems Over IoT Frameworks, Tools and Applications". Springer, Berlin, 2018.
- [11] X. Nie, T. Fan, B. Wang, Z. Li, A. Shankar and A. Manickam. "Big data analytics and IoT in operation safety management in under water management". *Computer Communications*, vol. 154, pp. 188-196, 2020.
- [12] A. Akbar, G. Kousiouris, H. Pervaiz, J. Sancho, P. Ta-Shma and F. C. K. Moessner. "Real-time probabilistic data fusion for large-scale IoT application". *IEEE Access*, vol. 6, pp. 10015-10027, 2018.
- [13] D. Serpanos and M. Wolf. "Internet-of-Things (IoT) Systems Architectures, Algorithms, Methodologies". Springer, Berlin, 2018.
- [14] S. A. Shah, D. Z. Seker, S. Hameed and D. Draheim. "The rising role of big data analytics and IoT in disaster management: Recent advances, taxonomy and prospects". *IEEE Access*, vol. 7, p. 54595-54614, 2019.
- [15] M. Babar, M. D. Alshehri, M. U. Tariq, F. Ullah, A. Khan, M. Irfan Uddin and A. S. Almasoud. "Energy-harvesting based on internet of things and big data analytics for smart health monitoring". *Sustainable Computing: Informatics and Systems*, vol. 20, pp. 155-164, 2018.
- [16] S. Singh and A. Yassine. "IoT big data analytics with fog computing for household energy management in smart grids". *Smart Grid and Internet of Things*. Springer, Berlin, pp. 13-22, 2018.
- [17] S. A. Shah, D. Z. Seker, M. M. Rathore, S. Hameed, S. B. Yahia

- and D. Draheim. "Towards disaster resilient smart cities: Can internet of things and big data analytics be the game changers?" *IEEE Access*, vol. 2, p. 1-19, 2019.
- [18] L. Syed, S. Jabeen, S. Manimala and A. Alsaeedi. "Smart health framework for ambient assisted living using IoMT and big data analytics techniques". *Future Generation Computer System*, vol. 101, pp. 136-151, 2019.
- [19] C. Li. "Information processing in Internet of Things using big data analytics". *Computer Communications*, vol. 160, pp. 718-729, 2020.
- [20] M. S. Hadi, A. Q. Lawey, T. E. El-Gorashi and J. M. Elmirghani. "Patient-centric HetNets powered by machine learning and big data analytics for 6G networks". *IEEE Access*, vol. 8, pp. 85639-85655, 2020.
- [21] C. Ge, C. Yin, Z. Liu, L. Fang, J. Zhu and H. Ling. "A privacy preserve big data analysis system for wearable wireless sensor network". *Computers and Security*, vol. 96, p. 101887, 2020.
- [22] Z. Lv, L. Qiao, K. Cai and Q. Wang. "Big data analysis technology for electric vehicle networks in smart cities". *IEEE Transactions on Intelligent Transportation Systems*, vol. 22, pp. 1807-1816, J 2020.
- [23] S. M. Kaya, A. Erdem and A. Güneş. "A smart data pre-processing approach to effective management of big health data in IoT edge". *Smart Homecare Technology and TeleHealth*, vol. 8, pp. 9-21, 2021.
- [24] I. Ahmed, M. Ahmad, G. Jeon and F. Piccialli. "A framework for pandemic prediction using big data analysis". *Big Data Research*, vol. 25, p. 100190, 2021.
- [25] T. Qin, P. Poovendran and S. BalaMurugan. "Student-centered learning environments based on multimedia bi data analytics". *Arabian Journal for Science and Engineering*, vol. 48, p. 1-11, 2021.

A Hybrid Artificial Bee Colony and Artificial Fish Swarm Algorithms for Software Cost Estimation



Hawar Othman Sharif¹, Mazen Ismaeel Ghareb², Hoshmen Murad Mohamedyusf³

¹Department of Computer Science, College of Science, University of Sulaimani, Iraq, ²Department of Computer Science, College of Science and Technology, University of Human Development, Kurdistan Region, Iraq, ³Department of Plastic Arts, Halabja Fine Arts Institute, Halabja, Iraq

ABSTRACT

Software cost estimation (SCE), estimating the cost and time required for software development, plays a highly significant role in managing software projects. A somewhat accurate SCE is necessary for a software project to be successful. It allows effective control of construction time and cost. In the past few decades, various models have been presented to evaluate software projects, including mathematical models and machine learning algorithms. In this paper, a new model based on the hybrid of the artificial fish swarm algorithm (AFSA) and the artificial bee colony (ABC) algorithm is presented for SCE. The initial population of AFSA, which includes the values of the effort factors, is generated using the ABC algorithm. ABC algorithm is used to solve the problems of the AFSA algorithm such as population diversity and getting stuck in a local optimum. ABC algorithm achieves the best solutions using observer and scout bees. The evaluation of the combined method has been implemented on eight different data sets and evaluated based on eight different criteria such as mean magnitude of relative error and PRED (0.25). The proposed method is more error-free than current SCE methods, according to the results. The error value of the proposed method is lower on NASA60, NASA63, and NASA93 datasets.

Index Terms: Artificial Fish Swarm Algorithm, Software Cost Estimation, Artificial Bee Colony Algorithm, Constructive Cost Model

1. INTRODUCTION

Software is the most expensive part of computer systems. Thus, Software cost estimation (SCE) is vital in the profit and loss of the company, and the smallest error in SCE can cause a lot of financial and time loss to the software development company [1]. One of the most challenging challenges for software engineers is SCE. Project failure might result from poor estimating. The estimating error is the primary cause of this issue. Estimating cost and time at

the beginning of the software production and development cycle is the biggest challenge for software projects. Knowing the cost of a software project is of particular importance for companies and software production companies. The cost of creating and producing the project is not known relatively precisely at the beginning of the software production, the company may have problems and the project may fail [2]. Among the problems that exist in SCE, we can mention the wrong use of the SCE process, not using the correct methods, or problems that may not allow accurate SCE. It is not accurately calculated because many variables influence the calculation of SCE, such as people, environment, and technology politics. The software engineering community frequently discusses estimation methods for software effort estimation (SEE) and SCE development. Correct forecasts may significantly improve a company's success in terms of SCE and resource allocation. Conversely, inaccurate estimates

Access this article online

DOI:10.21928/uhdjst.v8n1y2024.pp129-141

E-ISSN: 2521-4217

P-ISSN: 2521-4209

Copyright © 2024 Sharif, *et al.* This is an open access article distributed under the Creative Commons Attribution Non-Commercial No Derivatives License 4.0 (CC BY-NC-ND 4.0)

Corresponding author's e-mail: Hawar Othman Sharif, Department of Computer Science, College of Science, University of Sulaimani, Iraq. hawar.sharif@univsul.edu.iq

Received: 12-01-2024

Accepted: 05-04-2024

Published: 07-05-2024

can lead to significant financial losses and project failure [3]. Therefore, it is crucial to find novel models with improved estimate skills.

Over the past few decades, methods such as machine learning and meta-heuristic evolution have been employed to predict the time and cost of software projects. These models have shown their effectiveness compared to other approaches. Therefore, an appropriate model that can precisely forecast the SEE and ECE in software development is required. The production of software and its development is one of the inevitable problems of today's world, and these problems are not possible without accurate SCE. The success or failure of software depends on determining the required resources (including human, financial, and time resources) [4]. Algorithmic and non-algorithmic techniques are generally used in software project SCE, with algorithmic models being more significant due to their simplicity [5]. Among the algorithmic models, constructive cost model (COCOMO) SCE can be mentioned. This model is presented by Boehm in three basic, intermediate, and advanced types. It serves as a model for calculating the time, money, and effort required to complete software projects [6].

Despite the strengths of this model, the estimated cost is not sufficiently accurate the possibility of error is very high, and the dimensions of the problem expand with the increase in the number of factors and response variables. Software engineering has continuously sought ways to improve and increase the predictability of software development efforts and costs. Boehm and his colleagues pioneered this field by introducing COCOMO models [7]. These models serve as the foundation for SEE and SCE, which are necessary for every software project. The SCE of a software project strongly influences whether it is successful or not. The cost of the project should be estimated based on the basic information from the software.

Usually, the task of SCE in companies and programming teams is the responsibility of the project manager, who of course must be an experienced project manager and have previous knowledge in these fields [8]. Estimating resources, cost, and schedule for a software engineering activity depends on things like experience, and access to relevant statistical data. Inherently, software projects have risk, and this risk leads to ambiguity, which itself depends on things such as the ability to convert estimates based on size, human labor, time, software capabilities, and the stability of product requirements and the environment of software engineering activities. SCE is a key tool used by developers and project

managers to estimate the time and financial investment required for software projects. Although linear and gradient algorithms can nearly always discover the best solution, they are expensive and inefficient for difficult optimization tasks. Approximate algorithms are used to quickly solve complicated problems because they have a high possibility of finding solutions that are near to optimum. Heuristic and meta-heuristic algorithms are the two broad categories into which approximate algorithms are separated. The best solution is found using meta-heuristic algorithms, a class of stochastic algorithms.

In this paper, the hybrid model of artificial fish swarm algorithm (AFSA) [9] and artificial bee colony (ABC) algorithm [10] is used to manage software projects and the error of these algorithms is also investigated. Two measures, the effort adjustment factor and the number of lines of code (KLOC), play a fundamental role in SCE. The former indicates the size of the project, while the latter takes into account project-specific conditions and requirements such as hardware limitations, personnel capabilities, and project complexity. To acquire a reasonable estimate of the time and cost required for software development, both of these criteria are essential. This paper's primary contributions are as follows:

- Increase productivity by providing a hybrid method for accurate SCE projects
- Improvement of AFSA algorithm using ABC algorithm. AFSA algorithm is not able to find the best solutions due to the population diversity problem. Therefore, the ABC algorithm is used to generate the initial population of AFSA
- Evaluation of the proposed method on eight main data sets of cost estimation and comparison of the proposed method with other models.

The general structure of this paper is as follows: In Section 2, the previous studies in the field of SCE are reviewed. ABC algorithm is explained in Section 3. In Section 4, the proposed method and its steps are explained. In Section 5, the evaluation and results of the proposed method and its comparison with other models are done. And finally, in the ion 6, conclusions and future works are stated.

2. RELATED WORKS

Correct cost estimation makes the project manager a strong support for making different decisions during the software lifecycle. The software development team's project manager, analyst, designer, programmer, and other members should

be aware of how much time and effort will be needed to create a quality result. Software development employing AI techniques has been the subject of extensive research in recent years.

The development of large industrial software systems with the highest reliability and availability requirements results in a great cost. That's why different companies started to develop such costly systems by reusing already developed components. Sethy and Rani [11] stated that SCE is always done before project implementation. To measure the cost of a software project, accurately several estimation models are present in the literature. In this research, the author presents a hybrid model of SCE based on COCOMO and function points. Both the model's function point and COCOMO are considered accurate for SCE. This model uses a hybrid formula to calculate effort and project size. The IVR dataset was used to develop the proposed method in MATLAB. From the result, it was concluded that the hybrid model of COCOMO and function point.

SCE was discovered when the COCOMO II dataset was used to train a multilayered feed forward Artificial Neural Network (ANN) using the back-propagation approach [12]. MSE and mean magnitude of relative error (MMRE) were used to validate the findings of this study. However, providing a precise and accurate estimation for a software project is still considered the most challenging task. The major reason for this failure in a software project is inaccurate software development norms; the rapid change in the technology becomes more puzzling for the software development industry. ANN is to adjust different dependent and independent variables among complex sets of bonds. The data set of COCOMO is utilized to train and test the network. Performance measurement measures include mean square error (MSE) and MMRE. From the result, it was concluded that the presented model delivers superior and accurate predictions for software development efforts.

An ANN with two independent activation functions that are based on the Taguchi approach was proposed by Rankovic *et al.* [13]. Based on a procedural approach, six different datasets were employed in this study. The clustering technique was used to apply the input values. The validation of the results was based on the MMRE. This work reduces the execution time by requiring fewer repeats. Polynomial Analogy estimation was suggested by Shahpar *et al.* [14] to increase the SCE's accuracy of prediction. To determine the similar characteristics of the supplied project, an analogy approach is applied.

The Whale-crow optimization (WCO) method [15] combines the Crow Search Algorithm (CSA) with the Whale Optimization Algorithm (WOA). By identifying the ideal regression coefficients for regression models like the linear regression model and the kernel logistic regression model, the WCO technique aims to develop an optimal regression model for SCE. The experiment uses four datasets from the Promise software engineering repository to conduct the practical performance analysis. The provided Kernel Regression model achieves the average MMRE at a rate of 0.2692, whereas the recommended linear regression model does so at a rate of 0.2442, proving the usefulness of the suggested strategy of SCE. To optimize four COCOMO-II coefficients and get optimal estimation, the author of Puspaningrum and Sarno [16] presented a hybrid model combining harmony search algorithm and the cuckoo search algorithm (CSA). Utilizing the MRE and MMRE, the suggested methodology is tested on the NASA 93 dataset. The suggested technique outperforms COCOMO-II and the CSA, according to experimental data, in evaluating the work and time required to construct a software project.

A fuzzy inference system has been developed in [17] to determine the relevant effort multiplier for each cost driver. It offers guidance on how to improve fuzzy logic-based COCOMO utilizing the particle swarm optimization algorithm employing evolutionary-based optimization strategies. Utilizing assessment measures such as mean and amount of the relative error, which were calculated using COCOMO NASA2 and COCOMONASA datasets, it is verified. The model outperforms other optimization techniques like the genetic algorithm.

The authors of Singh *et al.* [18] suggest a brand-new multi-objective differential evolution (MODE) algorithm. It is validated in two phases during the validation process. First, the MODE algorithm is included in the novel homeostatic factor-based mutation operator. The Pareto optimality concept is applied. They use a MODE to increase candidate solution variety and convergence rates, resulting in improved solutions that support evolution. The efficiency of the suggested strategy is assessed using eight bi- and tri-objective test function benchmarks. In comparison to the most recent iterations of MOEAs, the proposed technique fared well. Second, using it for SCE, the suggested approach is put to use for an application-based test. Multiobjective parameters, such as two and three objectives-based SCE, are also included in this technique. In terms of lowering work and minimizing mistakes, the suggested strategy produces superior outcomes in the majority of software projects.

Turkish Industry software projects and NASA-93 are the two typical data sets used in the experiments. The Manhattan distance and the MMRE are two performance measures used to assess the performance of the proposed algorithm biogeography-based optimization (BBO)-COCOMO-II. The suggested BBO technique, according to simulation findings, enhances the COCOMO-II coefficients now in use for a more accurate prediction of software project cost or effort [19].

In Gouda and Mehta [20], the authors discuss the value of the meta-heuristic algorithms in tackling numerous optimization problems that arise in software applications and mathematical models. The novel evolutionism-based self-adaptive mutation operator is used in the proposed approach to address multi-objective optimization issues. The problems with MODE algorithms are addressed by this method. The Pareto optimality principle and the evolutionism-based self-adaptive mutation operator are integrated in a MODE technique to improve the diversity of potential solutions. They have used the non-dominated sorting method to lessen Pareto dominance's temporal complexity. Eight benchmark test functions were used to gauge the effectiveness of the proposed method, and it outperformed the most recent MOEAs. Further, research is conducted on the suggested method, which accurately predicts SCEs by improving the tuning parameters of the multi-objective COCOMO. For all objective tasks, the proposed approach outperforms the other traditional benchmark algorithms in mean absolute error (MAE), root mean square error, and terms of prediction.

3. ABC ALGORITHM

One of the population-based algorithms that was introduced in 2005 [10] is the ABC algorithm. The three groups into which the bees are divided using the ABC algorithm Bees that work, watch, and scout. About half of the colony is made up of worker bees, and the other half is made up of observation bees. Worker bees convey food information to observer bees as they look for food near the food source stored in their memory. Worker bees frequently discover an appropriate food supply, and observer bees frequently do the same. Scout bees are worker bees that leave their existing food sources to seek for new ones. Like other population-based algorithms, the ABC algorithm is an iterative process. In the ABC algorithm, the process of searching for food is started by the worker bees. Each worker bee performs a special dance upon finding food, and the observer bees inside the hive

look at the dance of the worker bees to use it to know the location of the food source. Scout bees randomly look for food in the surrounding environment. The ABC algorithm's initialization procedures for worker bees, spectator bees, and scout bees are carried out as follows:

3.1. Initial Population

Eq. (1) defines the starting population of solutions.

$$x_{ij} = x_{min,j} + \text{rand}[0,1](x_{max,j} - x_{minj})$$

$$i \in 1,2,\dots,SN; j \in 1,2,\dots,D \quad (1)$$

3.2. Worker Bees

At this step, artificial bees explore the area surrounding the food source at point x_i in search of new, better food sources v_i . Eq. (2) is used to pinpoint the new position of the food supply.

$$v_{ij} = x_{ij} + \phi_{ij}(x_{ij} - x_{kj}) \quad j = 1,2,\dots,D; k = 1,2,\dots,SN \quad (2)$$

In Eq. (2), $x_i = [x_{i1}, x_{i2}, \dots, x_{im}]$ is the position vector of the i^{th} bee, D is equal to the dimensions of the solutions. $v_i = [v_{i1}, v_{i2}, \dots, v_{im}]$ is the new position vector of the bees, an integer random number in the interval $[1, SN]$ is that SN is equal to the number of artificial bees. A uniformly distributed random number in the range $[-1, 1]$ makes up the parameter ϕ_{ij} . Using Eq. (3), the random number x_i is chosen at random from the problem's domain.

$$x_{ij} = L_i + \text{rand}(0,1) \times (U_i - L_i) \quad (3)$$

In Eq. (3), U_i and L_i are the upper and lower limits of variable x_{ij} , respectively, and the procedure $\text{rand}()$ uses random values between 0 and 1. After determining the location of the new food source, I have to calculate its optimality. For this purpose, the fitness level of vector x_{ij} is defined according to Eq. (4).

$$fit_i = \begin{cases} \frac{1}{1+f_i} & f_i \geq 0 \\ 1 + \text{abs}(f_i) & f_i < 0 \end{cases} \quad (4)$$

3.3. Onlooker Bees

At this stage, each of the onlooker bees decides to search around the found food sources with a certain probability. The onlooker bees make their choice based on the possible values of the worker bees. Therefore, Eq. (5) is used to calculate the likelihood that watcher bees will select a food source.

$$p_i = \frac{fit_i}{\sum_{j=1}^{SN} fit_j} \quad (5)$$

The surrounding food source's position is determined using the updated location of the food source after all of the spectator bees have chosen their preferred food sources using Eq. (5). This process continues until the condition required to terminate the program is met.

3.4. Scout Bees

In the ABC algorithm, if an optimal solution cannot be identified after a predefined number of iterations, some bees leave the several and return to their original roles as scout bees to conduct a random search. They deal with the scope of the problem. The likelihood of discovering the overall ideal solution might be considerably increased by implementing the scout bee's stage.

4. THE PROPOSED METHOD

4.1. COCOMO Model

Among algorithmic models, the COCOMO model is the most well-known and often applied. This model is a basic method used to predict the number of people needed each month for software development in the industry. This model is also able to provide an estimate of the development time per month, the amount of effort required in each phase of software development, and the amount of cost required. Boehm has offered three levels of this model, which include basic, intermediate, and advanced COCOMO. Most software projects use the baseline model to estimate software development costs.

The basic COCOMO model is good for estimating software cost estimates, says Boehm about this model. Its accuracy is necessarily limited because there are no factors known for the accuracy of various hardware limitations, the quality and experience of people, the use of modern technology, tools, and other project characteristics, to have a significant impact on the cost. In the COCOMO model, the average cost estimate of software projects is calculated according to Eq. (6) [21].

$$PM = a * (size)^b * \prod_{i=1}^{15} EM_i \quad (6)$$

The values of the fixed parameters a and b in Eq. (6) are determined by the dataset's data. The size argument indicates

TABLE 1: Values for the middle COCOMO model's parameters

Class of projects	A	B	C
Organic	2.4	1.05	2.5
Semidetached	3.0	1.12	2.5
Embedded	3.6	1.20	2.5

COCOMO: Constructive cost model

the project's size in thousands of lines of code (KSLOC). The EM parameter is a coefficient that increases or decreases the effort rate per person/month. Parameters a, b, and c are initialized in the intermediate COCOMO in accordance with (Table 1).

The relatively small tasks in the Organic class are completed by highly skilled teams. Typically, if a project is 100 KSLOC or larger, it is assigned to the organic class. Semidetached projects range in size from 100 to 300 KSLOC and are moderately sized; they are neither simple nor complex. Projects that are embedded in classes typically exceed 300 KSLOC. When hardware and operations are already established and do not require any adjustments, this class is utilized.

4.2. Hybrid ABC with AFSA

In this paper, the hybrid of ABC and AFSA is used for SCE. First, the initial formulation is generated by the ABC algorithm, and then, the optimized population is given as input to the AFSA algorithm. The purpose of the proposed method is to improve random answers in the AFSA algorithm. The proposed method's flowchart is shown in (Fig. 1). The proposed method uses the ABC algorithm to diversify the population and prevent it from hitting the local optimum. By creating the initial population and injecting them into the AFSA algorithm, the ABC algorithm strengthens the solutions and discovers global solutions. ABC algorithm increases the global position update probability and convergence speed.

(Fig. 2) shows the Pseudocode of the proposed method.

4.2.1. ABC algorithm

First, a population between 0.9 and 1.4 is formed as the initial population. The set of random values is stored in the matrix x, and then in the worker bee phase, according to Eq. (7), a solution is created in the neighborhood of the existing solution in the memory. The bees update the random values at each step and find the best values of the effort factors.

$$v_{ij} = x_{ij} + \phi_{ij} (x_{ij} - x_{kj}) \quad j = 1, 2, \dots, D; k = 1, 2, \dots, SN \quad (7)$$

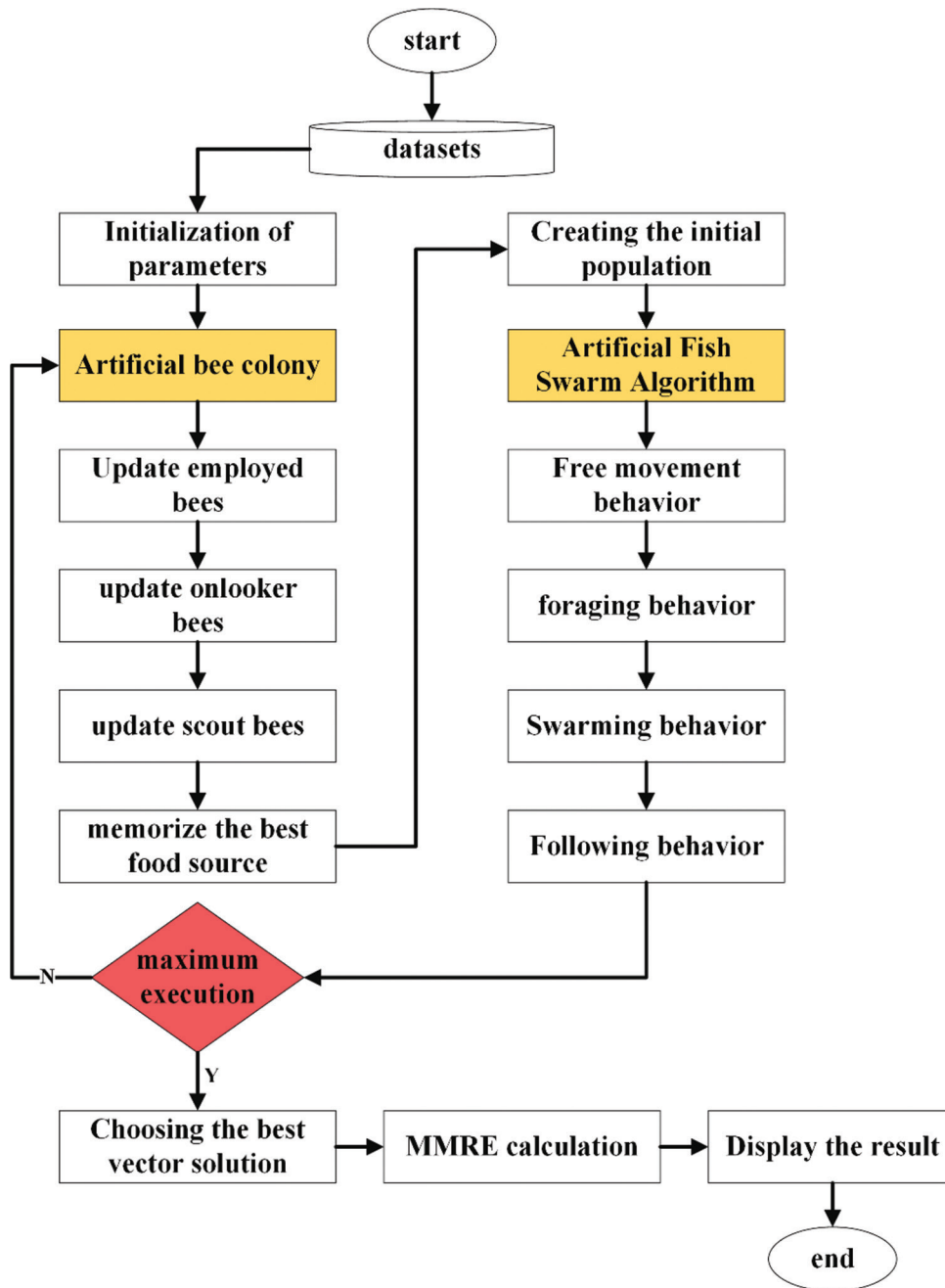


Fig. 1. Proposed method for Software cost estimation.

4.2.2. AFSA algorithm

This algorithm includes the following four behaviors: Free movement, foraging, group movement, and tracking behavior. When fishes fail to find food, they move freely according to Eq. (8). Random search leads to the discovery of all points of the problem space.

$$X(t+1) = X(t) + \text{Step} \times \text{Rand}(-1,1) \quad (8)$$

In Eq. (8), X_i is the i^{th} fish's location vector in the D-dimensional space. The uniformly distributed D-dimensional vector of random integers in the range [1 and -1] is produced by the *Rand* function. Food search behavior is defined using Eq. (9). If $X_j > X_i$ (in maximizing issues), the intended artificial fish advances from its present state in the direction of X_j . The food density in X_j is compared with the food density in the current state. In addition, another state, X_j , is chosen using

```

Read the datasets
Initialize the parameters
vector_length = 15
iteration_count = 0
WHILE iteration_count < maximum_execution DO
Perform ABC
Create Initial Population (vector_length, 0.9, 1.4)
For each bee in the population
Update the employed bee's position
Update the onlooker bee's position
Update the scout bee's position
Memorize the best food source
End for end
Perform the AFSA
Initialize the fish swarm
Perform the free movement behavior
Perform the foraging behavior
Perform the swarming behavior
Follow the best food source
Update the fish swarm
Calculate the fitness of each fish
Select the best fish
end
iteration_count = iteration_count + 1
End While
Choose the best vector solution
Calculate the MMRE
Display the result

```

Fig. 2. Pseudocode of the proposed method.

Eq. (8) if $X_j > X_i$ is not the case.

$$X_i^{(t+1)} = X_i^{(t)} + \frac{X_j - X_i^{(t)}}{X_j - X_i^{(t)}} \times \text{Step} \times \text{Rand}(0,1) \quad (9)$$

If X_i is the current state of the fish, a state (X) is randomly selected in the fish's field of view. The state of X_j is obtained using Eq. (10). The rand function generates a random number with a uniform distribution in the interval $[-1, 1]$.

$$X_j = X_i + \text{Visual} \times \text{Rand}(-1,1) \quad (10)$$

The group movement behavior of fishes is defined collectively according to Eq. (11). At this stage, each fish makes an effort to travel toward the central location, or X_C , which corresponds to the center of gravity of the fish group's members' vectors.

$$X_i^{(t+1)} = X_i^{(t)} + \frac{X_C - X_i^{(t)}}{X_C - X_i^{(t)}} \times \text{Step} \times \text{Rand}(0,1) \quad (11)$$

The following behavior is defined according to Eq. (12) that each of the fish is look or the fish that have found more food. In the process of group movement of fish, when a fish or a number of them find food, the neighbors and fishes close to them follow them and quickly reach the food. The update of the current state (X) is done by exploring the neighbors (X_j, k), so the movement toward the optimal points is done by checking the state of the neighbors. The segment step's maximum length is equal to the step. The Euclidean distance $d_{ij} = \|X_i - X_j\|$ denotes the separation between two artificial fish that are in the states X_i and X_j .

$$X_i^{(t+1)} = X_i^{(t)} + \frac{X_j - X_i^{(t)}}{X_j - X_i^{(t)}} \times \text{Step} \times \text{Rand}(0,1) \quad (12)$$

4.3. ABC-AFSA

A new hybrid model with the advantages of ABC and AFS is proposed to increase the discovery capability. The hybrid model leads to the improvement of the convergence rate and the quality of the solutions. The hybrid model creates a new method to find the best optimal solutions. Global exploration and local exploitation are executed in balanced mode. Exploratory search behavior is defined using Eq. (13).

$$X_i^{(t+1)} = \begin{cases} X_i^{(t)} + \frac{X_j - X_i^{(t)}}{X_j - X_i^{(t)}} \times \text{Step} \times \text{Rand}(0,1) & r_1 < 0.5 \\ X_i^{(t)} + \frac{X_{\min} - X_i^{(t)}}{X_{\min} - X_i^{(t)}} \times \left(1 - \left(\frac{t}{T}\right)^{e1}\right) \times \text{Rand}(0,1) & r_1 \geq 0.5 \end{cases} \quad (13)$$

In Eq. (13), is the current state. The state of is obtained using Eq. (14). The rand function generates a random number with a uniform distribution in the interval $[-1, 1]$. In the hybrid model, the value of Step and Visual is equal to 30 and 1, respectively. r_1 is a random number between

0 and 1. X_{min} represents the lowest value in the i^{th} vector. The parameters t and T are the current iteration and the maximum iteration, respectively. e_1 is a positive number between 0 and 1.

$$X_j = \begin{cases} X_i + \text{Visual} \times \text{Rand}(-1, 1) & r_2 < 0.5 \\ L_i + \text{rand}(0, 1) \times (U_i - L_i) & r_2 \geq 0.5 \end{cases} \quad (14)$$

In Eq. (14), U_i and L_i are variables with the upper and lower limits, respectively. $\text{Rand}()$ is also a function of random numbers in the interval (0,1). r_2 is a random number between 0 and 1.

AFSA has disadvantages such as early convergence and poor local search ability because it cannot use the local information of individuals in the population. ABC can enhance the search ability and avoid getting stuck in local optima. The hybrid model has good global discovery capability as well as local exploitation capability. It can obtain a better solution with a faster convergence speed. The exploitability in the combined model is defined according to Eq. (15). The X_{best} parameter represents the current best value found.

$$X_i^{(t+1)} = X_i^{(t)} + \frac{X_{best} - X_i^{(t)}}{X_{best} - X_i^{(t)}} \times ST \times \text{Rand}(0, 1) \quad (15)$$

$$ST = \frac{\text{rand}() \times \text{Visual}}{e^{(\text{rand}() \times \text{Visual})} - e^{\frac{t}{T} \times \text{Visual}}} \quad (16)$$

4.4. Evaluation Criteria

In the proposed method, the average relative error value [22] is considered as the fitness function. The proposed method's fitness function aims to reduce relative error values when compared to the COCOMO model. Eq. (17) is the definition of the fitness function for the proposed method. The y parameter is equal to the real value and the \bar{y} parameter is equal to the estimated value obtained by the proposed method.

Mean Magnitude of Relative Error (MMRE)

$$= \frac{1}{n} \sum_{i=1}^n \left(\frac{|y_i - \bar{y}_i|}{y_i} \times 100 \right) \quad (17)$$

Mean of Magnitude Error Relative (MMER)

$$= \frac{1}{n} \sum_{i=1}^n \left(\frac{|y_i - \bar{y}_i|}{\bar{y}_i} \times 100 \right) \quad (18)$$

$$\text{Mean Squared Error (MSE)} = \frac{1}{n} \sum_{i=1}^n (y_i - \bar{y}_i)^2 \quad (19)$$

$$\text{Root Mean Square Error (RMSE)} = \sqrt{\frac{1}{n} \sum_{i=1}^n (y_i - \bar{y}_i)^2} \quad (20)$$

Mean Absolute Percentage Error (MAPE)

$$= \sum_{i=1}^n \left(\frac{|y_i - \bar{y}_i|}{y_i} \right) / n \times 100 \quad (21)$$

$$\text{Mean of Absolute Errors (MAE)} = \frac{1}{n} \sum_{i=1}^n |y_i - \bar{y}_i| \quad (22)$$

Median Magnitude of Relative Error (MDMRE)

$$= \text{Median (MRE)} \quad (23)$$

5. EVALUATION AND RESULTS

In this paper, the SCE was computed using a mix of the ABC algorithm and AFSA, and the results were analyzed using a variety of techniques. The implementation of the hybrid method has been done in the VC#.NET 2021 environment. MMER, MMRE, MDMRE, PRED (0.25), MSE, RMSE, MAPE, and MAE criteria are used to evaluate the proposed method. The evaluation criteria are tested on eight datasets NASA60, NASA63, NASA93, Miyazaki, Maxwell, KEMERER, Desharnais, and Finnish. The initial population and the number of iterations in all algorithms are equal to 50 and 200, respectively. The value of k in the KNN algorithm is equal to 3. According to (Table 2)'s findings, the proposed method performs the best overall on NASA60. In the proposed method, MMRE has a value of 20.08. The MMRE value for COCOMO, ABC, AFSA, and KNN models is 16.09, 19.17, 16.17, and 14.52, respectively. The value of PRED for COCOMO, ABC, AFSA, and KNN models is 0.83, 0.75, 0.92, and 0.92, respectively.

According to Table 3's findings, the proposed method performs the best overall on NASA63 and MMRE has a value of 22.63. The MMRE value for COCOMO, ABC, AFSA, and KNN models is 16.60, 18.16, 15.24, and 15.16, respectively. The value of PRED for COCOMO, ABC, AFSA, and KNN models is 0.85, 0.77, 0.85, and 0.92, respectively.

TABLE 2: Evaluation of the proposed method on the NASA60 dataset

Function	COCOMO	ABC	AFSA	KNN	Proposed method
MMRE	19.43	16.03	16.92	16.67	16.02
MMRE	16.09	19.17	16.17	14.52	20.08
MDMRE	16.27	15.44	16.03	14.68	12.60
PRED	0.83	0.75	0.92	0.92	0.75
MSE	8521.40	5475.48	11570.14	6995.79	3408.14
RMSE	92.31	74.00	107.56	83.64	58.38
MAPE	16.09	19.17	16.17	14.52	20.08
MAE	50.34	42.55	59	43.30	39.24

AFSA: Artificial fish swarm algorithm, ABC: Artificial bee colony, MMRE: Mean magnitude of relative error, COCOMO: Constructive cost model, MAE: Mean absolute error

TABLE 3: Evaluation of the proposed method on the NASA63 dataset

Function	COCOMO	ABC	AFSA	KNN	Proposed method
MMRE	20.20	14.32	14.30	17.66	22.72
MMRE	16.60	18.16	15.24	15.16	22.63
MDMRE	16.27	10.33	14.04	14.68	16.97
PRED	0.85	0.77	0.85	0.92	0.77
MSE	8041.41	3925.67	6617.66	6633.15	16996.64
RMSE	89.67	62.66	81.35	81.44	130.37
MAPE	16.60	18.16	15.24	15.16	22.63
MAE	50.14	36.50	06.46	43.64	76.50

AFSA: Artificial fish swarm algorithm, ABC: Artificial bee colony, MMRE: Mean magnitude of relative error, COCOMO: Constructive cost model, MAE: Mean absolute error

TABLE 4: Evaluation of the proposed method on the NASA93 dataset

Function	COCOMO	ABC	AFSA	KNN	Proposed method
MMRE	23.10	12.28	38.90	21.27	15.65
MMRE	18.23	14.23	25.13	17.24	16.26
MDMRE	20.98	11.46	26.39	18.18	12.68
PRED	0.84	0.89	0.53	0.89	0.89
MSE	5933.62	3758.65	2255.6	4970.08	7518.1
RMSE	77.03	61.31	47.49	70.5	86.71
MAPE	18.23	14.23	25.13	17.24	16.26
MAE	44.49	34.32	36.68	40.04	50.06

AFSA: Artificial fish swarm algorithm, ABC: Artificial bee colony, MMRE: Mean magnitude of relative error, COCOMO: Constructive cost model, MAE: Mean absolute error

According to (Table 4)'s findings, the proposed method performs the best overall on NASA93 and MMRE has a value of 16.26. The MMRE value for COCOMO, ABC, AFSA, and KNN models is 18.23, 14.23, 25.13, and 17.24, respectively. The value of PRED for COCOMO, ABC, AFSA, and KNN models is 0.84, 0.89, 0.53, and 0.89, respectively.

According to (Table 5)'s findings, the proposed method performs the best overall on Miyazaki and MMRE in the proposed method is 31.22. The MMRE value for COCOMO, ABC, AFSA, and KNN models is 272.79, 33.52, 33.09, and 272.79, respectively. The value of PRED for ABC and AFSA models is 0.40 and 0.40, respectively.

According to (Table 6)'s findings, the proposed method performs the best overall on MAXWELL and MMRE in the

proposed method is 37.9. The MMRE value for COCOMO, ABC, AFSA, and KNN models is 76.43, 38.1, 37.81, and 43.76, respectively. The value of PRED for ABC and AFSA models and the proposed method is 0.46, 0.46, and 0.52, respectively.

According to (Table 7)'s findings, the proposed method performs the best overall on KEMERER and MMRE in the proposed method is 56.34. The MMRE value for COCOMO, ABC, AFSA, and KNN models is 687.64, 48.1, 45.8, and 687.64, respectively. The value of PRED for COCOMO, ABC, AFSA, and KNN models was obtained as 0, 0.44, 0.44, and 0 respectively.

According to (Table 8)'s findings, the proposed method performs the best overall on Desharnais and MMRE in the proposed method is 48.99. The MMRE value for COCOMO, ABC, AFSA, and KNN models is 99.11, 70.27, 1.71, and

TABLE 5: Evaluation of the proposed method on the Miyazaki dataset

Function	COCOMO	ABC	AFSA	KNN	Proposed method
MMRE	70.83	58.9	57.86	70.83	52.21
MMRE	272.79	33.52	33.09	272.79	31.22
MDMRE	277.48	41.04	40.52	277.48	37.46
PRED	0	0.40	0.40	0	0.50
MSE	18960.41	670.18	650.89	18960.41	555.1
RMSE	137.7	25.89	25.51	137.7	23.56
MAPE	272.79	33.52	33.09	272.79	31.22
MAE	122.16	20.71	20.49	122.16	19.22

AFSA: Artificial fish swarm algorithm, ABC: Artificial bee colony, MMRE: Mean magnitude of relative error, COCOMO: Constructive cost model, MAE: Mean absolute error

TABLE 6: Evaluation of the proposed method on the Maxwell dataset

Function	COCOMO	ABC	AFSA	KNN	Proposed method
MMRE	118.44	94.06	97.42	118.44	91.6
MMRE	76.43	38.1	37.81	43.76	37.9
MDMRE	36.58	34.67	31.31	36.58	32.93
PRED	0.38	0.46	0.46	0.38	0.52
MSE	14513588.9	21537730.41	23327134.14	14513588.9	22634329.41
RMSE	3809.67	4640.88	4829.82	3809.67	4757.55
MAPE	43.76	38.1	37.81	43.76	37.9
MAE	2603	2915.07	3031.72	2603	2964.61

AFSA: Artificial fish swarm algorithm, ABC: Artificial bee colony, MMRE: Mean magnitude of relative error, COCOMO: Constructive cost model, MAE: Mean absolute error

TABLE 7: Evaluation of the proposed method on KEMERER data set

Function	COCOMO	ABC	AFSA	KNN	Proposed method
MMRE	79.23	56.36	58.66	79.23	60.2
MMRE	687.64	48.1	45.8	687.64	56.34
MDMRE	626.6	39.5	31.2	626.6	39.29
PRED	0	0.44	0.44	0	0.44
MSE	3546018.29	68399.11	68923.45	3546018.29	3546018.29
RMSE	1883.09	261.53	262.53	1883.09	268.95
MAPE	687.67	48.1	45.8	687.64	56.34
MAE	1375.95	120.31	119.9	1375.95	130.43

AFSA: Artificial fish swarm algorithm, ABC: Artificial bee colony, MMRE: Mean magnitude of relative error, COCOMO: Constructive cost model, MAE: Mean absolute error

TABLE 8: Evaluation of the proposed method on the Desharnais dataset

Function	COCOMO	ABC	AFSA	KNN	Proposed method
MMRE	13882.49	559	31.562	29108.17	127.12
MMRE	99.11	70.27	1.71	99.35	48.99
MDMRE	99.28	72.29	01.74	99.6	51.9
PRED	0	0.06	0	0	0.12
MSE	19363264.14	9051856.53	9395487.52	176906010.58	86350530.51
RMSE	4400.37	3008.63	3065.21	13300.6	9292.5
MAPE	99.11	70.27	1.71	99.35	48.99
MAE	3879.66	2665.57	2701.35	10642.89	6638.94

AFSA: Artificial fish swarm algorithm, ABC: Artificial bee colony, MMRE: Mean magnitude of relative error, COCOMO: Constructive cost model, MAE: Mean absolute error

99.35 respectively. The value of PRED for ABC models and the proposed method is 0.06 and 0.12, respectively.

The results of (Table 9) show that the proposed method has the best overall performance on Finnish. The value of

MMRE in the proposed method is 48.82. The MMRE value for COCOMO, ABC, AFSA, and KNN models is 99.35, 55.75, 57.27, and 99.31, respectively. The value of PRED for ABC models and the proposed method is 0.12 and 0.12, respectively.

TABLE 9: Evaluation of the proposed method on the Finnish dataset

Function	COCOMO	ABC	AFSA	KNN	Proposed method
MMRE	29108.17	174.89	217.89	29108.17	127.12
MMRE	99.35	55.75	57.27	99.31	48.82
MDMRE	99.6	62.22	66.51	99.6	51.9
PRED	0	0.12	0.12	0	0.12
MSE	176906010.58	98437723.32	110721304.73	176906010.58	86350530.51
RMSE	13300.6	9921.58	10522.42	13300.6	9292.5
MAPE	99.35	55.75	57.27	99.35	48.99
MAE	1064.89	7358.82	7783.96	1064.89	6638.94

AFSA: Artificial fish swarm algorithm, ABC: Artificial bee colony, MMRE: Mean magnitude of relative error, COCOMO: Constructive cost model, MAE: Mean absolute error

TABLE 10: Comparison of the proposed model with meta-heuristic algorithms

Datasets	WOA	SCA	MFO	Proposed method
NASA60	21.52	20.48	21.94	20.08
NASA63	22.91	22.19	23.15	22.63
NASA93	16.54	16.82	17.24	16.26
Miyazaki	31.42	31.49	31.12	31.22
Maxwell	38.19	38.14	38.18	37.90
KEMERER	56.71	56.22	56.92	56.34
Desharnais	49.05	49.16	49.08	48.99
Finnish	48.97	49.02	48.95	48.82

WOA: Whale optimization algorithm, SCA: Sine cosine algorithm, MFO: Moth-Flame Optimization

To show the effectiveness of the proposed model, WOA [23], sine cosine algorithm (SCA) [24], and Moth-Flame Optimization (MFO) [25] have been used for comparison. The results of (Table 10) show that the SCA algorithm on NASA63 achieved an error rate of 22.19. The MFO algorithm on Miyazaki achieved an error rate of 31.12. The SCA algorithm on KEMERER has achieved an error rate of 56.22. In general, the proposed model has achieved a lower error value in most of the data sets. Of course, meta-heuristic algorithms have different results and the error value changes with each execution. The most important issue in meta-heuristic algorithms is the balance between exploration and exploitation, which is established in the proposed model.

In Table 11, the results of the models are shown based on the best, mean, and worst criteria. The values of the best, mean, and worst criteria on the NASA93 dataset for the proposed model are 16.26, 16.38, and 16.74, respectively. Furthermore, the values of the best, mean, and worst criteria on the Desharnais dataset for the proposed model are 48.99, 49.07, and 49.21, respectively. The worst value on the Miyazaki and Maxwell datasets for AFSA is 33.65 and 38.34, respectively.

The statistical results are confirmed using a non-parametric statistical test called Mann–Whitney U-test [26]. Statistical

tests are used to evaluate the results of the models statistically and meaningfully. For this purpose, the Mann–Whitney U-test has been used, which is a non-parametric statistical test. In Table 12, the results of the statistical test are shown that the models are compared with each other to determine whether the difference in the average errors for the combined model is significant or not. The hybrid model has a lower error value compared to other models.

6. CONCLUSION AND FUTURE WORK

SCE is one of the most challenging project management duties since project planning and budgeting are dependent on realized costs. Since there are a limited number of resources for a project, it is not possible to include all the required resources in the final product. In this paper, the combined method of ABC and AFSA was used for SCE. The proposed method was tested on NASA60, NASA63, NASA93, Miyazaki, Maxwell, KEMERER, Desharnais, and Finnish datasets. The proposed method performed better on the NASA60 dataset. In the NASA93 data set, MMRER, MMRE, MDMRE, PRED, MSE, and MAPE criteria have performed better. In the Finnish dataset, better performance is obtained in all measures except MAE. The main challenges of this study are as follows: (1) the data sets used are old. In old projects, all the factors involved in the construction of software projects are usually not mentioned. For example, current databases filter and process data using specific commands. Processing orders are specialized in a field and require specialized manpower. (2) Meta-heuristic algorithms for estimating software projects have a main limitation called local optimality. With the occurrence of local optimality, the algorithm is not able to find optimal values for the effort factors, and therefore, the error value increases. To solve the mentioned problems, weight and adaptive operators should be used in meta-heuristic algorithms. According to the obtained results, for future works, the combined method can

TABLE 11: The results of the models based on the best, mean, and worst criteria

Datasets	MMRE	COCOMO	ABC	AFSA	KNN	Proposed method
NASA60	Best	16.09	19.17	16.17	14.52	20.08
	Mean	16.09	19.32	16.29	14.30	20.15
	Worst	16.09	19.65	16.67	14.92	20.42
NASA63	Best	16.60	18.16	15.24	15.16	22.63
	Mean	16.60	18.25	15.38	15.33	22.91
	Worst	16.60	18.55	15.64	15.76	23.15
NASA93	Best	18.23	14.23	25.13	17.24	16.26
	Mean	18.23	14.81	25.67	17.48	16.38
	Worst	18.23	14.69	25.84	17.65	16.74
Miyazaki	Best	272.79	33.52	33.09	272.79	31.22
	Mean	272.79	33.84	33.24	273.61	31.35
	Worst	272.79	34.15	33.65	273.54	31.50
Maxwell	Best	76.43	38.10	37.81	43.76	37.90
	Mean	76.43	38.54	37.85	43.66	38.05
	Worst	76.43	38.64	38.34	44.21	38.12
KEMERER	Best	687.64	48.10	45.80	687.64	56.34
	Mean	687.64	48.23	46.20	688.11	56.46
	Worst	687.64	48.54	46.25	688.94	56.82
Desharnais	Best	99.11	70.27	1.71	99.35	48.99
	Mean	99.11	70.31	2.19	99.36	49.07
	Worst	99.11	70.56	2.84	99.49	49.21
Finnish	Best	99.35	55.75	57.27	99.31	48.82
	Mean	99.35	56.02	57.61	99.25	48.92
	Worst	99.35	56.16	57.94	99.51	49.25

AFSA: Artificial fish swarm algorithm, ABC: Artificial bee colony, MMRE: Mean magnitude of relative error, COCOMO: Constructive cost model

TABLE 12: The results of the Mann–Whitney U statistical test

Datasets	ρ value			
	ABC	AFSA	KNN	Proposed method
NASA60	2.362215e-16	3.257400e-12	5.000036e-14	3.261500e-12
NASA63	2.320164e-15	2.326010e-12	2.259487e-12	1.323265e-20
NASA93	4.002649e-12	2.993584e-15	4.013265e-14	3.265148e-15
Miyazaki	2.010062e-14	4.234901e-15	2.103284e-16	1.003261e-17
Maxwell	2.360014e-10	2.003947e-14	4.169500e-10	3.269501e-12
KEMERER	6.206554e-10	5.205974e-17	1.249014e-10	5.265491e-10
Desharnais	2.360057e-12	3.123500e-10	3.839142e-10	4.326514e-12
Finnish	3.142510e-14	3.320115e-12	5.760258e-12	2.365214e-15

AFSA: Artificial fish swarm algorithm, ABC: Artificial bee colony

be used for various problems in such fields as weather forecasting, disease forecasting, stock market forecasting, urban growth forecasting, license plate recognition, image recognition, etc.

REFERENCES

- [1] S. Hameed, Y. Elsheikh and M. Azzeh. "An optimized case-based software project effort estimation using genetic algorithm." *Information and Software Technology*, vol. 153, p. 107088, 2023.
- [2] N. Govil and A. Sharma. "Estimation of cost and development effort in Scrum-based software projects considering dimensional success factors." *Advances in Engineering Software*, vol. 172, p. 103209, 2022.
- [3] H. M. Sneed and C. Verhoef. "Cost-driven software migration: An experience report." *Journal of Software: Evolution and Process*, vol. 32, no. 7, p. e2236, 2020.
- [4] S. Tariq, M. Usman and A. C. Fong. "Selecting best predictors from large software repositories for highly accurate software effort estimation." *Journal of Software: Evolution and Process*, vol. 32, no. 10, p. e2271, 2020.
- [5] K. Rak, Ž. Car and I. Lovrek. "Effort estimation model for software development projects based on use case reuse." *Journal of Software: Evolution and Process*, vol. 31, no. 2, p. e2119, 2019.
- [6] T. Hacaloglu and O. Demirors. "An exploratory case study using events as a software size measure." *Information Technology and Management*, vol. 24, pp. 1-20, 2023.
- [7] E. Feizpour, H. Tahayori and A. Sami. "CoBRA without experts: New paradigm for software development effort estimation using COCOMO metrics." *Journal of Software: Evolution and Process*,

- vol. 35, p. e2569, 2023.
- [8] A. K. Bardsiri and S. M. Hashemi. "A differential evolution-based model to estimate the software services development effort." *Journal of Software: Evolution and Process*, vol. 28, no. 1, pp. 57-77, 2016.
- [9] X. L. Li, Z. J. Shao and J. X. Qian. "An optimizing method based on autonomous animats: Fish-swarm algorithm." *Systems Engineering-Theory and Practice*, vol. 22, no. 11, pp. 32-38, 2002.
- [10] D. Karaboga. "An Idea Based on Honey Bee Swarm for Numerical Optimization. Technical Report-tr06, Erciyes University, Engineering Faculty, Computer." Erciyes University, Engineering Faculty, Computer Engineering Department, Kayseri/Türkiye, 2005.
- [11] P. K. Sethy and S. Rani. "Improvement in COCOMO Modal Using Optimization Algorithms to Reduce MMRE Values for Effort Estimation. In: 2019 4th International Conference on Internet of Things: Smart Innovation and Usages (IoT-SIU)." pp. 1-4, 2019.
- [12] P. Rijwani and S. Jain. "Enhanced software effort estimation using multi layered feed forward artificial neural network technique." *Procedia Computer Science*, vol. 89, no. 1, pp. 307-312, 2016.
- [13] N. Rankovic, D. Rankovic, M. Ivanovic and L. Lazic. "Improved effort and cost estimation model using artificial neural networks and taguchi method with different activation functions." *Entropy*, vol. 23, p. 854, 2021.
- [14] Z. Shahpar, V. K. Bardsiri and A. K. Bardsiri. "Polynomial analogy-based software development effort estimation using combined particle swarm optimization and simulated annealing." *Concurrency and Computation: Practice and Experience*, vol. 33, no. 20, p. e6358, 2021.
- [15] S. W. Ahmad and G. R. Bamnote. "Whale-crow optimization (WCO)-based Optimal Regression model for Software Cost Estimation." *Sādhanā*, vol. 44, no. 4, p. 94, 2019.
- [16] A. Puspaningrum and R. Sarno. "A hybrid cuckoo optimization and harmony search algorithm for software cost estimation." *Procedia Computer Science*, vol. 124, no. 1, pp. 461-469, 2017.
- [17] S. Chhabra and H. Singh. "Optimizing design of fuzzy model for software cost estimation using particle swarm optimization algorithm." *International Journal of Computational Intelligence and Applications*, vol. 19, no. 1, p. 2050005, 2020.
- [18] S. P. Singh, G. Dhiman, P. Tiwari and R. H. Jhaveri. "A soft computing based multi-objective optimization approach for automatic prediction of software cost models." *Applied Soft Computing*, vol. 113, no. 1, p. 107981, 2021.
- [19] U. Aman, W. Bin, S. Jinfang, L. Jun, A. Muhammad and S. Zejun. "Optimization of software cost estimation model based on biogeography-based optimization algorithm." *Intelligent Decision Technologies*, vol. 14, no. 1, pp. 441-448, 2020.
- [20] S. K. Gouda and A. K. Mehta. "A new evolutionism based self-adaptive multi-objective optimization method to predict software cost estimation." *Software: Practice and Experience*, vol. 52, no. 8, pp. 1826-1848, 2022.
- [21] B. W. Boehm, C. Abts, A. W. Brown, S. Chulani, B. K. Clark, E. Horowitz, R. Madachy, D. J. Reifer and B. Steece. "Software Cost Estimation with COCOMO II." Prentice Hall Press, Upper Saddle River, NJ, USA, 2009.
- [22] R. H. Martin and D. Raffo. "A Comparison of Software Process Modeling Techniques. In: Innovation in Technology Management: The Key to Global Leadership, PICMET'97." pp. 577-580, 1997.
- [23] S. Mirjalili and A. Lewis. "The whale optimization algorithm." *Advances in Engineering Software*, vol. 95, pp. 51-67, 2016.
- [24] S. Mirjalili. "SCA: A Sine Cosine algorithm for solving optimization problems." *Knowledge-Based Systems*, vol. 96, pp. 120-133, 2016.
- [25] S. Mirjalili. "Moth-flame optimization algorithm: A novel nature-inspired heuristic paradigm." *Knowledge-Based Systems*, vol. 89, pp. 228-249, 2015.
- [26] Z. Abdelali, H. Mustapha and N. Abdelwahed. "Investigating the use of random forest in software effort estimation." *Procedia Computer Science*, vol. 148, no. pp. 343-352, 2019.

Black Hole Attack Detection in Wireless Sensor Networks Using Hybrid Optimization Algorithm



DiSoz Abdalkarim Rashid^{1*}, Marwan B. Mohammed²

¹Department of Computer Science, College of Science, University of Sulaimani, Sulaimani, Iraq, ²Department of Computer Science, College of Science, University of Al-Nahran, Baghdad, Iraq.

ABSTRACT

One of the types of denial of service attacks that target wireless sensor networks (WSNs) are black hole (BH) attacks, which are widely targeted at this form of network today. In this attack, data are blocked in the network, malware is installed on a group of nodes in the network, and ultimately, the data packet is blocked before reaching its destination. In other words, data cannot be transmitted in the vicinity of BH nodes. Because of the nature of WSNs that are readily available, these networks cannot be optimized without compromising energy consumption, and this problem becomes a non-deterministic polynomial-time hard problem. Despite some models that have been presented to resolve this issue, most of them have not had sufficient performance in dealing with BH attacks. Thus, we have presented a new and powerful model based on the hybrid meta-heuristic algorithm depending on the sine and cosine algorithm (SCA) and the whale optimization algorithm (WOA). This algorithm has been combined in such a way that the increase in computational load has been prevented, in addition, two algorithms are included in one algorithm in this case, using the positive features of these two algorithms, it escapes from the local optimal trap in the solution of the algorithm and also benefits from a very good convergence. Because the new production solutions have a good diversity and the intensification component also has a good performance the main goal of this article is to present a new type of robust optimization algorithm for BH detection in WSN. This model has been tested and evaluated using a network and compared with three other meta-heuristic algorithms to make a fair comparison. The results obtained from the proposed model indicate a high-quality performance of this model in detecting BH attacks. The proposed model can detect more than 85% of the BH nodes and the total warning rate in the proposed model is equal to 0.866.

Index Terms: Whale Optimization Algorithm, Sine and Cosine Algorithm, Black Hole Attack, Wireless Sensor Networks, Meta-Heuristic

1. INTRODUCTION

Wireless sensor networks (WSNs) consist of a set of sensors, each of which has a transmitter, and this processor is also used to communicate, observe, and respond to events in the environment [1]. In other words, these types of networks usually have more than tens of thousands of sensors that

are responsible for collecting information from nature and transmitting this information to the central device. WSN is a type of new technology that is widely used in various fields, including vehicles, health-care monitoring, accident detection, and emergency response at high speed [2]. Considering that these networks are very important, security is also of particular importance in these networks, and also, creating security in WSN can be a challenging operation. Regarding that WSN is physically interacting with the environment, network information can be at risk from security threats. In addition, the main goal of increasing security in WSN is to protect data and available resources against attacks and malicious behavior of hackers. Hence, in this case, reliable methods should be used to maximize security [3]. Not only

Access this article online

DOI: 10.21928/uhdjst.v8n1y2024.pp142-150

E-ISSN: 2521-4217

P-ISSN: 2521-4209

Copyright © 2024 DiSoz Abdalkarim Rashid and Marwan B. Mohammed. This is an open access article distributed under the Creative Commons Attribution Non-Commercial No Derivatives License 4.0 (CC BY-NC-ND 4.0)

Corresponding author's e-mail: DiSoz Abdalkarim Rashid, Department of Computer Science, College of Science, University of Sulaimani, Sulaimani, Iraq. E_mail: dlsorz.rashid@univsul.edu.iq

Received: 12-12-2024

Accepted: 22-04-2024

Published: 09-05-2024

providing a reliable and efficient model to increase security in WSN is a vital thing, but also analyzing the security method against security threats is very necessary.

Overall, trust in WSN can be separated into two groups: System reliability and user trust. In the proposed model, it is tried to propose a routing for the network and the system will receive a warning against malicious nodes [4]. Moreover, due to the nature of WSN, secure routing in WSN can be very challenging because resources are limited in these networks. In addition, due to limitations in processing capacity, data storage, and battery in sensor nodes are weak against attacks because they are placed in open environments and are attacked physically or by software. Hence, reliability in data transmission and security in these networks are not guaranteed [5]. In this paper, we have used the combined algorithm based on the whale optimization algorithm (WOA) and the sine and cosine algorithm (SCA) to detect black holes (BHs). In this model, the information of the requested messages, which include the ID of the sender, and the ID of the base station, are recorded. Then, if the requested message is received in any node, the sending node is added to the list that contains the information of the senders. If the requested message is found, it will be referred to the information in the list, and if the sender's information was in the list of previous senders, the normal procedure will continue. However, if there is no information in the list, a value is added to the variable related to the suspiciousness of the node. Then, it begins the optimization phase using the proposed hybrid algorithm, in which the node is tracked and surrounded, and then, the node is attacked. Finally, this node is included in the list of exclusions and attackers [6].

The proposed optimization algorithm is utilized to reduce the computational overhead to increase the accuracy in detecting BH attacks in WSN. This article has tried to eliminate the weaknesses of other methods that have less accuracy or lack of detection of multiple attackers. For this reason, to increase the accuracy in detecting attacks, we have used input parameters with many details obtained from the attackers' behavior. This approach not only increases accuracy but multi-attacker attacks are also detected. The output is evaluated with a threshold and if the output is large, the node is considered a BH node. This method is such that the input parameters of all three input variables are created and then optimized using the proposed optimizer algorithm, which also optimizes the number of attacks.

Some of the innovations made in this article are explained below.

- Providing a new optimization algorithm based on WOA and SCA algorithms
- BH attack detection
- Evaluation using the provided hypothetical network
- Comparison with the use of other optimization algorithms
- Display results using different graphs.

This article is divided in such a way that in the next section, the previous works are discussed and reviewed; then, the basic concepts are explained and the proposed model is fully explained. In the next section, the proposed model and other methods will be tested and compared, and in the final section, future works and conclusions will be elaborated.

2. RELATED WORKS

WSNs are vital in today's world. These networks also have some weaknesses that can be considered a very good target for hackers. For this reason, many models have been proposed to strengthen security in WSNs, each of which has advantages and disadvantages. In the following, various types of security-enhancing systems in WSN will be discussed. WSNs are applied in many fields, including industrial, commercial, and health. Previous studies show that the proposed models to avoid BH attacks suffer from very few false positives [7]. In Tripathi *et al.* [8], one of the popular clustering protocols in WSN, which is LEACH, is explained and it is explained how the network can be compromised by BH and gray hole attacks. In BH attacks, the hacker tries to take control of several sensors and then reprograms these sensors to prevent sending data packets to the main base. In Wazid *et al.* [9], the influence of BH attacks on the network is evaluated and then a new model for detecting BH attacks in WSN is presented. Radio communications are very vulnerable to wide and various attacks, one of which is BH attacks. In Kaushik and Sharma [10], the attacks carried out in the network layer that are related to BH attacks have been evaluated, and the security measures that lead to the reduction of the destructive effects of such attacks have been discussed.

In Pawar and Anuradha [2], a new system that depends on a deep learning model is presented to prevent and detect BH attacks in WSNs. In this model, different phases are considered, which are equal to collecting data assigning nodes identifying BH attacks, and mitigating BH attacks. This model initially considers a series of nodes to establish communication in the WSN. In this system, attacks are explored using the Bait approach, and wormhole attacks

are explored using round-trip validation operations. Data collection is also done using the round-trip time and Bait. Finally, the collected data are trained to utilize the long short-term memory (LSTM) deep learning model, the attack detection operation is performed, and the attacks are eliminated from the network by applying optimal and correct path detection. In Khare *et al.* [11] of this model, the shortest path is discovered using the WOA algorithm. To increase security in WSN, the BH optimization algorithm is presented to detect the attack node. Furthermore, this algorithm is implemented on a vertex participation function. An improved check agent method for detecting BH attacks is presented in Saputra Andika [12], which performs the discovery operation by sending a search agent to search for the malicious node. The implementation of this model is based on the WSN created using ZigBee technology. The topology of this model can have more than one routing table.

In Khan *et al.* [13], iterative route configuration based on reactive routing protocol and ant colony algorithm is used to avoid BH attacks in mobile networks. In Srinivas and Manivannan [14], a new method for finding and preventing BH attacks in WSN is presented, and this model has five different stages. In the first step of this method, cluster heads are selected, and then k-routing paths are created, and after that, security against BH attacks is created. The fourth stage is related to creating security for the selective sending attack, and finally, in the last stage, the most optimal possible path is discovered. In this model, a topology is created to discover cluster heads and then create an optimal path, which ultimately leads to the discovery and avoidance of BH attacks using the baiting process. A validation process based on sent and received packets has been used to detect selective sending attacks. Elliptic curve cryptography is used to maximize security. In this model, a combined algorithm based on the dragonfly algorithm and the Deer hunting optimization algorithm is used to discover the shortest possible path based on parameters such as trust and delay, packet loss ratio, and distance. In Pawar and Jagadeesan [15], a BH detection model based on a deep learning algorithm in WSN is presented. To discover useful features, the feature selection technique has been used using a self-adaptive-multi-verse optimization meta-heuristic algorithm. In the next step, the features discovered in the previous step are used to train and test the deep belief network (DBN) algorithm. Furthermore, to increase the detection rate, the optimizer algorithm is utilized to enhance the DBN to optimize the number of hidden neurons.

In Rani *et al.* [16], a deep learning algorithm and ant colony optimization algorithm are used to increase security in mobile

ad hoc networks. In this model, to increase the efficiency, the best nodes are selected to transmit data packets, and the results have been shown to signify the good ability of this model. BH attacks in the demand, distance vector routing protocol have been evaluated in Pullagura and Dhulipalla [17], which are discovered and avoided using a threshold mechanism of the intrusion detection system. Furthermore, maximum objectives are calculated using linear regression. Adaptive Taylor Sail fish optimizer algorithm is used to detect and prevent Sybil and BH attacks, routing is done using this optimizer algorithm, and the optimization parameters are energy, delay, and distance.

In Webber *et al.* [18], a new algorithm based on proportional overlapping score-based Minkowski K-means clustering was introduced for BH detection in beam sensor networks, which was the main goal of BH detection in health-care applications and it has little computational complexity. In another article [19], Bayesian theory and deep recurrent neural networks have been used to discover malicious nodes and BH in WSN by calculating the path discovery time. After removing the attacker node, a new optimal path is created using the grasshopper optimization algorithm.

According to the discussion and investigation, the presented models often have weaknesses, the main weakness of which is the long execution time. Because deep learning algorithms are often used and these models require a lot of time to train. Furthermore, in some cases, the selected optimizer algorithms have weaknesses in the exploration and exploitation phases, which, if faced with this problem, can in turn cause a decrease in the accuracy rate. In some cases, the optimization algorithms do not have good capabilities in the components of diversity and intensification, which easily causes the solutions to fall into the trap of local optimization during the optimization operation and does not happen with fast convergence. For this reason, the production solutions can have little diversity, which leads to the fact that the entire problem space is not explored. On the other hand, in the low number of iterations, the algorithm cannot discover high-quality solutions, which causes the algorithm to run in a large number of iterations, which increases the execution time. Therefore, choosing optimization algorithms to solve different problems can be a challenging task because each optimization algorithm has a series of strengths and weaknesses. Furthermore, by combining the two algorithms, the positive features of the two algorithms can be integrated and a powerful algorithm with a high search capability can be achieved. The proposed algorithm has very good capabilities in the exploration and exploitation phases because each of

the SSA and WOA algorithms has strong points that the WOA algorithm works better in the exploitation phase and SSA in the exploration phase. According to the combined method, the proposed algorithm has a better execution time than other optimization algorithms, and the production solutions have a very good variety, which has led to an increase in the accuracy rate of the proposed model.

In this paper, we have developed a new type of hybrid optimization algorithm with low execution time to detect and prevent BH.

3. PROPOSED METHODOLOGY

In this subsection, the basic concepts in the proposed model will be discussed and each of the mechanisms will be fully explained in the corresponding subsections.

3.1. BH Attack

BH attacks are carried out based on malicious nodes that repeatedly send information to neighboring nodes. This node receives sensitive and important data from neighboring nodes and refrains from sending it to other nodes. These nodes are called BH nodes and the areas close to these nodes are called BH regions. In Fig. 1 these attacks are shown.

In Fig. 1, the green areas are the sensor nodes and the red area is the BH region. If a node chooses a path to send data and there is a BH node in its path, if the data reaches the BH node, all the data received in this node will be lost and will not be transmitted. In this example, as can be seen, a large number of nodes are no longer able to send data outside the network. This type of attack takes place in the third layer of the network layer OSI model. Because these attacks take place in the network layer, all the activities in the network are disrupted, and functions such as delay, throughput, and packet loss take place in the network.

3.2. SCA

Meta-heuristic algorithms have shown very good performance in solving optimization problems and are a perfect option for solving problems in different optimization spaces. The SCA [20] is one of the powerful optimization algorithms that use cosine and sine functions to solve optimization problems. This algorithm has performed very well due to its approach to solving highly complex problems because it has a good capability in the diversity component. This algorithm mainly uses Eq. (1) to solve problems.

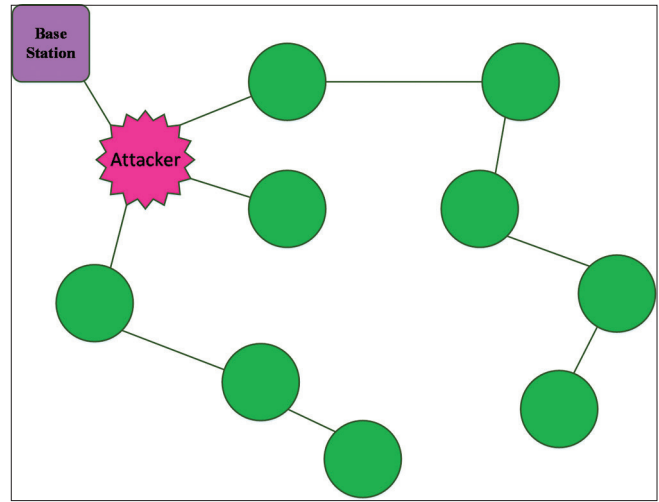


Fig. 1. Occurrence of black hole attack in wireless sensor networks.

$$x_i(t+1) = \begin{cases} x_i(t) + r_1 \times \sin(r_2) \times |r_3 P_i(t) - x_i(t)|, & r_4 < 0.5 \\ x_i(t) + r_1 \times \cos(r_2) \times |r_3 P_i(t) - x_i(t)|, & r_4 \geq 0.5 \end{cases} \quad (1)$$

In Eq. (1), *sin* and *cos* represent the sine and cosine functions, and $P_i(t)$ represents the location vector of the superior solution in the entire population, whereas $x_i(t)$ represents the current solution. Furthermore, r depicts the random number generated between 1 and 0. This algorithm uses Eq. (2) to change the exploration and exploitation phases and create balance.

$$r_1 = a - t \frac{a}{T} \quad (2)$$

In Eq. (2), a is a variable that must be set with a constant value before starting the optimization procedure, and t signifies the current iteration number and T indicates the value of all iterations for optimization reasons.

3.3. WOA

Meta-heuristic algorithms are modeled and then implemented based on the behavior of animals or natural events, which in the WOA [21] is inspired by group life and how these creatures hunt in nature and are implemented using mathematical equations. This algorithm generally uses two mechanisms to perform optimization operations. The first case is the web bubble attack and the second case is hunting. This algorithm uses Eq. (4) to perform the first phase of its optimization.

$$\vec{D} = \left| \vec{C} \cdot \overline{X_p}(t) - \vec{X}(t) \right| \quad (3)$$

$$\vec{X}(t+1) = \overline{X_p}(t) - \vec{A} \cdot \vec{D} \quad (4)$$

In Eqs. (3 and 4), X represents the current solution and X_p represents the vector of the best solution, whereas C and A are both coefficient vectors that are calculated using Eqs. (5 and 6).

$$\vec{A} = 2 \vec{a} \cdot r_1 - \vec{a} \quad (5)$$

$$\vec{C} = 2 \cdot r_2 \quad (6)$$

Where a is a coefficient vector that decreases linearly from the value of 2 to 0.

In the WOA, the spiral mathematical equation of the logarithm is used to perform the optimization operation, and this mathematical equation is shown in Eq. (7).

$$\vec{X}(t+1) = \vec{D}^i \cdot e^{b \cdot l} \cdot \cos(2 \pi l) + \overline{X_p}(t) \quad (7)$$

In Eq. (7), D^i refers to the distance between search agents and hunting, and b is a variable with a constant value, which must be set before starting the optimization procedure. In Eq. (8), two mechanisms used in the exploitation phase are shown, the first of which is related to the contraction mechanism.

$$\vec{X}(t+1) = \begin{cases} \overline{X_p}(t) - \vec{A} \cdot \vec{D} \\ \vec{D}^i \cdot e^{b \cdot l} \cdot \cos(2 \pi l) + \overline{X_p}(t) \end{cases} \quad (8)$$

In Eq. (8), P refers to the random number generated between 0 and 1.

In the natural world, whales often search for food randomly in the natural environment. The same thing has been modeled in the WOA, and if the value of vector A is >1 , the optimization algorithm enters the discovery phase, and the mathematical equation that models this behavior is shown in Eq. (9).

$$\vec{D} = \left| \vec{C} \cdot \overline{X_{rand}} - \vec{X} \right|$$

$$\vec{X}(t+1) = \overline{X_{rand}} - \vec{A} \cdot \vec{D} \quad (9)$$

In Eq. (9), X_{rand} refers to a search factor among the whole population which is randomly selected.

3.4. Proposed Model

Each optimization algorithm has a series of strengths and weaknesses, which can show very different and diverse effects

when faced with different problems. The main reason for this behavior can be the search algorithm of these algorithms in solving different problems. Because, each of these algorithms can be superior in one of the phases of exploitation or exploration, and in solving problems that one of these two cases can achieve good results, the efficiency of the algorithm is also better in the same problem. However, the problem of avoiding the BH requires good performance in both phases of exploitation exploration, and we have combined two SCAs and a WOA to solve this case. Because the SCA has a relative superiority in the exploration phase and the WOA has a better performance in the exploitation phase. Furthermore, the approach used to combine these two algorithms in this paper is to avoid increasing the computational complexity half of the population enters the SCA in each iteration, and the other half of the population enters the whale optimizer algorithm to perform optimization operations. In such a situation, the computational complexity is not increased and the optimization capabilities are maintained in both algorithms. Fig. 2 illustrates the general outline of the proposed optimizer algorithm.

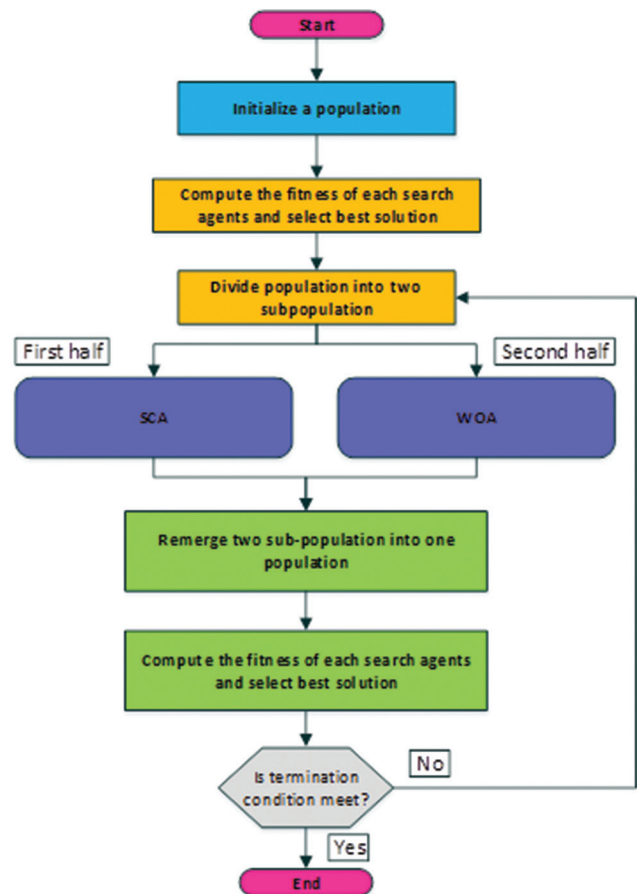


Fig. 2. Overall overview of the proposed model.

Different steps in the proposed model to discover the BH or avoid the BH, there are different steps, and each step has different processes, which are fully explained below. The proposed model goes through the following steps:

- Several nodes are randomly distributed in a square-shaped environment with adjustable dimensions
- Some of the nodes are considered BH randomly. These nodes do not send messages and by creating a hypothetical neighbor and inserting the ID of this hypothetical node in the list, they cause deception in the nodes that send the message. Because of this, the return time of the packets is very fast regardless of the specified path and can be used as a tip
- Normal nodes in the network have normal routing behavior and the return time of packets is also standard. If the packet return time from these nodes is less than the threshold, these nodes can be considered BH
- A central station undertakes the task of detecting BH using the proposed optimizer algorithm
- AODV algorithm is used for routing
- Identification stage, after detecting the suspicious nodes based on the response time, a command is issued through the central station to attack the neighboring nodes, which is the best solution of the central station in the proposed model. If the central node is adjacent to the suspicious node, the central station itself also participates in the attack process. The nodes that have the most warning and reception compared to the node in question are considered the three best nodes
- The top three nodes can change based on criteria at any moment. After being selected, these nodes start sending routing packets to discover BH nodes in a small range. In this phase, BH nodes that have not yet been definitively discovered may be present in the attack and disrupt the discovery of suspicious nodes of their colleagues
- If the number of warnings received in each enclosing node exceeds the first threshold value, it starts sharing this node with its neighbors. If the number of warnings received for the BH node exceeds the third threshold, this node will be saved as a BH node in its list. Furthermore, if the number of warnings of the first three solutions is greater than or equal to the third threshold, the suspicious node is considered a BH node. In addition, in the first three solutions, although the masked nodes warn their neighbors, the first node determines whether a node is a BH and transmits it to the hub. Then, after the definite discovery of a BH node, the station node warns this node to the neighbor so that the neighboring nodes are aware of the said node being a BH
- Neighboring nodes continue to communicate with all their neighboring nodes until the third threshold is reached, even if these nodes are suspicious nodes or BH nodes. However, when the warning level reaches the set value, these nodes are ignored
- In addition to the routing table, each node has another table called blacklist, in which the specifications of suspicious nodes are entered
- In each repetition of the simulation operation, the position of the nodes is updated, and the suspicious nodes are closely related to the number, type, and position of their neighboring nodes.

4. RESULTS AND DISCUSSION

In this section, the suggested model is tested and evaluated and the outcome gained from this evaluation will be depicted in tables and graphs. Furthermore, for a fair test, the results gained from the suggested model have been compared with gray wolf optimization [22], giant trevally optimizer [23], and particle swarm optimization (PSO) [24] algorithms. In addition, to perform this experiment, a computer with RAM 8 specifications and a Cori3-4005U CPU was used, and the implementation was done in MATLAB version 2016b. In this paper, we have used the face-centered central composite design [25] method to find the best parameter value. The best parameter value obtained from this experiment is shown in Table 1. The scenario used to test the proposed model is in the form of a virtual network, in which network nodes are randomly distributed in the network space every time it is executed. The network settings used for the experiment are shown in Table 1.

Regarding Table 2, this table shows the ratio of true and false alarms obtained from this test by the proposed model and other algorithms compared.

Focusing on the results demonstrated in Table 2, the proposed model has been able to show the best performance and is superior to other algorithms. The second-best performance is related to the PSO algorithm, which also has an acceptable rate. In the following, the proposed model has been carefully evaluated for a more accurate evaluation using different charts, which is shown in Fig. 3.

Fig. 2 shows the graphs of the cost and cumulative cost function. Considering that it is very difficult to discover BH nodes in the early stages, after each iteration, the values have decreased dramatically. In other words, in the initial stages, the

values were equal to 0.25, in the later stages of optimization, this value reached below 0.05. According to the cumulative cost diagram, the value of the cumulative function was more

than 12 in the first stage. It has been minimized to zero in the next stages, which shows the convergence process of the cost function.

TABLE 1: Parameter setting

Parameter name	Value
Network size	120×120
The total number of nodes	100/150
The number of black hole nodes	8/11
routing algorithm	AODV
Early warning level	2
Secondary warning level	6
Dimensions of the problem	3
Search range	(0 and 1)
The number of repetitions	50
Number of searchers	Variable and at least 3
Astana return time	25% of the shortest time interval

TABLE 2: Total warn with rate

Proposed Model	Gray wolf optimization	Particle swarm optimization	Giant trevally optimizer
0.8658	0.7458	0.8241	0.8068

Fig. 4 shows the graphs of the number of participating nodes and BH nodes in BH discovery. By referring to the diagram of the number of BH nodes, it is clear that the proposed model has been able to discover more BH nodes during the optimization operation, which indicates the good efficiency of the suggested model. According to the graph of the number of nodes that participated in BH detection, this graph is the percentage of nodes that participated in BH detection. Participated in the discovery of a BH at least once, it can be seen that most of the nodes participated during the optimization operation to discover the BH, which was almost more than 85%.

Fig. 5 shows the graphs of the total alerts received and the amount of correct and incorrect alerts. By carefully looking at the first diagram, it can be concluded that the number of warnings during the operation declined because the number

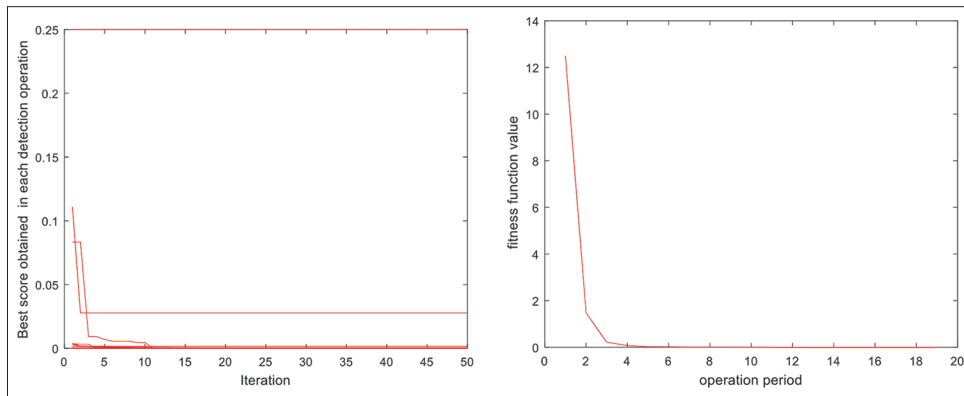


Fig. 3. Diagrams of the cost function set and the cumulative cost function.

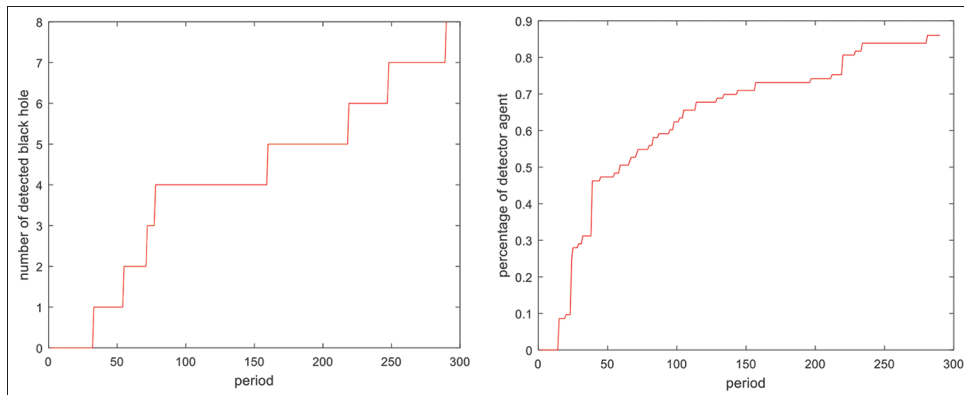


Fig. 4. Graphs of the number of detected black holes and the percentage of normal nodes detecting black holes.

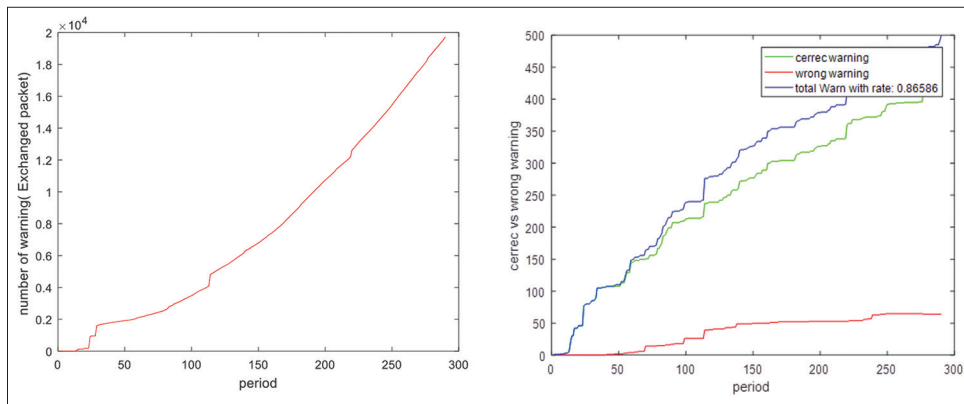


Fig. 5. Cumulative graphs of the received alarm of the whole network and the rate of false alarm and correct alarm.

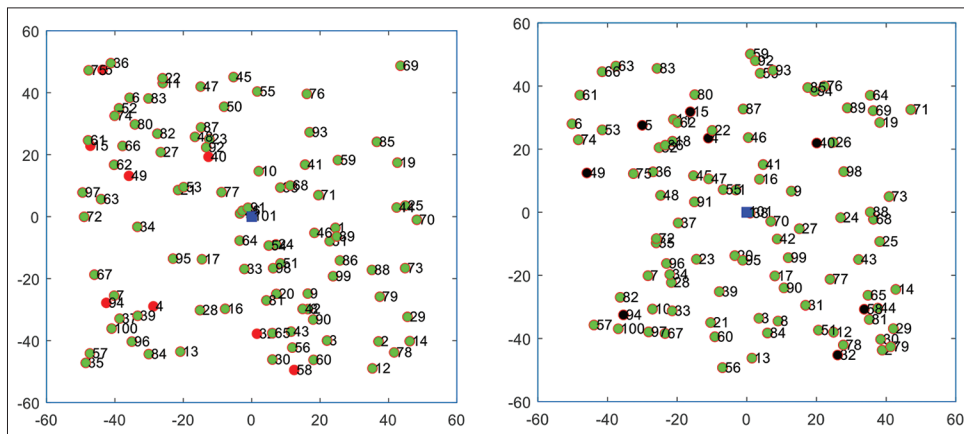


Fig. 6. Network environment before and after starting the simulation.

of BH nodes was discovered during the optimal procedure. Other normal nodes do not send information to these nodes. In the second graph, which is related to the amount of correct and false alarms, the ratio of correct alarms to false alarms is equal to 0.8658, the percentage of correct detection is equal to 100%, and the alarm ratio according to the error correction approach is equal to 0%.

Fig. 6 shows the simulation areas before and after the optimization operation. In this Fig., the suspicious nodes are shown with red circles, which change color to black if detected after the optimization operation. By looking carefully at this diagram, it is clear that the proposed model has almost been able to correctly discover all the nodes of the BH.

5. CONCLUSION AND FUTURE WORK

Minimizing energy and consumption and creating safety in WSN during the lifetime of the network is a vital issue

because otherwise, the network can easily be out of reach. In this article, a novel linked optimization algorithm depends on the WOA, and SCA is used for computing and also increasing the accuracy in finding BH attacks in WSN. In addition, it has been tried to eliminate the weaknesses in other algorithms, which include low accuracy and failure to detect multiple attackers. For this reason, in this model, an attempt has been made to use more detailed input data, which leads to increased accuracy and detection of multiple attacks. The output results are compared with a threshold value, and if this value is higher, the node in question is considered a BH node. Then, three input parameters in this model are given to the proposed optimizer algorithm to perform the optimization procedure. In this paper, a new type of optimization algorithm is presented to discover BH nodes in WSN. The above algorithm has a very good ability to explore the problem space due to its hybrid nature based on WOA and SCA algorithms. The above algorithm has shown that it has a very good performance in the exploitation and exploration phases.

The results of the experiment demonstrate that the suggested model has a perfect capability of detecting BH in WSNs.

In the future, the suggested algorithm can be applied to resolve various issues, or this model can be utilized to explore various attacks in WSN. Furthermore, in the future, a multi-objective algorithm depending on the proposed optimizer algorithm can be presented to solve multi-objective problems.

REFERENCES

- [1] S. Ali, M. A. Khan, J. Ahmad, A. W. Malik and A. U. Rehman. "Detection and Prevention of Black Hole Attacks in IOT and WSN. In: 2018 Third International Conference on Fog and Mobile Edge Computing (FMEC)". IEEE, United States, 2018.
- [2] M. V. Pawar and J. Anuradha. "Detection and prevention of black-hole and wormhole attacks in wireless sensor network using optimized LSTM". *International Journal of Pervasive Computing and Communications*, vol. 19, no. 1, pp. 124-153, 2023.
- [3] M. Shinde and D. Mehetre. "Black Hole and Selective Forwarding Attack Detection and Prevention in WSN. In: 2017 International Conference on Computing, Communication, Control and Automation (ICCUBEA)". IEEE, United States, 2017.
- [4] D. C. Mehetre, S. E. Roslin and S. J. Wagh. "Detection and prevention of black hole and selective forwarding attack in clustered WSN with active trust". *Cluster Computing*, vol. 22, pp. 1313-1328, 2019.
- [5] J. Kolangiappan. "A novel framework for the prevention of black-hole in wireless sensors using hybrid convolution network". *Scientific and Technical Journal of Information Technologies Mechanics and Optics*, vol. 22, no. 2, pp. 317-323, 2022.
- [6] M. H. Shirvani and A. Akbarifar. "Anomaly-based detection of blackhole attacks in WSN and MANET utilizing quantum-metaheuristic algorithms". *Journal of Communication Engineering*, vol. 9, no. 1, pp. 77-92, 2020.
- [7] B. K. Mishra, M. C. Nikam and P. Lakkadwala. "Security Against Black Hole Attack in Wireless Sensor Network-a Review. In: 2014 Fourth International Conference on Communication Systems and Network Technologies". IEEE, United States, 2014.
- [8] M. Tripathi, M. S. Gaur and V. Laxmi. "Comparing the impact of black hole and gray hole attack on LEACH in WSN". *Procedia Computer Science*, vol. 19, pp. 1101-1107, 2013.
- [9] M. Wazid, A. Katal, R. S. Sachan, R. H. Goudar and D. P. Singh. "Detection and Prevention Mechanism for Blackhole Attack in Wireless Sensor Network. In: 2013 International Conference on Communication and Signal Processing". IEEE, United States, 2013.
- [10] I. Kaushik and N. Sharma. "Black hole attack and its security measure in wireless sensors networks. In: Handbook of Wireless Sensor Networks: Issues and Challenges in Current Scenario's". Springer, Germany, pp. 401-416, 2020.
- [11] A. Khare, R. Gupta and P. K. Shukla. *Improving the Protection of Wireless Sensor Network Using a Black Hole Optimization Algorithm (BHOA) on Best Feasible Node Capture Attack. In: IoT and Analytics for Sensor Networks: Proceedings of ICWSNUCA 2021*". Springer, New York City, 2022.
- [12] R. Saputra, J. Andika and M. "Alaydrus. Detection of Blackhole Attack in Wireless Sensor Network Using Enhanced Check Agent. In: 2020 Fifth International Conference on Informatics and Computing (ICIC)". IEEE, United States, 2020.
- [13] D. M. Khan, T. Aslam, N. Akhtar, S. Qadri, N. A. Khan, I. M. Rabbani and M. Aslam. "Black hole attack prevention in mobile ad-hoc network (manet) using ant colony optimization technique". *Information Technology and Control*, vol. 49, no. 3, pp. 308-319, 2020.
- [14] T. A. S. Srinivas and S. S. Manivannan. "Black hole and selective forwarding attack detection and prevention in IoT in health care sector: Hybrid meta-heuristic-based shortest path routing". *Journal of Ambient Intelligence and Smart Environments*, vol. 13, no. 2, pp. 133-156, 2021.
- [15] M. V. Pawar and A. Jagadeesan. "Detection of blackhole and wormhole attacks in WSN enabled by optimal feature selection using self-adaptive multi-verse optimiser with deep learning". *International Journal of Communication Networks and Distributed Systems*, vol. 26, no. 4, pp. 409-445, 2021.
- [16] P. Rani, S. Verma and G. N. Nguyen. "Mitigation of black hole and gray hole attack using swarm inspired algorithm with artificial neural network". *IEEE Access*, vol. 8, pp. 121755-121764, 2020.
- [17] J. R. Pullagura and V. R. Dhulipalla. "Black hole attack and counter measure in ad hoc networks using traditional routing optimization". *Concurrency and Computation: Practice and Experience*, vol. 35, no. 9, p. e7643, 2023.
- [18] J. L. Webber, A. Arafa, A. Mehbodniya, S. Karupusamy, B. Shah, A. K. Dahiya and B. Kanani. "An efficient intrusion detection framework for mitigating blackhole and sinkhole attacks in healthcare wireless sensor networks". *Computers and Electrical Engineering*, vol. 111, p. 108964, 2023.
- [19] K. Cheena, T. Amgoth and G. Shankar. "Deep Learning-Based Black Hole Detection Model for WSN in Smart Grid. In: Computational Intelligence: Select Proceedings of InCITE 2022". Springer, Germany, pp. 19-30, 2023.
- [20] S. Mirjalili. "SCA: A sine cosine algorithm for solving optimization problems". *Knowledge-Based Systems*, vol. 96, pp. 120-133, 2016.
- [21] S. Mirjalili and A. Lewis. "The whale optimization algorithm". *Advances in Engineering Software*, vol. 95, pp. 51-67, 2016.
- [22] S. Mirjalili, S. M. Mirjalili and A. Lewis. "Grey wolf optimizer". *Advances in Engineering Software*, vol. 69, pp. 46-61, 2014.
- [23] B. Abdollahzadeh, F. S. Gharehchopogh and S. Mirjalili. "Artificial gorilla troops optimizer: A new nature-inspired metaheuristic algorithm for global optimization problems". *International Journal of Intelligent Systems*, vol. 36, no. 10, pp. 5887-5958, 2021.
- [24] J. Kennedy and R. Eberhart. "Particle Swarm Optimization. In: Proceedings of ICNN'95-International Conference on Neural Networks". IEEE, United States, 1995.
- [25] M. Balachandran, S. Devanathan, R. Muraleekrishnan and S. S. Bhagawan. "Optimizing properties of nanoclay-nitrile rubber (NBR) composites using face centered central composite design". *Materials and Design*, vol. 35, pp. 854-862, 2012.

Personalized Skincare: Correlating Genetics with Skin Phenotypes through DNA Analysis



Sirwan Aziz Akbar¹, Shkar M J Hassan¹, Zana Muhamad Raof², Mudhafar Mohamed M. Saeed³

¹Department of Pharmacy, Sulaimani Technical Institute, Sulaimani Polytechnic University, Sulaimani, Kurdistan Region, Iraq, ²Department of Pediatric Nursing, Sulaimani Technical Institute, Sulaimani Polytechnic University, Sulaimani, Kurdistan Region, Iraq, ³Department of Anesthesia, Sulaimani Technical Institute, Sulaimani Polytechnic University, Sulaimani, Kurdistan Region, Iraq

ABSTRACT

Genetic mapping through DNA sequencing for skin represents a novel method to elucidate detailed information regarding the relationship between genes and skin. This method analyzes genetic influences on various skin characteristics, crucial in the skin aging process. In this study, we aimed to explore the efficacy and potential of skin DNA sequencing as a valuable tool in dermatological research. Employing a purposive sampling method based on diverse skin types, we sought to ensure representativeness within the target population. The sample comprised four different skin types (five participants), selected to encompass a wide range of ages and diverse racial backgrounds. We precisely controlled for potential confounding factors such as age, gender, and race in study design. All participants exhibited consistent Fitzpatrick skin type classifications based on questionnaire responses and measurements from the Automatic Plasma Skin Type Analyzer or melanin reader. This consistency underscores the reliability of the Fitzpatrick skin type classification technique for determining skin phenotypes. Such classification holds significant importance in clinical research, guiding professionals and consumers in selecting suitable cosmetic products and skincare regimens. Furthermore, our study investigated into participants' skin characteristics and their genetic predispositions to various skin-related attributes including dermal sensitivity, protection against glycation, antioxidant capacity, freckles, and cellulite. DNA skin tests offer critical insights into understanding and managing one's unique skin traits. Our findings highlight the substantial impact of genetics on skin attributes. Notably, our observations indicate that individuals with similar skin types may harbor distinct genetic predispositions, underscoring the necessity for personalized skincare approaches. The results aim to empower clients, dermatologists, and beauty consultants to make knowledgeable skincare decisions based on genetic factors. The reliability of the Fitzpatrick skin type classification technique was validated through both questionnaire-based assessments and measurements from the Automatic Plasma Skin Type Analyzer or melanin reader, affirming its consistency and accuracy in describing participants' skin phenotypes. In summary, our study contributes to a deeper understanding of skin health and equips individuals, dermatologists, and beauty consultants to make knowledgeable skincare choices based on genetic insights.

Index Terms: DNA sequencing, Fitzpatrick skin type classification, Genetic predispositions, Genetic mapping, Personalized skincare solutions

1. INTRODUCTION

The skin is the largest organ that serves as a barrier, controls body temperature and fluids, and allows a person to perceive their surroundings [1]. It is commonly admitted as the primary defense mechanism shielding the body from external harm, which is composed of two main layers the epidermis and dermis [2].

Access this article online

DOI:10.21928/uhdjst.v8n1y2024.pp151-163

E-ISSN: 2521-4217

P-ISSN: 2521-4209

Copyright © 2024 Akbar, et al. This is an open access article distributed under the Creative Commons Attribution Non-Commercial No Derivatives License 4.0 (CC BY-NC-ND 4.0)

Corresponding author's e-mail: Sirwan Aziz Akbar, Department of Pharmacy, Sulaimani Technical Institute, Sulaimani Polytechnic University, Sulaimani, Kurdistan Region, Iraq. Email: sirwan.akbar@spu.edu.iq

Received: 02-01-2024

Accepted: 02-05-2024

Published: 29-05-2024

Despite significant advancements in dermatological research and practice, skin disorders remain a pervasive global health concern, affecting up to 1 billion people worldwide at any given time and, according to the global burden of disease project, ranking as the fourth most common cause of non-fatal diseases globally. This burden underscores the need for more targeted and effective approaches to skin health management, considering more than 3000 identified skin conditions. The prevalence and patterns of these diseases are shaped by a multitude of factors, including environmental conditions, hygiene standards, societal habits, and genetic predispositions. Notably, infections and infestations tend to be more prevalent in developing communities [1].

Skin conditions can impose financial, socioeconomic, and psychological challenges on communities, often leading to depression, frustration, social isolation, and even thoughts of self-harm or suicide. Common methods for diagnosing skin diseases involve patient history, symptom analysis, skin scraping, visual examination, dermatoscopy, and skin biopsies. Nonetheless, these diagnostic techniques can be labor-intensive, time-consuming, require experience and excellent visual perception, are subject to subjective interpretation, and are prone to error. Furthermore, they often necessitate the expertise and keen visual perception of dermatologists [1].

Recently, the relationship between an individual's genes and their skin characteristics has been a topic of interest in dermatological research. Despite growing interest, there is a notable absence of comprehensive studies directly investigating the genetic basis of individual skin characteristics and their correlation with skincare practices and treatment outcomes [3]. An analysis of the skin's DNA sequence provides comprehensive information about the connection between a person's genes and their skin, illustrating how the skin reacts to various conditions such as oxidation, premature ageing [4], varicose veins [5], redness and freckles [6] cellulite, and more [7].

According to our current understanding, there are insufficient studies in this area to provide a comprehensive understanding of the genetic basis of skin attributes. In many societies, and also in Kurdistan region of Iraq, skincare is becoming increasingly important for both women and men evident in the proliferation of skincare centers, rising dermatologist visits, and the extensive use of a range of skincare products and treatments. However, in certain circumstances, the haphazard use of skincare products and treatments can worsen skin problems [8]. This study aims to address the aforementioned gap by exploring the efficacy

and potential of skin DNA sequencing as a valuable method in dermatological research. By analyzing an individual's genetic sequencing, this method aims to provide personalized insights into skincare. The study seeks to enhance our comprehension of skin health by understanding the genetic basis of skin attributes such as sensitivity, predisposition to ageing, and susceptibility to various disorders such as redness, freckles, varicose veins, and cellulite. Ultimately, the precision offered by this information can empower individuals to make informed decisions when selecting skincare products and treatments. The additional objectives of this study were to determine skin type using different methods and evaluate their reliability in providing additional information about participants' skin, which all together aim to support specialists, including dermatologists, as further support during skin diagnosis and in prescribing interventions that are more likely to achieve positive results, thus satisfying the increasing demand for evidence-based skincare practices.

2. METHODS

In this study, we precisely conducted the selection of four different skin types (five participants or volunteers) through two distinct methods. The first method employed the Fitzpatrick skin type classification, which is a numerical classification scheme detailed in Table 1 and Fig. 1, in which participants were instructed to complete a concise questionnaire that sought information about genetic factors and personal tanning habits. The questionnaire was designed to evaluate their skin's response to sun exposure, considering factors such as burning and tanning tendencies, with the aim of establishing their self-reported Fitzpatrick skin type group [9].

TABLE 1: Total score equivalent to Fitzpatrick skin type [9]

Skin type score	Fitzpatrick skin type
0-7	I
8-16	II
17-25	III
25-30	IV
Over 30	V-VI

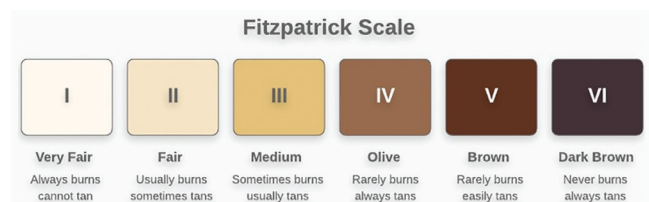


Fig. 1. Fitzpatrick scale for skin types classification [9].

The second method involved the use of an Automatic Plasma Skin Type Analyzer sensor for laser SPMU Melanin Fitzpatrick, a device manufactured under the SKINtastic brand. This device, manufactured under the SKINtastic brand, serves as a melanin reader and personnel operated it following the provided instructions.

We selected these four different skin types from a group of five unrelated participants or volunteers, consisting of three males (participants 1, 2, and 4) and two females (participants 3 and 5), with diverse skin pigmentation. They underwent thorough skin investigations using genetic sequencing. The group included individuals of varying ages, ranging from 25 to 58 years old, representing different genders, races, and a variety of skin tones, as detailed in Table 2.

Subsequently, we collected saliva samples from four different skin types (five participants) who had been previously selected for inclusion in this study. To ensure accuracy, participants followed specific guidelines in the 60–120 min preceding sample collection. They were instructed to abstain from drinking, eating, smoking, brushing their teeth, and chewing gum. During sample collection, both inner cheeks were vigorously rubbed with a swab for 1 min while personnel wore gloves and avoided contact with other surfaces. The collected samples were sealed in test tubes with stabilizer capsules, labeled with barcode stickers, and then sent to 24 Genetics DNA testing company in Spain. After the DNA extraction from the samples, 24 Genetics DNA testing company used high-throughput sequencing technologies to carry out the subsequent DNA analysis. Then, a comprehensive procedural

sequence starts, involving an in-depth analysis of the genetic material. This genetic testing relied exclusively on advanced Illumina technology, encompassing sequencing machines and chips, all within a reputable European laboratory. Following the genetic analysis, the resulting data were subjected to a comprehensive examination to identify genetic variants associated with different skin characteristics, such as oxidation, premature ageing, redness, freckles, varicose veins, and cellulite. The interpretation of the genetic map for each skin characteristic genotype depends on (Fig. 2). In this process, a comprehensive scrutiny of the approximately 0.7 million distinct gene markers present in the DNA samples was required. In this study, the DNA sequencing included only a sample of the genes that were analyzed.

Subsequently, algorithms were used to combine the individual genotypes from the markers examined. The scientific community broadly accepts the international genetic research standards on which this study's DNA sequencing method is based. Furthermore, the genetic tests utilized databases containing studies that achieved a certain level of consensus before including them in the analysis.

3. RESULTS

In this study, we assessed the participants' skin types and colors, and the results indicated Fitzpatrick skin types I, II, II, III, and IV, as determined by their questionnaire scores (4, 14, 13, 23, and 27, respectively), as presented in Table 2. In addition, when utilizing the Automatic Plasma Skin Type Analyzer or melanin reader, all participants displayed

TABLE 2: Total score (questionnaire) equivalent to Fitzpatrick skin type compared to the Automatic Plasma Skin Type Analyzer or melanin reader

Participants no	Gender	Age	Race	Skin type score based on a questionnaire	Skin type score	Fitzpatrick skin type	Skin type score based on the Automatic Plasma Skin Type Analyser or melanin reader	Skin type colour
Participant 1	M	25	Europeans	4	0–7	I	I	Very fair skin
Participant 2	M	58	Central Asian descent	14	8–16	II	II	Fair skin
Participant 3	F	31	Middle Eastern descent	13	8–16	II	II	Fair skin
Participant 4	M	43	Middle Eastern descent	23	17–25	III	III	Medium skin
Participant 5	F	47	Middle Eastern descent	27	25–30	IV	IV	Olive skin

identical results, aligning with the Fitzpatrick skin type scores obtained from the questionnaire, as illustrated in Table 2.

The results of skincare DNA sequencing, as shown in Table 3, revealed that Participant 1 (skin type I) possesses genetic variants associated with normal dermal sensitivity, representing a favorable genotype. Conversely, Participant 1 carries an unfavorable genotype, indicating a heightened susceptibility to potential damage caused by external agents. In addition, the genetic test shows that Participant 1 has a low

antioxidant capacity, which means that they have an unhealthy genotype and are more likely to be hurt by free radicals.

The genetic results for Participant 1 show that they are more likely to get acne, less likely to have skin that is excessively inflamed, and have an intermediate tendency to develop freckles.

In the context of genetic predisposition to varicose veins and protection against glycation, the analysis indicates a moderate

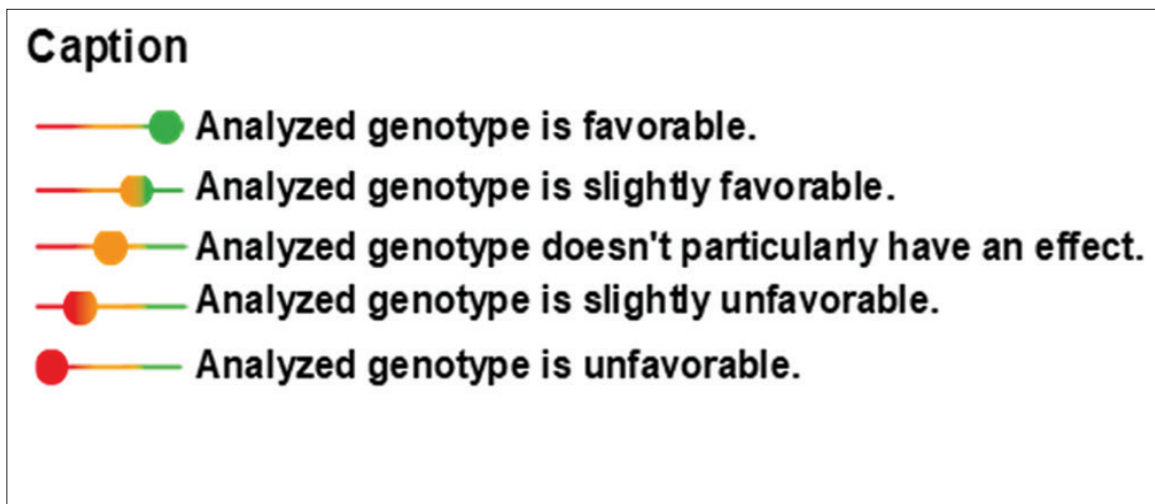


Fig. 2. Genotype interpretation of each skin characteristic genetic map (24 genetic).

TABLE 3: Genetic maps and interpretation results for skincare disease analysis of participant 1 (skin Type I)							
Skin Conditions	Genetic map		Genetic results	Skin Conditions	Genetic map		Genetic results
	Gene	Genotype			Gene	Genotype	
Dermal sensitivity	<i>IL18</i>	CC		Freckles	<i>intergenic</i>	TT	
	<i>ADAD1</i>	GG		<i>intergenic</i>	GG		
	<i>EPHX1</i>	TT		<i>IRF4</i>	TC		
Protection against pollution	<i>EPHX1</i>	TT		<i>TYR</i>	CC		
Antioxidant capacity	<i>NQO1</i>	AG		<i>TYR</i>	AG		
	<i>CAT</i>	CC		<i>MC1R</i>	CC		
	<i>NQO1</i>	GG	<i>MTHFR</i>	TT			
	<i>SOD2</i>	GG	<i>MTHFR</i>	AG			
	<i>EPHX1</i>	TC	Protection against glycation	<i>AGER</i>	AA		
Acne	<i>CAT</i>	TC	<i>AGER</i>	AG			
	<i>NQO1</i>	AG	<i>GLO1</i>	AG			
	<i>SELL</i>	GG	Cellulitis	<i>HIF1A</i>	CC		
	<i>TGFB2</i>	AG					
	<i>Intergenic</i>	GG					
Inflammation of the skin	<i>IL18</i>	CC					
	<i>IL6</i>	AG					
	<i>IFNG</i>	AG					
	<i>ADAD1</i>	GG					
	<i>IL10</i>	GG					
	<i>IL6</i>	GC					

influence (the analyzed genotype does not significantly impact these factors) and very limited protective capacity, respectively.

Finally, the results reveal that Participant 1 lacks the protective genotype, indicating a higher predisposition to cellulite, an unfavorable genotype.

In this study, as illustrated in as shown in Table 4, the skincare DNA sequencing analysis illustrated that Participant 2 (skin type II) harbors genetic variants associated with both normal dermal sensitivity and a high level of protection (a favorable genotype) against external factors capable of damaging their skin. The genotypes also indicated that Participant 2 exhibits very high antioxidant capacity.

In addition, Participant 2's genetic maps reveal a slightly unfavorable genotype predisposition (indicating a higher risk of developing acne) and a slightly favorable genotype predisposition (suggesting a lower risk of excessive inflammatory responses).

Regarding freckles and varicose veins, Participant 2's genotype is slightly unfavorable for freckles, indicating a higher probability of developing freckles, and genotype does not have particularly effect for varicose veins, suggesting an intermediate chance of suffering from varicose veins.

Furthermore, the genotype of this participant predisposes them to a high risk of glycation in their skin's components, while their predisposition to cellulite is considered average.

Table 5 illustrates that participant 3's (skin type II) genetic map exhibits favorable genotypes, signifying high potency for both dermal sensitivity and protection against pollution. However, the overall antioxidant capacity is at a moderate level. In addition, their genotypes indicate a slightly unfavorable predisposition (indicating a higher risk of acne) and a slightly favorable predisposition (suggesting a lower risk of excessive inflammatory responses).

The freckles genotype also indicated the slightly unfavorable, suggesting that their skin is at a high risk of developing freckles. In addition, the likelihood of their skin experiencing varicose veins is low. Finally, Participant 3's genetic map reveals a high risk of glycation in their skin's components and an average predisposition to cellulite.

Table 6 displays that participant 4's (skin type IV) genetic map exhibits favorable genotypes, signifying high potency for both dermal sensitivity and protection against pollution.

However, it was observed that Participant 4 exhibits a very low antioxidant capacity (unfavorable genotype), indicating a heightened susceptibility to the detrimental effects of free radicals. On the other hand, Participant's 4 genetic results

TABLE 4: Genetic maps and interpretation results for skincare disease analysis of participant 2 (Skin Type II)

Skin Conditions	Genetic map		Genetic results	Skin Conditions	Genetic map		Genetic results
	Gene	Genotype			Gene	Genotype	
Dermal sensitivity	<i>IL18</i>	CC		Freckles	<i>Intergenic</i>	TT	
	<i>ADAD1</i>	GG			<i>Intergenic</i>	GG	
	<i>EPHX1</i>	TC			<i>IRF4</i>	TC	
Protection against pollution	<i>EPHX1</i>	TC		Varicose veins	<i>TYR</i>	CC	
	<i>NQO1</i>	GG			<i>TYR</i>	AG	
Antioxidant capacity	<i>CAT</i>	TT		Protection against glycation	<i>MC1R</i>	CC	
	<i>NQO1</i>	GG			<i>MC1R</i>	CC	
	<i>SOD2</i>	AA			<i>MTHFR</i>	TT	
	<i>EPHX1</i>	TC			<i>MTHFR</i>	AG	
Acne	<i>CAT</i>	CC		Cellulitis	<i>AGER</i>	AA	
	<i>NQO1</i>	GG			<i>AGER</i>	AA	
	<i>SELL</i>	AA			<i>GLO1</i>	GG	
	<i>TGFB2</i>	AG			<i>HIF1A</i>	CC	
Inflammation of the skin	<i>intergenic</i>	GG					
	<i>IL18</i>	CC					
	<i>IL6</i>	GG					
	<i>IFNG</i>	AA					
	<i>ADAD1</i>	GG					
	<i>IL10</i>	AA					
	<i>IL6</i>	GG					

TABLE 5: Genetic maps and interpretation results for skincare disease analysis of participant 3 (Skin Type II)

Skin Conditions	Genetic map		Genetic results	Skin Conditions	Genetic map		Genetic results
	Gene	Genotype			Gene	Genotype	
Dermal sensitivity	<i>IL18</i>	CC		Freckles	<i>intergenic</i>	TT	
	<i>ADAD1</i>	GG		<i>intergenic</i>	GG		
	<i>EPHX1</i>	TC		<i>IRF4</i>	TC		
Protection against pollution	<i>EPHX1</i>	TC		<i>TYR</i>	CC		
	<i>NQO1</i>	GG		<i>TYR</i>	AG		
Antioxidant capacity	<i>CAT</i>	TC		<i>MC1R</i>	CC		
	<i>NQO1</i>	AG		Varicose veins	<i>MTHFR</i>		TT
	<i>SOD2</i>	AA		<i>MTHFR</i>	AG		
	<i>EPHX1</i>	TT		Protection against glycation	<i>AGER</i>		TA
Acne	<i>CAT</i>	TT		<i>AGER</i>	AA		
	<i>NQO1</i>	GG		Cellulitis	<i>GLO1</i>		AG
	<i>SELL</i>	AA		<i>HIF1A</i>	CC		
	<i>TGFB2</i>	AG					
Inflammation of the skin	<i>intergenic</i>	GG					
	<i>IL18</i>	CC					
	<i>IL6</i>	AA					
	<i>IFNG</i>	AG					
	<i>ADAD1</i>	GG					
	<i>IL10</i>	AG					
<i>IL6</i>	CC						










TABLE 6: Genetic maps and interpretation results for skincare disease analysis of Participant 4 (Skin Type III)

Skin Conditions	Genetic map		Genetic results	Skin Conditions	Genetic map		Genetic results
	Gene	Genotype			Gene	Genotype	
Dermal sensitivity	<i>IL18</i>	CG		Freckles	<i>intergenic</i>	TC	
	<i>ADAD1</i>	GG		<i>intergenic</i>	GG		
	<i>EPHX1</i>	TC		<i>IRF4</i>	CC		
Protection against pollution	<i>EPHX1</i>	TC		<i>TYR</i>	AC		
	<i>NQO1</i>	GG		<i>TYR</i>	GG		
Antioxidant capacity	<i>CAT</i>	CC		<i>MC1R</i>	CC		
	<i>NQO1</i>	GG		Varicose veins	<i>MC1R</i>		CC
	<i>SOD2</i>	AA		<i>MTHFR</i>	GG		
	<i>EPHX1</i>	TC		<i>MTHFR</i>	GG		
Acne	<i>CAT</i>	TC		Protection against glycation	<i>AGER</i>	AA	
	<i>NQO1</i>	GG		<i>AGER</i>	AA		
	<i>SELL</i>	AG		Cellulitis	<i>GLO1</i>	AA	
	<i>TGFB2</i>	AG		<i>HIF1A</i>	CC		
Inflammation of the skin	<i>Intergenic</i>	AG					
	<i>IL18</i>	CG					
	<i>IL6</i>	GG					
	<i>IFNG</i>	AA					
	<i>ADAD1</i>	GG					
	<i>IL10</i>	GG					
<i>IL6</i>	GG						

predispose to acne, high risk of excessive inflammatory responses on their skin, and unlikely to have freckles. The genotype also illustrated that Participant 4 is at an increased risk of varicose veins and protection against glycation (unfavorable genotype). The result also showed Participant 1 predisposition to cellulite is average.

The genetic map of Participant 5 (skin type V), as shown in Table 7, reveals a favorable genotype, indicating normal dermal sensitivity. Simultaneously, their genotype shows a very low tendency for protection (an unfavorable genotype) against external factors. The overall antioxidant capacity of Participant 4 is considered very high capacity. In addition,

TABLE 7: Genetic maps and interpretation results for skincare disease analysis of participant 5 (Skin Type IV)

Skin Conditions	Genetic map		Genetic results	Skin Conditions	Genetic map		Genetic results
	Gene	Genotype			Gene	Genotype	
Dermal sensitivity	<i>IL18</i>	CC		Freckles	<i>intergenic</i>	CC	
	<i>ADAD1</i>	GG			<i>intergenic</i>	GG	
	<i>EPHX1</i>	TT			<i>IRF4</i>	CC	
Protection against pollution	<i>EPHX1</i>	TT			<i>TYR</i>	AC	
	<i>NQO1</i>	AG			<i>TYR</i>	GG	
Antioxidant capacity	<i>CAT</i>	TT			<i>MC1R</i>	CC	
	<i>NQO1</i>	AG			<i>MC1R</i>	CC	
	<i>SOD2</i>	AA			<i>MTHFR</i>	TG	
Acne	<i>EPHX1</i>	TT		Varicose veins	<i>MTHFR</i>	GG	
	<i>CAT</i>	TT			<i>MTHFR</i>	GG	
	<i>NQO1</i>	AG		Protection against glycation	<i>AGER</i>	TA	
	<i>SELL</i>	GG			<i>AGER</i>	AA	
	<i>TGFB2</i>	GG			<i>GLO1</i>	AG	
Inflammation of the skin	<i>intergenic</i>	GG		Cellulitis	<i>HIF1A</i>	TC	
	<i>IL18</i>	CC					
	<i>IL6</i>	GG					
	<i>IFNG</i>	AG					
	<i>ADAD1</i>	GG					
	<i>IL10</i>	AA					
	<i>IL6</i>	GG					

this participant's genotype predisposes them to a higher risk of developing acne.

Furthermore, the genetic results suggest a heightened risk of excessive inflammatory responses in their skin. In addition, their freckle genotype is highly favorable, indicating a very low risk in their genetic predisposition to develop freckles.

Based on the genotype results, the probability of Participant 5 experiencing varicose veins and cellulitis is notably low and very low, respectively. Finally, Participant 5's genotype indicates a significantly reduced ability to protect against glycation (high risk of glycation).

4. DISCUSSION

In this age of advancing genetic testing, comprehending the genetic factors that impact skin characteristics can help individuals adapt their skincare routines according to their personal demands. DNA Skin Tests can help people customize skincare routines to fit their individual needs. Pinedo-Donelli and Ball (2020) considered DNA sequencing for skin, as a novel method to demonstrate detailed information about the relationship between genes and skin [10]. This test analyzes how genetics influence skin characteristics, such as hydration, elasticity, and antioxidant capacity, which play a key role in the skin aging process [3].

One of the findings of this study is that the Fitzpatrick skin type scores based on questionnaire responses and the Automatic Plasma Skin Type Analyzer or melanin reader consistently agree on how to classify skin types. This alignment is further corroborated by the findings of Magin *et al.*, who emphasized the reliability of the Fitzpatrick Skin Type Classification technique for determining skin phenotypes [11]. It is important to emphasize that the classification of skin types holds great significance in the realm of clinical research and plays an essential role in guiding professionals and consumers in their selection of appropriate cosmetic products and skincare routines [12]. Furthermore, even psychological morbidity in acne also tends to be significantly influenced by skin type [11].

To ensure proper skincare, understanding your skin well is the first step. Some of its attributes are readily noticeable through visual inspection. For instance, individuals with very pale skin are more sensitive to the sun's rays. On the other hand, certain characteristics, such as glycation, might not be visibly discernible. Nevertheless, a simple DNA skin test can uncover these hidden aspects and assist in selecting the most suitable treatments. Hence, genetic testing serves multiple purposes, including disease screening, diagnosis, and prognosis, when conditions are suspected to have a genetic basis. It is also employed to optimize drug therapy, enhancing both drug effectiveness and minimizing the risk of adverse effects [13]. Some single nucleotide polymorphisms (SNPs)

have been associated with skin characteristics as a result of recent developments in genomics and bioinformatics [3]: Skin diseases studied in this research include:

4.1. Dermal Sensitivity

The skin acts as a protective barrier that prevents harmful pathogens and toxins from entering the body. Increases the likelihood of skin sensitivity developing when there is an immune response overreaction to allergens or when there is a lack of defense against environmental toxins. This can result in atopic dermatitis, also known as eczema. Factors such as genetics and the environment appear to be the causes of increased dermal sensitivity. Researchers have identified various genetic variants associated with an increased risk of this condition through large-scale studies [14], [15].

Various immune and non-immune cells, including T and B lymphocytes, secrete interleukin-18 (IL-18), which is a member of the IL-1 cytokine family. IL-18 acts as an anticancer and pro-cancer. In common skin tumors, this protein has been shown to be overexpressed [16]. In the present study, all participants 1-5 with diverse skin types demonstrated a favorable genotype, indicating normal dermal sensitivity. Skin sensitivity can occur among all skin types; however, there is a restricted understanding of which skin types more frequently believe that they have sensitive skin. According to some sources, many factors of the biological basis of skin affect skin sensitivity, such as stratum corneum thickness, increased blood flow, and neuronal activation. However, other survey studies have shown similar rates of skin sensitivity across ethnic groups, and therefore, the correlation between skin sensitivity and skin type remains unclear, so the effect of Fitzpatrick skin type in relation to overall sensitivity remains unclear [17]. These findings align with the results of our study. In addition, the prevalence of eczema (atopic dermatitis), a common skin disorder affecting 15-20% of children and 1-3% of adult's worldwide [14], supports our findings. Since all participants in our study are adults over 25 years.

4.2. Protection Against Pollution

Environmental pollution can cause skin ageing, inflammation, and dark spots. Enzymes EPHX1 and NQO1 play crucial roles in protecting the skin's outer layer from toxins. EPHX1 converts epoxides into less reactive forms, while NQO1 alters coenzyme ubiquinone to ubiquinol, capturing free radicals and detoxifying quinones. Decreased enzyme levels can lead to reduced skin protection against environmental toxins. Genetic variations in the EPHX1 gene can cause deficiencies in these enzymes, and the NQO1 gene can decrease ubiquinol production [18]–[21]. In the present

study, Participants 1 and 5 exhibited genotypes indicating very low protection against pollution and toxins which mean that they are at a greater risk of not properly eliminating the external agents that can damage their skin. To address this concern, it is advisable for Participant 1 to consider the use of Coenzyme Q10 supplements, incorporate antioxidants like astaxanthin, also utilize products enriched with antioxidants and Coenzyme Q10, and employ a high sun protection factor. Reducing exposure to contaminants and implementing a nightly skincare routine are considered beneficial practices [22], [23], whereas Participants 2, 3, and 4 displayed genotypes suggesting very high protection against pollution.

4.3. Antioxidant Capacity

Stability between free radicals and antioxidants is necessary. To maintain proper physiological functioning and healthy-looking skin. In the skin, when the free radicals (known as oxidative stress) attack, the collagen (structural support of the skin) starts to breakdown, disrupting the cell regeneration cycle and leading to premature ageing (dull complexion, spots, and non-uniform texture), and altering proteins and lipids. Free radicals can affect all skin layers, including the hypodermis, dermis, and epidermis, making them particularly vulnerable [24], [25]. Antioxidants act as a natural defense system against free radicals, and they convert harmful free radicals into less harmful products. By reducing wrinkles and preserving the skin's natural shine, antioxidants can significantly reduce some signs of aging. Genetic variations in antioxidant enzymes, such as SOD2, EPHX1, CAT, and NQO1, have been linked to an increased risk of oxidative stress and a decline in antioxidant activity, which accelerates the aging of the skin [3], [26], [27].

In the present study, Participants 1 and 4 exhibited (an unfavorable genotype), which mean that they have a greater predisposition to suffer the harmful effects of free radicals. In response to this condition, it is recommended to maintain a diet rich in antioxidants. In addition, the use of antioxidant-rich skincare products, which may include ingredients such as green tea, caffeic acid, Vitamin C, carotenoids, Vitamin E, and glutathione, complements the antioxidants naturally presents in Participant 1's skin [28], whereas Participants 3 displayed genotypes indicating average antioxidant capacity, suggesting that some genetic variants are beneficial while others diminish the skin's antioxidant capacity. Participants 2 and 5 show high-capacity antioxidant.

4.4. Acne

Acne is a skin disorder that is especially frequent among adolescents and young adults, but can affect people of all ages.

It predominantly affects sebaceous glands linked to skin pores. These glands produce sebum, transporting dead skin cells to the skin's surface. Blockage of follicles leads to zit formation, exacerbated by bacterial growth. Anti-acne treatments are offered topically and orally. Acne is influenced by hormonal changes, stress, the use of certain medicines, and oily cosmetics. Acne is also influenced by hereditary factors, as this disorder is associated with numerous gene variants [29]–[31].

In the present study, the genotypes of all participants exhibited (slightly unfavorable genotypes), which mean a slight predisposition toward the development of acne, a trend supported by prior research indicating that individuals of various racial and ethnic backgrounds can be susceptible to acne. Furthermore, the prevalence of acne appears to be similar among individuals with lighter skin (Fitzpatrick skin types I–III) and those with darker skin (Fitzpatrick skin types IV–VI) [32]. Singh and Singh 2019 also indicated that acne can manifest in individuals across various skin types (all skin types) [33].

4.5. Inflammation of the Skin

An excessive response to allergens or toxins causes skin inflammation, which can be temporary and aid in skin regeneration. Various stressors such as UV radiation, toxins, and pathogen infections trigger persistent inflammation, leading to skin damage. Inflammation serves as the skin's basic defense mechanism, but excessive inflammation can accelerate skin aging. Chronic inflammation manifests as skin sensitivity, redness, and irritation, and variations in pro-inflammatory and anti-inflammatory genes elevate the risk of chronic skin inflammation [34]–[36].

In the present study, the genotypes of participants 1-3, representing skin types I–III, exhibited slightly favorable genotypes, indicating a lower risk of excessive inflammatory responses to inflammation. However, Participants 4 and 5 (skin types III and IV) displayed slightly unfavorable genotypes, suggesting a higher risk of excessive inflammatory responses to inflammation.

According to Bosma *et al.*, atopic dermatitis, also known as atopic eczema, is a chronic, inflammatory skin disorder with a higher prevalence among black and mixed-race communities, particularly those with darker skin types (IV-VI) compared to lighter individuals (I-III), attributed to genetic and immunological differences [37].

4.6. Freckles

Freckles are pigmentation features found in fair-skinned and red-haired individuals, categorized into ephelides and

solar lentigines (SL). Ephelides are small spots influenced by genetics and sunlight, appearing during childhood and increasing in adolescence. They are more susceptible to sunburn and skin cancer. SLs are larger, appearing after age 50 on sun-exposed skin. Freckles are viewed differently in Western and Asian cultures, leading to confusion about their nomenclature.

Freckles are associated with genetic variations in several genes, including the IRF4 gene (blue eyes, brown hair, freckles, and sun sensitivity), the MC1R gene (red hair, fair skin, UV sensitivity, and freckles), the ASIP gene (red hair, freckling, and sun sensitivity), the TYR gene (blond hair, blue eyes, and freckles), and the BNC2 gene (linked to freckles and skin color saturation) [38].

The genotypes of Participants 1-3 (skin Types I-III) indicated slightly unfavorable genotypes, signifying a high risk of developing freckles. Treatment for this disease involves various approaches, including the regular daily use of sunscreens, chemical peeling, cryotherapy, and laser therapy [39]. In contrast, Participants 4 and 5 (skin Types IV and V) showed low and very low risks, respectively, of developing freckles.

A previous study by Singh and Singh in 2019 effectively communicated that freckles are typically more common in individuals with Fitzpatrick skin types 1 and 2, but they can also be observed in those with skin types 3-5, particularly if they have red or blond hair [33].

4.7. Varicose Veins

Varicose veins, enlarged, twisted veins found in the legs, are strongly purple-blue and extend into the skin like roots. Genetic variations in the MTHFR gene increase the risk of developing varicose veins [40], while non-genetic factors increase the risk of developing varicose veins (chronic cough, constipation, family history of venous disease, being female, obesity, advanced age, pregnancy, and prolonged periods of standing). The exact cause of varicose veins is not entirely understood, but it involves a combination of genetic predisposition, weakened vessel walls, incompetent valves, and increased pressure in the veins [41].

The genetic mapping results revealed that Participants 1 and 2 (skin types I and II), exhibited a moderate genotype, indicating that the analyzed genotype has a limited impact on these aspects. In contrast, Participant 4 (skin type III) showed an unfavorable genotype, suggesting a very high risk of developing varicose veins. The recommended treatment

for varicose veins typically involves options such as oral inotropic drugs containing *Ginkgo biloba* plant that improves peripheral circulation [42].

More aggressive treatment options include external laser treatment, injection sclerotherapy, endovenous interventions, and surgery. Limited comparative data exist on the efficacy of different treatment modalities, and the choice of therapy is influenced by several factors, such as symptoms, patient preference, cost, potential complications, available medical resources, insurance coverage, and physician expertise [41].

Participants 3 and 5 (skin types II and IV) displayed slightly favorable genotypes, indicating a lower risk of developing the disease.

Based on a previous study by Aslam *et al.*, a population-based investigation conducted in San Diego found a higher prevalence of varicose veins among individuals of various racial and ethnic backgrounds. Specifically, the prevalence was 18% in Asians (Fitzpatrick skin types III–IV), 26% in Hispanics (Fitzpatrick skin types IV–VI), while varicose veins were more frequently observed in non-Hispanic Whites (Fitzpatrick skin types I–III), with a prevalence of 58%. However, various risk factors are associated with the development of varicose veins, including age, gender, occupation, pregnancy, family history, smoking, BMI, obesity, exercise, genetic factors, and current lifestyle [43].

4.8. Protection Against Glycation

Glycation is a non-enzymatic reaction between reducing sugars or reactive oxoaldehydes and proteins, lipids, or nucleic acids that leads to the creation of advanced glycation end products (AGEs) [44]. Glycation contributes to skin aging and affects the skin's capacity to regenerate and repair itself [45]. Glycated collagen fibers become inflexible and less elastic, leading to wrinkles, dryness, increased skin thickness, and a loss of firmness. AGEs develop with age and are dangerous when combined with UV exposure. Dietary measures can reduce glycation by lowering blood glucose, LDL cholesterol, and triglyceride levels. Gene variants such as GLO1 and AGER are linked to accelerated ageing and altered energy metabolism and glucose levels [44], [45].

All participants exhibited unfavorable genotypes, signifying a very low capacity for protection against glycation. Biological products caused by glycation are mostly linked to a number of age-related illnesses, such as neurodegenerative diseases, atherosclerosis, renal failure, immune system changes, retinopathy, skin photoaging, osteoporosis, and

the growth of some tumors. Epigenetic factors, oxidative stress, UV radiation, and nutrition all have an impact on the accumulation of AGEs [46]. In addition, studies done in 2022 by Zheng *et al.* suggest that exogenous factors like ultraviolet radiation make AGEs in the skin worse over time [47]. Green tea, Vitamin C, Vitamin E, niacinamide, and carnosine can lower the amount of advanced glycation products on the skin [45].

4.9. Cellulitis

Cellulite, also known as gynoid lipodystrophy or orange peel syndrome, is a common lipodystrophy disorder affecting post-adolescent women. It is characterized by subcutaneous tissue disorders such as nodules, edema, and aberrant fibrosis, giving an uneven skin appearance. Caucasian women are more likely to develop cellulitis. The pathophysiology of cellulite is complex and poorly understood, with hypotheses suggesting hormonal abnormalities, endothelial dysfunction, and genetic predispositions. Hormones such as estrogen and progesterone may contribute to fat distribution and tissue structure, while endothelial dysfunction can impair blood and lymphatic drainage. Genetic factors may also influence vulnerability to cellulite. Treatment methods for cellulite include topical creams, massages, and medical-aesthetic procedures, but their effectiveness may vary. Maintaining a healthy weight, staying active, adhering to a nutritious diet, and staying hydrated are recommended to reduce cellulitis risk [48]. Variations in the HIF1A and ACE genes, among others, have been associated with the risk of developing cellulitis [49].

The utilization of genetic mapping in the present study to assess the prevalence of cellulite unveiled distinct genetic predispositions among the participants. Participant 5, belonging to skin type IV, presented a favorable genotype, indicating a notably low susceptibility to cellulite. In contrast, Participants 2, 3, and 4, all representing skin types II and III, exhibited moderate genotypes. Notably, Participant 1 displayed an unfavorable genotype, indicating a significantly elevated risk of developing cellulite. The etiopathogenesis of cellulite is complex and not well-defined, but it is known to involve various factors, including environmental, hormonal, and genetic elements. In addition, factors like sex – where it is more prevalent in women than in men – and race – where Caucasians have a higher prevalence than other racial groups – have an impact on the incidence and severity of cellulite [48]. Another study by Friedmann revealed that despite its high incidence (80%–90%) in post-adolescent female patients of all races, cellulite is rare in male patients, which is linked to a deficiency of androgen as a result of

conditions such as castration, hypogonadism, Klinefelter's syndrome, or estrogen treatment for prostate cancer [50]. Caffeine and other ingredients such as retinol, carnitine, glucine, and tetrahydroxypropyl ethylenediamide are often used to treat cellulite [51].

In the present study, variations in skin types, ages, and genders among the participants have highlighted both differences and commonalities in their skin features. Besides genetics, other factors like lifestyle, and environmental influences are just a few of the variables that affect these differences and similarities. For instance, regardless of their diverse skin types (ranging from I to VI), all participants exhibit normal dermal sensitivity. They also share a very low capacity for protection against glycation. The characteristics of an individual's skin are determined by a combination of genetic and environmental factors. A person's DNA determines their skin type, color, and other physical characteristics. Nevertheless, environmental factors such as sun exposure, pollution, and lifestyle choices can also affect the health and appearance of their skin [52]. Recent research on twins has found that genetic factors account for up to 60% of the diversity in skin aging across individuals, while non-genetic factors such as environmental factors account for the remaining 40% [3]. This underscores the importance of considering not only genetic testing but also lifestyle and environmental factors when making skincare decisions. Furthermore, Vierkötter and Krutmann (2012) have pointed out that certain individuals may be more susceptible than others to skin injuries caused by environmental exposure. In addition, immense differences in the manifestation of extrinsic skin aging were observed between ethnic groups. The skin texture is a significant difference between the ethnic groups that is most likely relevant. However, additional genetic or behavioral differences may also be causal factors [53].

In the present study, for example, Participants 2 and 3, despite having similar skin types, exhibit variations in their antioxidant capacity and susceptibility to varicose veins. This highlights that even individuals with identical skin types may possess different genetic predispositions to photoaging [3], [54].

In the cosmetics and skincare industries, the concept of "one-size-fits-all" and "perfect for everyone" solutions is becoming obsolete as scientific research has demonstrated that every individual's skin is unique and has different requirements. Advances in technology and DNA testing have enabled the development of individualized beauty treatments tailored to the skin type, concerns, and requirements of each individual. By analyzing an individual's DNA, the cosmetics and skincare

industries can create personalized products and treatments that are more effective and efficient, resulting in improved outcomes for the individual. This personalized approach to cosmetic treatments is growing in popularity and will likely become the industry standard in the near future [55]. The skincare DNA test report provides the client, dermatologist or beauty consultant with useful information for devising a personalized skincare treatment.

While dermatoscopy and functional skin testing can be valuable tools in aiding the diagnostic process, but their application appears to be confined to specialized dermatology departments, and proficiency in their correct utilization and interpretation requires training [56]. On the other hand, DNA sequencing offers excellent diagnostic performance for skin diseases. This test holds the potential to serve as a valuable decision-support tool for dermatologists, general practitioners, and health-care professionals in the field of skin disease diagnosis [1].

Based on the report generated by DNA sequencing, an individual can select the most appropriate creams for their skin type with the help of DNA skin sequencing, which will improve the results of their dermatological treatments. Health experts such as geneticists or doctors (dermatologists) should examine and authorize any changes to health or skin treatments [3], [57]. Genes are undoubtedly a key component, but the body also reacts to a variety of other situations, including lifestyle, exercise, diet, and many more [58]. Despite the small sample size, the results serve as a starting point for further research.

5. CONCLUSIONS

The study confirms the reliability of the Fitzpatrick skin type classification based on both methods, which is crucial for clinical research and guiding skincare choices. In addition, genetic mapping through DNA sequencing provides detailed insights into how genetics influence skin attributes, a vital aspect of the aging process. The research highlights the necessity for personalized skincare solutions due to the significant impact of genetics on skin characteristics. These findings empower individuals, dermatologists, and beauty consultants to make informed decisions about skincare routines and product selections. Ultimately, understanding one's genetic predispositions enables tailored skincare approaches for better outcomes, emphasizing the importance of self-awareness in skin health management. Further research is necessary to explore these genetic influences more deeply and their implications for skincare practices.

REFERENCES

- [1] K. A. Muhaba, K. Dese, T. M. Aga, F. T. Zewdu and G. L. Simegn. "Automatic skin disease diagnosis using deep learning from clinical image and patient information". *Skin Health Disease*, vol. 2, no. 1, p. e81, 2022.
- [2] K. Park. "Role of micronutrients in skin health and function". *Biomolecules and Therapeutics*, vol. 23, no. 3, p. 207, 2015.
- [3] J. Naval, V. Alonso and M. A. Herranz. "Genetic polymorphisms and skin aging: The identification of population genotypic groups holds potential for personalized treatments". *Clinical, Cosmetic Investigational Dermatology*, vol. 7, pp. 207-214, 2014.
- [4] M. Hussain, S. Krishnamurthy, J. Patel, E. Kim, B. A. Baptiste, D. L. Croteau and V. A. Bohr. "Skin abnormalities in disorders with DNA repair defects, premature aging, and mitochondrial dysfunction". *Journal of Investigative Dermatology*, vol. 141, no. 4, pp. 968-975, 2021.
- [5] S. Li, Y. Liu, M. Liu, L. Wang and X. Li. "Comprehensive bioinformatics analysis reveals biomarkers of DNA methylation-related genes in varicose veins". *Frontiers in Genetics*, vol. 13, p. 1013803, 2022.
- [6] M. A. Farage, Y. Jiang, J. P. Tiesman, P. Fontanillas and R. Osborne. "Genome-wide association study identifies loci associated with sensitive skin". *Cosmetics*, vol. 7, no. 2, p. 49, 2020.
- [7] A. J. Rawlings. "Cellulite and its treatment". *International Journal of Cosmetic Science*, vol. 28, no. 3, pp. 175-190, 2006.
- [8] Y. V. N. Limam, A. C. de Oliveira Boeing, R. P. Júnior and T. M. G. da Silva. "The impact of social media on Acne Vulgaris treatment". *Surgical Cosmetic Dermatology*, vol. 15, p. e20230198, 2023.
- [9] S. Sachdeva. "Fitzpatrick skin typing: Applications in dermatology". *Indian Journal of Dermatology, Venereology Leprology*, vol. 75, p. 93, 2009.
- [10] S. Pinedo-Donelli and E. Ball. "Next generation sequencing: Use in dermatology". *Medicina Cutánea Ibero-Latino-Americana*, vol. 48, no. 1, pp. 47-62, 2020.
- [11] P. Magin, D. Pond, W. Smith, S. Goode and N. Paterson. "Reliability of skin-type self-assessment: Agreement of adolescents' repeated Fitzpatrick skin phototype classification ratings during a cohort study". *Journal of the European Academy of Dermatology Venereology*, vol. 26, no. 11, pp. 1396-1399, 2012.
- [12] R. Oliveira, J. Ferreira, L. F. Azevedo and I. F. Almeida. "An overview of methods to characterize skin type: Focus on visual rating scales and self-report instruments". *Cosmetics*, vol. 10, no. 1, p. 14, 2023.
- [13] N. Franceschini, A. Frick and J. B. Kopp. "Genetic testing in clinical settings". *American Journal of Kidney Diseases*, vol. 72, no. 4, pp. 569-581, 2018.
- [14] S. Nutten. "Atopic dermatitis: Global epidemiology and risk factors". *Annals of Nutrition and Metabolism*, vol. 66, no. Suppl. 1, pp. 8-16, 2015.
- [15] C. Beisswenger, K. Kandler, C. Hess, H. Garn, K. Felgentreff, M. Wegmann, H. Renz, C. Vogelmeier and R. Bals. "Allergic airway inflammation inhibits pulmonary antibacterial host defense". *The Journal of Immunology*, vol. 177, no. 3, pp. 1833-1837, 2006.
- [16] S. Yalçın, P. Mutlu, T. Çetin, M. Sarper, G. Özgür and F. Avcu. "The-137G/C polymorphism in interleukin-18 gene promoter contributes to chronic lymphocytic and chronic myelogenous leukemia risk in Turkish patients". *Turkish Journal of Hematology*, vol. 32, no. 4, p. 311, 2015.
- [17] C. E. Dubin, G. W. Kimmel, P. W. Hashim, J. K. Nia and J. A. Zeichner. "Objective evaluation of skin sensitivity across fitzpatrick skin types". *Journal of Drugs in Dermatology*, vol. 19, no. 7, pp. 699-701, 2020.
- [18] C. Parrado, S. Mercado-Saenz, A. Perez-Davo, Y. Gilaberte, S. Gonzalez and A. Juaranz. "Environmental stressors on skin aging. Mechanistic insights". *Frontiers in Pharmacology*, vol. 10, p. 759, 2019.
- [19] R. Václavíková, D. J. Hughes and P. Souček. "Microsomal epoxide hydrolase 1 (EPHX1): Gene, structure, function, and role in human disease". *Gene*, vol. 571, no. 1, pp. 1-8, 2015.
- [20] A. Parkinson and B. W. Ogilvie. "Biotransformation of xenobiotics. In: Casarett and Doull's Toxicology: The Basic Science of Poisons". Vol. 7. McGraw Hill, New York, pp. 161-304, 2008.
- [21] A. Atia and A. Abdullah. "NQO1 enzyme and its role in cellular protection; An insight". *Iberoamerican Journal of Medicine*, vol. 2, no. 4, pp. 306-313, 2020.
- [22] S. Davinelli, M. E. Nielsen and G. Scapagnini. "Astaxanthin in skin health, repair, and disease: A comprehensive review". *Nutrients*, vol. 10, no. 4, p. 522, 2018.
- [23] A. Knott, V. Achterberg, C. Smuda, H. Mielke, G. Sperling, K. Duncelmann, A. Vogelsang, A. Krüger, H. Schwengler, M. Behtash, S. Kristof, H. Diekmann, T. Eisenberg, A. Berroth, J. Hildebrand, R. Siegner, M. Winnefeld, F. Teuber, S. Fey, J. Möbius, D. Retzer, T. Burkhardt, J. Lüttke and T. Blatt. "Topical treatment with coenzyme Q10-containing formulas improves skin's Q10 level and provides antioxidative effects". *Biofactors*, vol. 41, no. 6, pp. 383-390, 2015.
- [24] V. Lobo, A. Patil, A. Phatak and N. Chandra. "Free radicals, antioxidants and functional foods: Impact on human health". *Pharmacognosy Reviews*, vol. 4, no. 8, p. 11, 2010.
- [25] M. Rinnerthaler, J. Bischof, M. K. Streubel, A. Trost and K. Richter. "Oxidative stress in aging human skin". *Biomolecules*, vol. 5, no. 2, pp. 545-589, 2015.
- [26] V. Sosa, T. Moliné, R. Somoza, R. Paciucci, H. Kondoh and M. E. LLeonart. "Oxidative stress and cancer: An overview". *Ageing Research Reviews*, vol. 12, no. 1, pp. 376-390, 2013.
- [27] J. D. Hayes, A. T. Dinkova-Kostova and K. D. Tew. "Oxidative stress in cancer". *Cancer Cell*, vol. 38, no. 2, pp. 167-197, 2020.
- [28] C. Kaur and H. C. Kapoor. "Antioxidants in fruits and vegetables-the millennium's health". *International Journal of Food Science and Technology*, vol. 36, no. 7, pp. 703-725, 2001.
- [29] N. Skroza, E. Tolino, A. Mambrin, S. Zuber, V. Balduzzi, A. Marchesiello, N. Bernardini, I. Proietti, and C. Potenza. "Adult acne versus adolescent acne: A retrospective study of 1,167 patients". *The Journal of Clinical Aesthetic Dermatology*, vol. 11, no. 1, p. 21, 2018.
- [30] K. Kameswararao, C. Sujani, N. V. N. Koteswararao, A. Rajarao and P. N. S. Satyanarayanamma. "A brief review on acne vulgaris". *Research Journal of Pharmacology Pharmacodynamics*, vol. 11, no. 3, pp. 109-119, 2019.
- [31] A. K. Mohiuddin. "A comprehensive review of acne vulgaris". *Journal of Clinical Pharmacy*, vol. 1, no. 1, p. 17-45, 2019.
- [32] N. Schmidt and E. H. Gans. "Clindamycin 1.2% tretinoin 0.025% gel versus clindamycin gel treatment in acne patients: A Focus on fitzpatrick skin types". *The Journal of Clinical Aesthetic Dermatology*, vol. 4, no. 6, p. 31, 2011.
- [33] R. Singh and R. G. Singh. "Efficacy and safety of radio frequency in acne and freckles". *Journal of Medical Science And clinical Research*, vol. 7, no. 7, pp. 362-368, 2019.

- [34] R. Huggenberger and M. Detmar. "The cutaneous vascular system in chronic skin inflammation". *Journal of Investigative Dermatology Symposium Proceedings*, vol. 15, pp. 24-32, 2011.
- [35] M. Pasparakis, I. Haase and F. O. Nestle. "Mechanisms regulating skin immunity and inflammation". *Nature Reviews Immunology*, vol. 14, no. 5, pp. 289-301, 2014.
- [36] T. P. Habif, M. S. Chapman, J. G. Dinulos and K. A. Zug. "*Skin Disease e-book: Diagnosis and Treatment*". Elsevier Health Sciences, Philadelphia, PA, 2017.
- [37] A. L. Bosma, W. Ouwerkerk, M. J. Heidema, D. Prieto-Merino, M. R. Ardern-Jones, P. Beattie, S. J. Brown, J. R. Ingram, A. D. Irvine, G. Ogg, P. Patel, N. J. Reynolds, R. M. Ross Hearn, M. Wan, R. B. Warren, R. T. Woolf, A. M. Hyseni, L. A. A. Gerbens, P. I. Spuls, C. Flohr, M. A. Middelkamp-Hup and TREAT NL Registry and UK-Irish A-STAR Study Groups. "Comparison of real-world treatment outcomes of systemic immunomodulating therapy in atopic dermatitis patients with dark and light skin types". *JAAD International*, vol. 10, pp. 14-24, 2023.
- [38] C. Praetorius, R. A. Sturm and E. Steingrimsson. "Sun-induced freckling: Ephelides and solar lentigines". *Pigment Cell Melanoma Research*, vol. 27, no. 3, pp. 339-350, 2014.
- [39] S. Noroozi, F. Fadaei, M. Rahbar, M. Tabarrai, P. Mansouri and L. Shirbeigi. "Novel preventive and therapeutic strategies for ephelides (freckles) from a Persian medicine perspective: A narrative review". *Journal of Skin Stem Cell*, vol. 9, no. 3, p. e123335, 2022.
- [40] M. Ekim and H. Ekim. "Incidence of the MTHFR polymorphisms in patients with varicose veins". *Hippokratia*, vol. 21, no. 4, p. 175, 2017.
- [41] R. H. Jones and P. J. Carek. "Management of varicose veins". *American Family Physician*, vol. 78, no. 11, pp. 1289-1294, 2008.
- [42] T. Arnould, C. Michiels, D. Janssens, N. Berna and J. Remacle. "Effect of Ginkor Fort on hypoxia-induced neutrophil adherence to human saphenous vein endothelium". *Journal of Cardiovascular Pharmacology*, vol. 31, no. 3, pp. 456-463, 1998.
- [43] M. R. Aslam, H. Muhammad Asif, K. Ahmad, S. Jabbar, A. Hayee, M. S. Sagheer, J. U. Rehman, S. Khalid, A. S. Hashmi and S. R. Rajpoot and A. Sharif. "Global impact and contributing factors in varicose vein disease development". *SAGE Open Medicine*, vol. 10, p. 1, 2022.
- [44] D. Indyk, A. Bronowicka-Szydelko, A. Gamian and A. Kuzan. "Advanced glycation end products and their receptors in serum of patients with type 2 diabetes". *Scientific Reports*, vol. 11, no. 1, p. 13264, 2021.
- [45] P. Gkogkolou and M. Böhm. "Advanced glycation end products: Key players in skin aging?" *Dermato-Endocrinology*, vol. 4, no. 3, pp. 259-270, 2012.
- [46] M. Fournet, F. Bonté and A. Desmoulière. "Glycation damage: A possible hub for major pathophysiological disorders and aging". *Aging Disease*, vol. 9, no. 5, p. 880, 2018.
- [47] M. Zhang, F. Song, L. Liang, H. Nan, J. Zhang, H. Liu, L. E. Wang, Q. Wei, J. E. Lee, and C. I. Amos, P. Kraft, A. A. Qureshi and J. Han. "Genome-wide association studies identify several new loci associated with pigmentation traits and skin cancer risk in European Americans". *Human Molecular Genetics*, vol. 22, no. 14, pp. 2948-2959, 2013.
- [48] K. Tokarska, S. Tokarski, A. Woźniacka, A. Sysa-Jędrzejowska and J. Bogaczewicz. "Cellulite: A cosmetic or systemic issue? Contemporary views on the etiopathogenesis of cellulite". *Advances in Dermatology and Allergology/Postępy Dermatologii i Alergologii*, vol. 35, no. 5, pp. 442-446, 2018.
- [49] E. Emanuele, M. Bertona and D. Geroldi. "A multilocus candidate approach identifies ACE and HIF1A as susceptibility genes for cellulite". *Journal of the European Academy of Dermatology*, vol. 24, no. 8, pp. 930-935, 2010.
- [50] D. P. Friedmann, G. L. Vick and V. Mishra. "Cellulite: A review with a focus on subcision". *Clinical, Cosmetic Investigational Dermatology*, vol. 10, pp. 17-23, 2017.
- [51] F. Turati, C. Pelucchi, F. Marzatico, M. Ferraroni, A. Decarli, S. Gallus, C. La Vecchia and C. Galeone. "Efficacy of cosmetic products in cellulite reduction: Systematic review and meta-analysis". *Journal of the European Academy of Dermatology Venereology*, vol. 28, no. 1, pp. 1-15, 2014.
- [52] G. M. DeStefano and A. M. Christiano. "The genetics of human skin disease". *Cold Spring Harbor Perspectives in Medicine*, vol. 4, no. 10, p. a015172, 2014.
- [53] A. Vierkötter and J. Krutmann. "Environmental influences on skin aging and ethnic-specific manifestations". *Dermato-Endocrinology*, vol. 4, no. 3, pp. 227-231, 2012.
- [54] S. Lautenschlager, H. C. Wulf and M. R. Pittelkow. "Photoprotection". *The Lancet*, vol. 370, no. 9586, pp. 528-537, 2007.
- [55] B. Perbal and S. Gabaron. "Mastering health: Liberating beauty: Will the cosmetics of tomorrow be genetic?" *Journal of Cell Communication and Signaling*, vol. 15, pp. 483-490, 2021.
- [56] A. Berekméri, A. Tiganescu, A. A. Alase, E. Vital, M. Stacey, and M. Wittmann. "Non-invasive approaches for the diagnosis of autoimmune/ autoinflammatory skin diseases-a focus on psoriasis and Lupus erythematosus". *Frontiers in Immunology*, vol. 10, p. 1931, 2019.
- [57] E. Rostkowska, E. Poleszak, K. Wojciechowska and K. Dos Santos Szewczyk. "Dermatological management of aged skin". *Cosmetics*, vol. 10, no. 2, p. 55, 2023.
- [58] D. G. Blazer and L. M. Hernandez. "*Genes, Behavior, and the Social Environment: Moving Beyond the Nature/Nurture Debate*". National Academies Press, Washington, DC, 2006.

p-ISSN 2521-4209
e-ISSN 2521-4217



UHD Journal of Science and Technology

A Scientific periodical issued by University of Human Development

Vol.8 No.(1) June 2024

2024

2724

e.mail:jst@uhd.edu.iq